

AD-785 024

**COMPARATIVE PERFORMANCE OF STRUCTURAL LAYERS IN
PAVEMENT SYSTEMS**

**VOLUME I. DESIGN, CONSTRUCTION, AND BEHAVIOR
UNDER TRAFFIC OF PAVEMENT TEST SECTIONS**

ARMY ENGINEER WATERWAYS EXPERIMENT STATION

**PREPARED FOR
FEDERAL AVIATION ADMINISTRATION**

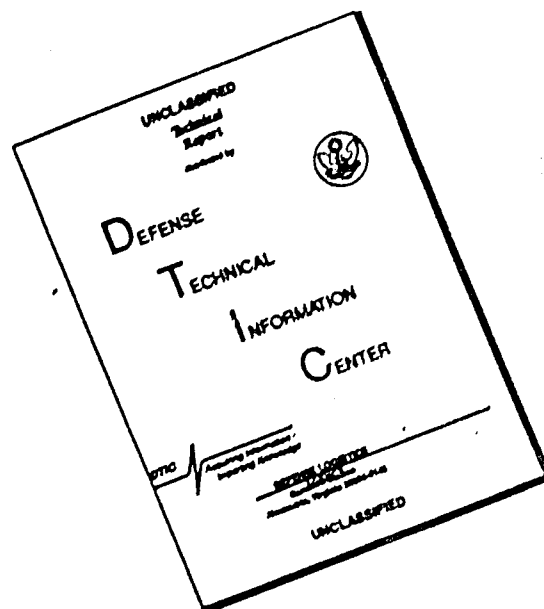
JUNE 1974

DISTRIBUTED BY:

NTIS

**National Technical Information Service
U. S. DEPARTMENT OF COMMERCE**

DISCLAIMER NOTICE



THIS DOCUMENT IS BEST QUALITY AVAILABLE. THE COPY FURNISHED TO DTIC CONTAINED A SIGNIFICANT NUMBER OF PAGES WHICH DO NOT REPRODUCE LEGIBLY.

1 Report No. FAA-RD-73-198, I	2 Government Accession No.	3 Recipient's Catalog No. AD785024
4 Title and Subtitle COMPARATIVE PERFORMANCE OF STRUCTURAL LAYERS IN PAVEMENT SYSTEMS; VOLUME I: DESIGN, CONSTRUCTION, AND BEHAVIOR UNDER TRAFFIC OF PAVEMENT TEST SECTIONS		5 Report Date June 1974
7 Author(s) C. D. Burns, C. L. Rone, W. N. Brabston, H. H. Ulery, Jr.		6 Performing Organization Code
9 Performing Organization Name and Address U. S. Army Engineer Waterways Experiment Station Soils and Pavements Laboratory, P. O. Box 631 Vicksburg, Miss. 39180		8 Performing Organization Report No.
12 Sponsoring Agency Name and Address Office, Chief of Engineers, U. S. Army, and Federal Aviation Administration Washington, D. C.		10 Work Unit No. (TRAIS)
		11 Contract or Grant No. FA71WAI-218
		13 Type of Report and Period Covered Final report
		14 Sponsoring Agency Code
15 Supplementary Notes		
16 Abstract Rigid and flexible pavement test sections were constructed to evaluate the performance of pavements incorporating a membrane-enveloped soil layer, insulating materials, chemically stabilized soil layers, and various types of surfacing including fibrous-reinforced concrete, plain portland cement concrete, and asphaltic concrete. These test sections were trafficked with 200- and 240-kip twin-tandem assemblies (Boeing 747 spacing) and a 50-kip single-wheel assembly. The design, construction, and behavior under traffic of the pavements are reported herein; the data will be used in further studies to determine the response of the pavement to both static and dynamic loads and to develop design and construction criteria. These studies will be reported in subsequent volumes.		
17 Key Words Stabilized layers Membrane-enveloped soil layers Insulating materials Rigid pavements Flexible pavements		18 Distribution Statement Document is available to the public through the National Technical Information Service, Springfield, Va. 22151.
19 Security Classif. (of this report) Unclassified	20 Security Classif. (of this page) Unclassified	21 No. of Pages 256
		22 Price 4.50. 3.25

Form DOT F 1700.7 (8-72)

Reproduction of completed page authorized

1
1.

Reproduced by
NATIONAL TECHNICAL
INFORMATION SERVICE
U. S. Department of Commerce
Springfield, VA 22151

ADDRESS for _____
 174
 NYC
 100
 A

NOTICES

This document is disseminated under the sponsorship of the Department of Transportation in the interest of information exchange. The United States Government assumes no liability for its contents or use thereof.

The United States Government does not endorse products of manufacturers. Trade or manufacturers' names appear herein solely because they are considered essential to the object of this report.

PREFACE

The investigation reported herein was jointly sponsored by the Office, Chief of Engineers, U. S. Army, as a part of the Military Engineering Design and Expedient Construction Criteria Program and the Military Construction Short-Range Airfield Pavement Research Program and by the Federal Aviation Administration as a part of Inter-Agency Agreement FA71WAI-218, "Development of Airport Pavement Criteria."

The investigation was conducted by personnel of the Soils and Pavements Laboratory (S&PL), U. S. Army Engineer Waterways Experiment Station (WES), under the general supervision of Messrs. J. P. Sale and R. G. Ahlvin, Chief and Assistant Chief, respectively, of S&PL. This report was prepared by Messrs. C. D. Burns, C. L. Rone, W. N. Brabston, and H. H. Ulery, Jr.

Directors of WES during the conduct of the investigation and the preparation of this report were BG E. D. Peixotto, CE, and COL G. H. Hilt, CE. Technical Director was Mr. F. R. Brown.

TABLE OF CONTENTS

INTRODUCTION	15
BACKGROUND	15
OBJECTIVES	15
SCOPE	16
DESIGN OF TEST SECTIONS	16
RIGID PAVEMENT TEST SECTION	16
FLEXIBLE PAVEMENT TEST SECTION	26
DESIGN CEMENT CONTENTS	38
INSTRUMENTATION OF TEST SECTIONS	42
DEFLECTION GAGES	42
PRESSURE CELLS	46
STRAIN SENSORS	46
INDUCTIVE PROBES	47
THERMISTORS	48
CONSTRUCTION OF TEST SECTIONS	49
RIGID PAVEMENT TEST SECTION	49
FLEXIBLE PAVEMENT TEST SECTION	65
INSTALLATION OF INSTRUMENTATION	70
TESTING AND SAMPLING DURING CONSTRUCTION	74
PROPERTIES OF AS-CONSTRUCTED PAVEMENTS	75
TESTING AND BEHAVIOR UNDER TRAFFIC	83
SELECTION OF TRAFFIC LOADINGS	83
TEST CONDITIONS AND PROCEDURES	83
COLLECTION OF INSTRUMENTATION DATA	90
BEHAVIOR OF PAVEMENTS UNDER TRAFFIC	97
SUMMARY OF TRAFFIC TEST DATA	103
SUMMARY OF FINDINGS	111
RIGID PAVEMENT TEST SECTION	111
FLEXIBLE PAVEMENT TEST SECTION	112

Preceding page blank

APPENDIX A: BEHAVIOR OF RIGID PAVEMENT TEST SECTION UNDER	
TRAFFIC	113
200-KIP LOAD, LANE 1	113
240-KIP LOAD, LANE 2	117
AFTER-TRAFFIC TESTING PROGRAMS	122
APPENDIX B: BEHAVIOR OF FLEXIBLE PAVEMENT TEST SECTION UNDER	
TRAFFIC	171
200-KIP LOAD, LANE 1	171
240-KIP LOAD, LANE 2	177
50-KIP SINGLE-WHEEL LOAD, LANE 3	182
VARIATION IN CEMENT CONTENT	187
REFERENCES	253

FIGURES

1	Layout of the rigid pavement test section	18
2	CBR, density, and water content data for heavy clay subgrade material	20
3	Gradations and classification data for subgrade materials	21
4	Laboratory compaction data for lean clay and clay gravel materials	22
5	Details of longitudinal construction joints in the rigid pavement test section	27
6	Details of transverse construction joints in the rigid pavement test section	28
7	Layout of the flexible pavement test section	29
8	Profiles of items in the flexible pavement test section with insulating materials	30
9	Gradations and classification data for base and subbase materials in items 1 and 3-5 of the flexible pavement section	33
10	Laboratory compaction data for gravelly sand (PI = 3) and crushed limestone materials	34
11	Laboratory compaction data for gravelly sand (PI = 0) and clayey sand materials	36
12	Aggregate gradation and CE and FAA specification limits for asphaltic concrete surface course in the flexible pavement test section	37
13	Instrumentation layout for flexible pavement test section	43
14	Instrumentation layout for flexible pavement test section	44
15	Instrumentation layout for rigid pavement test section	45
16	Pair of Bison strain sensors in micrometer calibration mount	47
17	Location of soil stabilization test sections within the existing MWHGL test section	50
18	Finished subgrade of item 1 of rigid pavement test section	52

19	Polyethylene membrane in place on the subgrade of item 1 of the rigid pavement test section	52
20	Placement of soil in the MESL	54
21	Completed MESL base course in item 1 of the rigid pavement test section	54
22	Bags of cement distributed over the surface of the base of item 2 of the rigid pavement test section	55
23	In-place mixing of soil and cement in item 2 of the rigid pavement test section	55
24	Compaction with the 30-ton self-propelled pneumatic-tired roller	57
25	Compaction with the 50-ton pneumatic-tired roller	57
26	Spreading hot-mix bituminous base material in item 3 of the rigid pavement test section	58
27	Specimen of bituminous base cut from item 3 of the rigid pavement test section	58
28	Polystyrene panels in place on the subgrade of item 5 of the rigid pavement test section	59
29	Surface texture of the lightweight concrete insulating layer in subitem 5b of the rigid pavement test section	60
30	Completed installation of insulating materials on subgrade of subitems 5a-d of the rigid pavement test section	61
31	Transition slabs in place between the rigid pavement test items	62
32	Placement of fibrous-reinforced concrete in item 2 of the rigid pavement test section	62
33	Placement of concrete over insulating materials in item 5 of the rigid pavement test section	63
34	Joint sawing operations in the rigid pavement test section	64
35	Completed subgrade of the flexible pavement test section	67
36	Bags of cement and fly ash distributed over the surface of the subgrade of items 1 and 2 of the flexible pavement test section	68
37	In-place mixing of treated soil with pulvimixer	68
38	Placement of lightweight concrete insulating materials in item 5 of the flexible pavement test section	71
39	Primed base courses prior to paving flexible pavement test section	71
40	Placement of 3-in.-thick asphaltic concrete surface course on the flexible pavement test section	72
41	Overall view of completed flexible pavement test section	72
42	Placement of a Bison strain sensor	73
43	Placement of a WES pressure cell	73
44	Twin-tandem assembly load cart	84
45	Wheel arrangement for twin-tandem assembly	85
46	Single-wheel assembly load cart	85
47	Traffic patterns	87
48	Traffic log for lane 1 of both test sections	91
49	Traffic log for lane 2 of the rigid pavement test section and for lanes 2 and 3 of the flexible pavement test section	92

50	Temperature data	93
51	Pavement temperature versus traffic distribution for lane 1 of the flexible pavement test section	94
52	Pavement temperature versus traffic distribution for lane 2 of the flexible pavement test section	95
A1	Item 1, lane 1, rigid pavement test section, prior to traffic	125
A2	Item 1, lane 1, rigid pavement test section, after 200 cov- erages by 200-kip twin-tandem assembly	125
A3	Item 1, lane 1, rigid pavement test section, after 1770 coverages by 200-kip twin-tandem assembly	126
A4	Item 1, lane 1, rigid pavement test section, after 3000 cov- erages by 200-kip twin-tandem assembly	126
A5	Crack development in lane 1, rigid pavement test section . . .	127
A6	Surface deformation in item 1, lane 1, rigid pavement test section	128
A7	Item 2, lane 1, rigid pavement test section, prior to traffic	129
A8	Item 2, lane 1, rigid pavement test section, after 200 coverages by 200-kip twin-tandem assembly	129
A9	Item 2, lane 1, rigid pavement test section, after 1000 coverages by 200-kip twin-tandem assembly	130
A10	Item 2, lane 1, rigid pavement test section, after 1770 coverages by 200-kip twin-tandem assembly	130
A11	Surface deformation in item 2, lane 1, rigid pavement test section	131
A12	Item 3, lane 1, rigid pavement test section, prior to traffic	132
A13	Item 3, lane 1, rigid pavement test section, after 200 coverages by 200-kip twin-tandem assembly	132
A14	Item 3, lane 1, rigid pavement test section, after 3000 coverages by 200-kip twin-tandem assembly	133
A15	Item 3, lane 1, rigid pavement test section, after 6360 coverages by 200-kip twin-tandem assembly	133
A16	Surface deformation in item 3, lane 1, rigid pavement test section	134
A17	Item 4, lane 1, rigid pavement test section, prior to traffic	135
A18	Item 4, lane 1, rigid pavement test section, after 1770 coverages by 200-kip twin-tandem assembly	135
A19	Item 4, lane 1, rigid pavement test section, after 6360 coverages by 200-kip twin-tandem assembly	136
A20	Surface deformation in item 4, lane 1, rigid pavement test section	137
A21	Item 5, lane 1, rigid pavement test section, prior to traffic	138
A22	Subitem 5a, lane 1, rigid pavement test section, after 1770 coverages by 200-kip twin-tandem assembly	138
A23	Subitem 5a, lane 1, rigid pavement test section, after 3000 coverages by 200-kip twin-tandem assembly	139

A24	Surface deformation in subitems 5a and b, lane 1, rigid pavement test section	140
A25	Subitem 5b, lane 1, rigid pavement test section, after 1770 coverages by 200-kip twin-tandem assembly	141
A26	Subitem 5b, lane 1, rigid pavement test section, after 3000 coverages by 200-kip twin-tandem assembly	141
A27	Subitem 5c, lane 1, rigid pavement test section, after 1000 coverages by 200-kip twin-tandem assembly	142
A28	Subitem 5c, lane 1, rigid pavement test section, after 1230 coverages by 200-kip twin-tandem assembly	142
A29	Surface deformation in subitems 5c and d, lane 1, rigid pavement test section	143
A30	Subitem 5d, lane 1, rigid pavement test section, after 3000 coverages by 200-kip twin-tandem assembly	144
A31	Item 1, lane 2, rigid pavement test section, prior to traffic	144
A32	Crack development in lane 2, rigid pavement test section . .	145
A33	Item 1, lane 2, rigid pavement test section, after 200 coverages by 240-kip twin-tandem assembly	146
A34	Item 1, lane 2, rigid pavement test section, after 1010 coverages by 240-kip twin-tandem assembly	146
A35	Surface deformation in item 1, lane 2, rigid test section .	147
A36	Item 2, lane 2, rigid pavement test section, prior to traffic	140
A37	Item 2, lane 2, rigid pavement test section after 200 coverages by 240-kip twin-tandem assembly	148
A38	Item 2, lane 2, rigid pavement test section, after 950 coverages by 240-kip twin-tandem assembly.	149
A39	Surface deformation in item 2, lane 2, rigid pavement test section	150
A40	Item 3, lane 2, rigid pavement test section, prior to traffic	151
A41	Item 3, lane 2, rigid pavement test section, after 200 coverages by 240-kip twin-tandem assembly	151
A42	Item 3, lane 2, rigid pavement test section, after 1200 coverages by 240-kip twin-tandem assembly	152
A43	Surface deformation in item 3, lane 2, rigid pavement test section	153
A44	Item 4, lane 2, rigid pavement test section, prior to traffic	154
A45	Item 4, lane 2, rigid pavement test section, after 200 coverages by 240-kip twin-tandem assembly	154
A46	Item 4, lane 2, rigid pavement test section, after 950 coverages by 240-kip twin-tandem assembly	155
A47	Surface deformation in item 4, lane 2, rigid pavement test section	156
A48	Subitem 5a, lane 2, rigid pavement test section, after 200 coverages by 240-kip twin-tandem assembly	157
A49	Subitem 5a, lane 2, rigid pavement test section, after 950 coverages by 240-kip twin-tandem assembly	157

A50	Surface deformation in subitems 5a and b, lane 2, rigid pavement test section	158
A51	Subitem 5b, lane 2, rigid pavement test section, after 200 coverages by 240-kip twin-tandem assembly	159
A52	Subitem 5b, lane 2, rigid pavement test section, after 950 coverages by 240-kip twin-tandem assembly	159
A53	Subitem 5c, lane 2, rigid pavement test section, after 200 coverages by 240-kip twin-tandem assembly	160
A54	Subitem 5c, lane 2, rigid pavement test section, after 840 coverages by 240-kip twin-tandem assembly	160
A55	Surface deformation in subitems 5c and d, lane 2, rigid pavement test section	161
A56	Subitem 5d, lane 2, rigid pavement test section, after 200 coverages by 240-kip twin-tandem assembly	162
A57	Subitem 5d, lane 2, rigid pavement test section, after 350 coverages by 240-kip twin-tandem assembly	162
A58	Locations of test pits, observation pits, and cores in rigid pavement test section	163
A59	Plate bearing tests, item 1, lanes 1 and 2, rigid pavement test section	164
A60	Plate bearing tests, item 2, lanes 1 and 2, rigid pavement test section	165
A61	Plate bearing tests, items 3 and 4, lanes 1 and 2, rigid pavement test section	166
A62	Plate bearing tests, items 5a-c, lanes 1 and 2, rigid pavement test section	167
A63	Plate bearing tests, items 5c and d, lanes 1 and 2, rigid pavement test section	168
B1	Item 1, lane 1, flexible pavement test section, prior to traffic	189
B2	Cracking in western quarter of item 1, lane 1, flexible pavement test section, at 2500 coverages of 200-kip twin-tandem assembly	189
B3	Cracking in eastern three-fourths of item 1, lane 1, flexible pavement test section, at 3660 coverages of 200-kip twin-tandem assembly	190
B4	Item 2, lane 1, flexible pavement test section, prior to traffic	190
B5	Cracking at instrumentation grid in item 2, lane 1, flexible pavement test section, at 2500 coverages of 200-kip twin-tandem assembly	191
B6	Item 2, lane 1, flexible pavement test section, at 3660 coverages of 200-kip twin-tandem assembly	191
B7	Item 3, lane 1, flexible pavement test section prior to traffic	192
B8	Item 3, lane 1, flexible pavement test section, when traffic was terminated after 7820 coverages of 200-kip twin-tandem assembly	192
B9	Item 4, lane 1, flexible pavement test section, prior to traffic	193

B10	Cracking in item 4, lane 1, flexible pavement test section, after 1200 coverages of 200-kip twin-tandem assembly	193
B11	Item 4, lane 1, flexible pavement test section, at 1380 coverages of 200-kip twin-tandem assembly	194
B12	Item 5, lane 1, flexible pavement test section, prior to traffic	194
B13	Cracking in item 5, lane 1, flexible pavement test section, after 1200 coverages of 200-kip twin-tandem assembly	195
B14	Item 5, lane 1, flexible pavement test section, at 2500 coverages of 200-kip twin-tandem assembly	195
B15	Deflections measured transverse to direction of traffic in items 1 and 2, lane 1, flexible pavement test section . . .	196
B16	Deflections measured transverse to direction of traffic in items 3 and 4, lane 1, flexible pavement test section . .	197
B17	Deflections measured transverse to direction of traffic in item 5, flexible pavement test section	198
B18	Surface deformation in item 1, lane 1, flexible pavement test section	199
B19	Surface deformation in item 2, lane 1, flexible pavement test section	200
B20	Surface deformation in item 3, lane 1, flexible pavement test section	201
B21	Surface deformation in item 4, lane 1, flexible pavement test section	202
B22	Surface deformation in item 5, lane 1, flexible pavement test section	203
B23	Test pit profile of item 1, lane 1, flexible pavement test section. Station 0+26.5 after 3660 coverages of 200-kip twin-tandem assembly	204
B24	Test pit profile of item 2, lane 1, flexible pavement test section. Station 0+65 after 3660 coverages of 200-kip twin-tandem assembly	205
B25	Test pit profile of item 3, lane 1, flexible pavement test section. Station 1+04 after 7820 coverages of 200-kip twin-tandem assembly	206
B26	Test pit profile of item 4, lane 1, flexible pavement test section. Station 1+27 after 1380 coverages of 200-kip twin-tandem assembly	207
B27	Test pit profile of item 5, lane 1, flexible pavement test section. Station 1+89 after 2500 coverages of 200-kip twin-tandem assembly	208
B28	Item 1, lane 2, flexible pavement test section, prior to traffic	209
B29	Cracking and deformation in item 1, lane 2, flexible pavement test section, after 600 coverages of 240-kip twin-tandem assembly	209
B30	Item 2, lane 2, flexible pavement test section, prior to traffic	210
B31	Item 2, lane 2, flexible pavement test section, after 320 coverages of 240-kip twin-tandem assembly	210

B32	Item 3, lane 2, flexible pavement test section, prior to traffic	211
B33	Deformation in item 3, lane 2, flexible pavement test section, at failure after 620 coverages of 240-kip twin-tandem assembly	211
B34	Item 4, lane 2, flexible pavement test section, prior to traffic	212
B35	Cracking and deformation in item 4, lane 2, flexible pavement test section, at failure after 120 coverages of 240-kip twin-tandem assembly	212
B36	Item 5, lane 2, flexible pavement test section, prior to traffic	213
B37	Cracking and deformation in item 5, lane 2, flexible pavement test section, at failure after 340 coverages of 240-kip twin-tandem assembly	213
B38	Deflections measured transverse to direction of traffic in items 1 and 2, lane 2, flexible pavement test section . . .	214
B39	Deflections measured transverse to direction of traffic in items 3 and 4, lane 2, flexible pavement test section . . .	215
B40	Deflections measured transverse to direction of traffic in item 5, lane 2, flexible pavement test section	216
B41	Surface deformation in item 1, lane 2, flexible pavement test section	217
B42	Surface deformation in item 2, lane 2, flexible pavement test section	218
B43	Surface deformation in item 3, lane 2, flexible pavement test section	219
B44	Surface deformation in item 4, lane 2, flexible pavement test section	220
B45	Surface deformation in item 5, lane 2, flexible pavement test section	221
B46	Test pit profile of item 1, lane 2, flexible pavement test section. Station 0+28 after 600 coverages of 240-kip twin-tandem assembly	222
B47	Test pit profile of item 2, lane 2, flexible pavement test section. Station 0+56 after 320 coverages of 240-kip twin-tandem assembly	223
B48	Test pit profile of item 3, lane 2, flexible pavement test section. Station 1+05 after 620 coverages of 240-kip twin-tandem assembly	224
B49	Test pit profile of item 4, lane 2, flexible pavement test section. Station 1+55 after 120 coverages of 240-kip twin-tandem assembly	225
B50	Test pit profile of item 5, lane 2, flexible pavement test section. Station 1+88 after 340 coverages of 240-kip twin-tandem assembly	226
B51	Subitem 4a, lane 3, flexible pavement test section, prior to traffic	227
B52	Cracking in subitem 4a, lane 3, flexible pavement test section, after 80 coverages of 50-kip single-wheel assembly	227

B53	Subitem 4b, lane 3, flexible pavement test section, prior to traffic	228
B54	Cracking and deformation in subitem 4b, lane 3, flexible pavement test section, at failure after 170 coverages of 50-kip single-wheel assembly	228
B55	Subitem 4c, lane 3, flexible pavement test section, prior to traffic	229
B56	Cracking in subitem 4c, lane 3, flexible pavement test section, at failure after 240 coverages of 50-kip single-wheel assembly	229
B57	Subitem 4d, lane 3, flexible pavement test section, prior to traffic	230
B58	Cracking in subitem 4d, lane 3, flexible pavement test section, at 170 coverages of 50-kip single-wheel assembly	230
B59	Cracking in subitem 4d, lane 3, flexible pavement test section, at failure after 240 coverages of 50-kip single-wheel assembly	231
B60	Subitem 5a, lane 3, flexible pavement test section, prior to traffic	231
B61	Cracking in subitem 5a, lane 3, flexible pavement test section, at failure after 240 coverages of 50-kip single-wheel assembly	232
B62	Subitem 5b, lane 3, flexible pavement test section, prior to traffic	232
B63	Subitem 5b, lane 3, flexible pavement test section, at failure after 240 coverages of 50-kip single-wheel assembly	233
B64	Subitem 5c, lane 3, flexible pavement test section, prior to traffic	233
B65	Cracking in subitem 5c, lane 3, flexible pavement test section, at failure after 240 coverages of 50-kip single-wheel assembly	234
B66	Subitem 5d, lane 3, flexible pavement test section, prior to traffic	234
B67	Cracking in subitem 5d, lane 3, flexible pavement test section, at failure after 240 coverages	235
B68	Deflections measured transverse to direction of traffic in subitems 4a and b, lane 3, flexible pavement test section	236
B69	Deflections measured transverse to direction of traffic in subitems 4c and d, lane 3, flexible pavement test section	237
B70	Deflections measured transverse to direction of traffic in subitems 5a and b, lane 3, flexible pavement test section	238
B71	Deflections measured transverse to direction of traffic in subitems 5c and d, lane 3, flexible pavement test section	239
B72	Surface deformation in subitems 4a-d, lane 3, flexible pavement test section	240
B73	Surface deformation in subitems 5a-d, lane 3, flexible pavement test section	241
B74	Test pit profile of subitem 4a, lane 3, flexible pavement test section. Station 1+25 after 240 coverages of 50-kip single-wheel assembly	242

B75	Test pit profile of subitem 5c, lane 3, flexible pavement test section. Station 1+85 after 240 coverages of 50-kip single-wheel assembly	243
B76	Test pit profile of subitem 4c, lane 3, flexible pavement test section. Station 1+45 after 240 coverages of 50-kip single-wheel assembly	244
B77	Test pit profile of subitem 5a, lane 3, flexible pavement test section. Station 1+65 after 240 coverages of 50-kip single-wheel assembly	245
B78	Cracks in polystyrene panels in subitem 4a, lane 3, flexible pavement test section, after traffic	246
B79	Cracks in polystyrene panels in subitem 4b, lane 3, flexible pavement test section, after traffic	247
B80	Cracks in lightweight concrete in subitems 4d and 5a, lane 3, flexible pavement test section, after 170 coverages of 50-kip load	247
B81	Surface of polystyrene panels in subitem 5c, lane 3, flexible pavement test section, after traffic	248
B82	Surface of polystyrene panels in subitem 5d, lane 3, flexible pavement test section, after traffic	248
B83	Vertical wall of test pit where samples were obtained to determine cement content of cement-stabilized soil layer . .	249
B84	Locations of observation trenches for cement content determinations	250
B85	Cement content versus depth. Samples from cement-stabilized lean clay base course, item 2, flexible pavement test section	251

CONVERSION FACTORS, U. S. CUSTOMARY TO METRIC (SI)
UNITS OF MEASUREMENT

U. S. customary units of measurement used in this report can be converted to metric (SI) units as follows:

<u>Multiply</u>	<u>By</u>	<u>To Obtain</u>
mils	0.0254	millimeters
inches	2.54	centimeters
feet	0.3048	meters
miles (U. S. statute)	1.609344	kilometers
feet per second	0.3048	meters per second
square inches	6.4516	square centimeters
square feet	0.092903	square meters
square yards	0.8361273	square meters
cubic yards	0.7645548	cubic meters
gallons (U. S. liquid)	3.785412	cubic decimeters
pounds	0.45359237	kilograms
kip	0.45359237	metric tons
tons	0.90718474	metric tons
pounds per square inch	0.6894757	newtons per square centimeter
pounds per cubic inch	0.027679911	kilograms per cubic centimeter
pounds per cubic foot	16.018489	kilograms per cubic meter
Fahrenheit degrees	5/9	Celsius or Kelvin degrees*

* To obtain Celsius (C) temperature readings from Fahrenheit (F) readings, use the following formula: $C = (5/9)(F - 32)$. To obtain Kelvin (K) readings, use: $K = (5/9)(F - 32) + 273.15$.

INTRODUCTION

BACKGROUND

In the past few years, new concepts have been developed involving the use of new construction techniques and materials in road and airfield pavements. The membrane-enveloped soil layer (MESL) concept, for example, involves using a membrane-enveloped, highly compacted, fine-grained soil as a structural layer in pavement systems. Innovations in regions where frost action is a continuing problem have included using prefabricated polystyrene panels and polystyrene bead concrete as insulating layers to reduce frost penetration. Extensive investigations have been conducted into using normally unsatisfactory soils in pavement structures by upgrading the quality of the materials through chemical stabilization. Much interest has also been generated in the use of fibrous-reinforced concrete pavements.

Various military and civilian agencies of the Federal Government have recognized the need for a full evaluation of these new concepts and for the development of design and construction criteria for their use in pavements. In early 1972, the U. S. Army Engineer Waterways Experiment Station (WES) had under consideration several investigational programs of this type proposed under separate sponsorships. Recognizing the mutual interest of the various agencies, WES began a comprehensive field and laboratory pavement investigation program that incorporated the objectives of all of the various sponsors.

OBJECTIVES

The objectives of this investigation were to evaluate the performance of several types of pavements that incorporated a MESL, insulating materials, chemically stabilized soil layers employing a range of soil types, and fibrous-reinforced concrete, portland cement concrete, and asphaltic concrete as structural elements and to develop criteria from the performance data for use of the materials in the design, evaluation, and construction of airfield pavements.

SCOPE

The objectives of the study were accomplished by the following:

- a. Design, construction, and traffic testing of full-scale test sections.
- b. Field and laboratory tests for classification and structural characterization of the materials used in the test sections.
- c. Instrumentation of the field test sections and measurements of deflection, strain, and pressure resulting from applied static and dynamic (slowly moving) single- and multiple-wheel loads.
- d. Analysis of test data based on material properties and performance data.
- e. Development of design and construction criteria.

This volume of the report describes the design, construction, and behavior under traffic of the full-scale test sections. The response of pavement to static and dynamic loads and design and construction criteria will be reported in subsequent volumes. .

DESIGN OF TEST SECTIONS

Two full-scale pavement test sections, one rigid and one flexible, were designed and constructed during the period March-August 1972. The test sections were designed to obtain comparative performance data for pavement structures incorporating a MESL, chemically stabilized layers for a range of soil types, insulating materials, and various types of pavement surfacing including fibrous-reinforced concrete, plain portland cement concrete, and asphaltic concrete. Descriptions of the design procedures and materials used in the test sections are given in the following paragraphs.

RIGID PAVEMENT TEST SECTION

DESIGN

A layout of the rigid pavement test section is shown in Figure 1. The test section was 290 ft long* and 50 ft wide and consisted of five test items, each 50 ft square and separated from the adjacent item(s) by 10-ft-wide transition zones. The initial thickness designs for the five rigid pavement test items were based on a 90-day flexural strength of 700 psi and a requirement that the items carry 1000 to 3000 coverages of a 240-kip twin-tandem gear having tires with a 44- by 58-in. spacing (B-747 configuration). Thicknesses of the pavement structures for items 1-4 were based on the following modulus of soil reaction k values for the various materials:

- a. Item 1. $k = 300$ pci at the surface of the MESL.
- b. Item 2. $k = 500$ pci at the surface of the clay gravel stabilized with portland cement.
- c. Item 3. $k = 300$ pci at the surface of the bituminous base course.
- d. Item 4. $k = 300$ pci at the surface of the lean clay stabilized with portland cement.

The thicknesses of the fibrous-reinforced concrete used in items 1 and 2

* A table of factors for converting U. S. customary units of measurement to metric (SI) units is presented on page 13.

were determined using a 2 to 1 equivalency factor from previous testing.¹ Item 5 was designed to study the structural behavior of pavement structures that incorporate polystyrene panels and a lightweight concrete, which are being considered for use as insulating materials in such structures. The item was divided equally into four subitems reducing the slab size to 12.5 ft square. (Theoretically, the reduction in slab size should not affect performance.) Subitem 5a was included to study the effect of placement of a stabilized layer between a concrete slab and polystyrene panels. Subitems 5b-d provided direct comparisons of the behavior of two different strengths of polystyrene panel and a lightweight concrete.

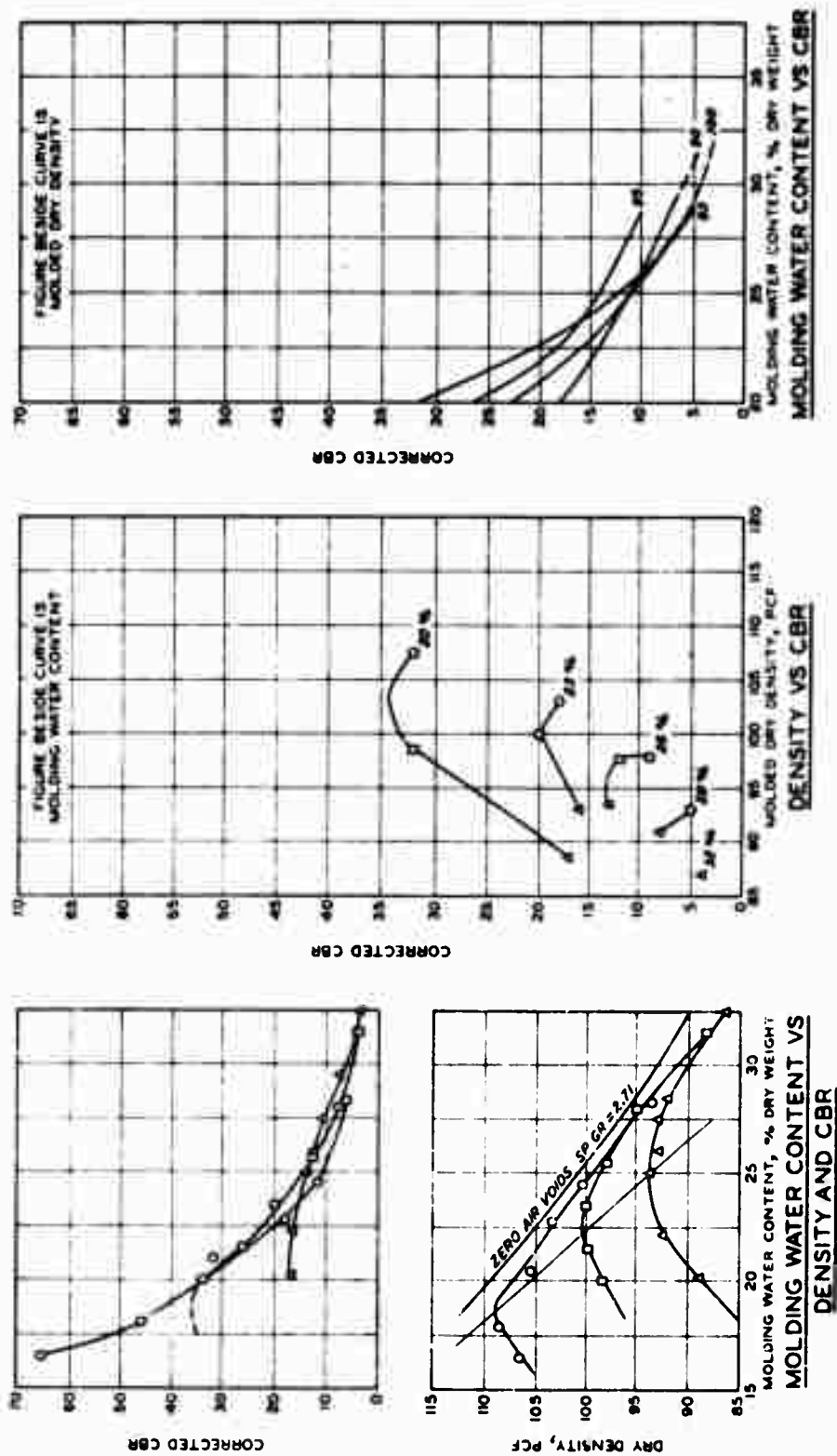
SUBGRADE

The top 3 ft of subgrade under the rigid pavement items was a processed 4-CBR heavy clay (CH, E-11) material* having a liquid limit (LL) of 73 and a plasticity index (PI) of 48. Laboratory CBR, density, and water content data for the heavy clay subgrade material are shown in Figure 2. Underlying the heavy clay to a depth of approximately 12 ft below the pavement surface was a processed lean clay (CL, E-7) soil having a LL of 43 and PI of 21. Both the lean and the heavy clay material had been previously placed in construction of the controlled strength subgrade for the multiple-wheel heavy hear load (MWHGL) tests conducted at WES in 1969.⁵ Below the processed lean clay was an identical clay in an undisturbed condition. Gradations and classification data for the heavy and lean clay materials are shown in Figure 3.

BASE COURSES

Item 1. The base course for item 1 consisted of a 20-in.-thick MESL. The soil used in the MESL was the same as the lean clay (CL, E-7) material described above for the subgrade. Laboratory compaction data for the lean clay soil are shown in Figure 4. Previous experience in

* Throughout this report, the first soil classification designation in parentheses indicates the classification according to the Unified Soil Classification System.² The second designation indicates the Federal Aviation Administration (FAA) soil classification.³



LEGEND	
COMPACTION EFFORT	NO. OF BLOWS PER LAYER
4	12
12	26
26	55
55	

Figure 2. CBR, density, and water content data for heavy clay subgrade material (tested as molded)

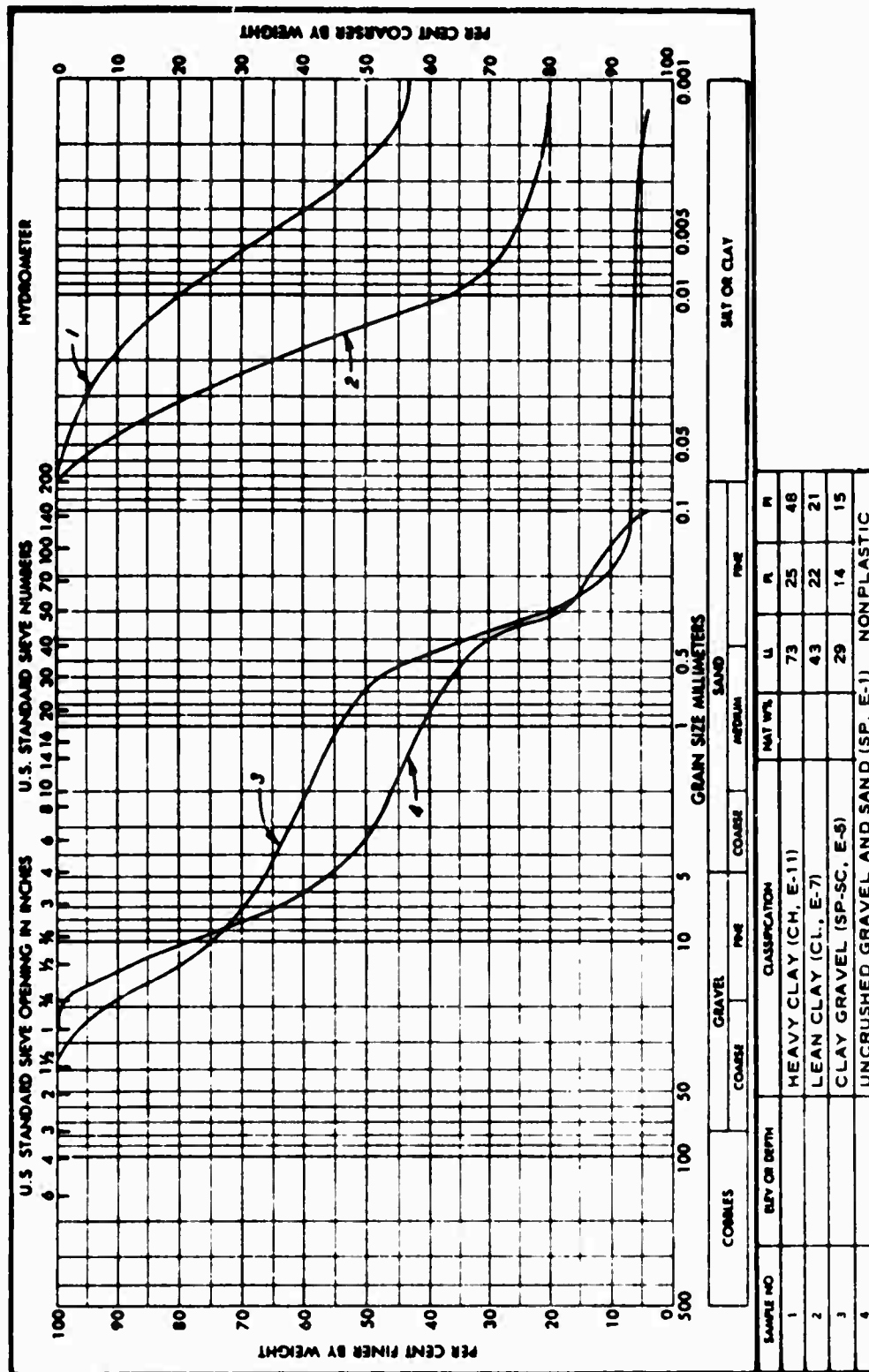


Figure 3. Gradations and classification data for subgrade materials

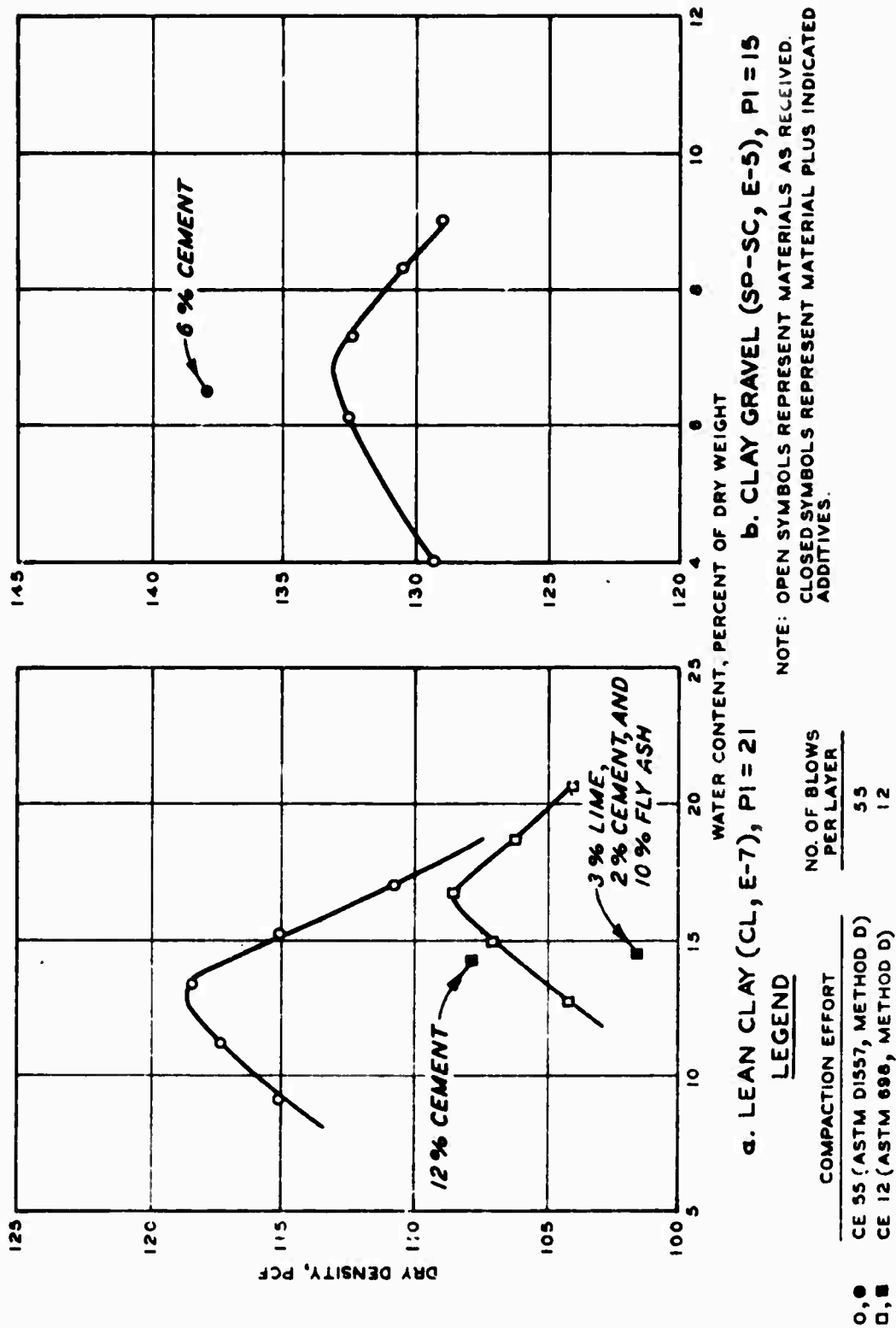


Figure 4. Laboratory compaction data for lean clay and clay gravel materials

compacting cohesive fine-grained soils of this type over low-strength subgrades (such as the heavy clay, 4-CBR material) has demonstrated that densities in excess of the laboratory Corps of Engineers (CE) 12 compaction effort⁶ (equivalent to American Society for Testing and Materials (ASTM) Designation: D 698-70,⁷ Method D) are very difficult to obtain in the field. Therefore, for the MESL base, it was desired to compact the soil in the field at a water content of about 15 percent (about 2 percent drier than CE 12 optimum) to approximately the equivalent of the CE 12 maximum density.

Item 2. The base course for item 2 consisted of a 17-in.-thick clay gravel (SP-SC, E-5) stabilized with portland cement. Classification data and gradation of the clay gravel material are shown in Figure 3, and laboratory compaction data are shown in Figure 4. A cement content of 6 percent by dry weight of soil was selected for stabilizing the material.

Item 3. A 6-in.-thick bituminous base course was used in item 3. The paving mixture consisted of 3/4-in. maximum-size uncrushed gravel and sand (SP, E-1) with 4.6 percent 85 to 100 penetration grade asphalt cement. The gradation of the aggregate is shown by Curve 4 in Figure 3.

Item 4. The base course for item 4 consisted of a 6-in.-thick, cement-stabilized layer of lean clay material with the same classification as that used for the MESL in item 1. The design cement content for stabilization of this soil was 12 percent.

Item 5. Test item 5, which was designed to study structural behavior of polystyrene panels and a lightweight (Styropor) concrete, was divided equally into subitems 5a-d. The insulating materials were to be placed between the heavy clay subgrade and the portland cement concrete surfacing with the exception of subitem 5a, in which a 6-in.-thick layer of cement-stabilized lean clay was to be placed over the polystyrene panels as indicated in Figure 1. The polystyrene panels were obtained from the Dow Chemical Company, Midland, Mich., and were identified as follows:

- a. Styrofoam HD-300: 3- by 16- by 108-in. panels with a minimum compressive strength of 120 psi (subitem 5c).

- b. Styrofoam SM: 3- by 24- by 48-in. panels with a minimum compressive strength of 35 psi (subitems 5a and d).

The mix proportions for the base course in subitem 5b were as follows:

<u>Component</u>	<u>Amount per Cubic Foot of Mix ft</u>
Preformed Styropor beads	1.10
HydrEpoxy A	0.23
HydrEpoxy B	0.23
Water	11.80
Concrete sand	3.00
Cement	<u>29.40</u>
	45.76

The mix design and the preformed Styropor beads and HydrEpoxy materials were furnished by BASF Wyandotte Corporation, Parsippany, N. J.

SURFACINGS

Fibrous-Reinforced Concrete. A mix design for the fibrous-reinforced concrete used to surface items 1 and 2 was prepared in the Concrete Laboratory at WES. Three different types of fibers were used in the concrete for these two items. Round fibers, 0.016 in. in diameter and 1 in. long, manufactured by Atlantic Wire Company, Branford, Conn., were used in item 1. Deformed fibers, 3/4 in. long, formed from 0.016-in.-diam wire were used in the north slab of item 2. Flat fibers, 0.10 by 0.14 in. in cross section and 3.4 in. long, were used in the south slab of item 2. All fibers used in item 2 were manufactured by National Standard Company, Niles, Mich. The coarse aggregate consisted of a 3/8-in. maximum-size chert pea gravel, and the fine aggregate was a natural sand. The cement was Dundee type 1P. This cement contained about 17 percent fly ash. The desired properties of the plastic concrete were for a slump of 2 to 4 in. and an air content of 4 to 6 percent. Trial mixes resulted in the following proportions:

<u>Component</u>	<u>Amount per Cubic-Yard Batch lb</u>
Coarse aggregate	728
Fine aggregate	1700
Wire fibers	250
Water	350
Cement	846
Air-entraining admixture	<u>--</u>
	3874

Portland Cement Concrete. Based on the following proportioning developed by laboratory mix design and using locally available gravel aggregates, concrete flexural strengths of 650 and 700 psi at 28 and 90 days, respectively, are reasonable. A 28-day strength of 650 psi was used for construction control. The mixture proportions were as follows:

<u>Component</u>	<u>Amount per Cubic-Yard Batch lb</u>
Type I cement (Federal Specification SS-C-192G ⁸)	611
Fine aggregate (minus 3/8-in. natural sand)	984
Coarse aggregate (1-1/2-in. maximum-size chert pea gravel)	2052
Water	231
Air-entraining admixture	<u>--</u>
	3878

The amount of air-entraining admixture required was considered to be the amount necessary to produce a 3 to 6 percent air content by volume of the concrete. The amount of water added was adjusted as necessary to maintain a slump of 3-1/2 in. or less.

JOINTS

Details of the design for the longitudinal construction joints

of the various items are shown in Figure 5. Based on results of the MWHGL study⁵ and a study of strengthening of keyed longitudinal construction joints in rigid pavements,⁹ keyed-and-tied joint design was selected for the 7-in.-thick fibrous-reinforced concrete surfacing in item 1 and for the plain portland cement concrete surfacing in items 3-5. For the 4-in.-thick fibrous-reinforced concrete surfacing in item 2, a thickened-edge butt joint was used. Details of the transverse construction joints are shown in Figure 6.

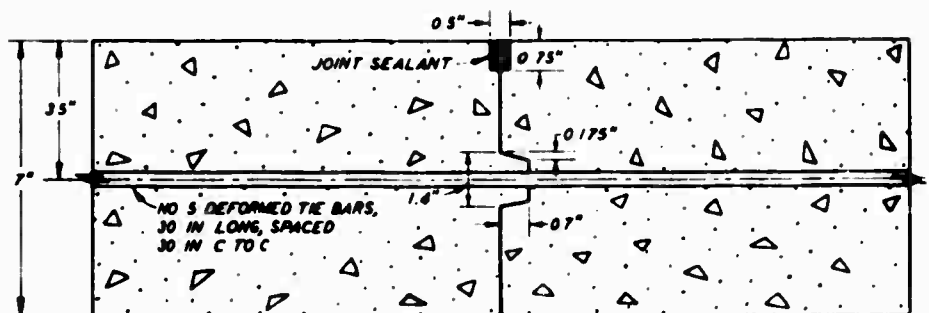
FLEXIBLE PAVEMENT TEST SECTION

LAYOUT

A layout of the flexible pavement test section is shown in Figure 7. The entire test section was surfaced with a 3-in.-thick layer of asphaltic concrete. The basic test section was 200 ft long by 40 ft wide and consisted of five test items, each 40 ft long by 40 ft wide, with foundations that included several types of chemically stabilized soil plus a conventional test item with unbound granular base and subbase materials (item 5). An additional 10-ft section was provided along the north side of test items 4 and 5 for the evaluation of the insulating materials being considered. This area was divided into 10-ft-square subitems designated 4a-d and 5a-d. A profile showing the type and location of the various insulating materials in the structure is shown in Figure 8.

DESIGN

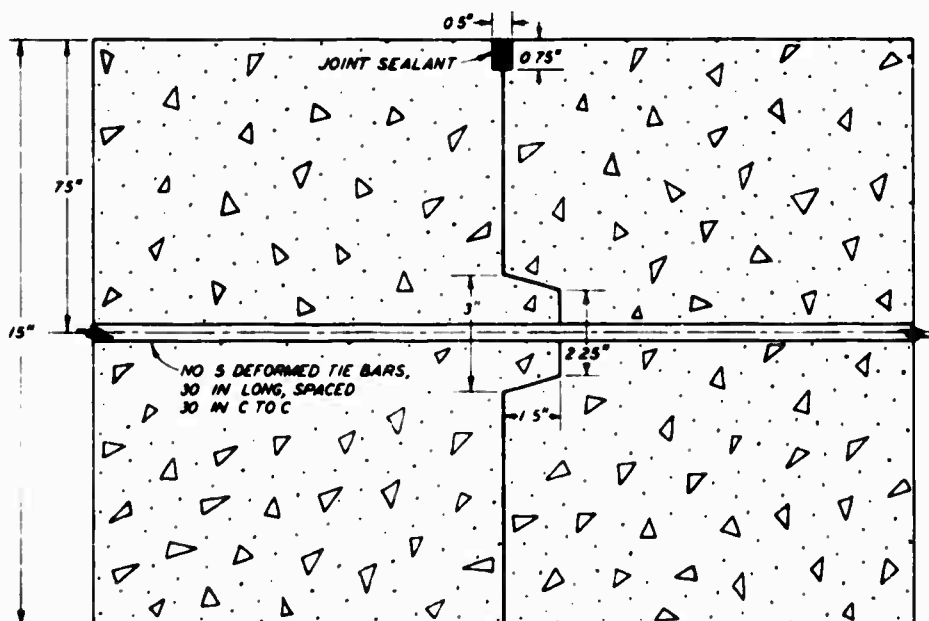
Stabilized and Conventional Structures. The thicknesses of the pavement structures for flexible pavement items 1-4 (Figure 7) were determined by the use of equivalency factors that were from an analysis of results of previous studies.¹⁰⁻¹² As was the case with the rigid pavement test section, the initial design loading was for a 240-kip twin-tandem assembly, and the assumed traffic level was on the order of 1000 to 3000 coverages. The subgrade was assumed to have a strength of 4 CBR. Item 5 of the flexible pavement test section was a conventional pavement structure and was identical with item 5 of the original MWHGL



ITEM 1, KEYED-AND-TIED JOINT



ITEM 2, THICKENED-EDGE JOINT



ITEMS 3, 4, AND 5
KEYED-AND-TIED JOINT

Figure 5. Details of longitudinal construction joints in the rigid pavement test section

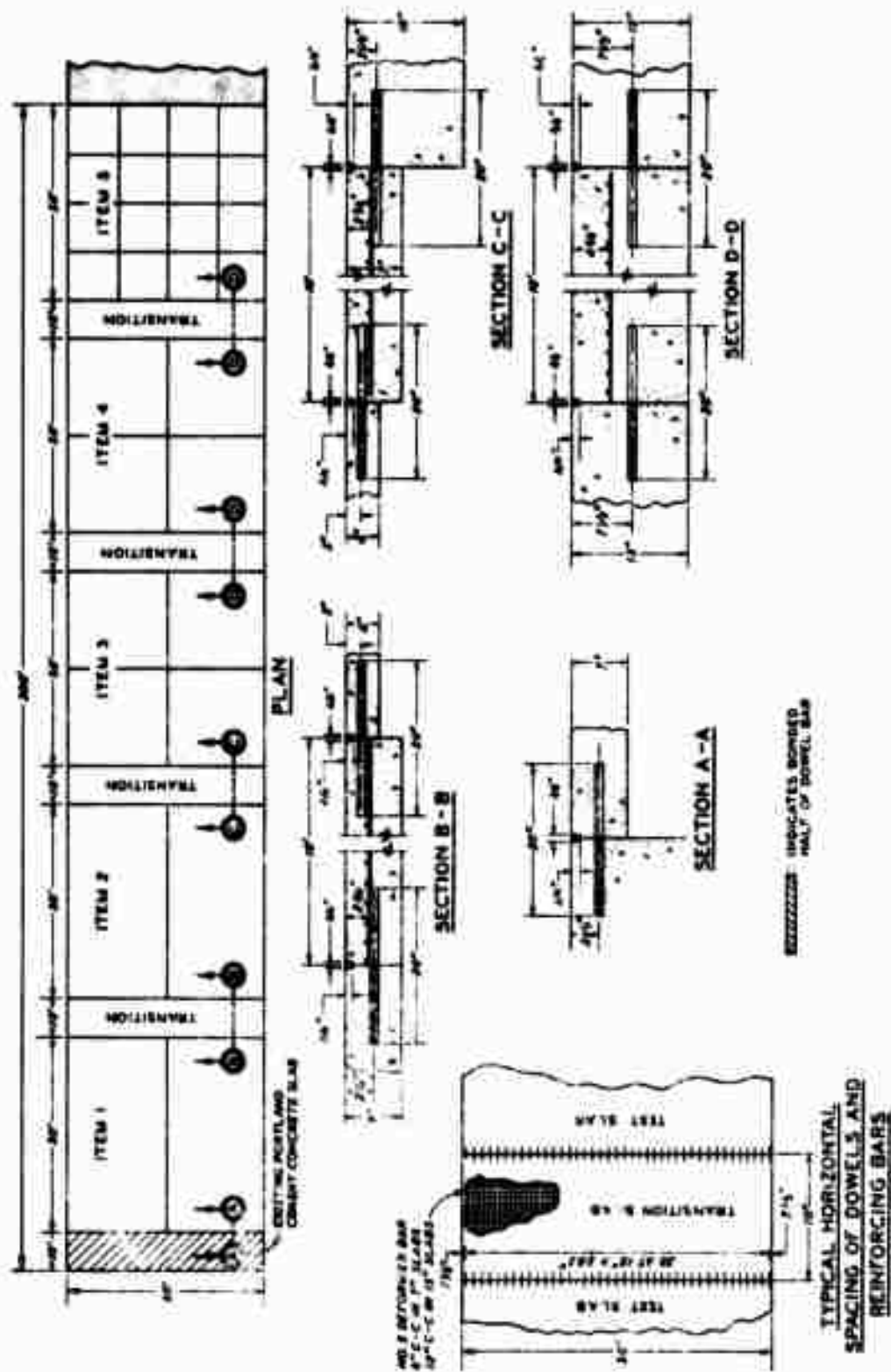
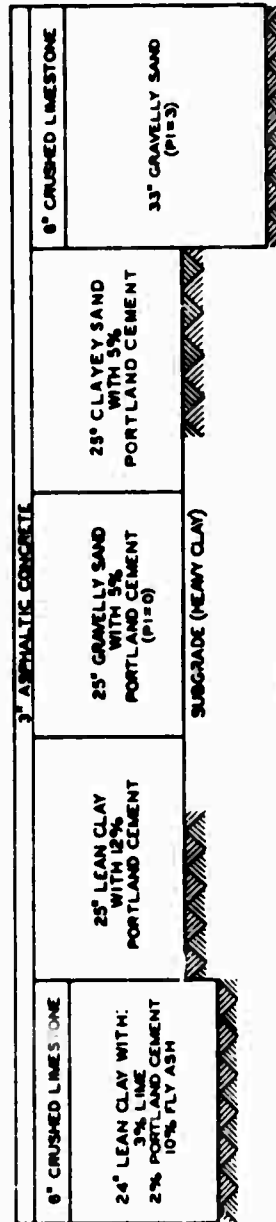
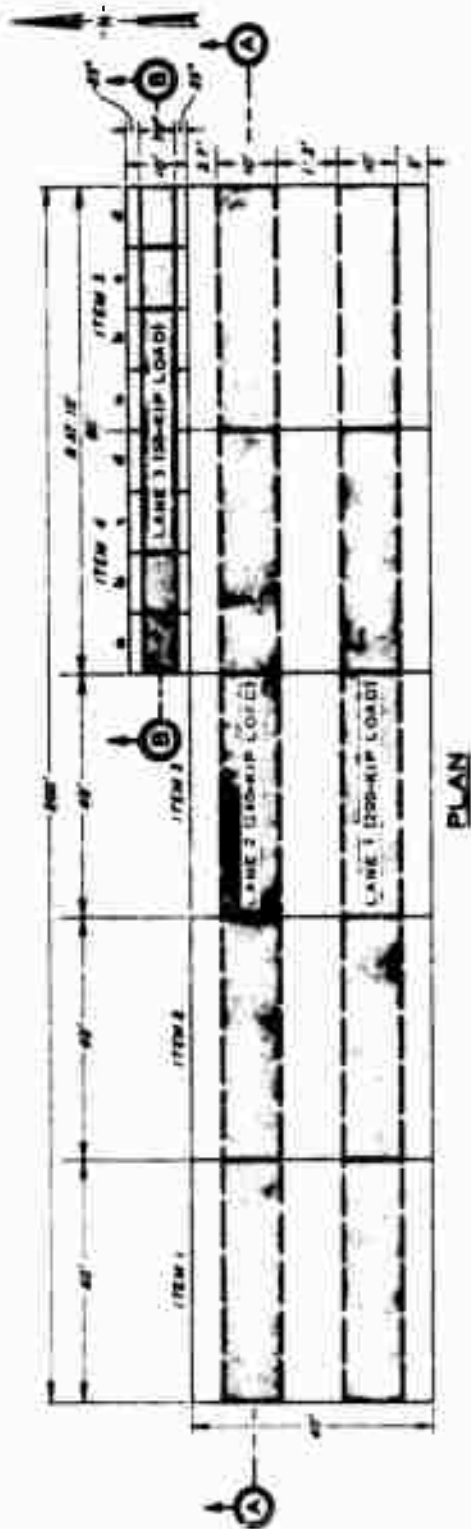


Figure 6 Details of transverse construction joints in the rigid pavement test section



NOTE: SEE FIGURE 8 FOR SECTION B - B.

Figure 7. Layout of the flexible pavement test section

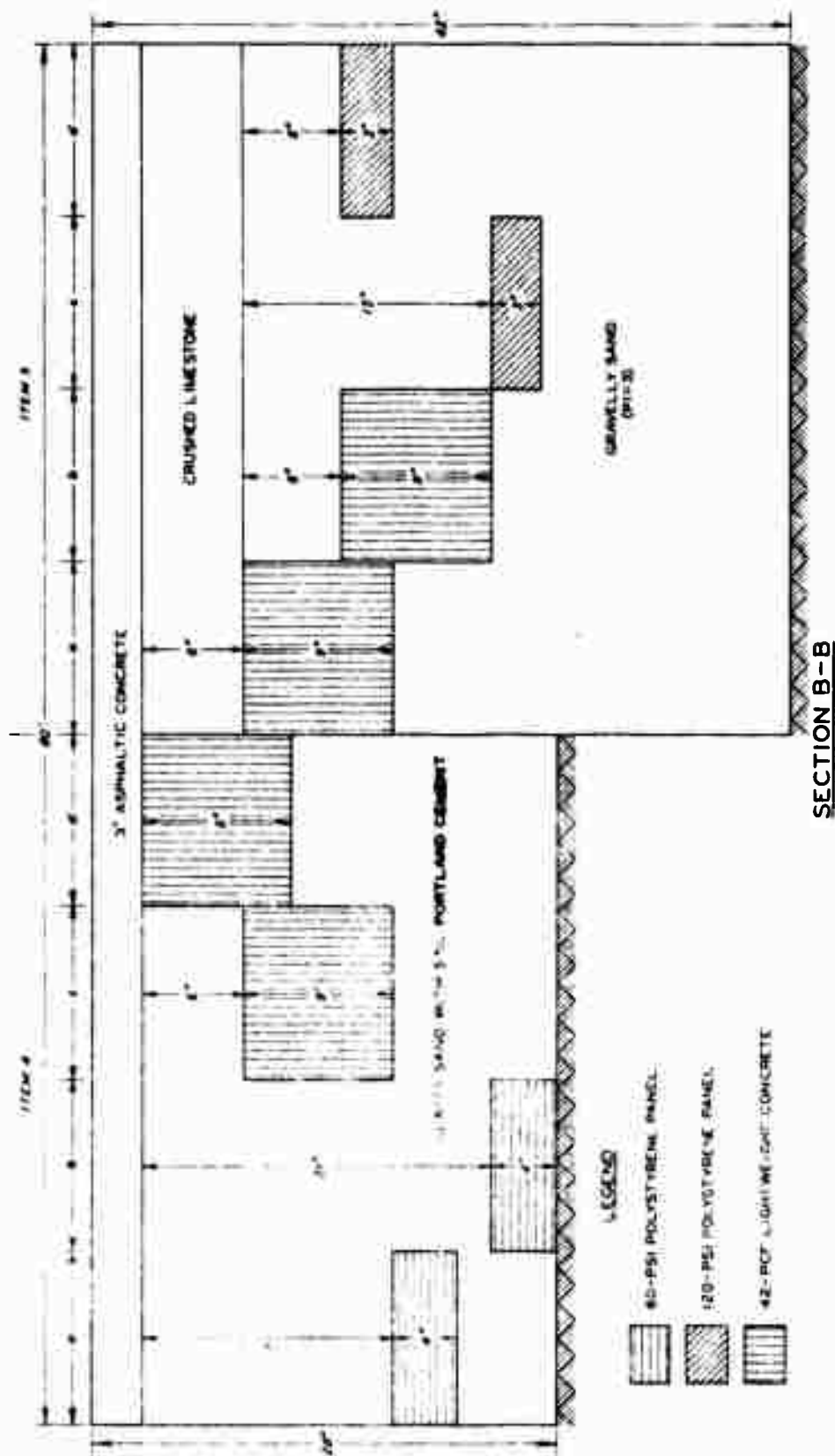


Figure 8. Profiles of items in the flexible pavement test section with insulating materials

flexible pavement test section,⁵ with the exception that a low-plasticity subbase material (PI = 3) was used in lieu of the cohesionless material (PI = 0) used in the MWHGL test section. The primary purpose of the item was to determine the effect of the subbase PI on the overall item performance.

Pavements Containing Insulating Material. In order to study the structural behavior of insulating materials in both a conventional pavement system and a pavement system having a stabilized layer, sub-items 4a-d and 5a-d were incorporated in the flexible pavement test section. Insulating materials included 60- and 120-psi polystyrene panels and a 42-pcf lightweight concrete. The polystyrene panels were obtained from the Dow Chemical Company and were identified as follows:

- a. Styrofoam HI: 4- by 24- by 96-in. panels with a minimum compressive strength of 60 psi.
- b. Styrofoam HD-300: 3- by 16- by 108-in. panels with a minimum compressive strength of 120 psi.

The mixture proportions for the lightweight concrete were the same as those used in the rigid pavement test section. A significant factor in the design of these items involved determination of the depth at which to place the insulating materials. To be most effective as insulation, it is desirable to locate insulating material at as high an elevation in a pavement system as permissible. This was a consideration in the final positioning of the insulating materials in the flexible pavement test section. The highest permissible locations were estimated based on computed vertical stresses due to a 60-kip single-wheel load with a tire pressure of 250 psi (one tire of the twin-tandem design loading) and by using layer elastic theory employing estimated material properties for the test section. The strength values for the polystyrene panels were obtained from unconfined compression tests; flexural and compressive strength data for the lightweight concrete were obtained from the manufacturer.¹³

Two depths from the surface of the pavement were selected for each strength polystyrene. The surfaces of the 60-psi polystyrene (sub-items 4a and b) were located 18 and 24 in. below the pavement surface,

where the vertical stresses were computed to be 45 and 15 psi, respectively. The surfaces of the 120-psi polystyrene (subitems 5c and d) were located 24 and 15 in. below the pavement surface, where the vertical stresses were computed to be 36 and 80 psi, respectively. The lower depth from surface for each of the materials was selected so that there would be no chance of compressive failure of the insulation. The profiles of the test items with insulated layers are shown in Figure 8.

SUBGRADES

The top 3 ft of the subgrade for the flexible pavement test section was the same heavy clay, 4-CBR material as previously described for the rigid pavement test section. The heavy clay soil was underlain with processed and natural lean clay materials as described for the rigid pavement test section. This subgrade also was originally constructed for the MWHGL study.⁵

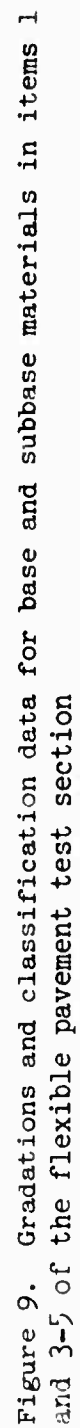
SUBBASES

Item 1. The subbase for item 1 consisted of a 24-in.-thick layer of lean clay (CL, E-7) soil (Figure 3) stabilized with a mixture of 3 percent hydrated lime, 2 percent portland cement, and 10 percent fly ash. The lime was type N, normal, hydrated, high-calcium lime meeting ASTM Specification C-207-49.¹⁴ The cement was type 1 normal portland cement of commercial grade conforming to Federal Specification SS-C-192G. The fly ash met the requirements of Federal Specification SS-P-570.¹⁵

Item 5. The subbase for test item 5 consisted of a 33-in.-thick layer of an unbound gravelly sand (SP-SC, E-1). Classification data and gradation of the gravelly sand are shown in Figure 9 (Curve 4). The material had a LL of 19 and a PI of 3. Laboratory compaction data are shown in Figure 10.

PASE COURSES

Items 1 and 5. The base course for items 1 and 5 consisted of a 6-in.-thick layer of unbound crushed limestone (SW-SM, E-1). Classification data and gradation of the material are shown in Figure 9.



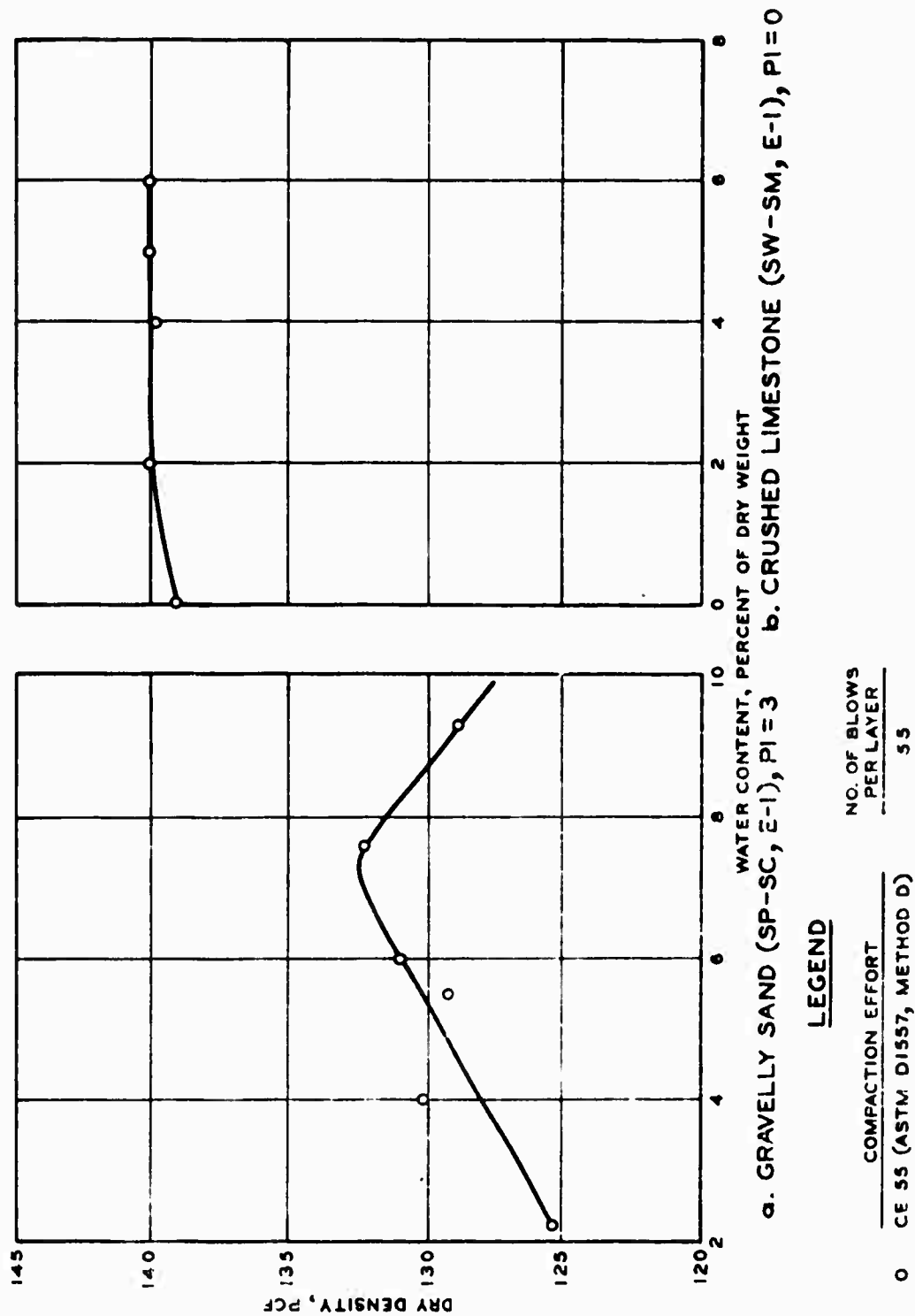


Figure 10. Laboratory compaction data for gravelly sand (PI = 3) and crushed limestone materials

Laboratory compaction data are shown in Figure 10. This crushed limestone met all requirement of CE Guide Specification CE-807.07¹⁶ and Item P-209 of FAA Advisory Circular AC 150/5370-1A.¹⁷

Item 2. The base course for item 2 consisted of a 25-in.-thick layer of lean clay material stabilized with 12 percent portland cement. The soil was the same as the material used for the stabilized subbases in flexible pavement item 1 and items 1 and 4 of the rigid pavement test section.

Item 3. The base course for item 3 consisted of a 25-in.-thick layer of gravelly sand (SP, E-1) material stabilized with 5 percent portland cement. Classification data and gradation of the gravelly sand are shown in Figure 9 (Curve 2). This soil was the same as the cohesionless gravelly sand used for the subbase in the original MWHGL test section. Laboratory compaction data for the material are shown in Figure 11.

Item 4. The base course for item 4 consisted of a 25-in.-thick layer of clayey sand stabilized with 5 percent portland cement. Classification data and gradation of the clayey sand material are shown in Figure 9 (Curve 3). The material had an LL of 34 and a PI of 21 and was classified as a clayey sand (SC, E-7). Laboratory compaction data for the clayey sand are shown in Figure 11.

ASPHALTIC CONCRETE SURFACING

The asphaltic concrete mixture used for the surface course layer over all flexible pavement items was obtained from a local contractor and was from a production quantity being used for a surface course on a local highway. The mixture consisted of a 1/2-in. maximum-size crushed gravel, natural sand, limestone mineral filler, and 85 to 100 penetration grade asphalt cement. A gradation curve for the aggregate and the CE¹⁶ and FAA¹⁷ specification limits are shown in Figure 12. A mix design using these aggregates was made in the Bituminous Laboratory at WES, and a design asphalt content of 3.9 percent was selected for the test section pavement.

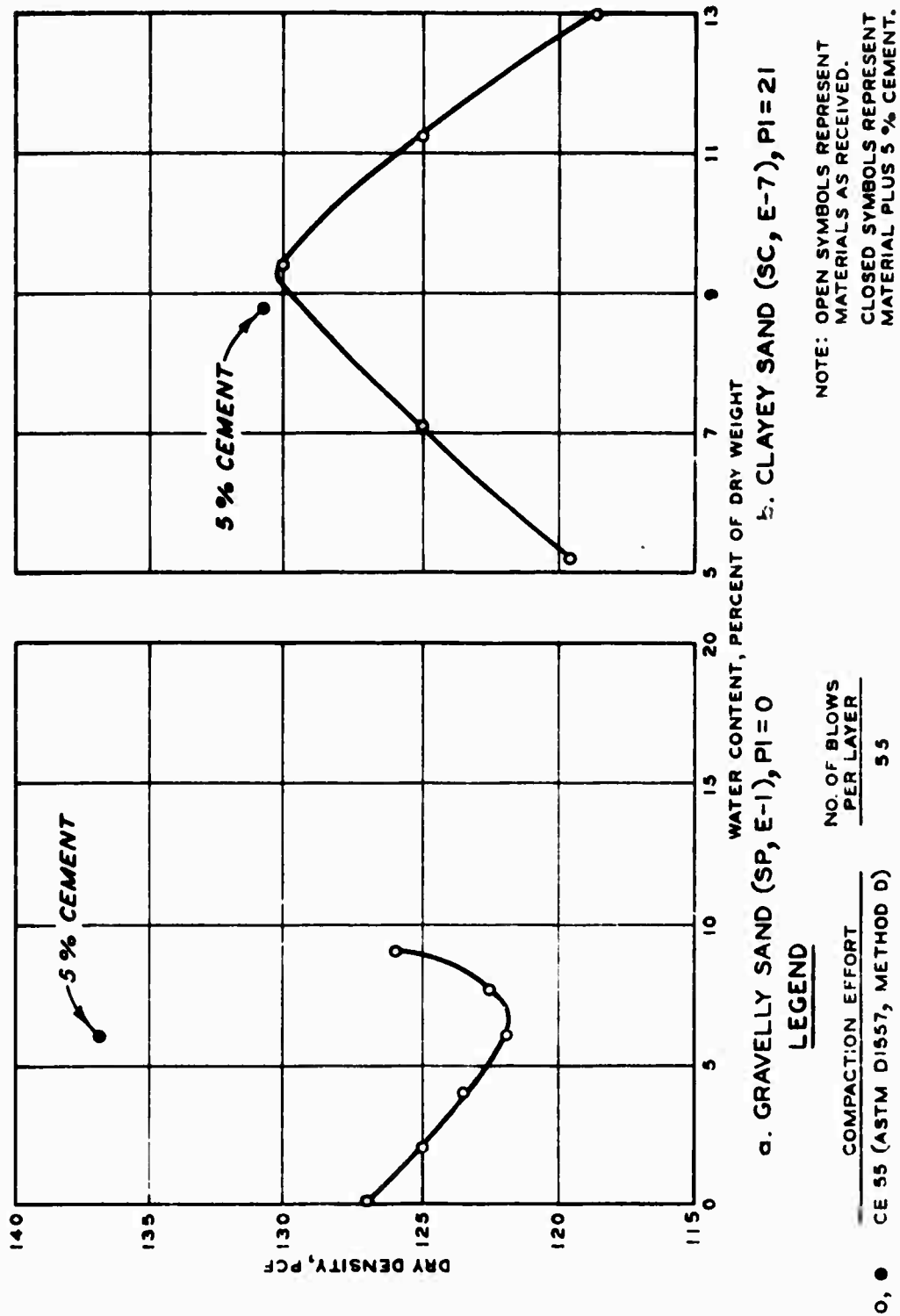


Figure 11. Laboratory compaction data for gravelly sand (PI = 0) and clayey sand materials

DESIGN CEMENT CONTENTS

The design cement contents used for stabilizing the various materials in both the rigid and flexible pavement test sections were based on procedures for estimating initial cement contents as indicated in the Portland Cement Association "Soil-Cement Laboratory Handbook."¹⁸ Based on the maximum laboratory dry density of the soil, one design cement content was selected. Test specimens were prepared in the laboratory for freeze-thaw and dynamic tests of the various soils containing the design cement content.

In preparation of the test specimens, the predetermined design percentages of stabilizing additives were mixed with the soil at the optimum water content as previously determined for the untreated soil. Eight duplicate specimens of each of the five soil-cement mixtures were prepared. Freeze-thaw tests were conducted on 35 specimens (7 specimens per mixture), 30 of which were subjected to the full test (12 cycles). Dynamic tests were conducted on 15 specimens (three specimens per mixture), 10 of which had been subjected to cycles of freezing and thawing.

The freeze-thaw tests were conducted in accordance with ASTM D 560-57.¹⁹ In these tests, three test specimens of each mixture were used to indicate volume change and water content; three other test specimens were used for determining soil-cement loss. One specimen from each mixture was tested for dynamic properties: (a) initially (before freezing and thawing); (b) after 6 cycles of freezing and thawing; and (c) after 12 cycles of freezing and thawing. The dynamic tests were conducted in accordance with ASTM D 2845-69.²⁰ The results of the freeze-thaw and dynamic tests are shown in Tables 1 and 2, respectively.

Laboratory maximum densities for the various soils treated with the design cement content are indicated in the compaction data plots, Figures 4 and 11. For the compaction tests, the stabilizing agents were mixed with the soil at the laboratory optimum water content for the untreated material, and then the treated soil was compacted with the indicated compaction effort. In Figure 4, it can be noted that the lime-cement-fly ash admixture resulted in a reduction in the maximum

Table 1

Summary of Results of Freeze-Thaw Tests on Laboratory Compacted Specimens of Stabilized Materials

Soil Classification	Test Section		Initial Soil Water Content Percent	Stabilizing Additive	Laboratory Compaction Effect	Laboratory Compaction Data			Maximum Volume Change Percent*	Maximum Water Content Percent*	Soil-Cement Loss Percent**
	Rigid Pavement	Flexible Pavement				Specimen No.	Welding Water Content Percent	Dry Density pcf			
Lean clay	4	2	17	12 percent portland cement	CE 12	1	14.2	107.3	+1.66	20.0	--
						2	14.3	106.7	--	--	29.6
						3	14.3	109.0	+1.66	19.0	--
						4	14.4	108.4	--	--	21.8
						5	14.5	108.7	+1.37	19.6	--
						6	14.5	107.2	--	--	33.3
Clayey sand	-	4	9.2	2 percent portland cement, 3 percent lime, 10 percent fly ash	CE 12	33	14.5	101.4	+0.71	23.8	--
						34	14.5	102.1	--	--	100+
						35	14.5	101.5	+0.66	24.4	--
						36	14.5	101.7	--	--	100+
						37	14.6	101.4	+0.66	23.2	--
						38	14.5	101.6	--	--	100+
						9	8.8	130.5	+0.43	9.4	--
						10	8.6	130.9	--	--	17.4
						11	8.6	130.9	-0.50	9.3	--
						12	8.7	130.7	--	--	13.7
Gravelly sand	-	3	6.0	5 percent portland cement	CE 55	13	9.1	130.2	-0.72	9.3	--
						14	9.0	130.7	--	--	15.2
						17	5.9	137.1	+2.38	5.3	--
						18	6.1	136.5	--	--	2.1
						19	5.4	136.7	+2.11	6.1	--
						20	6.1	136.5	--	--	1.4
Clay gravel	2	-	7.0	6 percent portland cement	CE 55	21	5.9	137.4	+2.11	5.2	--
						22	5.8	136.6	--	--	2.3
						25	6.0	138.4	-0.50	5.9	--
						26	6.4	137.8	--	--	1.7
						27	5.7	138.3	+0.50	6.1	--
						28	6.0	138.2	--	--	1.7
						29	6.6	137.2	-0.73	6.3	--
						30	6.2	138.2	--	--	1.6

* During freeze-thaw test (ASTM D 560-57).

** For 12 cycles of freezing and thawing.

+ Specimens were friable.

Table 2

Results of Dynamic Tests on Soil-Cement Specimens

Soil Identification	No.	Laboratory Compaction Data			No. of Freeze- Thaw Cycles	Dynamic Test Properties								Ratio of Shear to Compressive Velocity
		Molding Water Content Percent	Dry Density pcf			Compressive Velocity fps	Shear Velocity fps	Young's Modulus 10 ⁸ psi	Shear Modulus 10 ⁸ psi	Bulk Modulus 10 ⁸ psi	Poisson's Ratio	Lame's Constant 10 ⁷ psi		
Lean clay with 12 percent portland cement	7 8 1	14.5 14.5 14.2	107.6 107.9 107.3		0 6 12	6,077 6,146 --	3480 2049 --	0.51 0.21 --	0.20 0.07 --	0.35 0.55 --	0.26 0.44 --	2.13 5.01 --		0.58 0.33 --
Lean clay with 2 percent portland cement, 3 percent lime, 10 percent fly ash	39 40 23	14.5 14.6 14.5	101.4 101.0 101.4		0 6 12	4,846 -- --	2438 -- --	0.27 -- --	0.10 -- --	0.26 -- --	0.33 -- --	1.94 -- --		0.50 -- --
Clayey sand with 5 per- cent port- land cement	15 16 9	8.7 8.8 8.8	140.5 140.6 140.5		0 6 12	10,068 9,101 4,408	5931 5791 2950	1.67 1.48 0.33	0.68 0.64 0.15	1.04 0.72 0.035	0.23 0.16 0.09	5.96 2.99 0.35		0.59 0.64 0.67
Gravelly sand with 5 per- cent port- land cement	23 24 17	6.0 5.5 5.3	136.9 137.0 137.1		0 6 12	14,689 14,737 12,350	9093 8708 5982	3.82 3.60 1.76	1.60 1.46 0.65	2.05 2.24 1.91	0.19 0.23 0.35	9.78 12.6 14.7		0.62 0.59 0.48
Clay gravel with 6 per- cent port- land cement	31 32 25	6.9 6.5 6.0	137.5 137.6 138.4		0 6 12*	10,347 10,033 8,410	6716 5525 6165	2.03 1.55 1.26	0.89 0.60 0.71	0.93 1.18 0.34	0.14 0.28 -0.11	3.33 7.83 -1.3		0.65 0.55 0.74

* Entries indicate satisfactory results were not obtained.

* Satisfactory results were not obtained as indicated by a negative value for Poisson's ratio. Test values were apparently influenced by deficiencies in test specimens brought about by freezing and thawing.

density of the lean clay soil for the CE 12 (ASTM D 698-70) compaction effort, whereas the density of the same soil treated with 12 percent cement was about the same as the density of the untreated material. The addition of 6 percent cement to the clay gravel material (Figure 4) resulted in an increase in density. Likewise, addition of 5 percent cement to the gravelly sand material (Figure 11) resulted in a considerable increase in density. The addition of 5 percent cement to the clayey sand material (Figure 11) had very little effect on the maximum laboratory density.

INSTRUMENTATION OF TEST SECTIONS

Instrumentation was installed during construction of the flexible and rigid pavement test sections for the purpose of collecting response data under static and dynamic (slowly moving) traffic loadings. The response data were to be used not only in this investigation but also for future investigations and comparisons of the applicability of theoretical treatments to pavement design. Instruments for the measurement of vertical stresses, vertical deflections, vertical and horizontal strains, and temperatures were included in both test sections. Locations of the instrumentation are shown in Figures 13 and 14 for the flexible pavement test section and in Figure 15 for the rigid pavement test section. A brief description of the instrumentation is given in the following paragraphs; detailed descriptions can be found in Gray¹¹ and Ledbetter et al.²¹

DEFLECTION GAGES

In item 4 of the flexible pavement test section, vertical deflections were measured with a d-c linear variable differential transformer (LVDT) displacement transducer mounted within a WES deflection gage housing located at the center of the stabilized layer. The LVDT transducer produces d-c output voltages directly proportional to the movement of the sensing unit. The transducer consists of a main body (which houses the sensing coil and its associated electronics) and a core (which is movable) through the center of the sensing coil to transfer the mechanical movement of the core to record a change in an electrical signal in the soil. The LVDT transducer was mounted on a reference rod that extended to a reference flange located approximately 13 ft deep in the subgrade.

In item 4 of the rigid pavement test section, the main body of the gage was embedded in the concrete, and the core was mounted on a reference rod that was anchored 14 ft deep in the subgrade. This placement gave a measurement of the deflection of the pavement relative to the anchorage point of the reference rod.

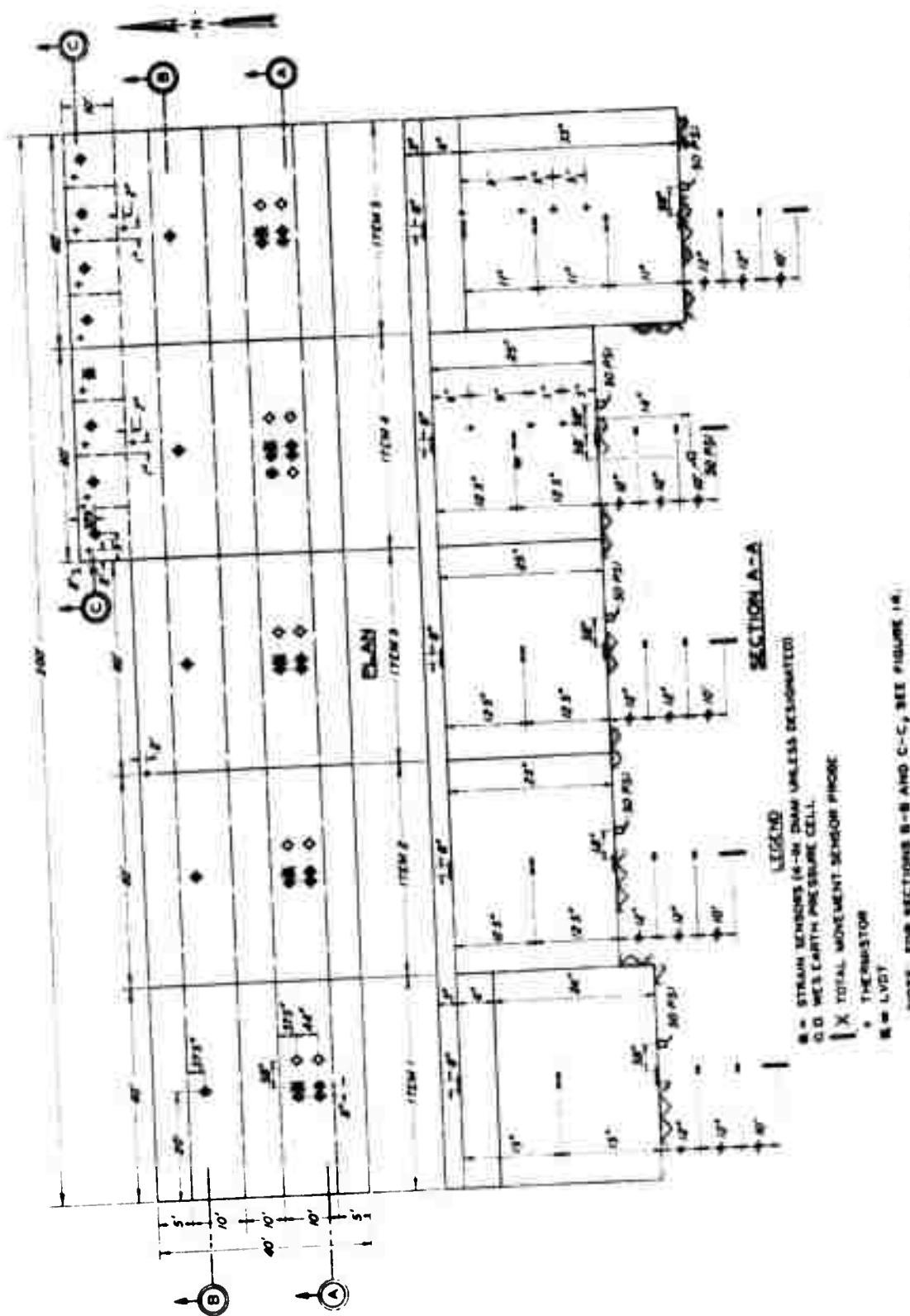


Figure 13. Instrumentation layout for flexible pavement test section (Plan view and Section A-A)

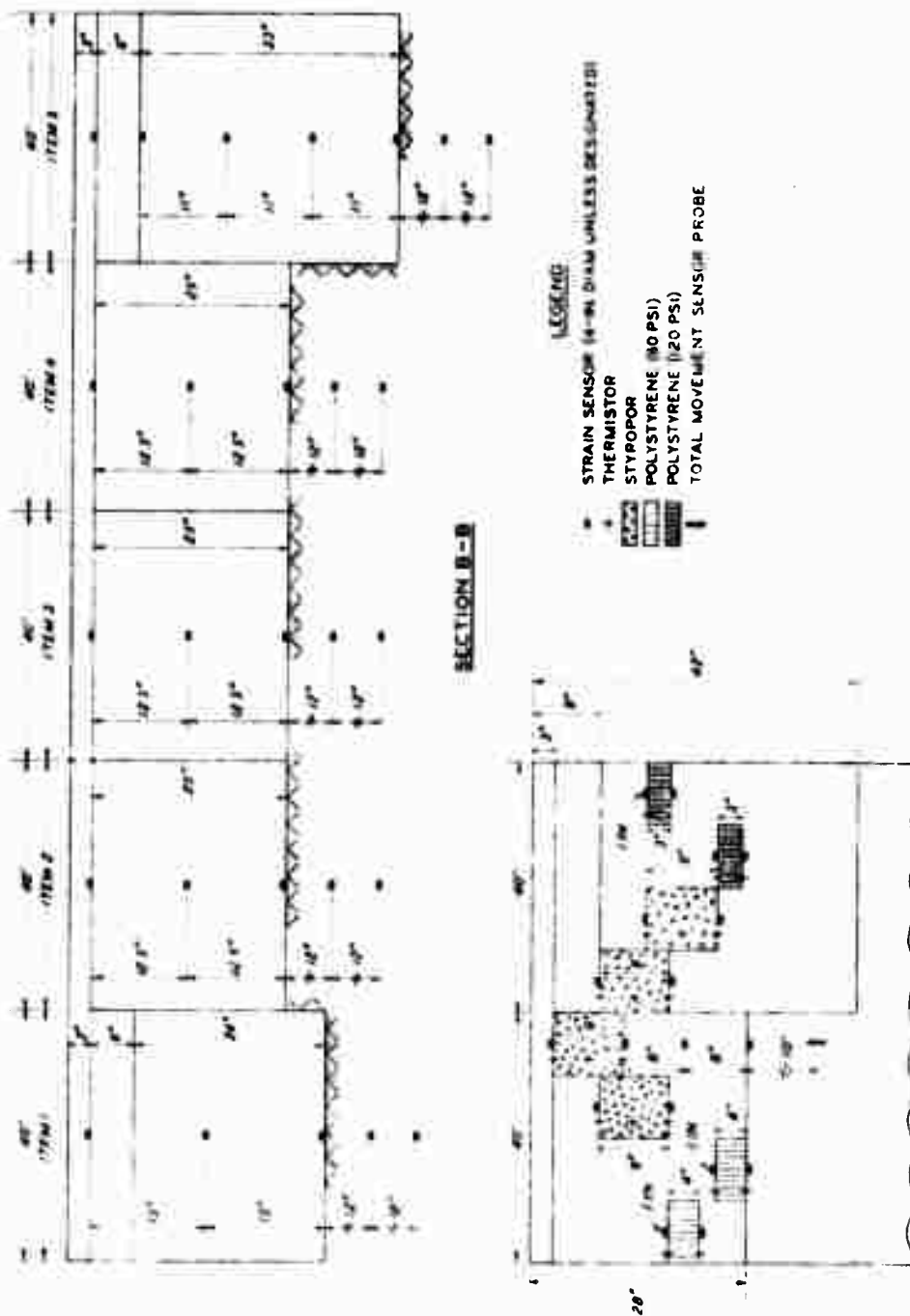


Figure 14. Instrumentation layout for flexible pavement test section (Sections B-B and C-C)

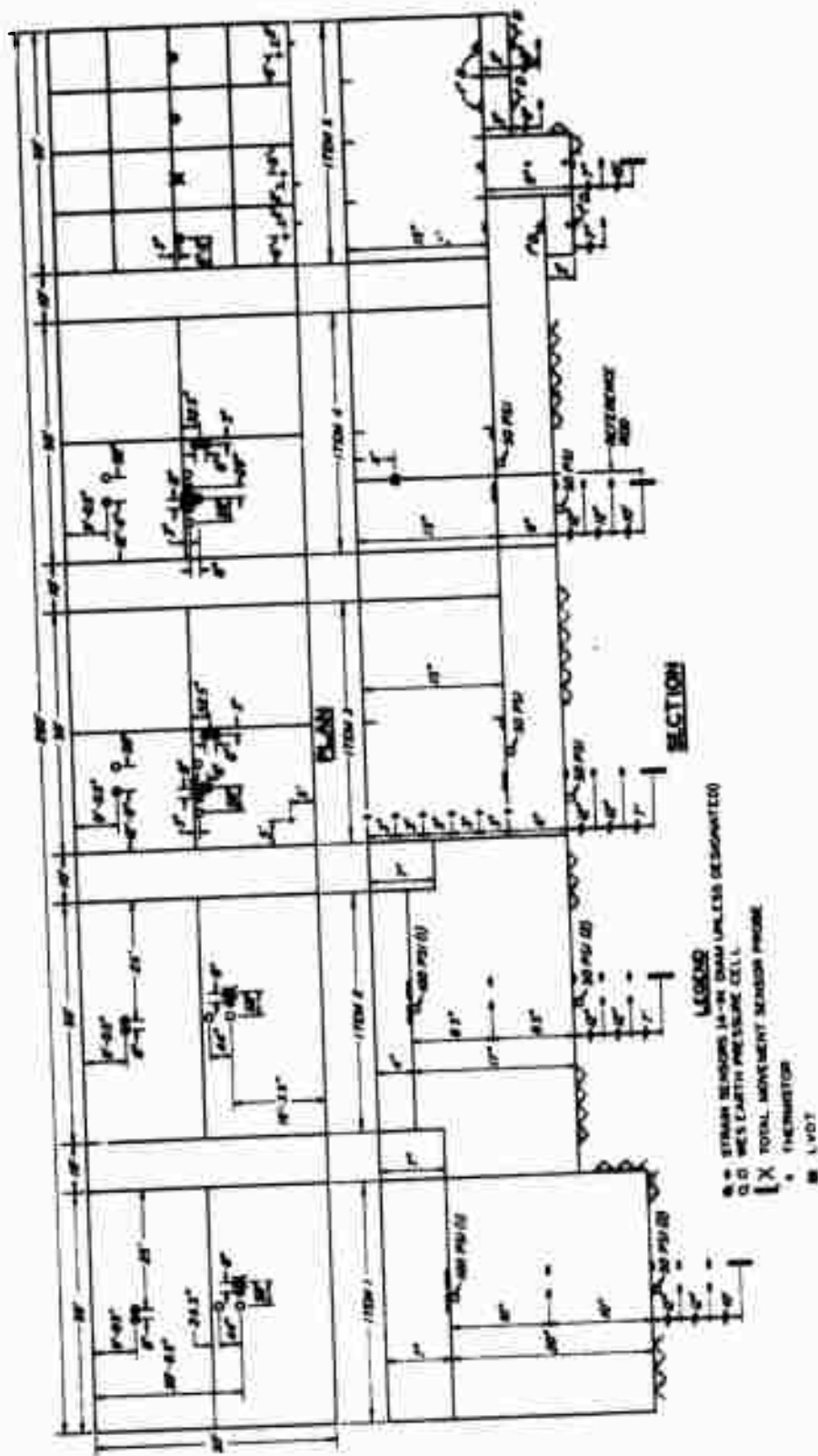


Figure 15. Instrumentation layout for rigid pavement test section

PRESSURE CELLS

WES earth pressure cells were installed in both the rigid and flexible pavement test sections. These cells are 6 in. in diameter, are fabricated from stainless steel, and use a mercury-filled fluid chamber with a diaphragm and a full Wheatstone bridge circuit consisting of four SR-4 strain gages hermetically sealed within the cell. Pressure applied to the faceplate of the cell is transmitted through the mercury in the fluid chamber to an internal flexible diaphragm and produces deflection of the diaphragm proportional to the load. The four SR-4 strain gages are mounted on the diaphragm and are actuated by its deflection. The full Wheatstone bridge circuit practically eliminates the effects of temperature and of resistance variations in the lead wires. The cells used were rated at either 50- or 100-psi capacity but can withstand greater pressures without damage.

STRAIN SENSORS

The strain sensors were manufactured by Bison Instruments, Inc., Minneapolis, Minn. The sensors are individual disk-shaped coils, and their principle of operation involves the electromagnetic mutual inductance coupling of any two sensors. They may be placed in one of three alignments: lateral, parallel, or perpendicular. A receiver sensor can be placed anywhere within the electromagnetic field surrounding a sensor excited by an oscillating current. Movement of one sensor with respect to the other results in a change of the electromagnetic coupling between the two. The change in electromagnetic coupling is a nonlinear function of movement; however, the change can be calibrated very accurately with resolution and repeatability of spacing change better than 0.0001 in.

The sensors have no mechanical connection between them and operate at any spacing between one and four times the nominal sensor diameter as long as there is no disturbance of the induced electromagnetic field, such as metal between or around the sensors. Bison strain sensors are available in 1-, 2-, and 4-in.-diam sizes; the 1- and 4-in.-diam sizes were used in this study. Figure 16 shows a pair of 4-in.-diam sensors mounted in a calibration stand.

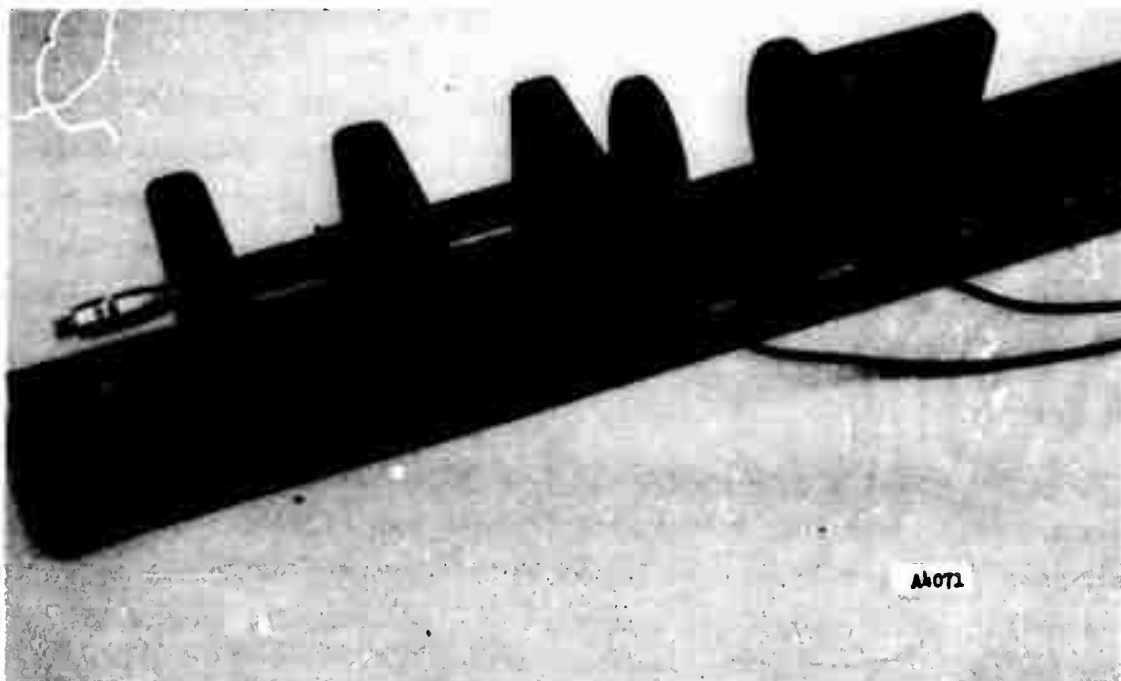


Figure 16. Pair of Bison strain sensors in micrometer calibration mount

Two types of readout equipment were used during the conduct of the study. A field-use instrument manufactured by Bison Instruments, Inc., which contains all necessary driving, amplification, balancing, readout, and calibration controls, as well as a self-contained power supply, was used mainly to collect static load data. Changes in sensor spacing could be determined by means of bridge balance, meter deflection from zero, or voltage output on a recorder connected to the rear panel of the instrument package. The instrument package used for this study could detect both static and dynamic strain. Response time of the instrument was about 0.1 msec. WES-developed multichannel recording equipment was also used to record static and dynamic load responses. This equipment is described in Horn.²²

INDUCTIVE PROBES

In addition to the standard Bison sensors, a number of experimental inductive coils were also installed. Physically, these probes

consist of an encapsulated coil of wire 18 in. long and 1 in. in diameter. These were installed simply by drilling a 1-1/2-in.-diam hole to the desired depth and lowering the probe into the hole. The hole was then backfilled with the cable running up to ground level at which point it was diverted to the side of the test section. The inductive probes were intended to work as lower reference coils for the standard Bison coils installed at the higher levels. These probes plus the standard coil configuration offered the advantages of easier installation than the standard Bison coils and the ability to reference upper coil motion to a relatively stable lower level.

THERMISTORS

Thermistor probes manufactured by United Systems Corporation, Dayton, Ohio, were installed in the flexible and rigid pavement test sections. The probes were monitored with a direct-reading digital temperature meter, which was connected to a recorder for automatic monitoring.

CONSTRUCTION OF TEST SECTIONS

Construction of the rigid and flexible pavement test sections was accomplished during the period 17 March-3 August 1972. As indicated earlier, the test sections were located within the area used previously for the MWHGL test section (Figure 17). Since the MWHGL tests, other pavement tests have also been conducted on this site using the original subgrade. Therefore, it was necessary to remove the rigid and flexible pavements remaining from previous tests prior to construction.

RIGID PAVEMENT TEST SECTION

SUBGRADE

The top 6 to 12 in. of subgrade was reprocessed, compacted, and graded as necessary to obtain the desired strength and elevation. Plate bearing and CBR tests were conducted on the subgrade in each item immediately prior to placing the base courses. The k_u values* of the subgrade ranged from 40 to 85 pci, with an average of 65 pci, and the average CBR of the top 12 in. of the subgrade was 3.4 (see Table 3). A view of the finished subgrade in item 1 is shown in Figure 18.

BASE COURSES

Item 1. In item 1, the bottom membrane for the MESL consisted of 6-mil-thick polyethylene that was placed over the prepared subgrade (Figure 19). The membrane was fabricated from two smaller sheets that were bonded together at the center to form a continuous membrane of sufficient size to provide waterproof protection at the bottom and sides of the finished soil layer. The lean clay soil was preprocessed to a moisture content of about 51 percent, hauled to the site, dumped, spread, and compacted. The 20-in.-thick base was placed and compacted in three lifts. The first or bottom lift was about 8 in. thick, and the thicknesses of the top two lifts were each about 6 in. after compaction.

* The k_u value is the modulus of soil reaction uncorrected for saturation.

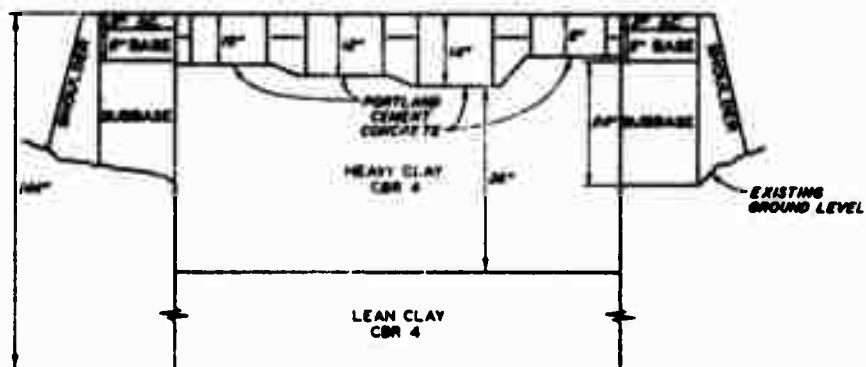
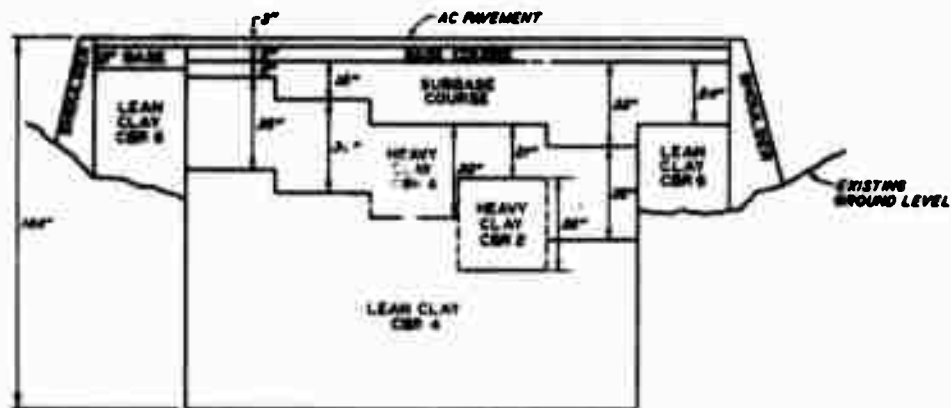
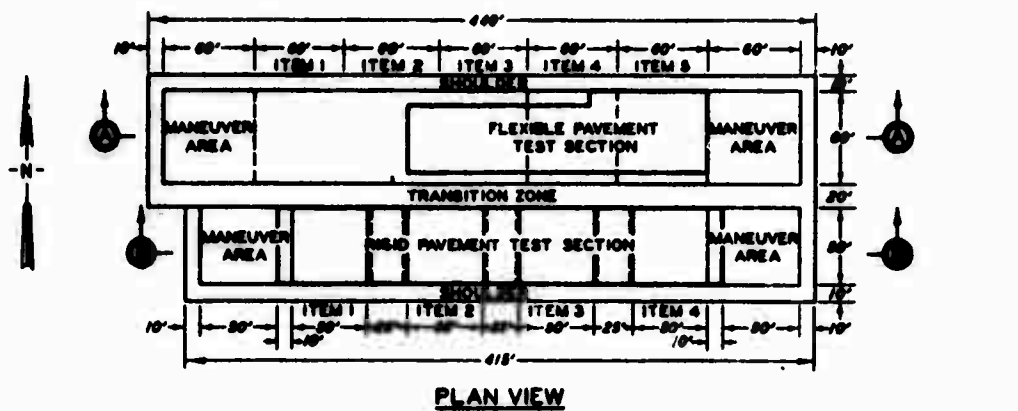


Figure 17. Location of soil stabilization test sections within the existing MWHGL test section (Sections A-A and B-B represent original pavement structure)

Table 3

Summary of Plate Bearing, Field CBR, Water Content, and Dry Density
Data for the Rigid Pavement Test Section as Constructed

Test Item No.	Material	Depth in.	k_u Value pci	CBR	Water Content percent	Dry Density pcf
1	Lean clay MESL	7	175	33	15.9	104.2
		13	--	19	12.2	96.1
		19	--	18	12.8	98.6
	Heavy clay subgrade	27	47	3.5	29.8	89.1
		33	--	2.4	32.0	84.3
		39	--	2.7	33.4	85.8
2	Clay gravel with 6 percent port- land cement	4	545	150+	5.8	135.1
	Heavy clay subgrade	21	85	3.4	34.1	85.0
		27	--	3.3	34.5	84.4
		33	--	3.4	34.0	84.1
3	Bituminous base	15	99	--	--	--
3	Heavy clay subgrade	21	84	3.5	32.2	87.0
		27	--	3.1	32.3	86.3
		33	--	4.0	31.7	87.1
4	Lean clay with 12 percent port- land cement	15	167	50	15.8	105.2
	Heavy clay subgrade	21	40	3.3	33.1	86.1
		27	--	4.0	33.4	85.9
		33	--	4.5	32.2	87.3

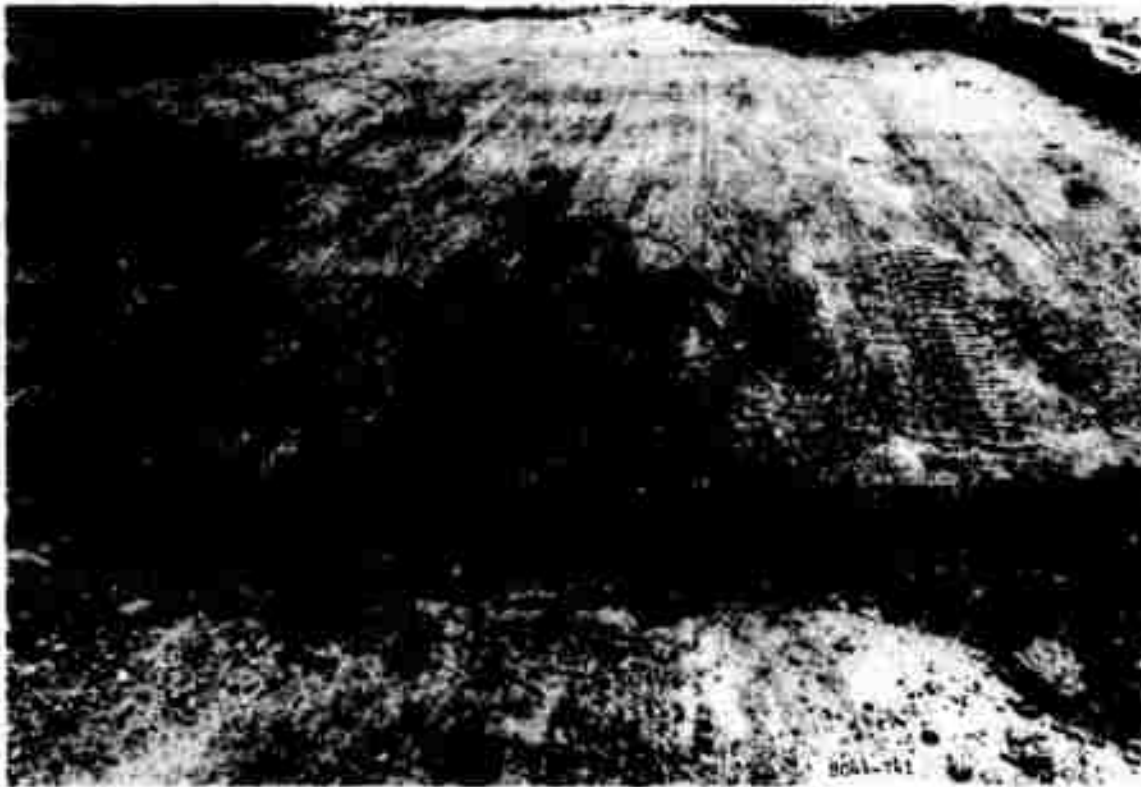


Figure 18. Finished subgrade of item 1 of rigid pavement test section



Figure 19. Polyethylene membrane in place on the subgrade of item 1 of the rigid pavement test section

Care was exercised in placement of the first lift of soil to prevent damage to the thin polyethylene membrane. The soil was end-dumped starting at one edge, pushed forward, and then spread with a D-4 bulldozer. Compaction was accomplished with a 30-ton self-propelled pneumatic-tired roller having a tire pressure of about 90 psi. Placement of the top layer of soil of the MESL is shown in Figure 20. The top layer of the soil base was compacted by eight coverages of the pneumatic-tired roller with tire pressure of 90 psi. After compaction, plate bearing tests conducted at the surface of the soil base indicated a k_u value of approximately 175 pci, and an average CBR value of 33 was obtained (Table 3). After grading the surface of the soil base to the desired elevation, the encapsulation was completed by placing a polypropylene-asphalt membrane over the surface area and bonding it to the polyethylene that was used as the bottom and sides of the MESL. The membrane was formed by spraying the surface of the soil layer with cationic emulsified asphalt (ASTM C-RS-2²³) at a rate of about 0.5 gal per square yard, covering the soil layer with polypropylene fabric, and spraying an additional application of the emulsified asphalt at a rate of about 0.3 gal per square yard. A blotter course of sand was applied over the asphalt-impregnated polypropylene material. A view of the completed MESL base is shown in Figure 21.

Item 2. The base course of item 2 was cement-stabilized clay gravel. The 17-in.-thick cement-stabilized base was constructed in three lifts of about equal thicknesses. The untreated soil was pre-processed to the desired water content of about 8 percent, and a sufficient quantity for one lift was hauled and spread uniformly over the surface area. Bags of cement were distributed over the surface area at a spacing to provide the desired proportioning (Figure 22). Hand tools were used to distribute the cement uniformly over the surface area, and then the cement was admixed in place with a rotary tiller (Figure 23). Immediately after mixing, the treated soil was compacted with the 30-ton self-propelled pneumatic-tired roller



Figure 20. Placement of soil in the MESL



Figure 21. Completed MESL base course in item 1 of the rigid pavement test section



Figure 22. Bags of cement distributed over the surface of the base of item 2 of the rigid pavement test section



Figure 23. In-place mixing of soil and cement in item 2 of the rigid pavement test section

(Figure 24). The surface of the compacted lift was scarified lightly, and the same procedure was followed in constructing the additional lifts. The top lift was subjected to 16 coverages of compaction rolling with a 50-ton pneumatic-tired roller (Figure 25) following the initial compaction with the 30-ton roller. Plate bearing tests conducted after a 6-day curing period indicated a k_u value of 545 pci, and the average CBR of the stabilized base 1 day after construction was in excess of 150 (Table 3).

Item 3. The 6-in.-thick bituminous base of item 3 was constructed in a single lift. The hot material was dumped from trucks directly onto the clay subgrade and spread with a D-4 bulldozer (Figure 26). Compaction was accomplished with a 10-ton tandem steel-wheeled roller and the 30-ton pneumatic-tired roller. Density specimens cut from the base indicated that 100 percent of 75-blow Marshall density was obtained. A view of a specimen cut from the base is shown in Figure 27. Plate bearing tests conducted 6 days after construction indicated a k_u value of 99 pci at a temperature of about 85 to 90 F (Table 3).

Item 4. The cement-stabilized lean clay soil used in item 4 was similar to the lean clay used in the MESL in item 1. The untreated soil was processed in a stockpile to the desired water content of about 18 percent, hauled to the test site, dumped, and spread directly over the subgrade. The cement was then distributed and mixed into the soil in place to yield a cement content of about 12 percent by dry weight of soil. The procedures used for distributing and mixing the cement were the same as those previously described for test item 2. Compaction was accomplished using the 30-ton pneumatic-tired roller. Plate bearing tests conducted after a 6-day curing period indicated a k_u value of 167 pci, and the average CBR of the stabilized base 1 day after construction was 50 (Table 3).

Item 5. The subgrade for subitems 5a and b was excavated to an elevation 6 in. deeper than that for subitems 5c and d to allow for a 9-in. thickness of the lightweight concrete in subitem 5b and for a 6-in.



S044-780

Figure 24. Compaction with the 30-ton self-propelled pneumatic-tired roller



S044-781

Figure 25. Compaction with the 50-ton pneumatic-tired roller



Figure 26. Spreading hot-mix bituminous base material in item 3 of the rigid pavement test section



Figure 27. Specimen of bituminous base cut from item 3 of the rigid pavement test section

layer of cement-stabilized lean clay over 3-in.-thick, 35-psi polystyrene panels in subitem 5a. All of the insulating materials were placed directly on the clay subgrade. The polystyrene panels in subitems 5a, c, and d were placed by hand in the pattern shown in Figure 28. The lightweight concrete was mixed in the Concrete Laboratory at WES in 1/2-cu-yd batches, hauled to the test site, and placed directly on the subgrade between forms. The surface was screeded to grade and immediately covered with wet burlap and wet-cured for 48 hr. Forty-eight batches of lightweight concrete were used. For the first 24 batches, the wet unit weight was about 52 pcf; this material was placed in the south paving lane. After the first 24 batches, the quantity of Styropor beads was increased slightly in order to bring the wet unit weight nearer design requirements (45.76 pcf). The increase in Styropor beads gave a unit weight of 44 pcf, which when cured resulted in a unit weight of about 38 pcf. The lighter weight material was placed in the north paving lane. A closeup view of the textural finish of the lightweight concrete



Figure 28. Polystyrene panels in place on the subgrade of item 5 of the rigid pavement test section

is shown in Figure 29. The cement-stabilized lean clay used over the 35-psi polystyrene panels in subitem 5a was the same as that used in



Figure 29. Surface texture of the lightweight concrete insulating layer in subitem 5b of the rigid pavement test section

item 4, except that the cement was premixed with the soil prior to placement over the polystyrene. The premixed material was end-dumped on top of the polystyrene and spread with a D-4 bulldozer. Compaction was accomplished with the 30-ton roller with a tire pressure of about 60 psi. A view of the finished sublayers in item 5 is shown in Figure 30.

SURFACINGS

All concrete mixtures including the fibrous-reinforced concrete were dry-batched at the plant of the Vicksburg Concrete Co., Inc. The batch proportions were in accordance with the mix designs furnished by WES. The mixtures were transit-mixed and delivered to the construction site, a distance of about 5 miles, in ready-mix trucks. Due to the small, confined working areas, the mixtures were placed and finished by

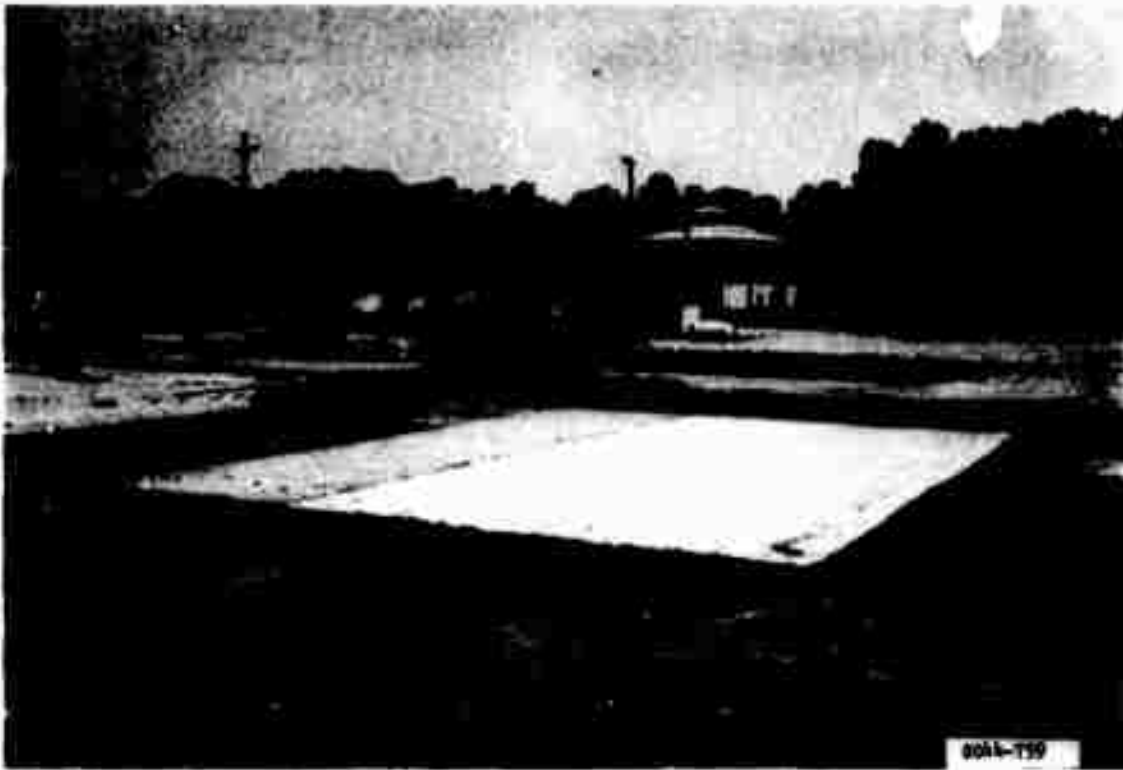


Figure 30. Completed installation of insulating materials on subgrade of subitems 5a-d of the rigid pavement test section

hand. Details of the placement and finishing operations are discussed in the following paragraphs.

The 10- by 50-ft reinforced transition slabs were placed prior to placing the actual test slabs. Forms were set into or on top of the various base course layers to provide for the desired thicknesses. Details of the horizontal spacing of dowels and reinforcing bars are shown in Figure 6. The transition slabs between items 1 and 2, 2 and 3, and 3 and 4 are shown in Figure 31. Note the exposed dowel bars.

The concrete in each test item was first placed in the north paving lane (25- by 50-ft section) between the previously placed transition slabs. The material was discharged from the ready-mix trucks directly onto the base course between the paving forms. Placement of fibrous-reinforced concrete in item 2 is shown in Figure 32. The concrete was spread by use of shovels and was screeded off with a straightedge with a small vibrator mounted on the straightedge, as shown in Figure 32.

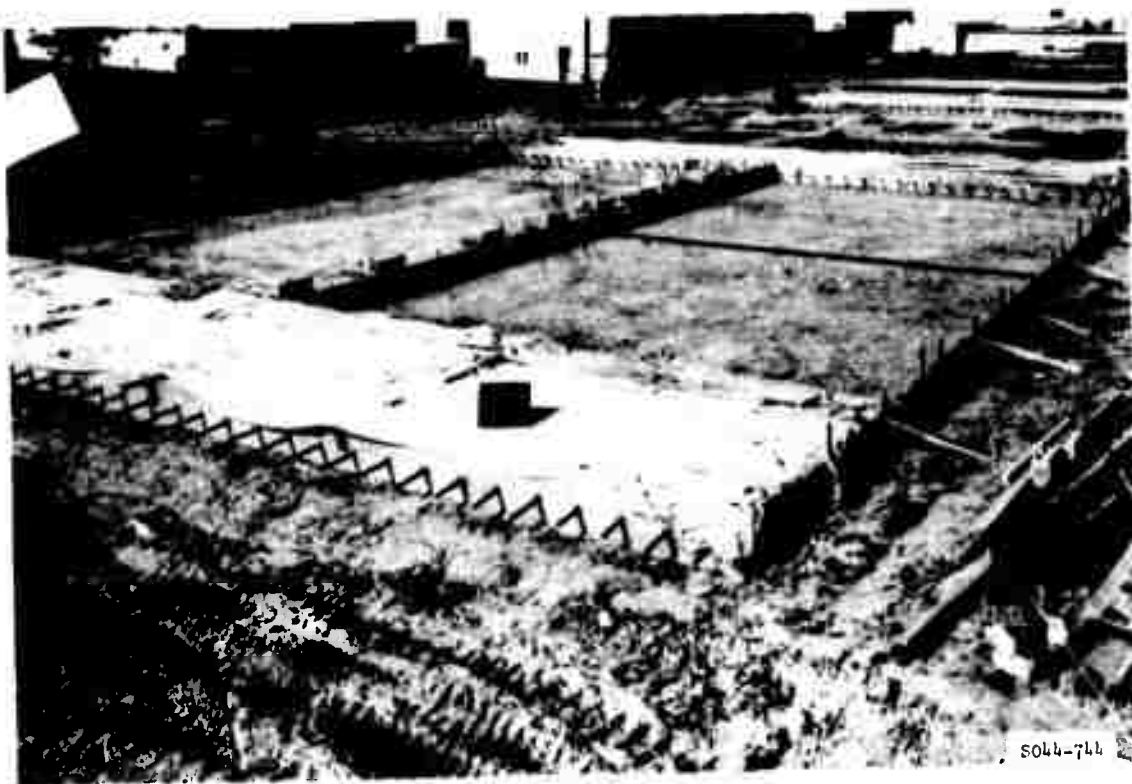


Figure 31. Transition slabs in place between the rigid pavement test items



Figure 32. Placement of fibrous-reinforced concrete over insulating materials in item 2 of the rigid pavement test section

Internal vibration was not used in items 1 and 2. Finishing was accomplished by hand with trowels and bull floats. The same procedures were used in placement and finishing of the plain portland cement concrete in items 3 and 4, except that internal vibration was accomplished with stinger-type hand vibrators. A crane with a concrete bucket was used to distribute the concrete mixture over the insulating materials in item 5, as shown in Figure 33.



Figure 33. Placement of concrete over insulating materials in item 5 of the rigid pavement test section

The concrete was moist-cured for 7 days. Wet burlap was placed on the fresh concrete and kept wet by spraying during the first 24 hr. After the first day, the burlap was covered with plastic sheeting that was kept in place for the remainder of the 7-day curing period.

A keyed-and-tied longitudinal construction joint was used between the north and south paving lanes in all items except for the 4-in.-thick fibrous-reinforced concrete in item 2. A thickened-edge joint was used for this item. The keyway was formed using wooden strips of the

required shape and size fastened to the form of the north paving lane. Keyway dimensions and locations, which are a function of the pavement thickness, are shown in Figure 5.

Transverse weakened-plane construction joints were provided on 25-ft spacings in both paving lanes for items 3 and 4 and on 12.5-ft spacings for item 5. Also, in item 5, a longitudinal weakened-plane joint was provided on 12.5-ft spacings in each lane. The weakened plane was formed by placing thin metal strips in the bottom of the concrete and sawing grooves in the surface of the pavement directly over the metal strips. In order to control construction cracking to prevent damage to instrumentation gages located near the weakened-plane joints, metal strips were located on the surface of the finished base and held in place during concrete placement by metal pegs driven into the base. A view of one of the strips in place prior to placing concrete in item 4 can be seen in Figure 31. In most cases, the sawed grooves were cut in the concrete within 24 hr after placement of the concrete. A view of



Figure 34. Joint sawing operations in the rigid pavement test section

Internal vibration was not used in items 1 and 2. Finishing was accomplished by hand with trowels and bull floats. The same procedures were used in placement and finishing of the plain portland cement concrete in items 3 and 4, except that internal vibration was accomplished with stinger-type hand vibrators. A crane with a concrete bucket was used to distribute the concrete mixture over the insulating materials in item 5, as shown in Figure 33.



Figure 33. Placement of concrete over insulating materials in item 5 of the rigid pavement test section

The concrete was moist-cured for 7 days. Wet burlap was placed on the fresh concrete and kept wet by spraying during the first 24 hr. After the first day, the burlap was covered with plastic sheeting that was kept in place for the remainder of the 7-day curing period.

A keyed-and-tied longitudinal construction joint was used between the north and south paving lanes in all items except for the 4-in.-thick fibrous-reinforced concrete in item 2. A thickened-edge joint was used for this item. The keyway was formed using wooden strips of the

required shape and size fastened to the form of the north paving lane. Keyway dimensions and locations, which are a function of the pavement thickness, are shown in Figure 5.

Transverse weakened-plane construction joints were provided on 25-ft spacings in both paving lanes for items 3 and 4 and on 12.5-ft spacings for item 5. Also, in item 5, a longitudinal weakened-plane joint was provided on 12.5-ft spacings in each lane. The weakened plane was formed by placing thin metal strips in the bottom of the concrete and sawing grooves in the surface of the pavement directly over the metal strips. In order to control construction cracking to prevent damage to instrumentation gages located near the weakened-plane joints, metal strips were located on the surface of the finished base and held in place during concrete placement by metal pegs driven into the base. A view of one of the strips in place prior to placing concrete in item 4 can be seen in Figure 31. In most cases, the sawed grooves were cut in the concrete within 24 hr after placement of the concrete. A view of



Figure 34. Joint sawing operations in the rigid pavement test section

Grooves for joint seal installation were formed by sawing to the dimensions shown in Figures 5 and 6. The longitudinal construction joints were sawed on the day following placement of the south paving lane. Almost all transverse joints were sawed the day following placement. After a 2- to 3-week curing period, the sawed joints were thoroughly cleaned with compressed air and sealed with a hot-poured joint sealing compound meeting Federal Specification SS-S-164(4).²⁴

FLEXIBLE PAVEMENT TEST SECTION

SUBGRADES

The flexible pavement test section was located as indicated in Figure 17. The existing asphaltic concrete pavement was broken up and removed. The crushed-stone base material and gravelly sand subbase material that had been used in a previous test section were salvaged and stockpiled for future use.

The top 6 to 12 in. of the in-place heavy clay was reprocessed, with material added or removed where necessary to obtain the desired grades; the water content was adjusted as required; and the soil was compacted with the 30-ton pneumatic-tired roller. The elevation of the surface subgrade was established in each item so that the finished pavement elevation would match the existing grade of the MWHGL test section. In-place CBR and plate bearing tests were conducted to verify that the soil strength was within the desired range. The k_u values averaged 60 pci, and the average CBR of the top 12 in. of the subgrade was about 5 (Table 4). An overall view of the completed subgrade is shown in Figure 35.

SUBBASE AND BASE COURSES

The stabilized soil layers used as subbase in item 1 and as base course in items 2-4 were constructed concurrently. Prior to applying the stabilizing agent, the subbase and base materials to be stabilized were processed to the desired water content and then placed in the various test items in approximately 7-in.-thick loose lifts that resulted in about 6-in.-thick compacted layers. After placing and spreading the

Table 4
Summary of Laboratory Compression Data and
As-Constructed Plate Bearing, Field CBR, Water Content, and Dry Density Data
for the Flexible Pavement Test Section

Test Item	Material	Laboratory Data				As-Constructed Data						
		Water Content		Maximum Dry Density pcf	Compaction Effort	Depth in.	Water Content Untreated Material percent	k, psi	CBR	Water Content percent	Dry Density pcf	Percent Laboratory Density
		Untreated percent	Treated percent									
(1)	(2)	(3)	(4)	(5)	(6)	(7)	(8)	(9)	(10)	(11)	(12)	(13)
1	Crushed limestone (base)	6.0	--	140.0	CE 55	3	--	--	110*	1.0	151.9	108.0
	Lean clay with 3 percent lime, 2 percent portland cement, 10 percent fly ash (subbase)	17.0	14.5	101.5	CE 12	9	19.6	470	94	17.7	96.5	95.1
						13	17.3	--	94	15.8	98.8	97.3
						19	17.3	--	47	8.9	92.6	91.2
	Heavy clay (subgrade)	25.0	--	94.0	CE 12	33	--	--	3.3	30.9	87.3	97.0*
						39	--	--	4.1	32.4	85.3	99.0*
						45	--	--	4.4	32.8	85.9	100.0*
	Lean clay with 12 percent portland cement (base)	17.0	14.5	107.9	CE 12	3	16.1	345	105	16.0	102.9	95.3
						7	19.6	--	150*	12.5	103.5	95.9
						14	18.3	--	68	15.2	98.1	90.9
						21	17.3	--	14	12.2	93.1	86.3
	Heavy clay (subgrade)	25.0	--	94.0	CE 12	28	--	--	3.6	30.2	86.5	96.0*
						30	--	--	3.7	30.6	88.1	97.5*
						40	--	--	4.4	31.6	87.2	100.0*
3	Gravelly sand with 5 percent portland cement	6.0	5.9	137.0	CE 55	3	6.3	645	150*	3.2	133.4	97.3
						7	6.1	--	150*	1.6	134.6	98.2
						14	--	--	136*	3.9	126.2	92.1
						21	7.0	--	129	2.1	120.3	87.8
	Heavy clay (subgrade)	25.0	--	94.0	CE 12	28	--	68	3.6	30.3	87.0	97.0*
						34	--	--	3.2	30.8	87.2	97.5*
						40	--	--	3.9	32.6	85.9	100.0*
	Clayey sand with 5 percent portland cement (base)	9.2	8.7	130.5	CE 55	3	9.7	448	150*	8.9	116.9	89.6
						7	9.8	--	150*	4.6	121.5	93.1
						14	9.4	--	93	6.3	112.8	86.4
						21	9.4	--	103	7.8	119.3	91.4
	Heavy clay (subgrade)	25.0	--	94.0	CE 12	28	--	--	3.7	30.5	86.9	98.0*
						34	--	--	4.1	29.3	88.8	98.5*
						40	--	--	4.0	32.0	84.2	97.5*
	Crushed limestone (base)	6.0	--	140.0	CE 55	3	--	--	104	2.4	145.7	103.8
						9	--	--	56	5.4	136.7	103.2
						15	--	--	46	4.6	135.2	100.6
						21	--	--	9	9.4	127.5	96.2
	Heavy clay (subgrade)	25.0	--	94.0	CE 12	42	--	55	4.2	29.9	89.2	99.0*
						48	--	--	3.5	31.1	86.0	97.2*
						54	--	--	4.6	31.5	86.5	98.0*
4a	Clayey sand with 5 percent portland cement over 60-psi polystyrene	--	8.7	130.5	CE 55	14	--	--	--	3.8	123.1	94.5
4b	Clayey sand with 5 percent portland cement over 60-psi polystyrene	--	8.7	130.5	CE 55	10	--	--	--	7.0	119.5	91.5
4c	Clayey sand with 5 percent portland cement over lightweight concrete	--	8.7	130.5	CE 55	3	--	--	--	12.3	112.5	86.5
5b	Gravelly sand over lightweight concrete	7.5	--	132.4	--	9	--	--	--	10.9	123.1	93.3
5c	Gravelly sand over 120-psi polystyrene	7.5	--	132.4	--	15	--	--	--	4.9	132.9	100.3
5d	Gravelly sand over 120-psi polystyrene	7.5	--	132.4	--	9	--	--	--	6.3	132.1	100.0

* Percent of CE 12 (ASTM D 696-70) maximum density corresponding to the field in-place water content.



Figure 35. Completed subgrade of the flexible pavement test section

loose material for each lift, bags of lime, fly ash, and/or cement were placed in the respective items at predetermined intervals to give the desired proportioning (Figure 36). After distributing the additive uniformly over the surface area, in-place mixing was accomplished with a pulvimixer as shown in Figure 37. Compaction was accomplished by the application of eight coverages of the 30-ton roller on the surface of each lift, plus an additional eight coverages of the 50-ton roller on the top two lifts of each item.

During the in-place mixing operations, visual checks were made to insure that uniform mixing of the soil and additive was obtained for the full depth of each lift. These checks were made by digging holes in the mixed material down to the previously compacted lift and inspecting the material. In general, it appeared that fairly uniform mixing was obtained. However, after construction of the top lift, an open, gage installation trench that was cut across item 4 down to the bottom of the



Figure 36. Bags of cement and fly ash distributed over the surface of the subgrade of items 1 and 2 of the flexible pavement test section



Figure 37. In-place mixing of treated soil with pulvimixer

top lift was filled with rain and some erosion occurred in the bottom 1 to 2 in. of the lift. Examination of the material indicated that the cement was concentrated in the upper part of the lift with very little cement in the bottom 1 to 2 in. A further check in item 3 revealed the same condition. Therefore, the top lifts of stabilized materials were removed from items 3 and 4. Sufficient quantities of the gravelly sand and the clayey sand used in the base courses of items 3 and 4, respectively, were premixed in windrows on a paved working area adjacent to the test site. The premixed materials were then placed in the respective test items and compacted as previously described. Checks made in item 1 and 2 at the same time indicated fairly uniform mixtures of soil and additives through the full depth of each surface layer of stabilized material. Therefore, no corrective action was required for these items.

The untreated gravelly sand subbase in item 5 was placed and compacted at optimum water content using the same lift thicknesses and compaction efforts previously described for the stabilized materials.

The crushed limestone base material used in items 1 and 5 was thoroughly mixed and wetted in a windrow adjacent to the test site, spread with a dozer, and compacted with the pneumatic-tired rollers as previously described for the stabilized base courses.

SUBITEMS CONTAINING INSULATING MATERIALS

As indicated in Figures 7 and 8, a special test area designed to study the structural behavior of materials used for insulating purposes was constructed adjacent to items 4 and 5 of the flexible pavement test section. Composition of the pavement structures in this area was identical with that previously discussed for items 4 and 5, except that the insulating layers were incorporated into the pavement structure at the various depths indicated in Figure 8. The type of insulating material or the elevation in the structure was varied in these subitems. The polystyrene panels were placed by hand during construction. The lightweight concrete was mixed in the WES Concrete Laboratory and placed in the test section between forms at the locations and elevations indicated in Figure 8. The same procedures were used in placement, finishing, and

curing as described previously for the lightweight concrete in the rigid pavement test section. A view of the placement operation is shown in Figure 38. The soil and cement for subitems 4a-d were premixed in a windrow adjacent to the test section, placed with a front-end loader, and spread in about 6-in.-thick loose layers. The untreated material in subitems 5a-d was placed in the same manner. Each layer was compacted by 8 coverages of the 30-ton roller with tire pressures of about 70 psi. The heavy 50-ton roller was not used over the insulating materials in subitems 4a-d or 5a-d for fear of damaging the insulating materials.

ASPHALTIC CONCRETE SURFACING

The finished base courses of the entire test section were primed with MC-1 cutback asphalt at a rate of about 0.15 gal per square yard (Figure 39). After a 2-day curing period, the 3-in.-thick asphaltic concrete mixture was hauled from the contractor's central batch plant (a distance of 10 miles) and was placed with a Barber-Green finisher in 10-ft-wide paving lanes (Figure 40). The mix temperature was about 300 to 325 F, and the laydown temperature was about the same. Compaction was accomplished with the 10-ton tandem roller and the 30-ton pneumatic-tired roller. The completed flexible pavement test section is shown in Figure 41.

INSTALLATION OF INSTRUMENTATION

RIGID PAVEMENT TEST SECTION

The deflection gages, pressure cells, thermistors, and strain sensors were installed during construction operations at the locations and elevations shown in Figure 15. Pressure cells and strain sensors located within the subgrade were placed by excavating trenches and pits to the proper elevations, placing the instruments, backfilling the excavations, and hand-compacting the fill material. Pressure cells and strain sensors located at the top of the subgrade were placed directly on the subgrade surface (Figures 42 and 43) in items 1, 3, and 5; the gages in item 2 were installed after the first layer of stabilized material was placed; in item 4 the gages were placed after the



Figure 38. Placement of lightweight concrete insulating materials in item 5 of the flexible pavement test section



Figure 39. Primed base courses prior to paving flexible pavement test section



Figure 4C. Placement of 3-in.-thick asphaltic concrete surface course on the flexible pavement test section



Figure 41. Overall view of completed flexible pavement test section



Figure 42. Placement of a Bison strain sensor

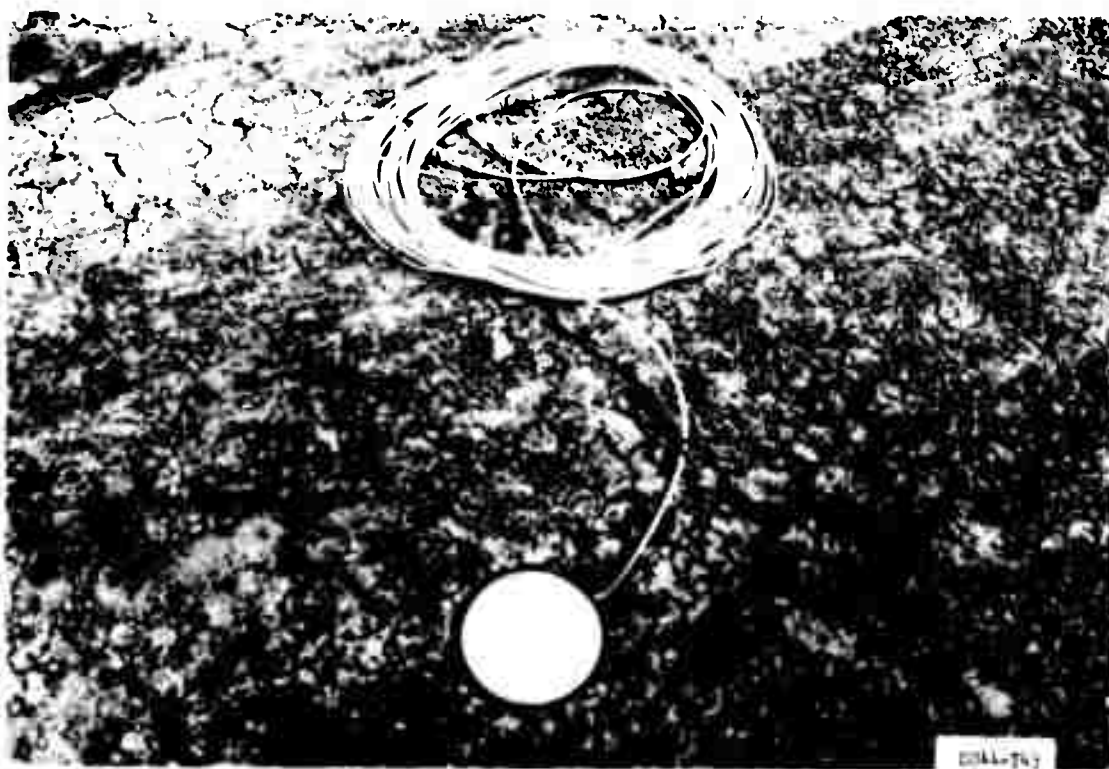


Figure 43. Placement of a WES pressure cell

bituminous-stabilized base course was completed. Inductive probes were placed in core holes drilled from the top of the subgrade. Strain sensors placed at the center of the stabilized base courses in items 1 and 2 were placed after one lift of base course material had been completed at the desired elevation. Instruments located directly beneath the concrete slab were placed on the underlying surface immediately prior to concrete placement. Strain sensors were taped in place on the top of the insulated layers in item 5. A deflection gage was installed in item 4 adjacent to the longitudinal construction joint near the midpoint of the southwest slab. Details of deflection gage installation are described in Horn.²²

FLEXIBLE PAVEMENT TEST SECTION

Plan and section views of the instrumentation for the flexible pavement test section are shown in Figures 13 and 14. As was the case with the rigid pavement installation, gages were placed in the subgrade by trenching to the proper elevations, placing the gages, backfilling, and compacting by hand. Gages located on top of the subgrade and in the base course of all five test items were placed by overbuilding, and then excavating to the desired elevation. Strain sensors placed at the top of the base course were covered with a thin layer of cold-mix asphalt-aggregate blend prior to placement of the hot-mix asphaltic concrete surface course. Gages placed on top of the insulating layers were taped in place. Inductive probes were placed in core holes drilled to the elevations shown in Figures 13 and 14. One deflection gage was installed in item 4; details of the installation can be found in Horn.²²

TESTING AND SAMPLING DURING CONSTRUCTION

Water content, density, and CBR determinations were made at the surface of the subgrade, at 6- and 12-in. depths in the subgrade, and at the surface of each layer of subbase and/or base course during construction. The density determinations were made in the subgrade by use of the drive-cylinder method (ASTM D 2937-71²⁵) and in the subbase and base materials by use of the rubber-balloon method (ASTM D 2167-66²⁶).

Plate bearing tests were made on the finished subgrade and on the top of the base course in each item of both the rigid and flexible pavement test sections. The tests were performed in accordance with Method 104 of MIL-STD-621A.

Specimens of the lightweight concrete, fibrous-reinforced concrete, and plain portland cement concrete mixtures were obtained during the paving operations. Beams that were 6 by 6 by 36 in. and 6-in.-diam, 12-in.-high cylinders were taken that were representative of the concrete placed in each test item. All test specimens were moist-cured in a 100 percent humidity environment at 73 F until time for tests of strength properties.

Disturbed samples of the subgrade, subbase, and base materials were obtained for future laboratory tests. Samples of both untreated and field-mixed treated materials were obtained for testing. Also, undisturbed samples of the subgrade from both the rigid and flexible test sections were obtained for future testing. All samples were stored in a humid room for testing. Test results and analysis will be reported in subsequent volumes of this report.

PROPERTIES OF AS-CONSTRUCTED PAVEMENTS

RIGID PAVEMENT TEST SECTION

A summary of results from plate bearing, in-place CBR, water content, and density tests conducted on the subgrade and base course layers of the rigid pavement test section is shown in Table 3. The plate bearing tests on the subgrade were made immediately prior to placing base courses, and the plate bearing tests on the surface of the base courses were made after a 5- to 7-day curing period. The CBR, water content, and density data for the subgrade were obtained in test pits at the surface and at depths of 6 and 12 in. just prior to placing the base course layers. The CBR, water content, and density data for the MESL base were obtained at the surface of each layer during construction. Marshall stability, flow, voids, and density data for the bituminous base material with 4.6 percent asphalt content used in item 3 are summarized as follows:

<u>Type Compaction</u>	<u>Stability lb</u>	<u>Flow Units of 1/100 in.</u>	<u>Voids, percent</u>		<u>Density pcf</u>	<u>Percent Lab Density</u>
			<u>Total Mix</u>	<u>Filled</u>		
Laboratory*	1426	5	5.3	66.0	144.5	--
Field**	760	10	5.2	66.5	144.6	100

* 75-blow Marshall effort.

** Tests were performed on field cores.

The test values above are averages of three or more determinations. The laboratory compacted specimens were prepared from plant-mixed material.

Flexural strength and modulus of elasticity data obtained from the lightweight concrete beams are shown in Table 5. Also shown in the table are the specimen ages at time of testing and the unit weight of the concrete. Results of compressive strength and static modulus of elasticity tests on 6- by 12-in. cylinders of lightweight concrete cast at the time of placing material in the rigid and flexible pavement test sections are shown in Table 6.

Flexural and compressive strength data for the plain concrete used in items 3-5 of the rigid pavement test section are shown in Table 7. The tests were conducted after 7- and 28-day curing times, as indicated.

Flexural strength, compressive strength, and modulus of elasticity data for the fibrous-reinforced concrete placed in test items 1 and 2 of the rigid pavement test section are shown in Table 8. These specimens, cast on 5 and 6 June 1972, were tested at three different ages, 28 days, 150 days (at the initiation of traffic), and 328 days (at the end of traffic). Beams were tested in accordance with ASTM C 78-64,²⁷ except that they were tested in the as-cast position.

FLEXIBLE PAVEMENT TEST SECTION

A summary of laboratory compaction data and as-constructed k_u , CBR, water content, and density of the various elements of the pavement structure is given in Table 4. The laboratory density values shown in

Table 5
Flexural Strength and Modulus of Elasticity of
Lightweight Concrete Beams*

<u>Specimen No.</u>	<u>Age days</u>	<u>Unit Weight pcf</u>	<u>Flexural Strength psi</u>	<u>Modulus of Elasticity E 10⁶ psi</u>
2-1	7	44	145	0.364
2-4	7	44	140	0.649
2-7	7	44	125	0.406
1-44-3	66	44	155	0.568
2-2	280	44	150	0.425
2-8	280	44	175	0.482
2-9	280	44	175	0.478
1-44-1	339	44	150	0.394
1-44-2	339	44	160	0.363
1-52-4	66	52	195	0.760
1-52-5	66	52	160	0.543
1-52-1	339	52	160	0.595
1-52-3	339	52	165	0.676
1-52-3	339	52	165	0.659

* Beams were 6 by 6 by 36 in.

Table 6

Compressive Strength and Modulus of Elasticity
of Lightweight Concrete Cylinders*

<u>Specimen No.</u>	<u>Age days</u>	<u>Unit Weight pcf</u>	<u>Compressive Strength psi</u>	<u>Modulus of Elasticity E 10⁶ psi</u>
2-3	227	44	370	0.178
2-6	227	44	640	0.256
2-9	227	44	570	0.265
1-44-1	336	44	300	0.171
1-44-2	336	44	350	0.207
1-52-1	336	52	750	0.313
1-52-2	336	52	780	0.297
1-52-3	336	52	780	0.294

* Cylinders were 6 in. in diameter and 12 in. long.

Table 7

Flexural and Compressive Strength Data for Plain Portland Cement
Concrete Used In the Rigid Pavement Test Section

Test Item No.	Slab	Slump in.	Entrained Air percent	Flexural Strength, psi		Splitting	Compressive	
				Beams*		Tensile**	Strength	
				7-day	28-day	28-day	7-day	28-day
3	North	2.5	2.5	576	515	530	4382	5717
3	South	3.6	2.4	--	500	505	3800	4910
4	North	3.0	3.7	--	470	530	3560	4590
4	South	4.0	2.8	--	540	495	3600	5110
5	North	3.2	2.0	--	545	510	3780	5320
5	South	2.75	2.4	--	540	607	3370	4980

Note: All test specimens were moist-cured.

* Flexural test beams were 6 by 6 by 36 in. and were subjected to third-point loading. Strength values shown are averages of four tests.

** Splitting tensile tests were conducted on cylindrical samples 6 in. in diameter and 12 in. high. Values shown are averages of two tests.

† Compressive strength tests were conducted on cylindrical samples 6 in. in diameter and 12 in. high. Values shown are averages of four to eight tests.

Table 8

Summary of Flexural and Compressive Strengths and Modulus
of Elasticity of Fibrous-Reinforced Concrete Used
in the Rigid Pavement Test Section

Test Item No.	Slab	Slump in.	Age days*	Flexural Strength psi**	Compressive Strength psi†	Modulus of Elasticity 10 ⁶ psi††
1	North	4	28	805	5860	--
1	South	5	28	735	4660	--
2	North	4	28	810	6100	--
2	South	5	28	695	4540	--
1	North	4	150	1145	6770	6.93
1	South	5	150	935	6140	5.34
2	North	4	150	835	8125	6.58
2	South	5	150	900	6155	6.34
1	North	4	328	1390	--	6.33
1	South	5	328	1165	--	6.98
2	North	4	328	945	--	6.35
2	South	5	328	1115	--	6.31

* Age of 150 days represents the pavement at the time of initiation of traffic, 328 days represents the pavement at the completion of traffic.

** Flexural strength was determined from 6- by 6- by 36-in. beams subjected to third-point loading.

† Compressive strength tests were conducted on cylindrical samples 6 in. in diameter and 12 in. high. Values shown are averages of two tests.

†† Modulus of elasticity tests were conducted on beam specimens prior to loading to complete failure.

Column 5 of this table are for the materials as used in the test section (i.e., treated or untreated). In preparation of the treated laboratory test specimens, the soil was prepared at the optimum water content of the natural or untreated soil, as indicated in Column 3. The stabilizing additive to be used with the soil was then uniformly mixed with the soil and the specimens compacted by the effort indicated in Column 6. The differences in water content values shown in Columns 3 and 4 indicate the drying effect of the stabilizing additive. Column 8 indicates that the field water content of the various soils had stabilized just prior to adding and mixing the additives.

Plate bearing tests were conducted at the top of subgrade in items 3 and 5, at the top of stabilized subbase in test item 1, and at the top of the base course in items 2-4. Plate bearing tests were run 10, 8, 9, and 5 days after completion of construction in items 1, 2, 3, and 4, respectively. The k_u values as determined from the plate bearing tests are shown in Column 9 of Table 4. The CBR, water content, and density data shown in Columns 10, 11, and 12 were obtained at the completion of compaction of the various layers of material. The percent laboratory density was based on the laboratory density of treated or untreated material (including additives) as actually used in the test section. As can be seen, the heavy clay subgrade soil was compacted at a water content considerably on the wet side of optimum. Therefore, the percent compaction indicated for this material was based on the laboratory density at the field in-place water content.

A summary of stability, flow, voids, and density data for laboratory and field-compacted asphaltic concrete specimens is given in Table 9. The mixture used for laboratory compaction was plant-mixed and was the same as the mixture placed in the field except that the asphalt content was reduced from 4.1 to 3.9 percent for the test section pavement. Data from the field-compacted mixture were determined from cores cut immediately after compaction and after various coverages of traffic. These data will be discussed in more detail later in this report.

Table 9

Summary of Stability, Flow, Voids, and Density Data for Asphaltic Concrete Specimens

Test Item No.	Traffic Lane No.	Surfaces	Asphalt		Marshall Stability lb	Flow Units of 1/100 in.	Percent Voids		Unit Weight Total Mix pcf	Percent Laboratory Density
			Content Percent of Total Weight				Total Mix	Filled with Asphaltic Concrete		
--	--	--	4.1		2393	10	4.5	67.6	147.2	100.0
Plant-Mixed Laboratory Compacted Samples*										
Field Cores										
1	1,2	0	3.9		549	12	7.6	53.4	142.8	97.0
	1	1200	3.9		1231	13	6.0	59.9	145.4	98.8
	1	2500	3.9		839	11	7.5	53.7	143.1	97.2
	1	4000	3.9		848	16	6.6	57.3	144.4	98.1
2	1,2	0	3.9		648	11	8.4	50.6	141.7	96.3
	1	1200	3.9		1098	12	6.7	56.8	144.5	98.2
	1	2500	3.9		840	11	6.4	57.9	144.7	98.3
	1	3600	3.9		900	14	6.2	58.5	145.0	98.5
3	1,2	0	3.9		539	12	8.0	51.8	142.2	96.6
	1	1200	3.9		1061	12	6.8	56.5	144.2	98.0
	1	2500	3.9		1163	8	6.5	57.5	144.6	98.2
	1	3600	3.9		1310	12	5.8	60.5	145.7	99.0
4	1,2	0	3.9		519	10	8.6	50.0	141.3	96.0
	1	1200	3.9		1112	12	6.4	58.0	144.8	98.4
5	1,2	0	3.9		454	14	8.4	50.6	141.6	96.2
	1	1200	3.9		1077	10	7.2	53.4	143.6	97.6
	1	2500	3.9		1005	9	6.5	57.5	144.6	98.2
1	2	600	3.9		1536	12	6.2	58.7	145.0	98.5
2	2	400	3.9		1588	13	6.7	56.7	144.3	98.0
3	2	400	3.9		1215	13	6.0	59.7	145.4	98.8
4	2	1200	3.9		566	15	9.3	50.9	141.8	96.3
5	2	300	3.9		1444	15	5.9	59.9	145.5	98.8

* Specimens were compacted with a gyratory compactor at 240-psi pressure and 1-deg pitch for 30 revolutions.

TESTING AND BEHAVIOR UNDER TRAFFIC

SELECTION OF TRAFFIC LOADINGS

Prior to the start of traffic, evaluations of the load-carrying capacity of the rigid pavement test items were made using the as-constructed material test data shown in Tables 3 and 4. The evaluations resulted in the selection of a 200-kip twin-tandem loading (B-747 spacing) for lane 1 of the rigid pavement test section.

Using results of unconfined compression tests of field-mixed, laboratory compacted samples, estimates were made of stiffness and strength values for the stabilized items of the flexible pavement test section. Then, by using layered elastic theory, stresses, strains, and deflections were computed for three loadings (200, 220, 240 kips on twin-tandem assemblies). Estimates of the number of coverages each item could carry were then made using the correlations developed and presented in Barker et al.²⁸ Based on this analysis, the 200-kip twin-tandem load was also chosen for lane 1 of the flexible pavement test section, and a 50-kip single-wheel load was selected for the test items with insulated layers. At the conclusion of traffic on lane 1 of both the rigid and the flexible pavement test sections, the responses of the various items were evaluated, and a 240-kip twin-tandem load was selected for trafficking lane 2 of both test sections.

TEST CONDITIONS AND PROCEDURES

Traffic tests were performed on two test lanes on the 50-ft-wide, 290-ft-long rigid pavement test section (Figure 1) and on three test lanes on the flexible pavement test section (Figure 7). Lanes 1 and 2 of the flexible pavement test section were on the 40-ft-wide, 200-ft-long section, and lane 3 was on the 10-ft-wide, 80-ft-long insulating materials section. The load carts, test lanes, traffic patterns, pavement conditions, and failure criteria are discussed in the following paragraphs.

LOAD CARTS

Traffic was applied to lanes 1 and 2 on both test sections with the twin-tandem load cart shown in Figure 44. The test cart consisted of a load box supported by an A-frame and was towed by a Caterpillar Model 619 tractor. The load box was carried by four wheels arranged as shown in Figure 45. The test cart was loaded to a net weight of 200 kips (50 kips per wheel) for trafficking lane 1 and to 240 kips (60 kips per wheel) for trafficking lane 2. Tires on the load cart were 56x16 with a 38 ply rating. The tire contact area for both loads was maintained at 267 sq in. by using inflation pressures of 190 and 250 psi for the 200- and the 240-kip loads, respectively. The 50-kip single-wheel assembly load cart used to apply traffic on lane 3 of the flexible pavement test section is shown in Figure 46. The load cart consisted of a load box supported by an A-frame and was towed by a Tournapull Super C tractor. The load box was carried by a single 56x16, 32-ply tire and was loaded to 50 kips. The tire was inflated to 200 psi, giving a contact area of 267 sq in.



Figure 44. Twin-tandem assembly load cart

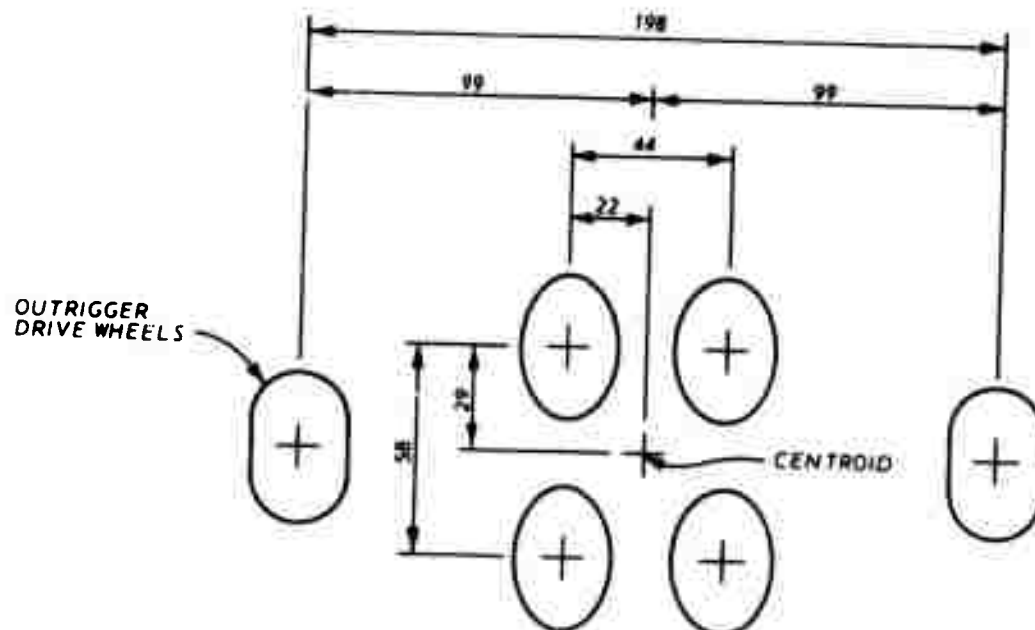


Figure 45. Wheel arrangement for twin-tandem assembly



Figure 46. Single-wheel assembly load cart

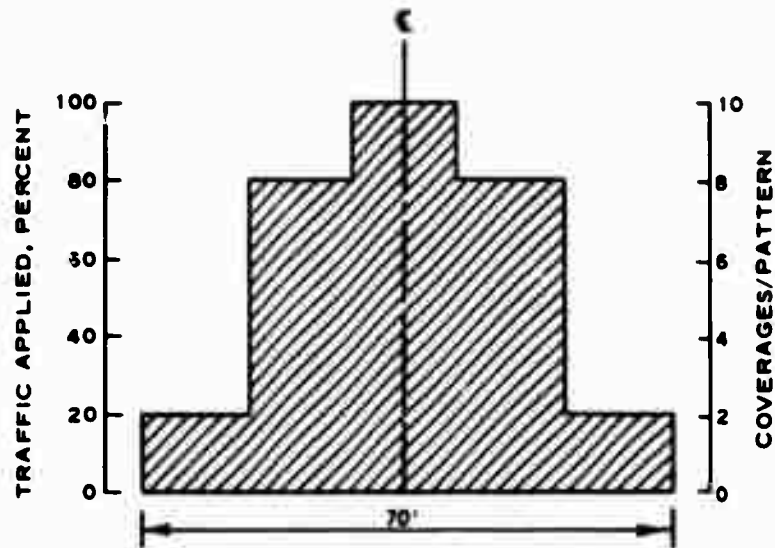
TRAFFIC LANES

Figures 1 and 7 show the location and width of each test lane on the rigid and flexible pavement sections, respectively. Each lane consisted of a portion of the test section on which no traffic had previously been applied. Lanes 1 and 2 on both the rigid and flexible pavement sections were 10 ft wide and ran the full length of the test sections. Lane 1 on the rigid pavement section was laid out so that the longitudinal construction joint in the section coincided with the edge of the area that received 100 percent of the traffic. Test lane 2 on the rigid pavement section was laid out approximately at the center of the north slabs with no longitudinal joints in the traffic lane in items 1-4, but a weakened-plane longitudinal joint was included in item 5. Test lane 3 was 5.83 ft (70 in.) wide and 80 ft long.

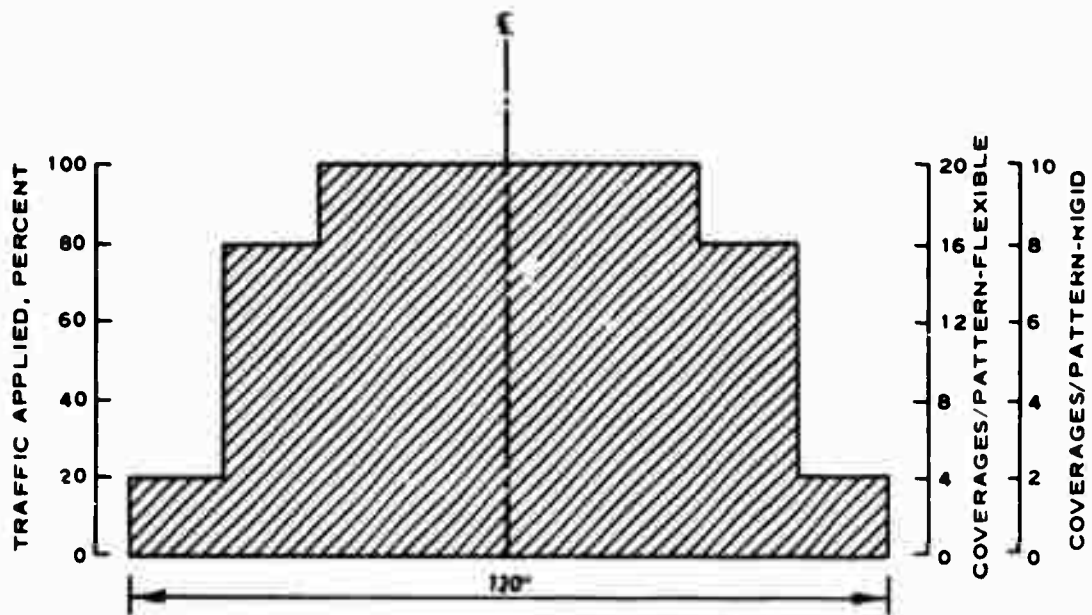
TRAFFIC PATTERNS

Two types of traffic patterns were used in applying the test traffic. Layouts of the two patterns are shown in Figure 47. The lateral distribution of traffic over the traffic lanes was arranged in a pattern to simulate the actual traffic distribution experienced on a prototype runway. The coverage levels referred to in this report are the total number of coverages applied in the 100 percent coverage zone.

Traffic was applied with the twin-tandem assembly load cart in the pattern shown in Figure 47b using five guidelines which were painted on the pavement 15 in. apart. To apply the traffic over the 10-ft-wide traffic lane in the pattern depicted, the load cart first traveled the full length of the test lane along guideline 1 (south side of the traffic lane) and then traveled back along the same line. The cart was shifted laterally to guidelines 2-5 in succession, and a pass in each direction was applied along these guidelines. Additional passes in each direction were applied to guidelines 4, 3, 2, 2, 3, 4, 4, 3, 2, and 3, in that order. A traffic pattern for the twin-tandem assembly required



a. 50-KIP SINGLE-WHEEL ASSEMBLY



b. 200- OR 240-KIP TWIN-TANDEM ASSEMBLY

Figure 47. Traffic patterns

30 passes of the load cart and resulted in 10 coverages* in the center 60 in. of the test lane for the rigid pavement and 20 coverages in the center 60 in. for the flexible pavement and a lesser number of coverages along the edges.

Traffic applied with the single-wheel assembly load cart on lane 3 was in the pattern shown in Figure 47a using five guidelines painted on the pavement approximately 14 in. apart. To apply the traffic pattern depicted, the load cart first traveled the full length of the test lane along guideline 1 (south edge of the traffic lane) and then was shifted laterally to guidelines 2-5 in succession for 1 pass in each direction on each line. Therefore, when the load cart had traversed the full distance across the test lane, a total of 2 coverages had been applied over the test lane. Guidelines 2 and 4 were traveled three more times in each direction, and guideline 3 was traveled four more times in each direction. This application resulted in the desired coverage pattern. The interior 14 in. of the traffic lane received 100 percent of the traffic, and the exterior portions of the lane received 80 and 20 percent as shown in Figure 47a.

FAILURE CRITERIA

Flexible Pavement Items. In judging failure of the flexible pavement test items, a distinction was made between settlement due to traffic compaction and distortion due to shear deformation. Settlement, which is the result of densification of the base or subbase under accelerated traffic, was anticipated because it was not possible to apply a heavy compaction effort on the lower layers of the subbase or base course in the thin layers placed over the subgrade or in the thin layers placed over insulating materials. The term "shear deformation" as used

* For rigid pavements, the number of coverages is a measure of the number of maximum stress repetitions that occur in the pavement due to the applied traffic. A coverage occurs when each point of the pavement within the test lane has been subjected to a maximum stress, assuming the stress is equal under the full tire print width. For the twin-tandem gear, the front and rear twin wheels are sufficiently close that only one maximum stress repetition occurs for each pass of the gear.

herein refers to excessive plastic movement or, in extreme cases, to rupture of any element in the pavement structure. A flexible pavement item was considered failed when either of the following conditions occurred:

- a. Surface upheaval of the pavement adjacent to the traffic lane reaches 1 in. or more.
- b. Cracking extends through the asphaltic concrete layer.

Plain Portland Cement Concrete Items. For the plain portland cement concrete items in the rigid pavement test section, there were three conditions that were considered to constitute failure:

- a. Initial crack failure. A crack that is visible at the surface of the pavement, extends through the depth of the concrete slab, and is caused by traffic loading constitutes the initial crack failure condition. This should not be confused with surface cracking resulting from such minor defects as spalls, popouts, shrinkage, etc. It must also be recognized that concrete may crack during its early life due to causes other than traffic loadings, and any such cracks should not be construed as denoting the initial crack failure condition.
- b. Shattered slab failure. Cracking that is visible on the pavement surface or subdivides a pavement slab into six pieces or more constitutes the shattered slab failure condition. The cracking must be associated with traffic loading rather than resulting from some minor defect or early life cracking prior to application of traffic.
- c. Complete failure. Cracking that is visible on the pavement surface and subdivides the pavement slab into individual pieces having an area of less than about 15 to 20 sq ft each and that is characterized by relatively large permanent deformations and faulted cracks or joints constitutes complete failure.

Fibrous-Reinforced Concrete Items. In identifying failure of the fibrous-reinforced concrete items, consideration was given to the extent of cracking in the pavement and the amount of permanent deformation in the traffic lane. The initial cracks in fibrous-reinforced concrete do not appear to affect the structural performance of the pavement as they do in nonreinforced concrete. Cracks in the fibrous-reinforced concrete do not open up and spall under traffic as is the case with nonreinforced concrete. The fibrous-reinforced concrete was considered failed when either of the following conditions occurred:

- a. The crack pattern becomes concentrated enough that small areas of the pavement begin to break away and develop into potentially damaging foreign objects.
- b. Permanent deformation in the traffic lane exceeds 1 in.

APPLICATION OF TRAFFIC

Traffic was applied to the test sections during the period 4 October 1972-8 May 1973. Schedules of the application of traffic on lane 1 of both test sections are shown in Figure 48. Schedules of the application of traffic on lane 2 of the rigid pavement test section and lanes 2 and 3 of the flexible permanent test section are shown in Figure 49. Most of the traffic was applied on days with no rain, but some traffic was applied during light rainfall and immediately after rainfall.

PAVEMENT TEMPERATURES

Thermistors installed at various elevations in the pavement structure as shown in the instrumentation layout in Figures 13-15 were used to record temperature readings periodically during the application of traffic. Figure 50 shows the maximum and minimum temperatures recorded at 1/4 in. below the surface of pavement, the maximum and minimum ambient temperatures, and the average temperature at the interface of the portland cement concrete surfacing and the bituminous base course in item 3 of the rigid pavement test section. Pavement temperature versus traffic distribution curves for each item of lanes 1 and 2 of the flexible pavement test section are shown in Figures 51 and 52, respectively.

COLLECTION OF INSTRUMENTATION DATA

Before applying any traffic, static load instrumentation measurements were made on all items of the test sections. Single-wheel loadings used were 30 and 50 kips, with 90- and 190-psi tire pressures, respectively. In addition, before applying any traffic, static load instrumentation readings were made with the 240-kip twin-tandem assembly (250-psi tire pressure) on lane 2 of both test sections. As shown in Table 10, static load measurements were made throughout the traffic life of the test sections. At frequent intervals during traffic, dynamic

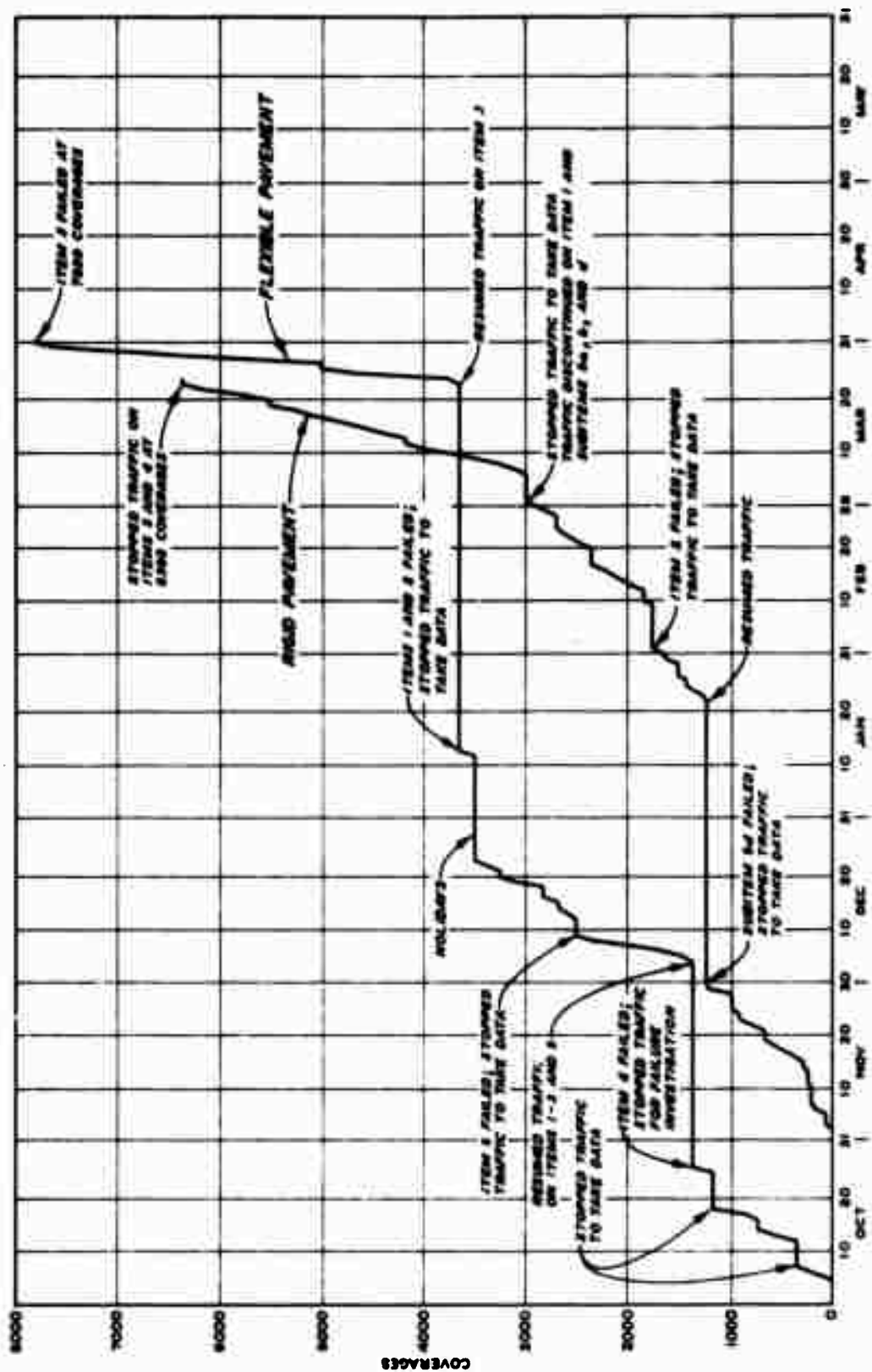


Figure 48. Traffic log for lane 1 of both test sections

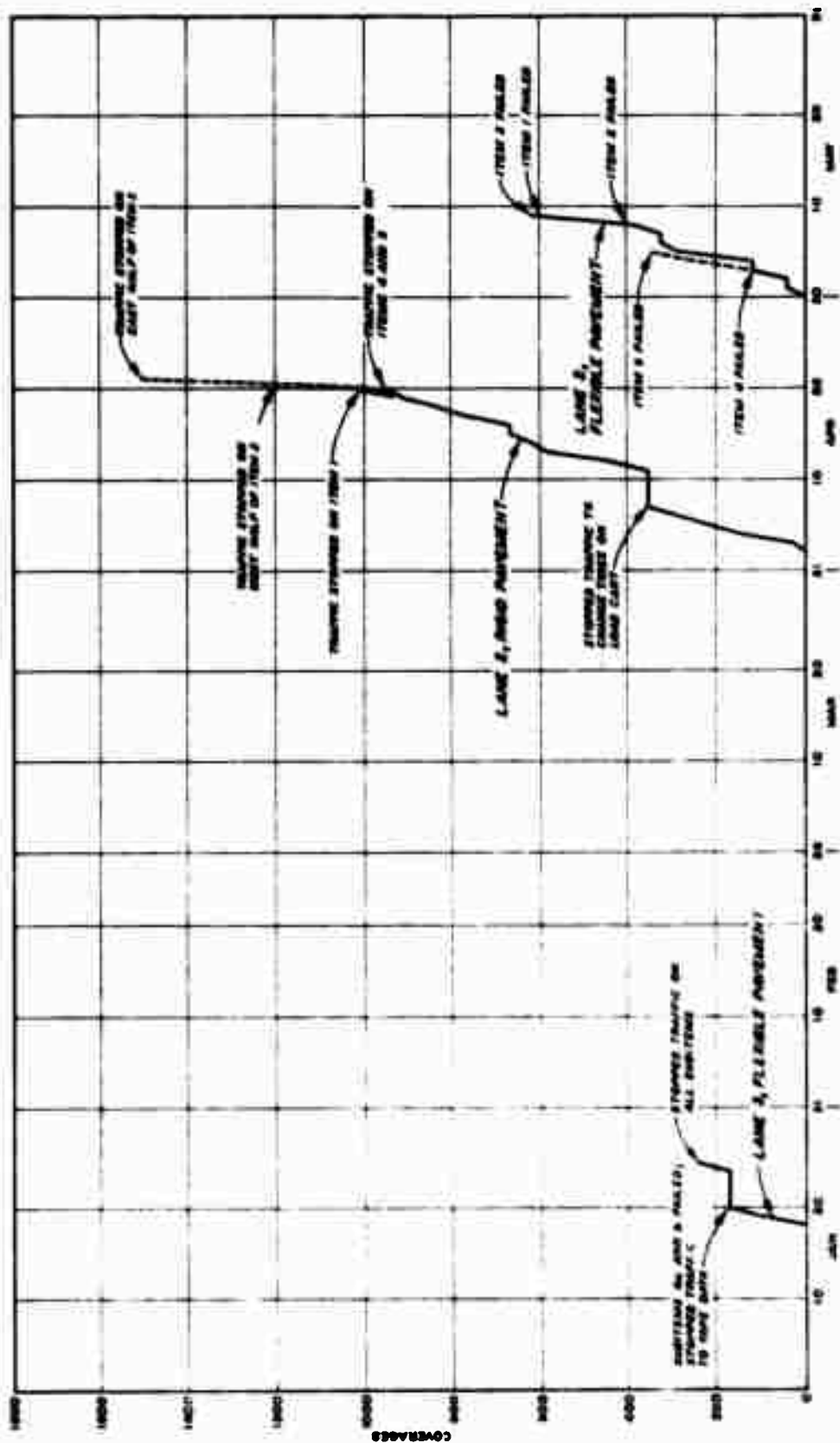


Figure 49. Traffic log for lane 2 of the rigid pavement test section and for lanes 2 and 3 of the flexible pavement test section

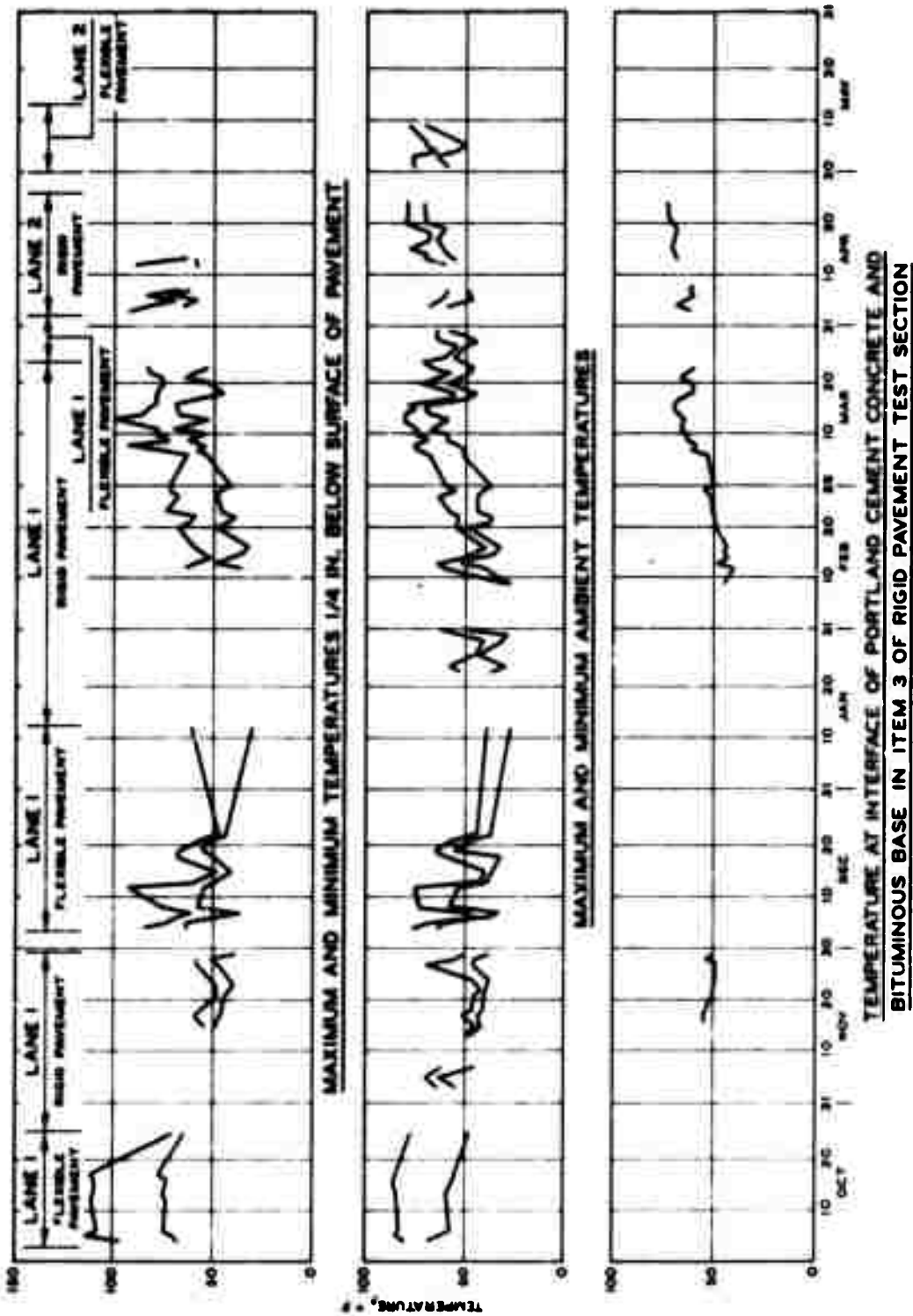


Figure 50. Temperature data

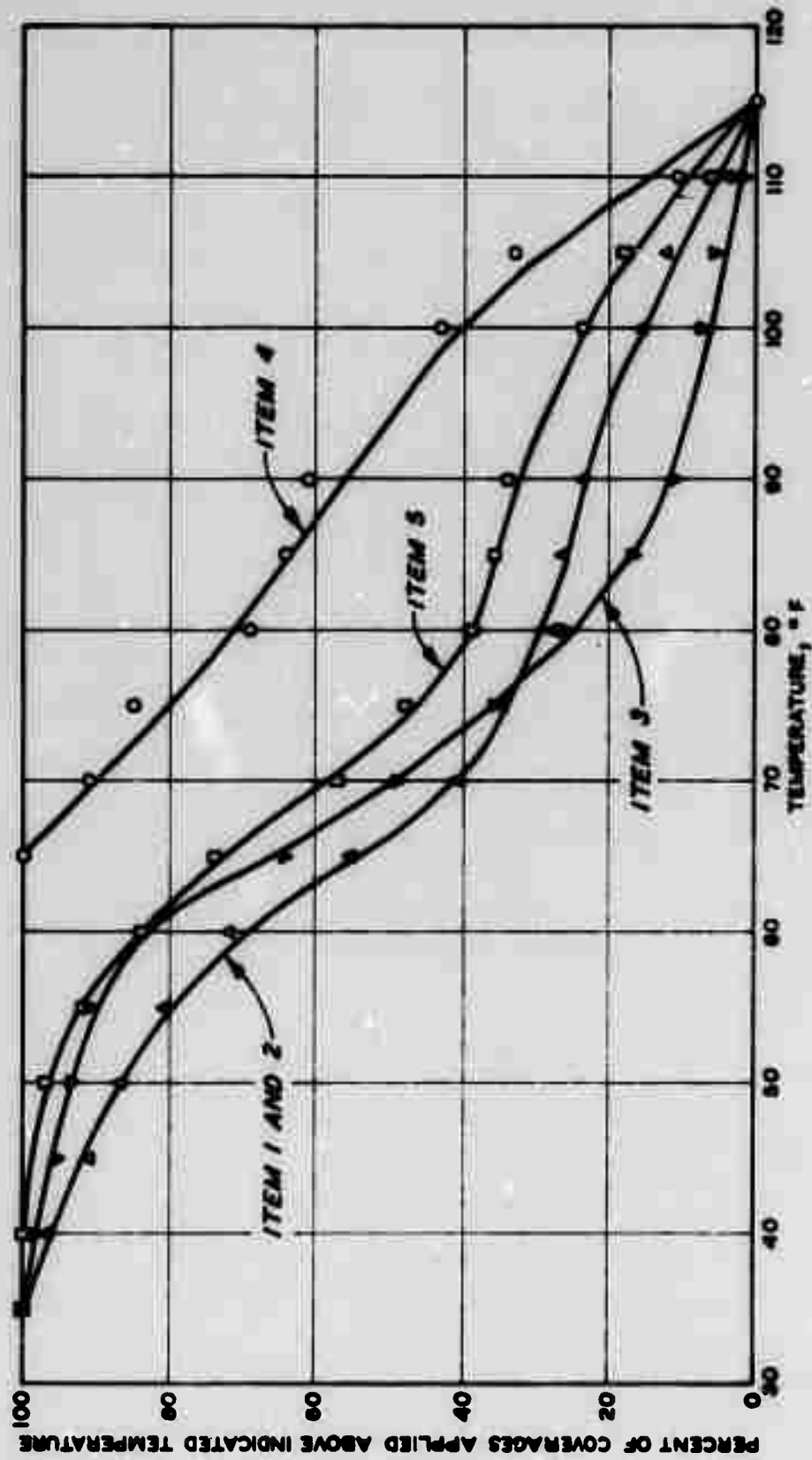


Figure 51. Pavement temperature versus traffic distribution for lane 1 of the flexible pavement test section

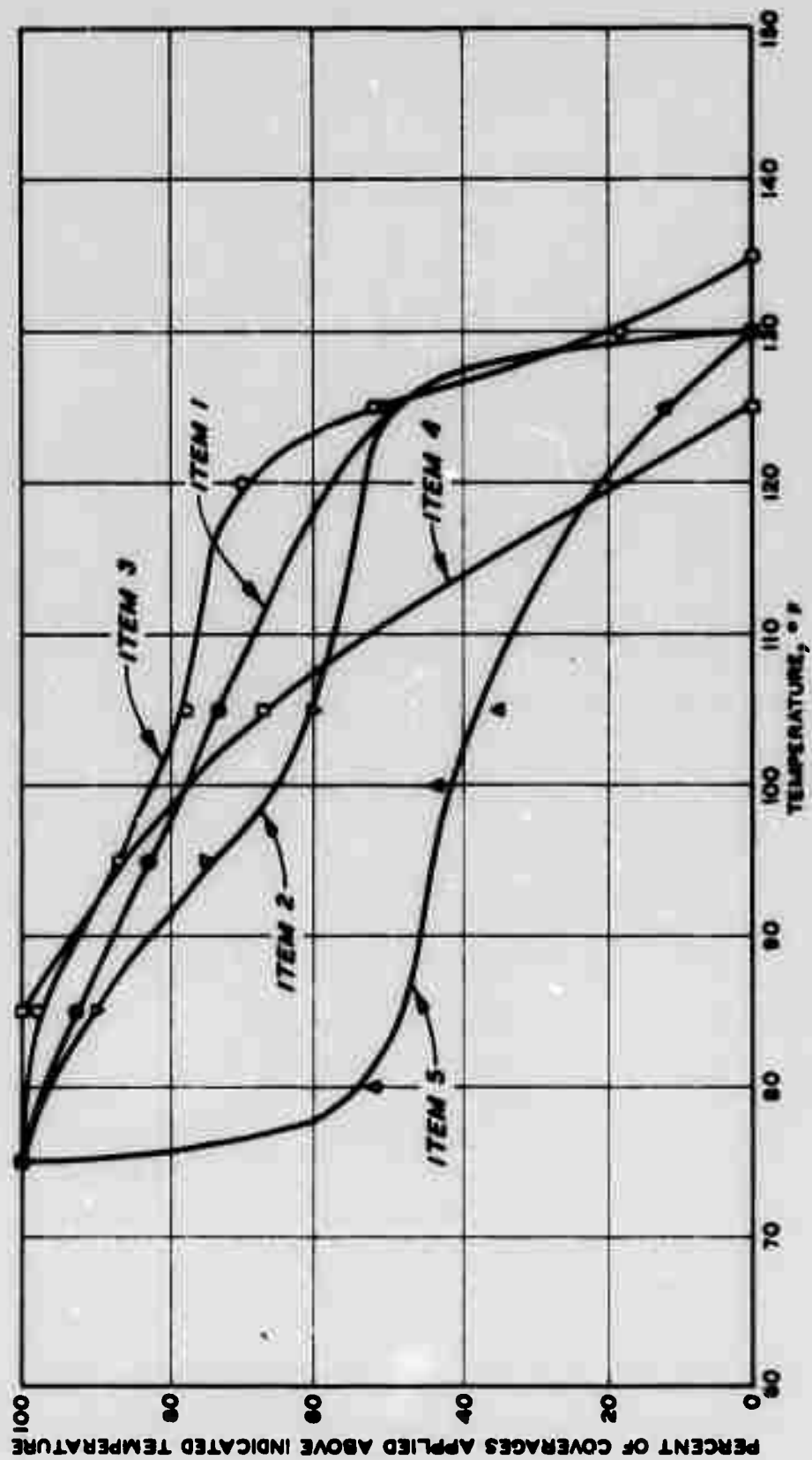


Figure 52. Pavement temperature versus traffic distribution for lane 2 of the flexible pavement test section

Table 10
Coverage Levels of Static Load Instrumentation Tests

[illegible]

- Strain sensors recorded on WEC multichannel equipment.

The instruments in Lane 2 of item 5.

* Strain sensors recorded with both Bison console and VES multichannel equipment.

(slowly moving) load response measurements were also recorded. The results of these measurements will be reported in subsequent volumes.

BEHAVIOR OF PAVEMENTS UNDER TRAFFIC

Visual observations of the behavior of the test items for each lane were recorded throughout the traffic test period. These observations were supplemented by photographs, electronic instrumentation readings, rod and level readings, and plots of cracks occurring at various locations. Rod and level readings were taken on the pavement surface at preselected points on each item prior to and at intervals during traffic to show the development of permanent pavement deformation and deflection of the pavement under the assembly load for the lane being observed. After failure, a thorough investigation was made by excavating test trenches across the traffic lanes and by establishing profiles of the surface of the various layers in the structure, along with strength measurements and other pertinent tests to determine where failure had occurred. Tables 11 and 12 summarize the pertinent physical property data and results of traffic testing on the rigid and flexible pavement test sections, respectively. The behavior of each item under traffic is summarized below. The data obtained during the traffic tests are presented in Appendixes A and B for the rigid and flexible pavement test sections, respectively.

RIGID PAVEMENT TEST SECTION

Item 1. The pavement structure in item 1 consisted of 7 in. of fibrous-reinforced concrete over a 20-in.-thick MESL base course. At 3000 coverages of the 200-kip load, the entire item was severely cracked and was considered to have reached the complete failure condition. Under the 240-kip load in lane 2, cracking became severe over the entire item at 1010 coverages, and the item was considered to have reached the complete failure condition.

Item 2. Item 2 consisted of 4 in. of fibrous-reinforced concrete on a 17-in.-thick base course composed of clay gravel stabilized with 6 percent portland cement. The item was considered completely failed at

Table 11

Summary of Traffic Test Data for Rigid Pavement Test Section

Item No.	Trsf. Lane No.	Subgrade				Base Course				Pavement				Performance Data			
		Water Content, %		Dry Density, pcf.		Modulus of Soil Reaction		Thick-ness		Thick-ness, in.		Concrete Strength, psi		Maximum Static Deflection, in.		Maximum Permanent Deflection, in.	
		As Constructed	After Trsf.	As Constructed	After Trsf.	As Constructed	After Trsf.	As Constructed	After Trsf.	As Constructed	After Trsf.	As Constructed	After Trsf.	As Constructed	After Trsf.	As Constructed	After Trsf.
1	1	29.8	--	89.1	--	47	180	175	230	7.1	7.0	735	992	0.54	0.7	1000	1800
2	1	29.8	27.7	89.1	92.1	47	200	175	290	7.3	7.8	805	1097	0.37	0.7	200	690
	2	34.1	33.1	85.0	85.5	85	118	545	490	4.4	4.0	695	1177	0.42	2.1	500	1200
3	1	34.1	--	85.0	--	85	--	545	375	4.3	4.0	810	1120	0.46	3.2	150	400
	2	32.2	--	87.0	--	84	--	99	255	14.8	14.6	500	897	0.30	0.8	1770	6360
4	1	32.2	--	87.0	--	84	--	99	255	14.7	--	500	897	0.17	0.8	1660	--
	2	32.2	33.5	87.0	--	84	164	99	--	14.9	--	515	910	0.20	0.2	390	--
5	1	32.2	33.5	87.0	--	84	164	99	--	15.2	14.9	515	910	0.24	0.2	--	--
	2	33.1	33.3	86.2	86.0	40	68	167	200	14.4	--	540	982	0.16	1.5	1660	5500
6	1	33.1	33.3	86.1	86.0	40	68	167	200	14.4	14.6	540	982	0.15	1.5	1660	5850
	2	33.1	--	86.1	--	40	--	167	328	14.3	14.8	470	605	0.26	0.2	100	--
7	1	33.1	--	86.1	--	40	--	167	328	14.5	--	470	605	0.23	0.2	40	--
	2	--	--	--	--	--	--	--	180	14.7	14.7	540	965	0.38	1.4	--	Joint failure
8	1	--	--	--	--	--	--	--	--	15.5	--	545	--	0.40	0.7	290	Joint failure
	2	--	--	--	--	--	--	--	--	14.7	--	540	--	0.28	0.9	--	Joint failure
9	1	--	--	--	--	--	--	--	120	15.2	--	545	--	0.42	1.9	390	Joint failure
	2	--	--	--	--	--	--	--	--	15.0	--	540	--	0.15	0.6	1000	1230
10	1	--	--	--	--	--	--	--	63	15.3	15.1	545	868	0.43	1.1	390	Joint failure
	2	30.0	--	90.4	--	120	--	--	--	15.1	--	540	--	0.21	0.4	1080	Joint failure
11	1	30.9	--	89.1	--	143	--	--	103	15.1	--	540	--	0.21	0.4	1080	Joint failure
	2	--	--	--	--	--	--	--	--	15.4	--	545	--	0.53	0.7	20	700

* Determined from level readings.

** Measured from beam samples.

† Determined from 28-day construction control tests.

†† Representative values based on beam samples cut from pavement.

‡ Traffic was discontinued before item reached failure condition shown.

Table 12
Summary of Traffic Test Data for Flexible Pavement Test Section

Traffic Load	Load per Tire lb	Tire Inflation Pressure psi	Tire Contact Area sq. in.	Item No.	Rated Subgrade CB	No. of Cycles	Maximum Permanent Deformation in.	Maximum Deflection in.	Maximum Upheaval in.	Pavement Cracking	Rating of Item
1 750-kip twin-tandem	30,000	180	267	1	3.8	0	0.0	0.17	--	--	--
						1200	0.8	0.23	--	None	Satisfactory
						3660	1.2	0.21	--	Severe	Failed
				2	3.4	0	0.0	0.28	--	--	--
						1200	0.7	0.30	--	Slight	Satisfactory
						3660	1.1	0.23	--	Severe	Failed
				3	3.0	0	0.0	0.23	--	--	--
						3660	1.4	0.21	--	None	Satisfactory
						7820	1.5	0.21	--	Severe	Failed
				4	4.9	0	0.0	0.34	--	--	--
						320	0.7	0.29	--	None	Satisfactory
						1380	1.3	0.49	0.4	Severe	Failed
2 240-kip twin-tandem	60,000	250	267	1	4.4	0	0.0	0.25	--	--	--
						320	1.4	0.47	0.4	Slight	Satisfactory
						600	3.2	0.60	1.0	Severe	Failed
				2	4.0	0	0.0	0.24	--	--	--
						120	0.7	0.42	1.2	Slight	Satisfactory
						340	1.4	0.44	1.7	Severe	Failed
				3	3.2	0	0.0	0.21	--	--	--
						320	1.2	0.38	1.0	None	Satisfactory
						620	2.5	0.48	2.3	Slight	Failed
				4	5.2	0	0.0	0.38	--	--	--
						40	0.8	0.43	--	Slight	Satisfactory
						120	1.7	0.90	--	Severe	Failed
3 50-kip single-wheel	50,000	200	267	4a	4.2	0	0.0	0.16	--	--	--
						170	1.3	0.36	0.3	Severe	Failed
						240	1.5	--	1.1	Severe	
				4b	4.2	0	0.0	0.10	--	--	--
						170	1.4	0.28	0.2	Severe	Failed
						240	1.8	--	1.1	Severe	
				4c	4.2	0	0.0	0.06	--	--	--
						170	1.0	0.20	0.3	Slight	Satisfactory
						240	2.7	--	1.5	Severe	Failed
				4d	4.2	0	0.0	0.06	--	--	--
						170	1.0	0.29	0.3	Slight	Satisfactory
						240	2.7	--	1.4	Severe	Failed
				5a	4.1	0	0.0	0.08	--	--	--
						170	0.8	0.08	--	Slight	Satisfactory
						240	1.0	--	--	Severe	Failed
				5b	4.1	0	0.0	0.09	--	--	--
						170	0.6	0.08	--	None	Satisfactory
						240	1.0	--	0.3	Slight	Failed
				5c	4.1	0	0.0	0.15	--	--	--
						170	1.0	0.12	--	Slight	Satisfactory
						240	1.2	--	0.3	Severe	Failed
				5d	4.1	0	0.0	0.14	--	--	--
						170	1.2	0.12	--	Slight	Satisfactory
						240	1.3	--	0.2	Severe	Failed

1770 coverages of the 200-kip load and at 740 coverages of the 240-kip load. Both failures were due to severe cracking of the fibrous-reinforced concrete.

Item 3. Item 3 consisted of 15 in. of plain portland cement concrete over a 6-in.-thick bituminous base course. At the conclusion of traffic of the 200-kip load (6360 coverages), a shattered slab failure had developed in the southwest slab; only initial crack failure had been reached in the northwest and southeast slabs; and no cracks had developed in the northeast slab. Under the 240-kip load, severe spalling occurred along crack paths and at transverse joints. In lane 2, 1200 coverages of the 240-kip load were applied to the western half of the item, and 1500 coverages were applied to the eastern half of the item.

Item 4. Item 4 consisted of 15 in. of plain portland cement concrete over a 6-in.-thick base course of lean clay stabilized with 12 percent portland cement. After 6360 coverages of the 200-kip load, the item had numerous severe cracks, and pumping had occurred at the transitions and at the transverse weakened-plane joint. Shattered slab conditions were reached at 5500 coverages and 5850 coverages on the southwest and southeast slabs, respectively. Traffic was discontinued on the item before complete failure occurred. Under the 240-kip load, the initial crack failure condition was reached at 100 coverages and 40 coverages on the northwest and northeast slabs, respectively. Traffic was discontinued before other failure conditions were reached.

Subitem 5a. The pavement structure in subitem 5a was composed of 15 in. of plain portland cement concrete and a 6-in.-thick base course of lean clay stabilized with 12 percent portland cement over 3-in.-thick 35-psi polystyrene panels. At 3000 coverages of the 200-kip load, spalling along the longitudinal joint became severe, and two hairline transverse cracks developed in the north slab. Pumping, which was first noted at the transverse joints after 750 coverages, became more severe with application of additional traffic and continued for 2 to 3 hr after rainfall stopped. The initial crack failure condition was reached in

subitem 5a at 290 coverages of the 240-kip load. Severe spalling along the weakened-plane joint occurred by 740 coverages. The cement-stabilized lean clay base course material began pumping through the cracks in the pavement at about 350 coverages, and the pumping became progressively more severe with additional applications of the 240-kip load.

Subitem 5b. Subitem 5b consisted of 15 in. of plain portland cement concrete over 9 in. of lightweight concrete. Spalling parallel to the longitudinal construction joint was severe when traffic with the 200-kip load was discontinued after 3000 coverages. During the 200-kip load trafficking, pumping was first observed along the transverse joint on the east edge of the subitem at 340 coverages and then occurred at 750 coverages along the transverse joint on the west edge of the subitem. Under the 240-kip load, the initial crack failure condition occurred at 350 coverages, and traffic was discontinued at 740 coverages. Pumping began along the east end transverse joint at 320 coverages and increased with continued application of traffic.

Subitem 5c. Subitem 5c consisted of a 15-in.-thick layer of plain portland cement concrete over 3-in.-thick 120-psi polystyrene panels. At 1230 coverages of the 200-kip load, the south slab of the subitem had reached the shattered slab failure condition. Pumping was observed along the east transverse joint at 220 coverages. At 340 coverages, pumping had become severe with liquified subgrade material being extruded through the transverse joints on both sides of the south slab. Pumping continued with application of additional traffic and was observed for 2 to 3 hr after rainfall stopped. Under the 240-kip load, the initial crack failure condition was reached at 350 coverages. At 740 coverages, severe spalling had occurred along the weakened-plane joint. Pumping began between subitems 5b and 5c at 320 coverages and became more severe as cracks developed in the pavement of the subitems.

Subitem 5d. Subitem 5d consisted of 15 in. of plain portland cement concrete over 3-in.-thick 35-psi polystyrene panels. The initial crack failure condition was reached at 1080 coverages of the 200-kip

load. When traffic on lane 1 was discontinued at 3000 coverages, spalling along the longitudinal construction joint extended almost the full length of the subitem. Minor pumping occurred under traffic. Under the 240-kip load, the shattered slab condition was reached at 200 coverages, and severe spalling was occurring at 350 coverages when traffic was discontinued.

FLEXIBLE PAVEMENT TEST SECTION

Item 1. The pavement structure in item 1 was a 3-in.-thick asphaltic concrete wearing course over 6 in. of crushed limestone base course material and a 24-in.-thick subbase of lean clay that was stabilized with 3 percent hydrated lime, 2 percent portland cement, and 10 percent fly ash. This item was failed by 3660 coverages in lane 1 of the 200-kip load and by 600 coverages in lane 2 of the 240-kip load. Severe cracking that extended through the asphaltic concrete occurred under traffic in both lanes.

Item 2. Item 2 contained 3 in. of asphaltic concrete wearing course over a 25-in.-thick base course of lean clay stabilized with 12 percent portland cement. This item failed under 3660 and 320 coverages of the 200- and 240-kip loads on lanes 1 and 2, respectively. In both traffic lanes, severe cracks penetrated the full depth of the asphaltic concrete.

Item 3. Item 3 consisted of 3 in. of asphaltic concrete over 25 in. of gravelly sand stabilized with 5 percent portland cement. Traffic by the 200-kip load was discontinued after 7820 coverages in lane 1 when cracks penetrated the full depth of the asphaltic concrete. Cracking of the pavement in lane 2 (under the 240-kip load) was never severe, but the item was considered failed after 620 coverages because of the excessive upheaval and deformation of the pavement.

Item 4. Item 4 consisted of 3 in. of asphaltic concrete with a 25-in.-thick base course of clayey sand stabilized with 5 percent portland cement. The item was failed by 1380 coverages of the 200-kip load and by 120 coverages of the 240-kip load. Failure was attributed to

shear deformation in the base course and to severe cracks that extended through the asphaltic concrete of each lane.

Item 5. Item 5 contained 3 in. of asphaltic concrete over 6 in. of crushed limestone and 33 in. of gravelly sand. Under the 200- and 240-kip loads, the item was considered failed at 2500 and 340 coverages, respectively, due to severe cracking that had penetrated the full depth of the asphaltic concrete in each lane.

Subitems 4a-d. Subitems 4a-d of the insulating materials section (lane 3) consisted of 3 in. of wearing course over a 25-in.-thick stabilized clayey sand subbase course that included insulating materials that were placed at the depths in the subitems shown in Figure 8. All four subitems developed severe cracks under the 50-kip single-wheel load and were considered failed when the cracks penetrated the full depth of the asphaltic concrete. Subitems 4a and b failed at 170 coverages, and subitems 4c and d failed at 240 coverages.

Subitems 5a-d. Subitems 5a-d contained 3 in. of asphaltic concrete over 6 in. of crushed limestone base course and a 33-in.-thick subbase course of gravelly sand that incorporated insulating materials at the depths shown in Figure 8. Subitems 5a, 5c, and 5d sustained severe cracks and 5b sustained slight cracks under the 50-kip single-wheel load. All subitems were considered failed at 240 coverages when the cracks extended through the full depth of the asphaltic concrete.

SUMMARY OF TRAFFIC TEST DATA

RIGID PAVEMENT TEST SECTION

Table 11 presents a summary of pertinent physical property data and results of traffic testing on the rigid pavement test section. Much of this data is self-explanatory; however, some of the columns needing further explanation are discussed in the following paragraphs.

Subgrade Modulus of Soil Reaction. After-traffic tests showed that the modulus of soil reaction k_u of the subgrade increased in all items. The largest increase occurred in item 1 where the value increased

from 47 pci during construction to an average of 180 pci after traffic. This increase was probably due to the increase in dry density from 89.1 to 92.1 pcf, with a corresponding decrease in water content of 29.8 to 27.7 percent. The increase in density probably occurred during construction of the MESL base course in the item. Items 2 and 4 showed smaller increases in k_u (see Table 11), but the water content and density in these items were approximately the same after traffic as before traffic. Item 3 showed an increase in k_u from 84 to 164 pci; the water content in the subgrade was approximately the same after traffic as before traffic, but no density measurements were taken after traffic. Determinations of k_u were not made in item 5 during construction. Since k_u values obtained in items 1-4 were about the same during construction and since the subgrades in all items were constructed at the same time, it is assumed that the subgrade modulus in item 5 was about the same as that in the other items during construction and that the increase in subgrade modulus in item 5 during traffic was about the same as the increase in the moduli in items 2 and 3.

Base Course Modulus of Soil Reaction. Values of k_u for the base courses determined after traffic were higher than those obtained during construction in all items where construction values were available, except in item 2. In item 1, the average water content after traffic was slightly lower in lane 1 and about 3 percent lower in lane 2 (see Tables 3 and 13) than that during construction. This probably accounts for the increase in k_u in item 1. In item 2, k_u was lower after traffic than during construction (Table 11). During traffic on this item, deformations of 2.1 and 3.2 in. occurred in traffic lanes 1 and 2, respectively. This deformation probably caused a breakdown in the cement-stabilized base course, which resulted in the lower k_u values of the base course. k_u for item 3 was 255 pci after traffic and 99 pci during construction. The temperature of the bituminous base course recorded during the after-traffic testing ranged from 70 to 72 F. The temperature of the bituminous base course was not recorded while the plate bearing tests were being run during construction, but the ambient

Table 13
After-Traffic Test Data for Rigid Pavement Test Section

Item No.	Material	Depth Below Pavement Surface in.	Lane 1			Lane 2		
			k _u Value pci	Water Content Percent	Dry Density pcf	k _u Value pci	Water Content Percent	Dry Density pcf
1	Lean clay MESL	7	230	15.9	100.6	250	12.5	100.1
		13		14.6	96.6	--	--	--
		19		15.0	100.5	--	--	--
		7*	--	--	--	--	20.7*	101.5*
		13*		--	--		22.6*	98.5*
		19*		--	--		22.6*	--
	Heavy clay subgrade	27	180	--	--	200	27.7	92.1
2	Clay gravel with 6 percent port-land cement	4	490	33.1	85.5	375	--	--
	Heavy clay subgrade	21	118	--	--	--	--	--
3	Bituminous base	15	255	--	--	--	--	--
	Heavy clay subgrade	21	--	--	--	164	33.5	--
4	Lean clay with 12 percent port-land cement	15	200	--	--	328	23.3	--
	Heavy clay subgrade	21	68	33.3	86.0	--	--	--
5a	Lean clay with 12 percent port-land cement	15	188	--	--	--	--	--
	Heavy clay subgrade	24	--	--	--	--	--	--
5b	Heavy clay subgrade	24	--	--	--	--	--	--
5c	Heavy clay subgrade	18	--	--	--	120	30.0	90.4
				34.4	85.4			
				34.0	84.8			
5d	Heavy clay subgrade	18	143	30.9	89.1	--	--	--

* Data obtained from observation pit in lane 2 of item 1.

high temperature for that day was 75 F with partly cloudy conditions. This would indicate that the pavement temperature was about 15 to 20 F higher during the construction testing than during the after-traffic testing, which may account for the low k_u value obtained during construction. In item 4, the k_u value was determined 7 days after compaction of the cement-stabilized base course. The higher values obtained after traffic were mainly due to the additional aging of the cement-stabilized material. No tests were conducted during construction of the base courses in item 5; therefore, no comparisons can be made.

Pavements. The as-constructed portland cement concrete pavement thicknesses shown in Table 11 are average values that were determined from a number of level readings taken on the surface of the completed base courses and then on the surface of the pavement in each item. The after-traffic thickness values were determined from the concrete beam samples and were measured at the point at which the beam specimen broke. Flexural strengths in all items were higher after traffic than during construction; however, this was expected because of the aging of the concrete. The increase in strength was within the range anticipated on mixes of this type.

Pavement Performance. Structural cracking and spalling were used for evaluating the performance of the items, and deflection measurements were made to assist in predicting performance. In items 3-5, traffic was stopped before structural cracking had reached any of the conditions of failure except in subitem 5d of lane 2. In both lanes, spalling was severe along the longitudinal joints in most of the subitems of item 5. Maximum deflections were higher in some cases (in item 1 and the west slab of item 3) for lane 1, which was trafficked with the 200-kip twin-tandem load, than in lane 2, which was trafficked with the 240-kip twin-tandem load. The deflection measurements in lane 1 were taken with the load wheels of the load cart adjacent to the longitudinal construction joints, and vertical displacement occurred at this joint. The deflection measurements in lane 2 were taken in the center of the north slab.

FLEXIBLE PAVEMENT TEST SECTION

A summary of the traffic test results for the three traffic lanes on the flexible pavement test section is shown in Table 12. Much of this data is self-explanatory; however, some of the columns needing further explanation are discussed in the following paragraphs.

Rated Subgrade CBR. The rated CBR values of the subgrade shown in Table 12 are based on the numerical averages of the CBR values measured during construction (Table 4) and after traffic (Table 14). The CBR values used were from tests conducted at the surface of the subgrade and at depths of 6 and 12 in. in the subgrade. In lane 1, CBR values obtained after traffic on items 1-4 were somewhat higher than values obtained during construction, but values obtained after traffic on item 5 were about the same as the as-constructed values. Rated subgrade CBR values for lane 1 were 5.6, 5.4, 3.8, 4.9, and 4.0 for items 1, 2, 3, 4, and 5, respectively. The CBR's of the subgrade in items 1-4 were probably affected somewhat by the presence of the cement-treated bases directly over the subgrade. In lane 2, CBR values obtained after traffic were also slightly higher than those obtained during construction in all items except item 3, where the value was slightly lower after traffic than during construction. This decrease in strength was due to an increase in water content of the subgrade. Rated CBR values for lane 2 were 4.4, 4.0, 3.2, 5.2, and 4.2 for items 1, 2, 3, 4, and 5, respectively. In lane 3, CBR values obtained after traffic and during construction were approximately the same. The rated CBR for all subitems in item 4 was 4.2 and for all subitems of item 5 was 4.1.

Deflection. The deflection values shown in Table 12 represent the maximum values measured in the items at the number of coverages indicated.

Maximum Permanent Deformation. The values listed in Table 12 were obtained from cross-sectional measurements taken prior to traffic and at the coverage levels indicated. The maximum deformation occurred within the 100 percent traffic zone and normally was at the center line of the traffic lane.

Table 14
After-Traffic Water Content, Density, and CBR Data for Flexible Pavement Test Section

Item No.	Material	No. of Cored Areas	Depth Below Pavement Surface in.	Inside Traffic Lane				Outside Traffic Lane			
				CBR	Water Content Percent	Dry Density pcf	Percent Lab Density	CBR	Water Content Percent	Dry Density pcf	Percent Lab Density
Lane 1, 800,000-lb Twin-Tandom Assembly											
1	Crushed-stone base	3660	3	65	2.3	154.3	107.2	75	3.3	147.0	102.1
	Lean clay subbase with 3 percent lime, 2 percent portland cement, 10 percent flyash		9	123	20.4	100.1	98.6	97	23.5	97.4	96.0
	Heavy clay sub-grade		33 39 45	7 7 7	31.4 31.8 32.1	88.2 86.0 88.9	100.2 ^a 97.7 ^a 101.2 ^a	8 7 8	30.2 32.0 30.2	87.2 86.9 88.6	96.9 ^a 97.6 ^a 98.1 ^a
2	Lean clay base with 12 percent portland cement	3660	3 9 21	150 ^a 150 ^a 87	15.9 -- --	108.3 -- --	100.4 -- --	150 ^a 150 ^a 77	14.1 -- --	113.4 -- --	105.1 -- --
	Heavy clay sub-grade		28 34 40	7 8 5	29.8 29.2 31.3	89.2 90.2 87.3	99.1 ^a 99.1 ^a 98.1 ^a	7 8 6	30.3 29.0 31.1	89.0 89.7 87.1	98.9 ^a 97.5 ^a 97.9 ^a
	Gravelly sand base with 5 percent portland cement		3	150 ^a	--	--	--	150 ^a	--	--	--
3	Gravelly sand base with 5 percent portland cement	7820	3	150 ^a	--	--	--	150 ^a	--	--	--
	Heavy clay sub-grade		28 34 40	4.8 3.5 3.9	30.6 31.8 32.9	89.0 87.9 86.5	100.0 ^a 99.9 ^a 100.6 ^a	2.7 3.6 3.1	32.7 31.5 32.1	86.7 88.2 86.8	100.8 ^a 100.2 ^a 98.6 ^a
	Clayey sand base with 5 percent portland cement		3 12	70 50	13.1 14.1	118.0 117.8	90.4 90.3	150 ^a 107	11.9 11.4	122.6 115.6	93.9 88.6
4	Heavy clay sub-grade	1380	28 34 40	7 6 4.3	27.3 29.3 32.9	92.4 89.6 84.9	99.4 ^a 98.5 ^a 98.7 ^a	8 6 4.0	25.8 29.1 34.2	91.2 90.3 83.9	97.0 ^a 98.2 ^a 98.7 ^a
	Crushed-stone base		3	150 ^a	1.9	155.2	107.8	150 ^a	1.2	152.2	105.7
	Untreated gravelly sand subbase (PI = 3)		9 21 27	52 40 25	5.2 6.2 5.7	141.0 141.2 136.7	106.5 106.6 103.2	57 41 34	5.1 5.5 6.0	140.5 135.9 135.6	106.1 102.6 102.4
5	Heavy clay sub-grade	2500	42 48 54	2.5 3.0 4.3	33.3 33.4 33.6	86.5 85.2 85.9	100.6 ^a 99.1 ^a 99.9 ^a	4.3 4.1 4.7	32.5 33.4 33.2	87.2 85.3 84.9	101.4 ^a 99.2 ^a 98.7 ^a
	Lane 2, 240,000-lb Twin-Tandom Assembly										
	1		Crushed-stone base	600	3	141	1.1	153.2	106.4	105	1.2
Lean clay subbase with 3 percent lime, 2 percent portland cement, 10 percent flyash		9	126		20.4	100.7	99.2	147	25.6	98.3	96.8
Heavy clay sub-grade		33 39 45	4.2 5.1 5.4		32.6 32.7 33.2	86.7 87.2 86.2	100.8 ^a 101.4 ^a 100.2 ^a	4.1 5.5 5.3	35.4 32.2 32.9	83.5 87.4 86.3	100.6 ^a 101.6 ^a 100.3 ^a
2	Lean clay base with 12 percent portland cement	400	3	150 ^a	15.1	109.8	101.8	144	14.8	106.1	98.3
	Heavy clay sub-grade		28 34 40	5 5 4.6	31.6 30.4 31.4	87.4 89.1 87.9	99.3 ^a 99.0 ^a 99.9 ^a	3.6 3.2 3.6	33.9 33.0 31.9	84.2 85.7 87.3	99.0 ^a 99.7 ^a 100.3 ^a
	Gravelly sand base with 5 percent portland cement		3 15	150 ^a 105	3.3 --	137.0 --	100.0 --	150 ^a 150 ^a	2.8 --	135.3 --	98.8 --
3	Heavy clay sub-grade	620	28 34 40	1.5 3.9 3.3	32.9 31.4 33.3	85.8 87.9 85.7	99.8 ^a 99.9 ^a 99.7 ^a	1.8 2.9 3.9	34.1 33.2 33.1	84.5 85.7 86.0	99.4 ^a 99.7 ^a 100.0 ^a

(Continued)

* Percent of CE 12 (ASTM D 698-70) maximum density corresponding to field in-place water content.

Table 14 (Concluded)
After-Traffic Water Content, Density, and CBR Data for Flexible Pavement Test Section

Item No.	Material	No. of Coverages	Depth Below Pavement Surface in.	Inside Traffic Lane				Outside Traffic Lane			
				CBR	Water Content percent	Dry Density pcf	Percent Lab Density	CBR	Water Content percent	Dry Density pcf	Percent Lab Density
4	Clayey sand base with 5 percent portland cement	120	3	150*	14.0	116.4	89.2	150*	14.1	116.4	89.2
			15	26	12.3	112.5	86.2	112	11.2	121.0	92.7
	Heavy clay sub-grade		28	6	29.6	90.4	100.4*	3.9	29.4	89.8	98.7*
			34	10	27.8	92.6	100.7*	9	28.5	91.3	100.3*
			40	4.5	31.8	87.0	100.0*	6	31.0	87.9	98.8*
5	Crushed-stone base	340	3	133	2.0	158.9	110.3	133	2.0	155.5	108.0
			9	24	4.4	138.5	104.6	25	5.1	143.3	108.2
	Untreated gravelly sand subbase (PI = 3)										
			42	3.9	32.3	87.4	100.5*	3.4	32.0	87.4	100.5*
			48	4.1	30.2	89.1	99.0*	4.3	32.7	87.0	101.2*
Heavy clay sub-grade		54	6	31.4	88.1	99.0*	3.5	32.8	86.9	101.0*	
		<u>Lane 3, 50,000-lb Single-Wheel Assembly</u>									
4a	Clayey sand with 5 percent portland cement	240	3	67	14.1	109.3	83.8	114	11.6	115.8	88.7
			15	27	16.8	110.4	84.6	33	10.7	121.6	93.2
	60-psi polystyrene		18	8	--	--	--	7	--	--	--
			22	56	17.8	109.5	83.9	22	16.8	116.5	89.3
	Heavy clay sub-grade		28	2.8	30.9	83.0	93.3*	4.4	27.2	87.3	93.9*
34			3.1	32.2	87.3	100.3*	3.8	28.6	86.3	94.8*	
40			2.6	34.5	85.5	100.6*	2.8	33.9	84.7	99.6*	
4b	Clayey sand with 5 percent portland cement	240	3	--	13.5	116.8	89.5	--	13.0	117.4	90.0
4c	Clayey sand with 5 percent portland cement	240	3	104	14.0	110.9	85.0	130*	14.2	115.2	88.3
			9	39	--	--	--	66	--	--	--
	Clayey sand with 5 percent portland cement		18	51	12.8	112.5	86.2	18	13.4	118.8	91.0
			28	4.8	28.7	89.5	98.4*	6	28.9	86.6	95.2*
	Heavy clay sub-grade		34	6	30.7	88.9	99.9*	8	28.9	89.0	97.8*
40			4.5	33.5	84.9	99.9*	5	32.0	85.4	98.2*	
5a	Crushed limestone	240	3	63	4.3	144.3	100.2	53	2.5	146.5	101.7
			9	45	--	--	--	82	--	--	--
	Gravelly sand		18	20	6.1	137.8	104.1	20	9.3	132.8	100.3
			30	20	8.9	136.4	103.0	16	6.1	134.9	101.9
	Heavy clay sub-grade		42	3.6	31.4	87.5	98.3*	3.4	31.7	87.8	100.9*
48			3.7	31.1	89.6	100.7*	3.9	32.6	86.7	100.8*	
54			3.4	33.4	85.0	100.0*	4.3	32.0	85.3	98.0*	
5c	Crushed limestone	240	3	68	3.2	148.2	102.9	85	2.2	146.5	101.7
			9	69	4.9	139.2	105.1	49	4.0	142.0	107.3
	Gravelly sand		24	14	--	--	--	15	--	--	--
			27	31	6.7	137.7	104.0	23	7.5	135.9	102.6
	Heavy clay sub-grade		39	9	6.9	130.4	98.5	9	7.0	137.1	103.5
42			3.6	32.6	85.3	99.2*	4.5	28.0	90.4	98.3*	
48			4.4	33.1	85.2	100.2*	4.3	32.3	86.5	99.4*	
			54	5.0	32.9	86.5	100.6*	5.1	31.8	86.9	99.9*

* Percent of CE 12 (ASTM D 698-70) maximum density corresponding to field in-place water content.

Unheaval. The upheaval values shown in Table 12 were obtained from cross-sectional measurements taken at the indicated coverage levels and are the maximum values obtained on any cross section. Upheaval adjacent to the traffic lane is an indication of shear deformation in some element of the pavement structure. In this study, a test item was considered failed when an upheaval of 1 in. or more was measured.

Pavement Cracking. Pavement cracking through the full 3-in. thickness of asphaltic concrete was another failure criterion. Where pavement cracking is indicated in Table 12 as "severe," such a condition existed and the pavement items were considered failed. "Slight" cracking indicates narrow, shallow surface cracks that did not extend through the asphaltic concrete surface layer.

Rating of Test Items. Pavement failure developed in all test items under the 200-kip load in lane 1. In lane 1, the primary cause of failure was fatigue cracking of the asphaltic concrete, except for item 4. In item 4, shear failure that developed in the cement-stabilized base course between 1200 and 1380 coverages resulted in rupture of the base course and a loss in strength as indicated by the CBR tests after traffic. All items of lane 2 were failed by the 240-kip loading. The primary cause of failure in lane 2 was subgrade shear deformation in items 1-3. Failure of lane 2 of item 4 was due to shear deformation in the stabilized base course. Lane 2 of item 5 failed due to excessive cracking of the asphaltic concrete layer accompanied by excessive deformation and some lateral movement and upheaval in the gravelly sand subbase. All items in lane 3 failed under the 50-kip single-wheel load due to fatigue cracking and excessive deformation.

SUMMARY OF FINDINGS

RIGID PAVEMENT TEST SECTION

The significant findings from the tests of the rigid pavement test section are summarized as follows:

- a. The MESL base under the fibrous-reinforced concrete in item 1 performed quite well under traffic and gained strength during traffic. Localized failures occurred at each end of the item. These were the result of a failure of the load transfer mechanism between the fibrous-reinforced concrete and the transition slab. Excessive deflection resulted in a rupture of the membrane allowing infiltration of water into the MESL and a loss in soil strength.
- b. All base courses in the rigid pavement test section were effective in preventing pumping of the subgrade soils. However, some pumping of the cement-stabilized lean clay was noted in item 4, and some subgrade pumping occurred through the joints and cracks of the insulating materials and concrete in item 5.
- c. The keyed-and-tied longitudinal joints in test items 1, 3, and 4 performed satisfactorily except for a portion of the west slab in item 3 where a joint failure developed.
- d. In lane 1 of item 5, the spalling initiated at the key and progressed to the surface at about a 45-deg angle.
- e. The transverse weakened-plane joints in items 3 and 4 performed satisfactorily under both the 200- and 240-kip twin-tandem assembly loads with little or no faulting or joint deterioration.
- f. The transverse and longitudinal weakened-plane joints in lane 2 of item 5 failed under the 240-kip twin-tandem loading, with considerable faulting and joint deterioration accompanied by pumping of subgrade soil through the joints.
- g. The thickened-edge longitudinal joint in the 4-in.-thick fibrous-reinforced concrete of item 2 did not perform entirely satisfactorily as faulting along the joint on the south paving lane developed quite early during traffic in lane 1.
- h. The overall performance of the 7-in.-thick fibrous-reinforced concrete in item 1 over the MESL base course was very good and somewhat better in both lanes 1 and 2 than that for the 4-in.-thick fibrous-reinforced concrete over the cement-stabilized clay gravel base in item 2.
- i. The overall performance of the 15-in.-thick portland cement concrete was about the same over the bituminous base course

in item 3 as that of the 15-in.-thick portland cement concrete over the cement-stabilized lean clay in item 4.

- j. The overall performance of the 15-in.-thick portland cement concrete in test items 3 and 4 was somewhat better than that of the 15-in.-thick concrete in all subitems of item 5 over the insulating materials.

FLEXIBLE PAVEMENT TEST SECTION

The significant findings from the tests of the flexible pavement test section are summarized as follows:

- a. The primary mode of failure for the flexible pavement under the 200-kip twin-tandem loading was excessive cracking of the asphaltic concrete surface layer in test items 1-3 and 5. Item 4 failed due to shear deformation in the cement-stabilized clayey sand base course.
- b. The primary mode of failure for test items 1-3 of lane 2 under the 240-kip twin-tandem loading was shear deformation in the subgrade accompanied by excessive cracking of the asphaltic concrete surface layer in items 1 and 2. The mode of failure in item 4 was shear deformation in the base course accompanied by excessive cracking of the asphaltic concrete surface layer. The mode of failure in item 5 was excessive cracking in the asphaltic concrete accompanied by excessive deformation and some lateral movement and upheaval of the sand subbase.
- c. The order of overall performance of the items for both lanes 1 and 2, from best to worst, was items 3, 1, 2, 5, and 4.
- d. The cement was most effective in stabilizing the cohesionless gravelly sand in item 3 and least effective in stabilizing the clayey sand ($PI = 21$) in item 4.
- e. The overall performance of items 1-3 (total thicknesses over the subgrade of 33, 28, and 28 in., respectively) was better than that of item 5, which consisted of 42 in. total thickness of conventional construction over essentially the same strength subgrade.
- f. The performance of item 5 under the 240-kip twin-tandem gear loading was essentially the same as that for item 5 of the original MWHGL test section under the same loading. The only difference in these two items was that a cohesionless gravelly sand subbase was used in the MWHGL test section as compared with a low-plasticity ($PI = 3$) gravelly sand in this test section.
- g. Under a single-wheel load, the performance of the items incorporating insulating materials at various depths in the structure was not as good as that of the same pavement items without the insulating materials under either the 200- or 240-kip load.

APPENDIX A: BEHAVIOR OF RIGID PAVEMENT TEST SECTION UNDER TRAFFIC

200-KIP LOAD, LANE 1

ITEM 1

A general view of the item prior to traffic is shown in Figure A1. No cracks were visible in the item at this time. At 200 coverages, a few transverse hairline cracks were observed, and one crack near the west end of the item extended across the entire traffic lane (Figure A2). The crack at the west end of the item appeared to have been caused by a load transfer failure between the transition slab and the 7-in.-thick fibrous-reinforced concrete. This area was repaired after 280 coverages, and traffic was continued. Cracks continued to develop with additional application of traffic. At 1770 coverages, each end of the item was severely cracked; however, the center of the item had only a moderate amount of cracks (Figure A3). At 3000 coverages, the entire item was severely cracked (Figure A4) and was considered to have reached the shattered slab condition.

Figure A5 shows the progression of cracks with the application of traffic. Permanent deformations of the pavement surface are shown by the cross sections in Figure A6, and the maximum deformation is shown in Table 11 of the main text. Deformations at each end of the item were not representative of those in the rest of the item since failure at these points occurred due to a load transfer failure at the transition slabs. Excluding the deformation at the two ends of the item, an average deformation of about 0.55 in. and a maximum of 0.70 in. were recorded at the end of traffic (3000 coverages).

ITEM 2

A general view of the item prior to traffic is shown in Figure A7. No cracks were visible in the item prior to traffic. At 200 coverages, several longitudinal cracks were noted in the pavement (Figure A8), and approximately 0.1 in. of vertical displacement had occurred along the longitudinal butt joint between the north and south slabs. At 1000 coverages, cracking at the west end of the item and along the south edge of

the traffic lane was fairly heavy (Figure A9). The average vertical movement along the longitudinal butt joint was about 0.5 in. Cracking continued with the application of traffic, and at 1770 coverages complete failure had occurred (Figure A10). Differential displacement between the north and south slabs along the butt joint averaged about 0.6 in. Figure A5 shows the progression of cracks with the application of traffic. Permanent deformations of the pavement surface are shown by the cross sections in Figure A11. An average deformation of 1.58 in. developed along the longitudinal joint, and a maximum of 2.1 in. was recorded.

ITEM 3

A general view of the item prior to traffic is shown in Figure A12. Prior to traffic, a transverse shrinkage crack had developed in the southwest slab. At 200 coverages, a transverse crack developed in the southwest slab approximately 6 in. from the weakened-plane joint between the east and west slabs (Figure A13). At 1770 coverages of the 200-kip load, the initial failure condition was noted in the northwest slab. At approximately 2050 coverages, semicircular cracks began to develop in the southwest slab adjacent to the longitudinal construction joint. These semicircular cracks continued to develop along with spalling, and, at 3000 coverages, a diagonal crack developed in the southwest slab. The condition of the item at 3000 coverages is shown in Figure A14. A corner break developed at the northwest corner of the southeast slab at 4460 coverages. Progressive spalling of the concrete along cracks was observed with additional cracking in the southwest slab to 6360 coverages when traffic was terminated. At 6360 coverages, a shattered slab failure had developed in the southwest slab; only the initial crack failure condition had been reached in the northwest and southeast slabs; and no cracks had developed in the northeast slab. The condition of the item at the conclusion of traffic is shown in Figure A15.

The progression and extent of cracking at selected levels of traffic are shown in Figure A5. Permanent deformation in the test lane is shown in Figure A16. As is shown in these cross sections, a

2

differential movement of about 0.5 in. occurred between the north and south slabs on the east half of the west slabs. An average deformation of 0.63 in. and a maximum deformation of 0.8 in. were recorded. Slight pumping began at about 1500 coverages at transverse joints at each end of the item and became more noticeable with continued application of traffic. Pumping was apparent at the transitions during and immediately after rainfall. There was no pumping through the longitudinal construction joint, the weakened-plane joint, or the cracks noted within the test item proper.

ITEM 4

The condition of item 4 prior to traffic is shown in Figure A17. No visible defects were noted in the item before traffic. At 1770 coverages, a hairline crack was noted at approximately the center of the northwest slab and extended from the longitudinal construction joint to the north edge of the traffic lane (Figure A18), and minor spalling was noted in the northwest slab at the transverse weakened-plane joint. No further cracking developed until 4630 coverages. Between 4630 coverages and 4660 coverages, all interior corners cracked except the southeast corner of the northeast slab. Cracking progressed with continued traffic; at 6360 coverages, the item had numerous cracks as shown in Figure A19. The progression and extent of cracking at selected levels of traffic are shown in Figure A5. Permanent deformation in the test lane is shown in Figure A20. An average deformation of 1.0 in. and a maximum deformation of 1.5 in. were recorded. Pumping at the transitions and at the transverse weakened-plane joint was first observed at 750 coverages and increased with the application of traffic.

ITEM 5

The condition of all subitems in item 5 prior to traffic is shown in Figure A21. Prior to traffic, the only cracks noted were in the north slab between subitems 5b and 5c where the transverse weakened-plane joint had not been sawed and at the east end of the subitem 5c parallel to the transverse weakened-plane joint. The behavior of each

of the subitems under traffic is discussed in the following paragraphs.

Subitem 5a. At 1770 coverages, a crack developed parallel to and about 1 ft south of the longitudinal construction joint (Figure A22). With continued application of traffic to 3000 coverages, spalling along the crack path became severe and two hairline transverse cracks developed in the north slab (Figure A23). Traffic was stopped at 3000 coverages because of severe spalling along the longitudinal joint. Permanent deformation in the traffic lane is shown in Figure A24. As shown in these cross sections, a differential movement of about 0.6 in. occurred between the north and south slabs. An average deformation of 1.13 in. and a maximum deformation of 1.4 in. were recorded. Pumping, first noted at the transverse joints at 750 coverages, became more severe with the continued application of traffic and continued long after rainfall.

Subitem 5b. Spalling was noted parallel to the longitudinal construction joint at 1770 coverages (Figure A25). Cracking progressed with the application of traffic, and, at 3000 coverages, spalling along the longitudinal construction joint was severe (Figure A26). Permanent deformation in the traffic lane is shown in Figure 24. Only about 0.3 in. of differential movement occurred between the north and south slabs near the west end of the subitem. An average deformation of 0.65 in. and a maximum deformation of 0.9 in. were recorded. Pumping was first observed along the transverse joint on the east edge of the subitem at 340 coverages, and at 750 coverages pumping was observed along the transverse joint on the west edge.

Subitem 5c. With the exception of spalling along the transverse joint at the east edge of the subitem, the initial cracks were observed at 1000 coverages (Figure A27). At 1230 coverages, the south slab of the subitem had reached the shattered slab condition, as shown in Figure A28. Pumping was observed along the east transverse joint at 200 coverages. At 340 coverages, pumping had become severe, with the heavy clay pumping through the transverse joints on both sides of the south slab. Pumping continued with traffic and was observed long after rainfall. Permanent deformation in the traffic lane is shown in Figure A29.

Cross sections taken at 1000 coverages show that there was 0.3 in. of permanent deformation, but, at the time of failure at 1230 coverages, about 0.6 in. of differential movement was measured at the longitudinal joint between the north and south slabs.

Subitem 5d. The first crack was recorded at 1080 coverages and was located parallel to and about 2 ft south of the south edge of the traffic lane. At 2220 coverages, spalling began developing parallel to the longitudinal construction joint. At 3000 coverages, spalling along the longitudinal construction joint extended almost the full length of the subitem (Figure A30). Pumping was observed along the transverse joint between subitems 5c and d at 220 coverages but was not observed along the east edge of subitem 5d at the transitions until 750 coverages. Pumping continued with traffic but was never as serious as in subitem 5c. The cross sections shown in Figure A29 indicate that 0.3 in. of permanent deformation developed in the traffic lane during the application of traffic.

240-KIP LOAD, LANE 2

ITEM 1

A general view of item 1 prior to traffic is shown in Figure A31. No cracks were observed in the pavement surface prior to static loading for instrumentation readings, but, during static loading, several cracks developed in the item (Figure A32). Cracks continued to develop with the application of traffic, and, at 200 coverages, cracking was heavy at the west end and moderate at the east end of the item (Figure A33). Traffic was continued, and, at 430 coverages, severe cracking had developed at the west end of the item. Landing mat was placed over the area, and traffic was continued to 1010 coverages. At 1010 coverages, cracking had become severe over the entire item (Figure A34), and the item was considered to have reached the complete failure condition. Permanent deformation of the pavement is shown in the cross sections in Figure A35. The west end of the item is not included in the profiles because the polypropylene used to encase the lean clay was torn, probably during

construction, and the lean clay became wet causing a premature failure in about 10 ft of the extreme west end. The large deformation at the east end of the item was probably due to a load transfer failure where the fibrous-reinforced concrete slab joined the transition slab. Permanent deformation in the traffic lane, not including the two ends, averaged 0.5 in. with a maximum deformation of 0.7 in. A slight upheaval (0.3 in.) of the pavement surface occurred outside the traffic lane at the north edge of the pavement.

ITEM 2

A general view of item 2 prior to traffic is shown in Figure A36. No cracks were observed in the pavement until 40 coverages of traffic had been applied. At 40 coverages, a few small hairline cracks had developed near the west end of the item. At 200 coverages, cracking was moderate at the west end, and a few small hairline cracks were developing near the east end (Figure A37). Cracking continued to develop with the application of traffic. At 740 coverages, severe cracking had developed throughout the entire traffic lane, and the item was considered completely failed. The progression of cracks with the application of traffic is shown in Figure A32. Although the item was considered failed at 740 coverages, traffic was continued to 950 coverages. Cracking became extreme, and permanent deformation increased (Figure A38). The amount of permanent deformation is shown in the cross-sections in Figure A39. Permanent deformation in the traffic lane averaged 1.78 in., and the maximum deformation was 3.2 in. As is shown by the cross sections, an upheaval occurred along the outside of the traffic lane on the north side. Upheaval along the north edge averaged 1.02 in., with a maximum of 2.1 in.

ITEM 3

A general view of item 3 prior to traffic is shown in Figure A40. Prior to traffic, the item had one crack located at about the middle of the west slab and transverse to the direction of traffic. During the instrumentation readings prior to trafficking lane 2, a longitudinal

crack developed in the center of the traffic lane. After 200 coverages, these were the only cracks in the item except for minor spalling at the west transition slab (Figure A41). Traffic was continued to 1200 coverages on the west half of the item and to 1500 coverages on the east half of the item, with severe spalling occurring along the crack paths and at transverse joints (Figure A42). The progression of cracks with the application of traffic is shown in Figure A32. Cross sections of the pavement surface at selected intervals of traffic are shown in Figure A43. These profiles show that an average of 0.13 in. of permanent deformation occurred in the traffic lane during the application of traffic.

ITEM 4

A general view of item 4 prior to traffic is shown in Figure A44. Cracks that occurred during trafficking of lane 1 extended to the south edge of traffic lane 2. During the application of static load traffic for taking instrumentation readings, a longitudinal crack developed near the center of the traffic lane in the west slab and near the south edge of the traffic lane in the east slab. During the application of traffic, the first crack developed in the northeast slab at 40 coverages. At 100 coverages, cracks had developed transverse to the traffic lane in both slabs, and the longitudinal cracks at the center of the traffic lane extended the entire length of the item (Figure A45). At 950 coverages, severe spalling was occurring along crack paths (Figure A46). The progression of cracks with the application of traffic is shown in Figure A32. Cross sections of the pavement surface at selected intervals of traffic are shown in Figure A47. These cross sections show that an average of 0.15 in. of permanent deformation occurred in the traffic lane during the application of traffic.

ITEM 5

Test item 5 was divided into four subitems. Prior to traffic no cracks were noted in any of the subitems. The behavior of each subitem will be discussed separately in the following paragraphs.

Subitem 5a. During static loading, cracks developed at the east end of the subitem at the intersection of the transverse and longitudinal weakened-plane joints. These were the only cracks to develop during the first 200 coverages (Figure A48). With continued traffic, the transverse cracks at the east end progressed across the subitem. The initial crack failure condition was reached at 290 coverages. At 500 coverages, spalling was noted at the west end of the subitem parallel to the longitudinal joint. With continued application of traffic, spalling became severe the full length of the subitem. At 740 coverages, the weakened-plane joint was considered failed, but traffic was continued to 950 coverages (Figure A49). The progression and extent of cracking at selected levels of traffic is shown in Figure A32. Permanent deformation in the traffic lane is shown in Figure A50. An average deformation of 0.63 in. and a maximum deformation of 0.7 in. were recorded. Cross sections at stations 2+46 and 2+52 taken at 950 coverages indicated that the weakened-plane joint sheared since there was definite vertical displacement between the north and south slabs. Pumping of the cement-stabilized lean clay base course material through the cracks was first noted at 350 coverages and became more severe with the application of traffic.

Subitem 5b. At 200 coverages, the subitem was in excellent condition except for a minor amount of spalling at the joint between subitems 5b and c (Figure A51). The first crack caused by loading was noted outside the traffic lane at 350 coverages. The weakened-plane joint began spalling at 540 coverages and at 740 coverages, spalling extended the full length of the subitem. The joint was considered failed at 740 coverages, but traffic was continued on the item to 950 coverages, with spalling becoming severe along the weakened-plane joint (Figure A52). The progression and extent of cracking at selected levels of traffic are shown in Figure A32. Permanent deformation in the traffic lane is shown in Figure A50. An average deformation of 1.3 in. and a maximum deformation of 1.9 in. were recorded. The cross sections show differential movement of about 1 in. between the north and south slabs

along the weakened-plane joint. Pumping was first observed along the transverse joint on the east end of the subitem at 320 coverages and increased with the application of traffic.

Subitem 5c. At 160 coverages, spalling began parallel to the longitudinal weakened-plane joint near the east end of the subitem (Figure A53). At 350 coverages, the first load-associated crack was noted outside the traffic lane. With continued application of traffic, spalling along the weakened-plane joint increased and, at 430 coverages, extended the entire length of the subitem. Spalling along the joint was severe at 740 coverages and the joint was considered failed. Traffic was continued on the subitem to 840 coverages; the condition of the pavement at that coverage level is shown in Figure A54. The progression and extent of cracking at selected levels of traffic are shown in Figure A32. Permanent deformation of the traffic lane is shown in Figure A55. An average deformation of 1.0 in. and a maximum deformation of 1.1 in. were recorded. The cross sections show a differential movement of about 0.6 in. between the north and south slabs along the weakened-plane joint. Pumping was noted between subitems 5b and c at 320 coverages. As cracks developed, pumping became more severe.

Subitem 5d. At 20 coverages, the first load-associated crack developed near the center of the traffic lane on the east end and ran diagonally across the subitem from the center of the subitem to both edges of the traffic lane at the west end (Figure A32). At 200 coverages, cracking and spalling along crack paths had become severe (Figure A56), and a shattered slab condition of failure was reached. Traffic was continued to 350 coverages (Figure A57). The progression and extent of cracking at selected levels of traffic are shown in Figure A32. Permanent deformation in the traffic lane is shown in Figure A55. An average deformation of about 0.6 in. and a maximum deformation of 0.7 in. were recorded. Only a very slight differential movement occurred at the weakened-plane joint between the north and south slabs.

AFTER-TRAFFIC TESTING PROGRAMS

Comprehensive after-traffic testing programs were conducted in both paving lanes to establish the physical properties of the pavement, base course, and subgrade materials that were needed for an evaluation of the behavior of each test item. Beams and cores were used to determine the pertinent properties of the paving materials. Results of plate bearing tests and density and water content determinations were used to evaluate the base courses and subgrade. The test program included both laboratory and field tests.

The locations of after-traffic test pits and cores are shown in Figure A58. Test pits in items 1 and 2 of lane 1 were excavated across the longitudinal construction joint between the north and south slabs in order to examine the differential movement between the two slabs. Test pits in items 3-5 of lane 1 were located in the south slab adjacent to the longitudinal construction joint so that the keyed joints and tie bars could be examined. It was found that the keyed-and-tied joints in items 1, 3, and 4 performed satisfactorily except in the east half of the west slab of item 3, where the keyed joint failed resulting in a surface differential of about 0.5 in. between the north and south sides of the joint. In item 5, an initial crack developed about 1 ft south of and parallel to the longitudinal joint. As traffic continued, spalling and cracking developed rather rapidly in all subitems. This initial crack was located at about the end of the tie bars in the longitudinal joint and formed an angle of about 45 deg with the joint. In removal of the slab from the test pits, the tie bars and keyed joints were disturbed so that the actual condition of the joint could not be verified. Test pits in lane 2 were located near the center of the traffic lane in all items except item 1, 2, and 4, where test pits extended from the center to the north edge of the test section.

Concrete slabs removed from the test pits were taken to the WES Concrete Laboratory for sawing into test specimens and testing. Three beams were cut from each slab except for the slab from test pit 5, for which only two beams could be obtained. Each beam had a depth and

width equal to the pavement thickness. Beams were only slightly longer than three times their depth, so only one break was obtained on each beam. Beams were tested for modulus of elasticity in accordance with CRD-C-21.²⁹ When the modulus of elasticity test was completed, loading was continued to failure of the beam. Results of flexural strength and modulus of elasticity tests obtained on the beams are shown in Table A1. Also shown in Table A1 are the results of modulus of elasticity and flexural strength tests performed on beams of lightweight concrete from sub-item 5b.

Four cores were taken from the portland cement concrete in each test item, and two cores were taken from the lightweight concrete base in subitem 5b. The four cores taken from item 1 were 4 in. in diameter; all other cores were 6 in. in diameter. All cores were tested according to the applicable part of CRD-C-107²⁹ for unit weight. The four cores from item 2 were tested for splitting tensile strength according to CRD-C-77.²⁹ Compressive strength and static modulus of elasticity were determined on cores from items 1 and 3-5. Dynamic modulus of elasticity was determined on portland cement concrete cores from items 3-5. The two lightweight concrete cores were tested for unit weight, and compressive strength and the static modulus of elasticity were determined on one of the cores. The results of all tests on cores are shown in Table A2.

Plate bearing tests were performed at the surface of the base courses, insulating layers, and subgrade. Plate bearing tests were not performed on the surface of each layer in every test pit due to the time and cost that would have been involved, but tests were performed at selected locations to obtain values representative of the entire test section. Load-deflection plots for each plate bearing test are shown in Figures A59-A63, and the moduli of soil reaction are shown in Table 11 of the main text. Moisture content and density determination were made at the surface of the base course and at the surface of the subgrade in various test pits. Moisture content determinations were made from samples of materials from an observation pit at the west end of item 1,

lane 2, to determine if there had been any change in the moisture content of the lean clay in the MESL. The results of all the moisture content and density determinations are shown in Table 13 of the main text.



Figure A1. Item 1, lane 1, rigid pavement test section, prior to traffic



Figure A2. Item 1, lane 1, rigid pavement test section, after 200 coverages by 200-kip twin-tandem assembly

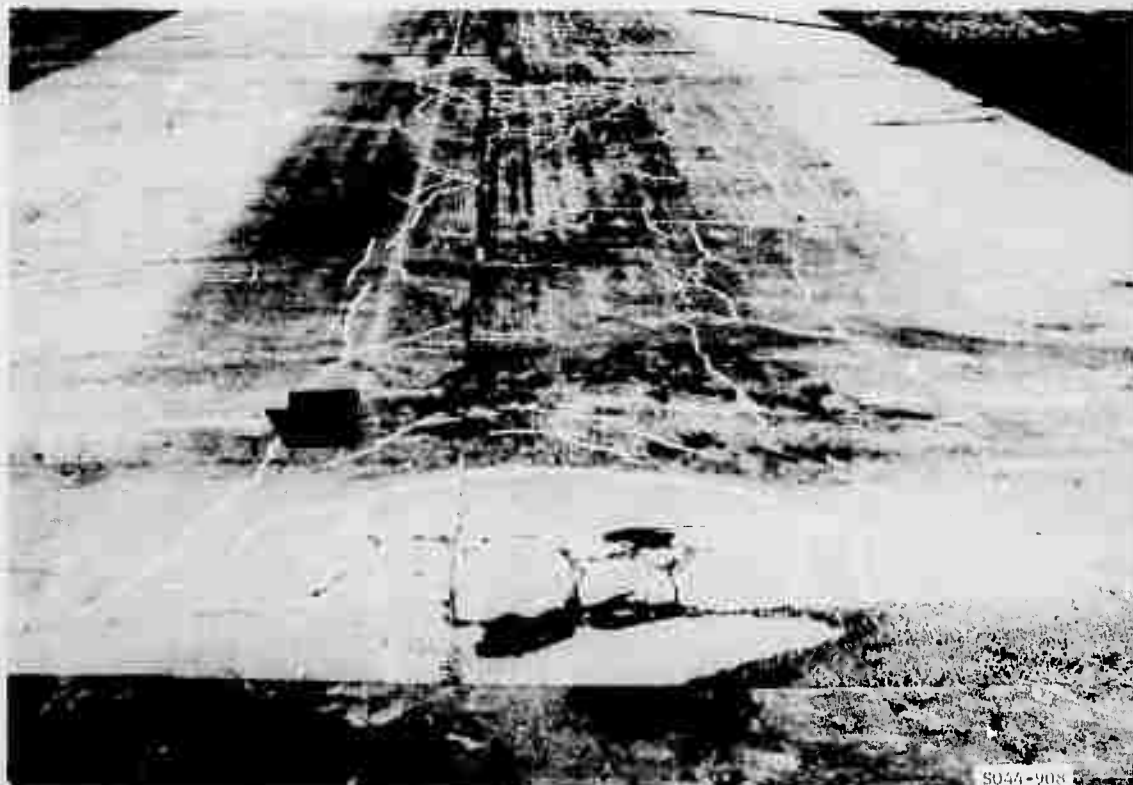


Figure A3. Item 1, lane 1, rigid pavement test section, after 1770 coverages by 200-kip twin-tandem assembly



Figure A4. Item 1, lane 1, rigid pavement test section, after 3000 coverages by 200-kip twin-tandem assembly

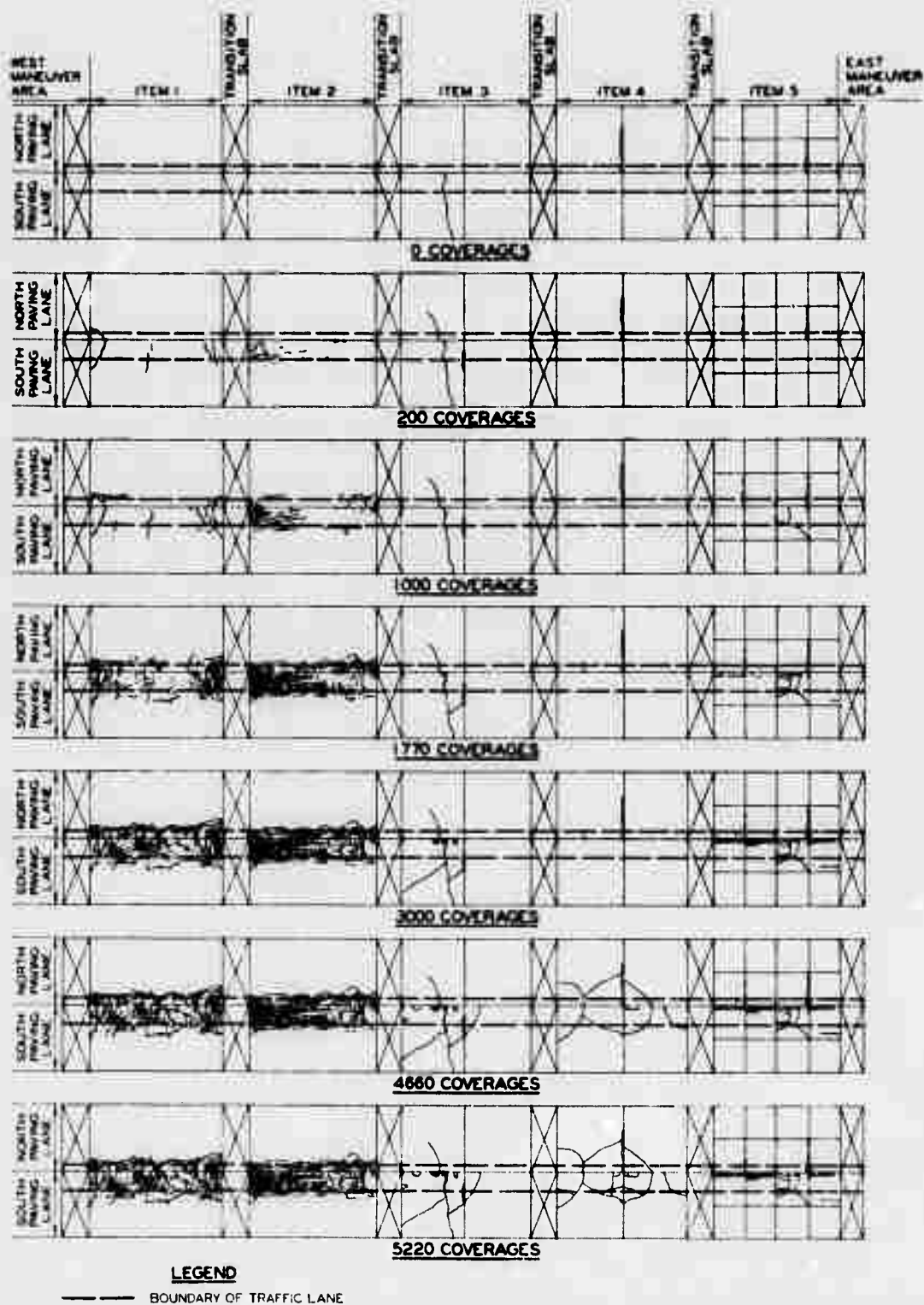


Figure A5. Crack development in lane 1, rigid pavement test section

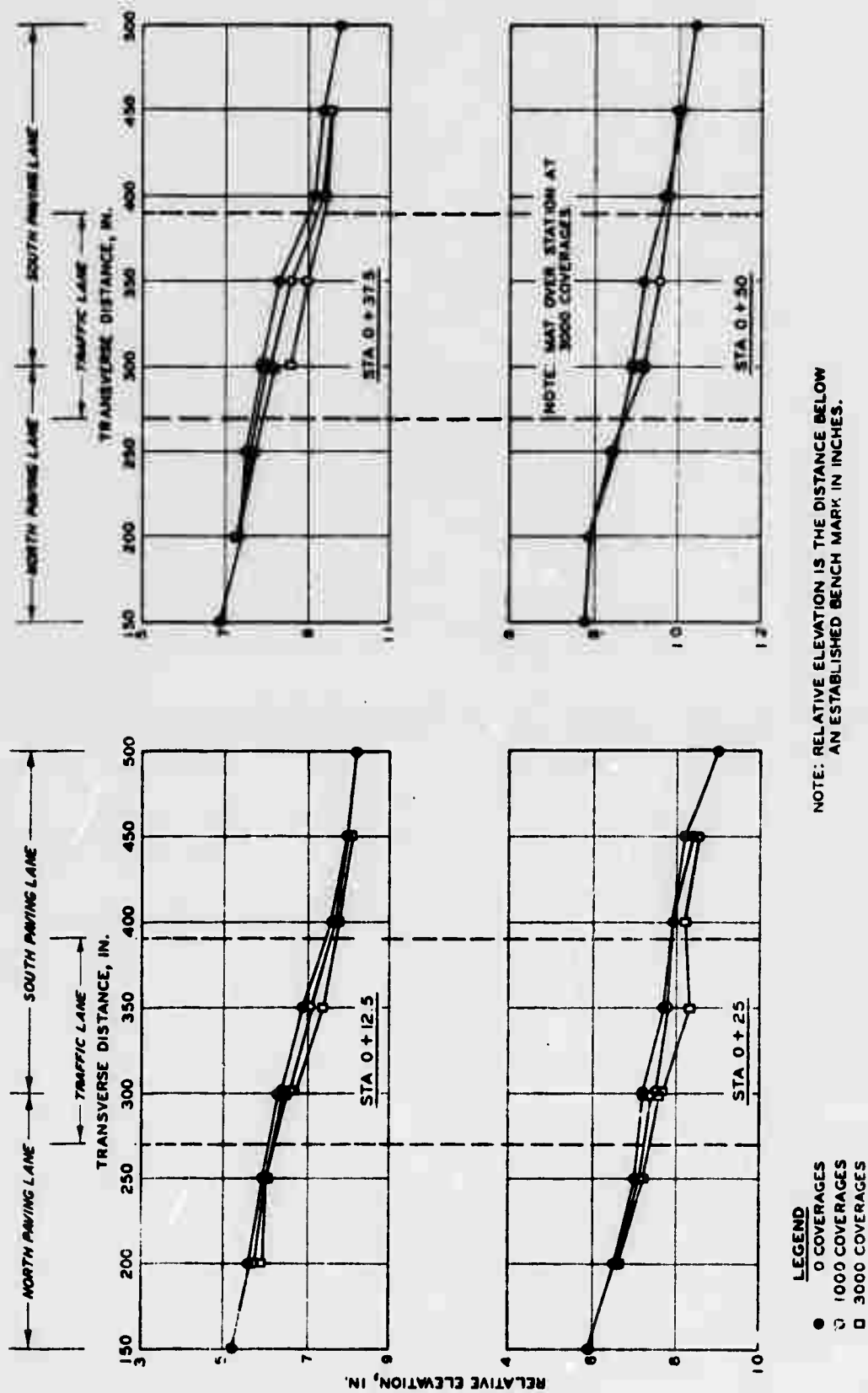


Figure A6. Surface deformation in item 1, lane 1, rigid pavement test section

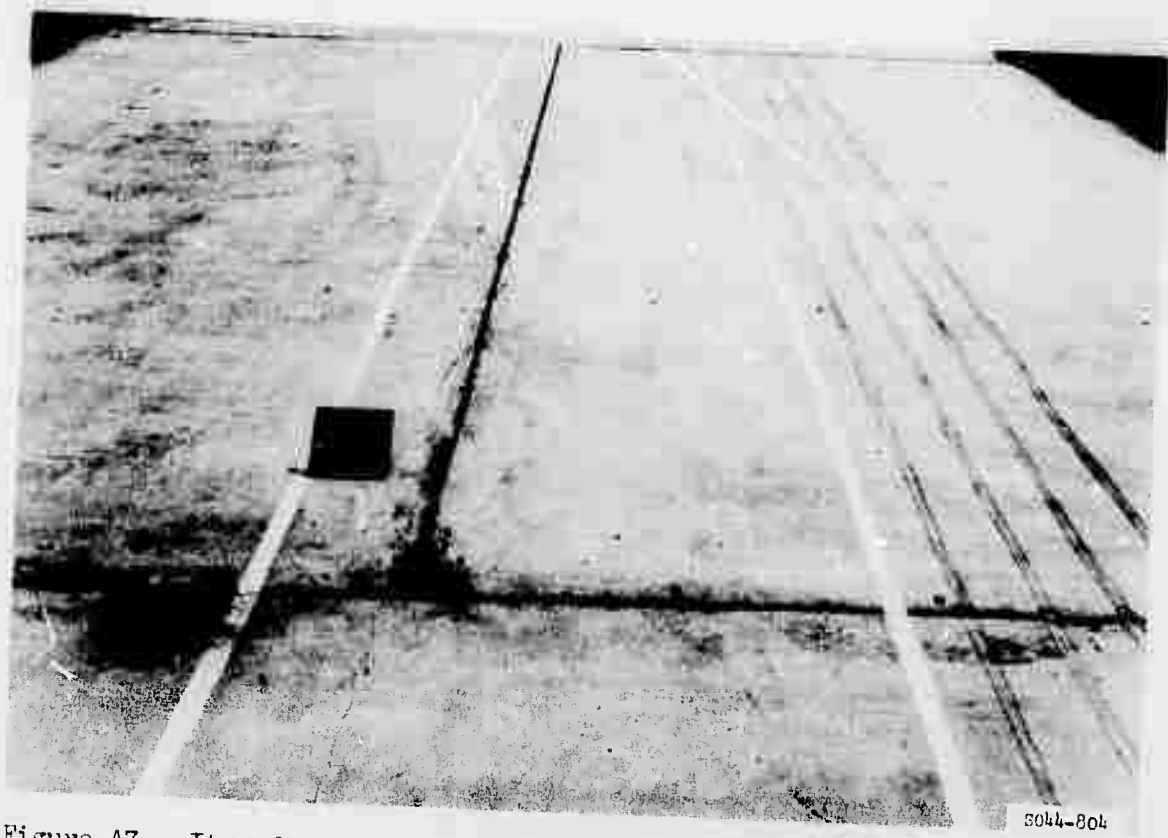


Figure A7. Item 2, lane 1, rigid pavement test section, prior to traffic



Figure A8. Item 2, lane 1, rigid pavement test section, after 200 coverages by 200-kip twin-tandem assembly

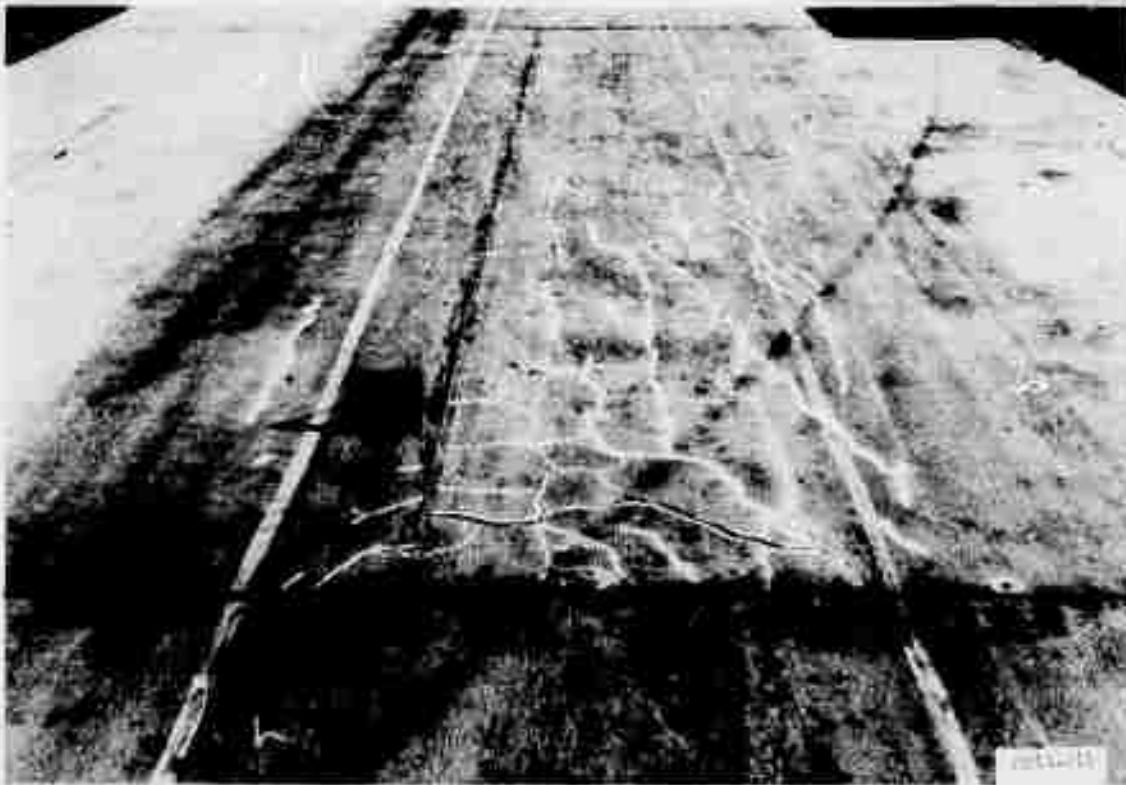


Figure A9. Item 2, lane 1, rigid pavement test section, after 1000 coverages by 200-kip twin-tandem assembly



Figure A10. Item 2, lane 1, rigid pavement test section, after 1770 coverages by 200-kip twin-tandem assembly

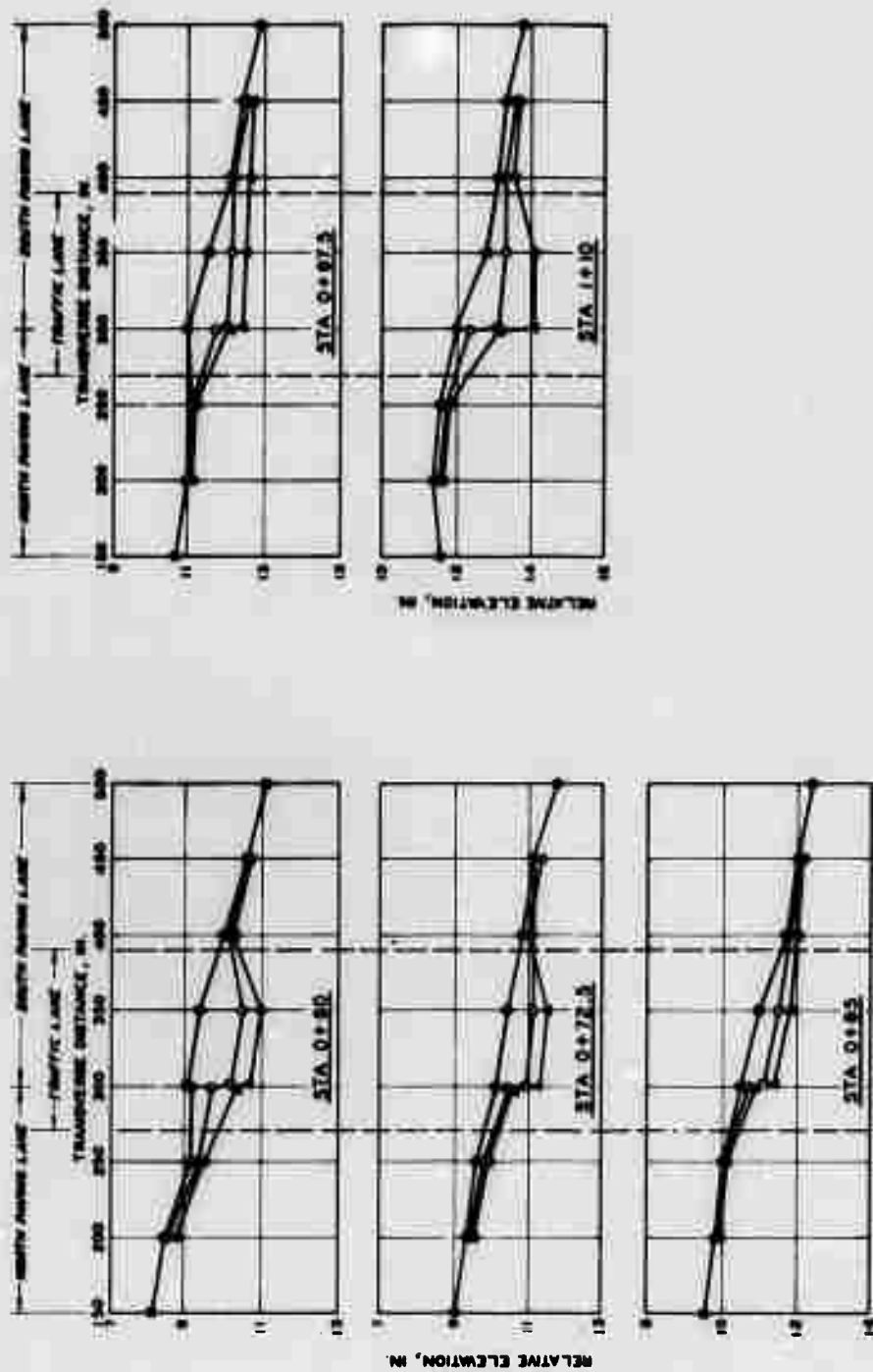


Figure All. Surface deformation in item 2, lane 1, rigid pavement test section

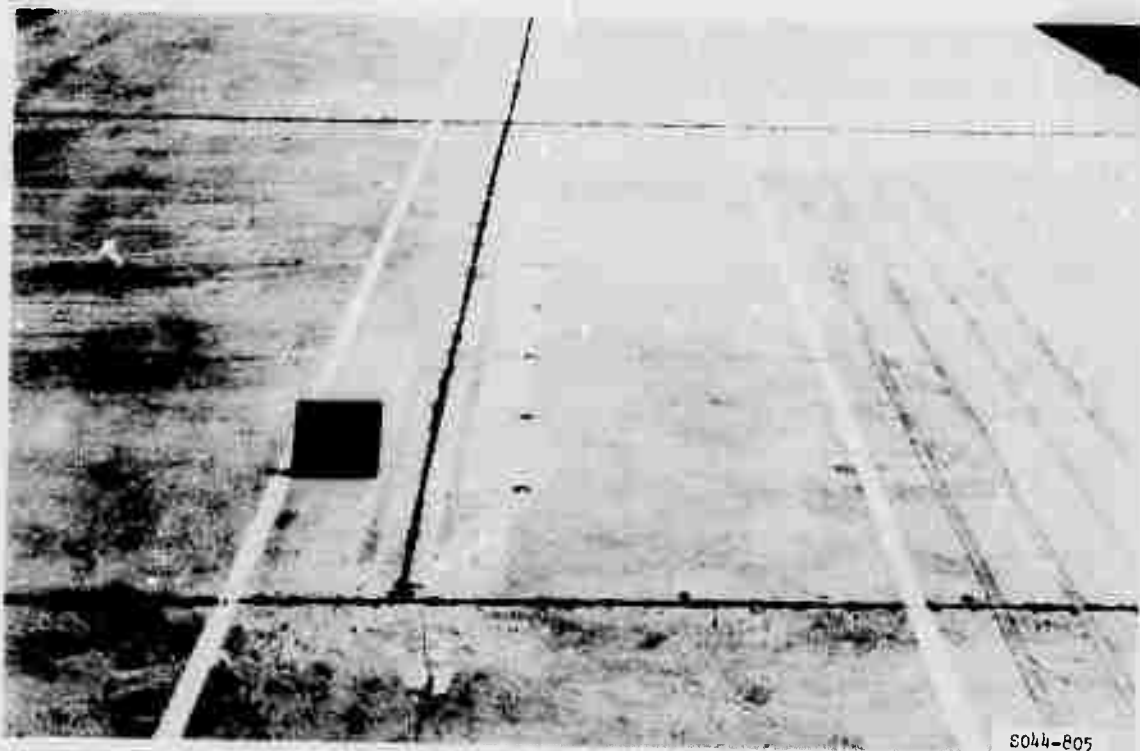


Figure A12. Item 3, lane 1, rigid pavement test section, prior to traffic



Figure A13. Item 3, lane 1, rigid pavement test section, after 200 coverages by 200-kip twin-tandem assembly

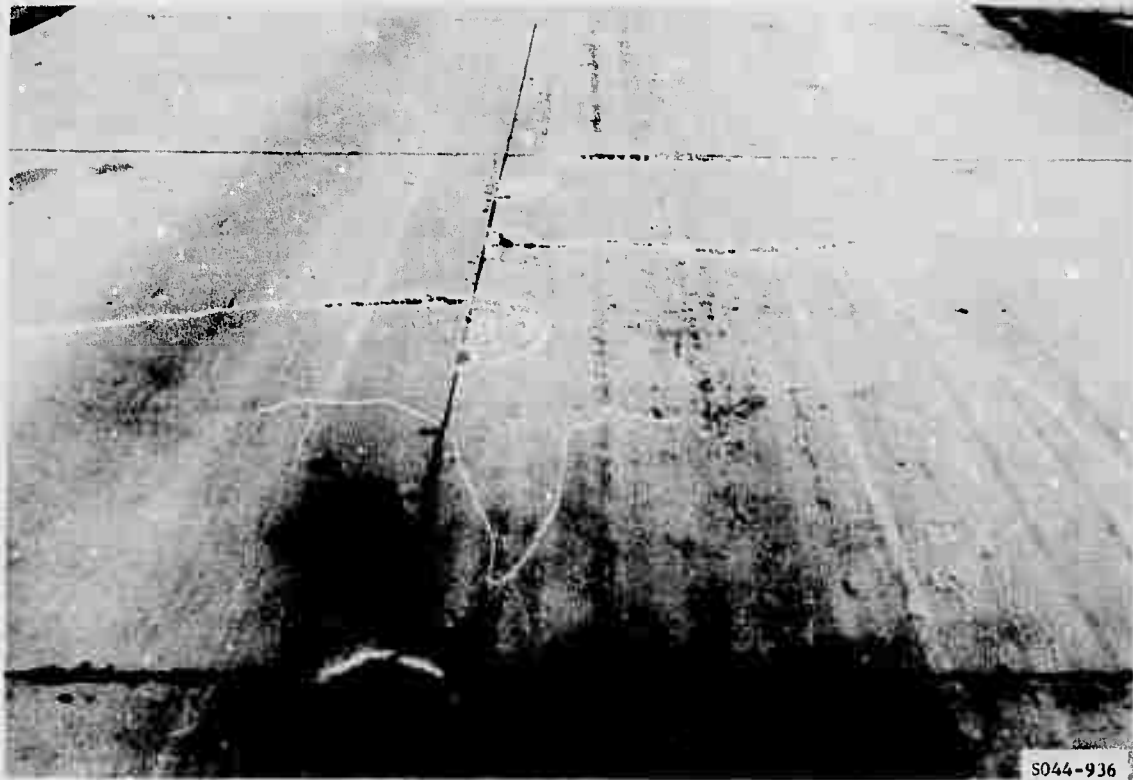


Figure A14. Item 3, lane 1, rigid pavement test section, after 3000 coverages by 200-kip twin-tandem assembly



Figure A15. Item 3, lane 1, rigid pavement test section, after 6360 coverages by 200-kip twin-tandem assembly

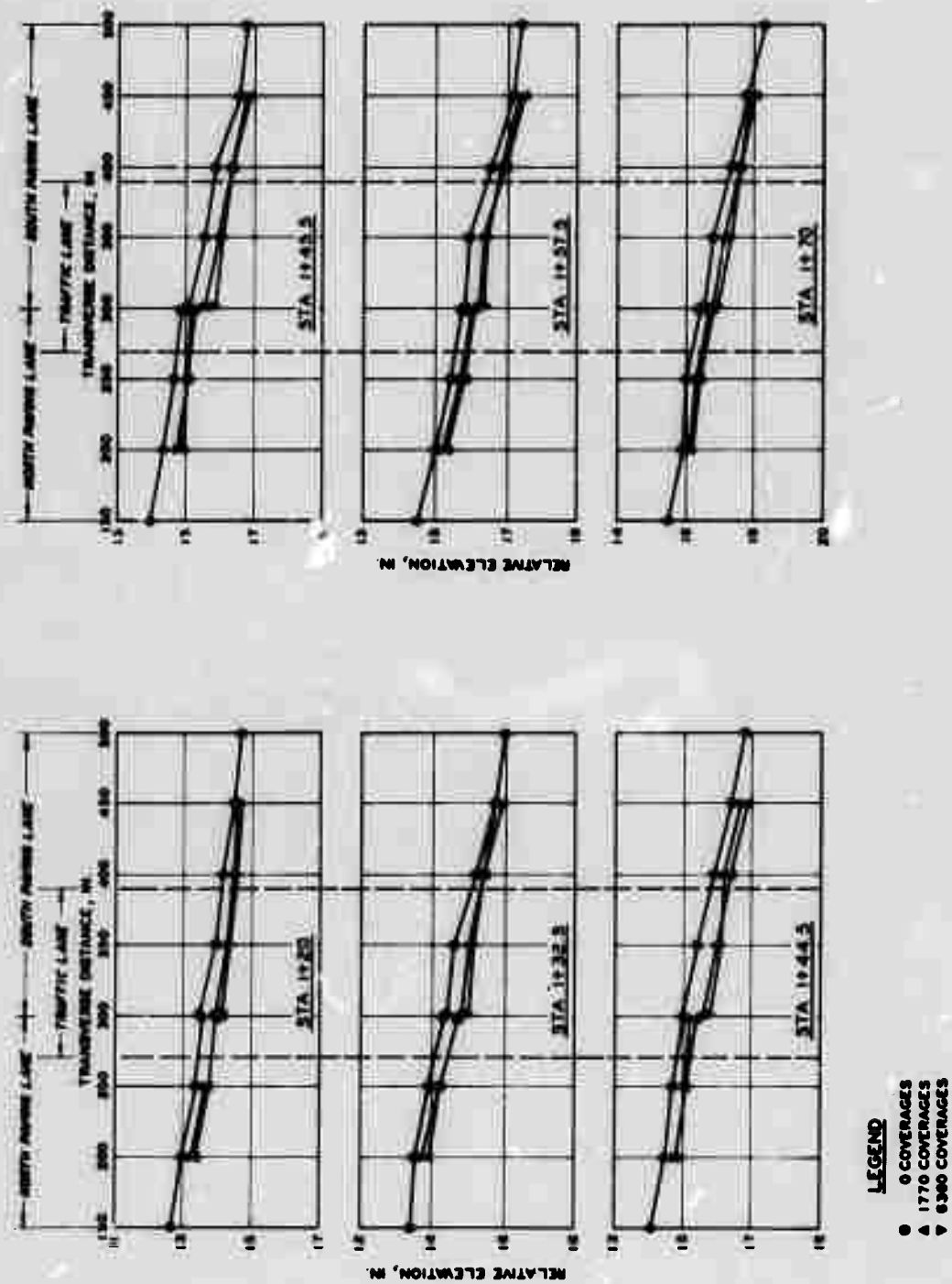


Figure A16. Surface deformation in item 3, lane 1, rigid pavement test section

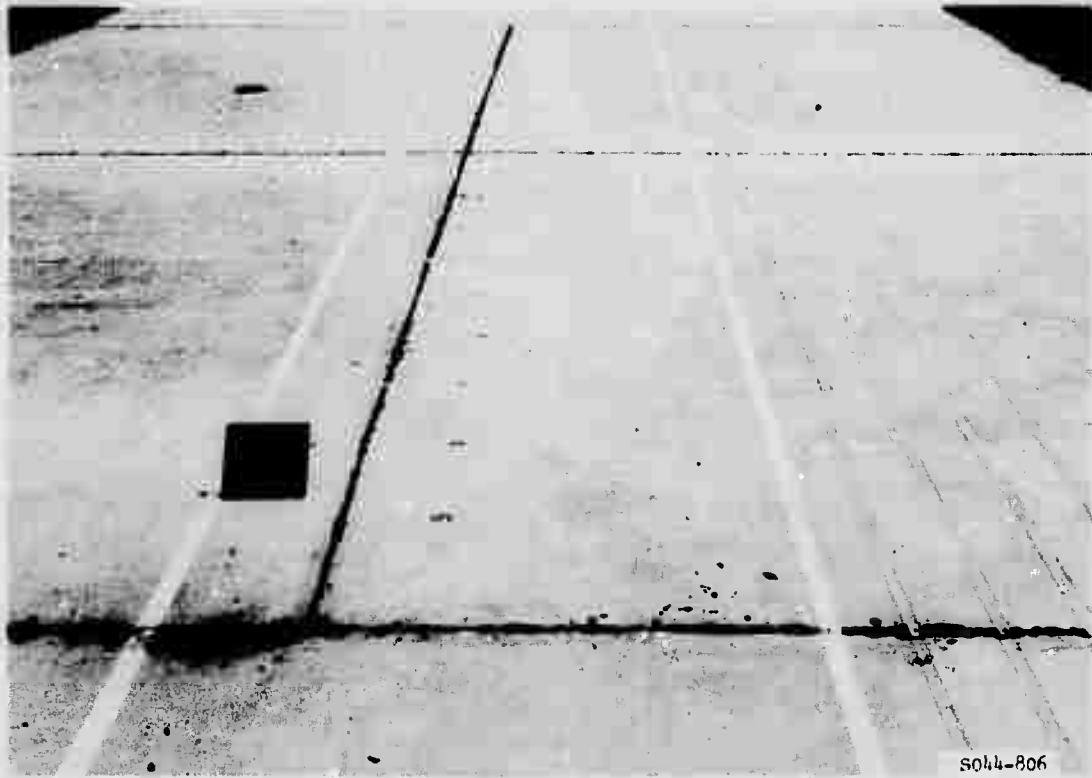


Figure A17. Item 4, lane 1, rigid pavement test section, prior to traffic



Figure A18. Item 4, lane 1, rigid pavement test section, after 1770 coverages by 200-kip twin-tandem assembly

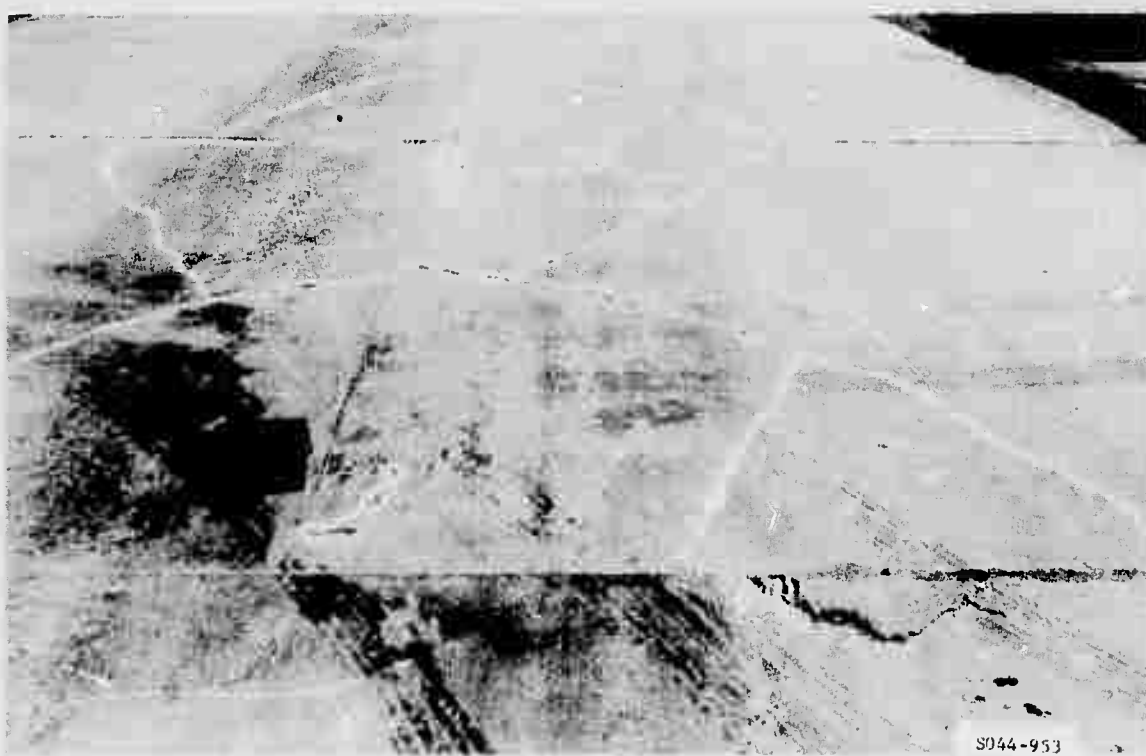
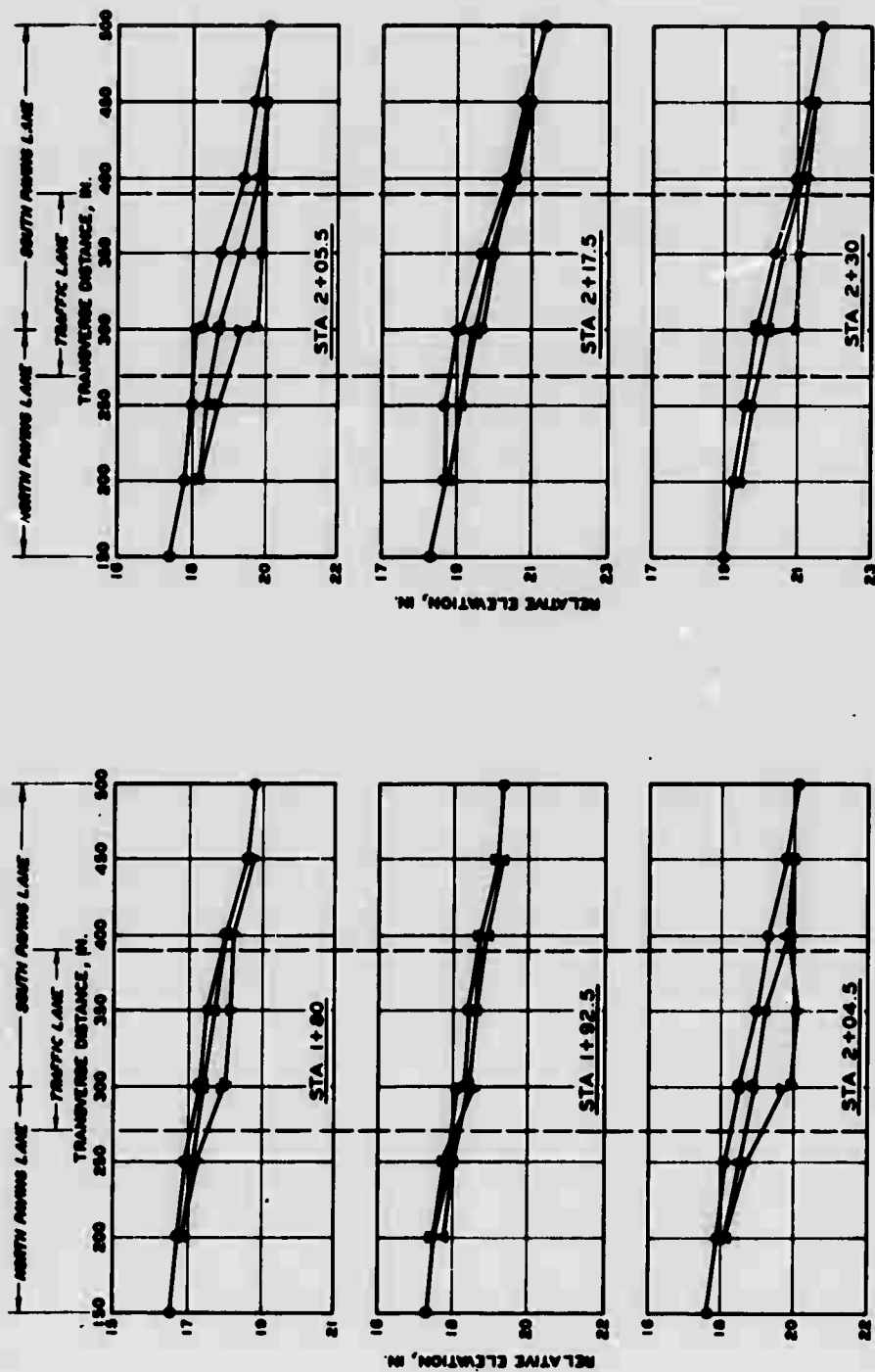


Figure A19. Item 4, lane 1, rigid pavement test section, after 6360 coverages by 200-kip twin-tandem assembly



LEGEND
 ○ 0 COVERAGES
 ▲ 1775 COVERAGES
 ▼ 8300 COVERAGES

Figure A20. Surface deformation in item 4, lane 1, rigid pavement test section

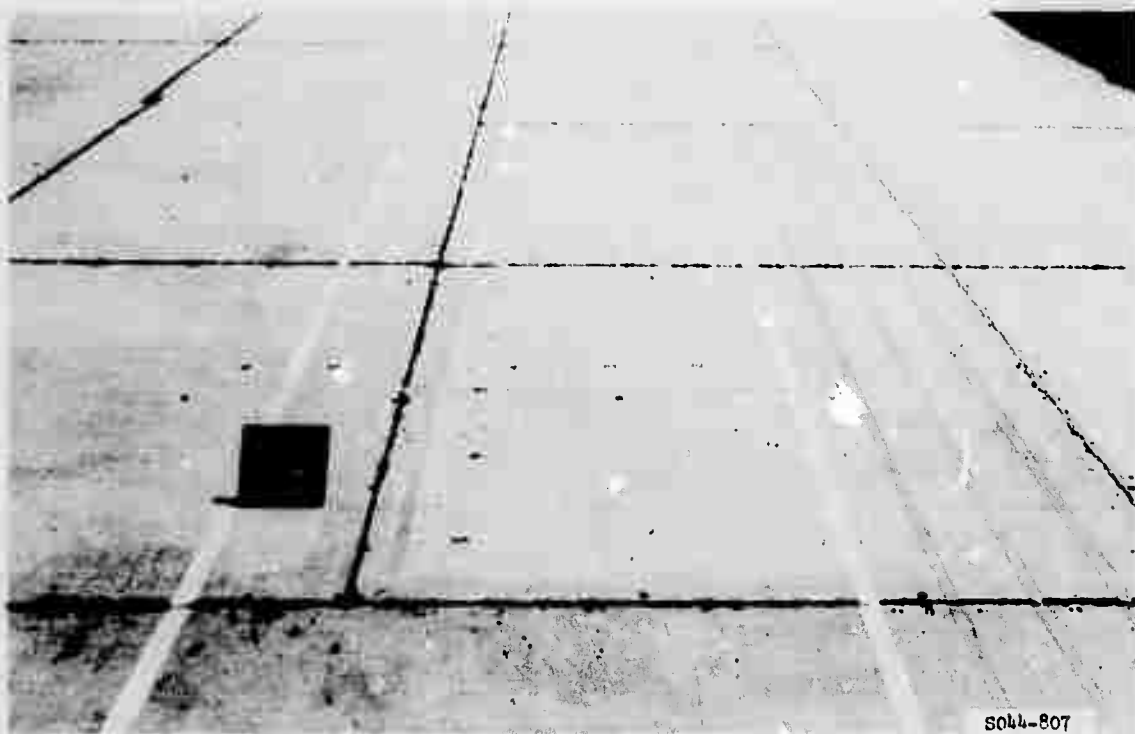


Figure A21. Item 5, lane 1, rigid pavement test section, prior to traffic



Figure A22. Subitem 5a, lane 1, rigid pavement test section, after 1770 coverages by 200-kip twin-tandem assembly

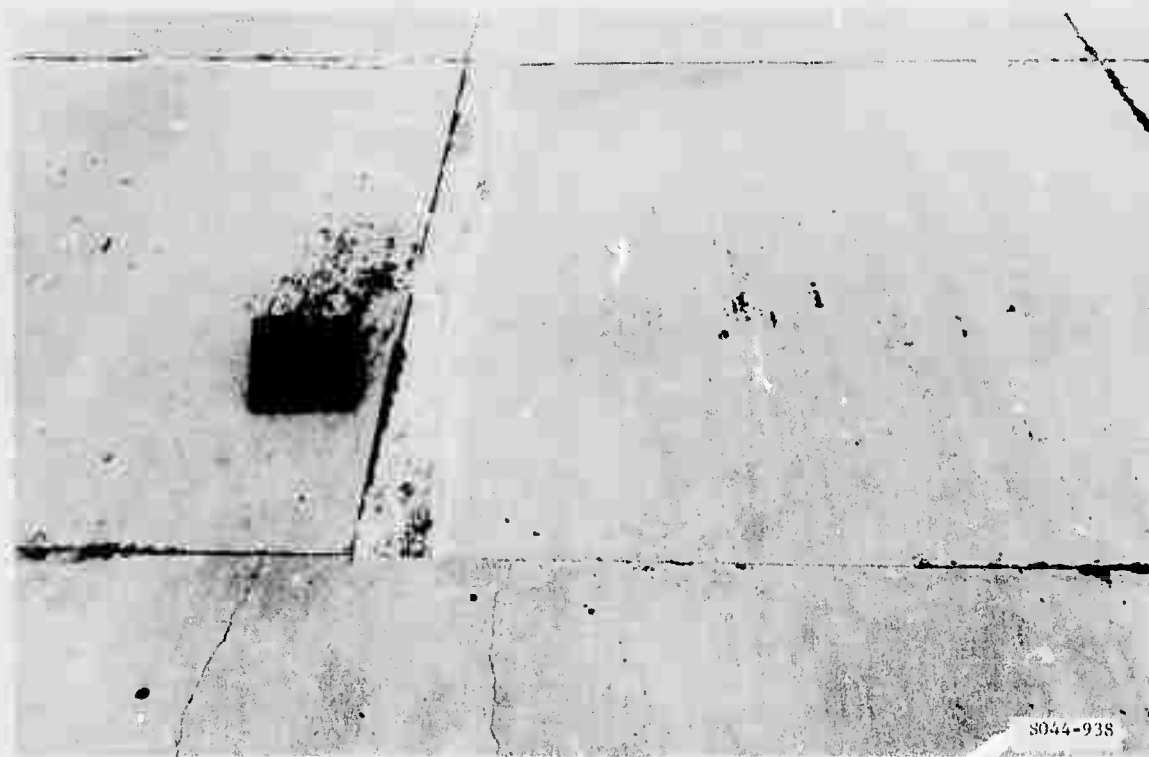


Figure A23. Subitem 5a, lane 1, rigid pavement test section, after 3000 coverages by 200-kip twin-tandem assembly

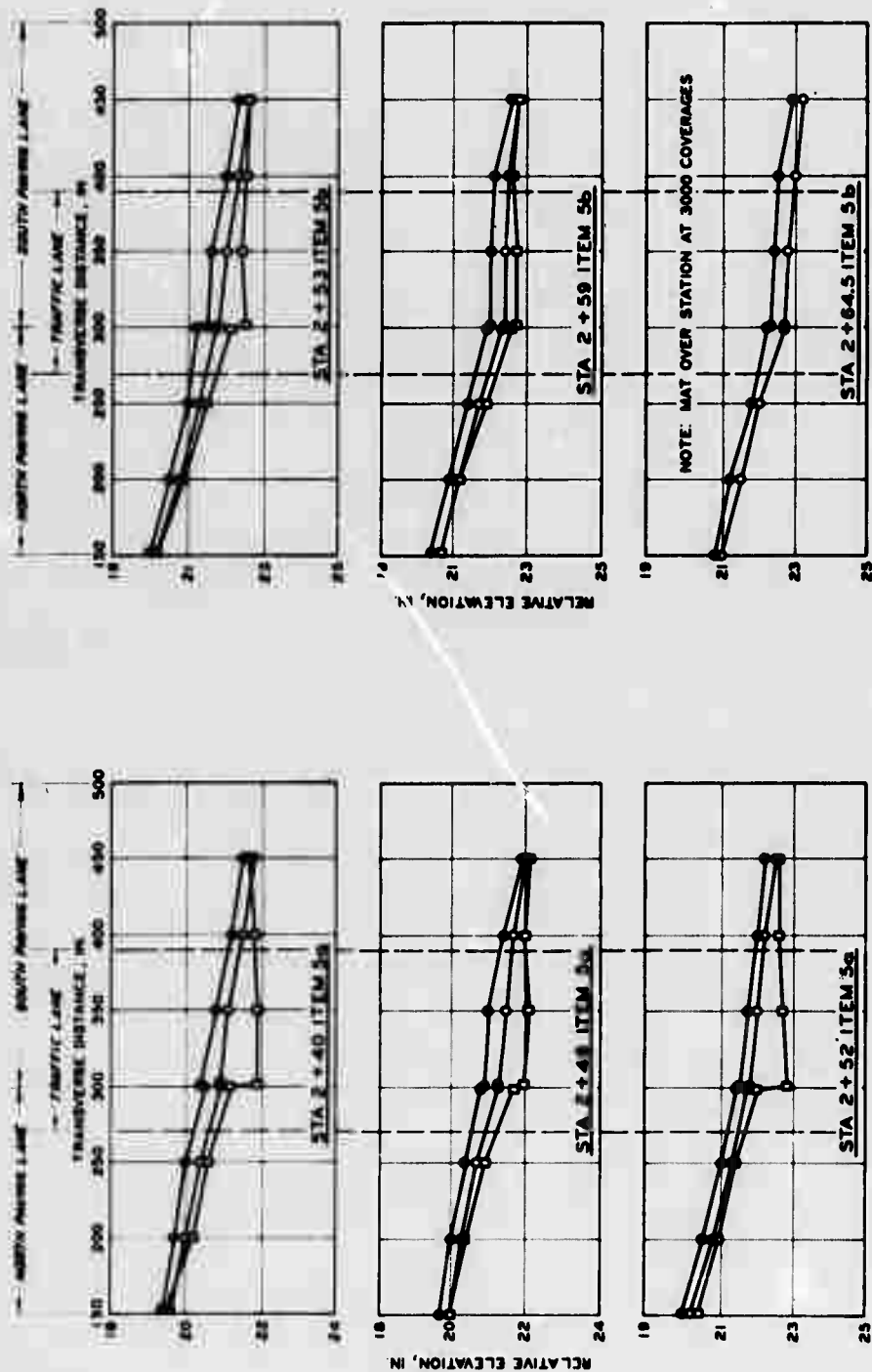


Figure A24. Surface deformation in subitems 5a and b, lane 1, rigid pavement test section



Figure A25. Subitem 5b, lane 1, rigid pavement test section,
after 1770 coverages by 200-kip twin-tandem assembly



Figure A26. Subitem 5b, lane 1, rigid pavement test section,
after 3000 coverages by 200-kip twin-tandem assembly

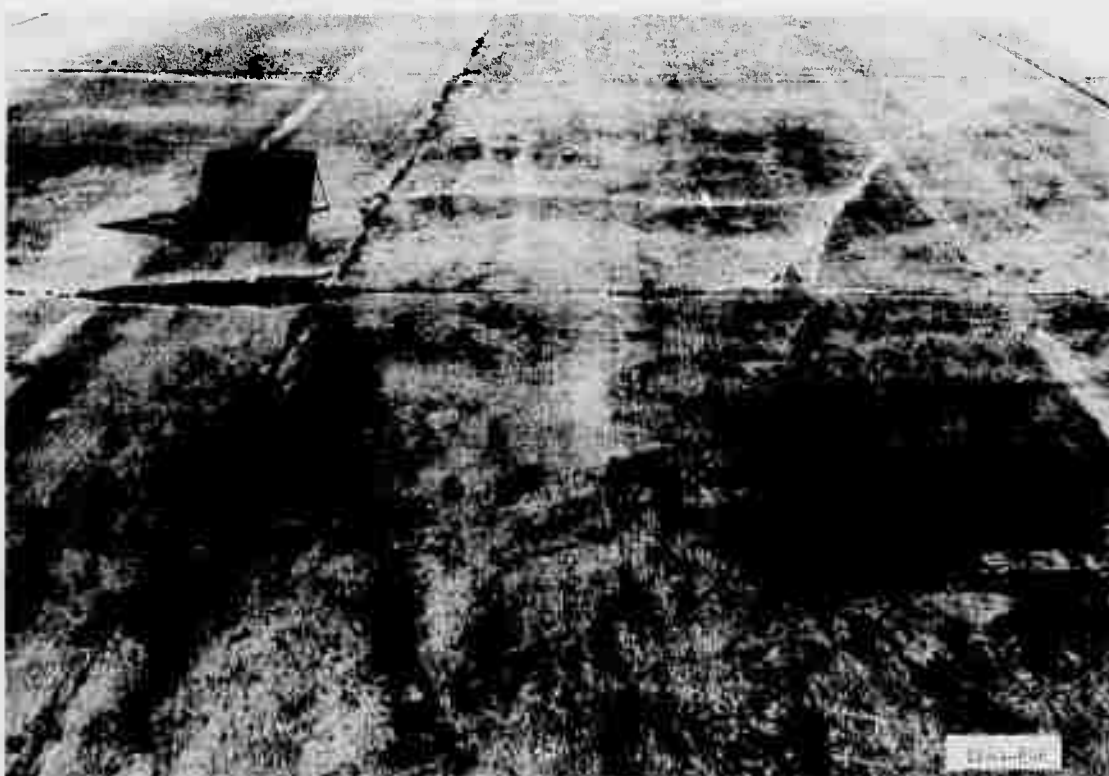


Figure A27. Subitem 5c, lane 1, rigid pavement test section, after 1000 coverages by 200-kip twin-tandem assembly



Figure A28. Subitem 5c, lane 1, rigid pavement test section, after 1230 coverages by 200-kip twin-tandem assembly

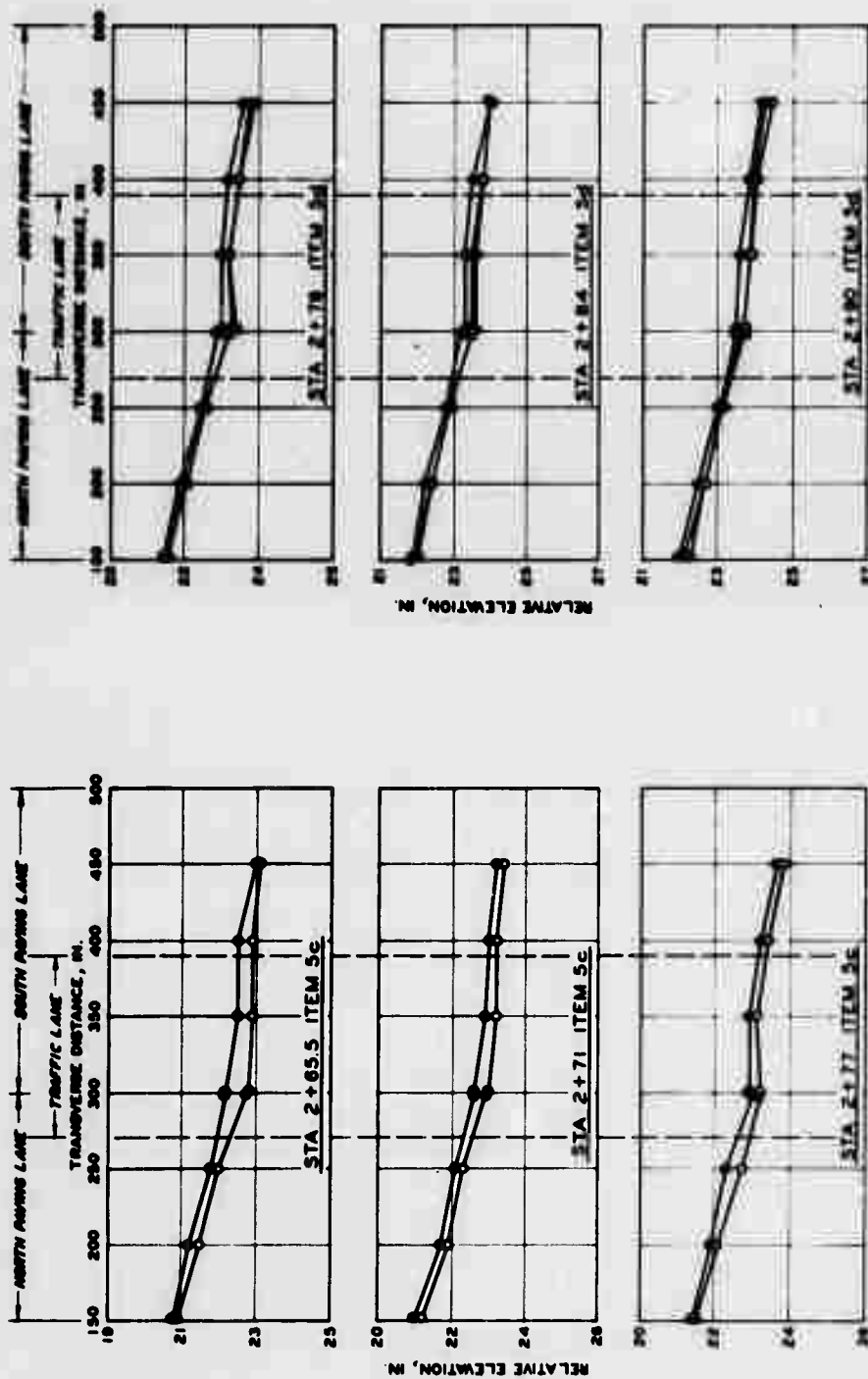


Figure A29. Surface deformation in subitems 5c and d, lane 1, rigid pavement test section

LEGEND

- 0 COVERAGES
- 1000 COVERAGES
- 3000 COVERAGES

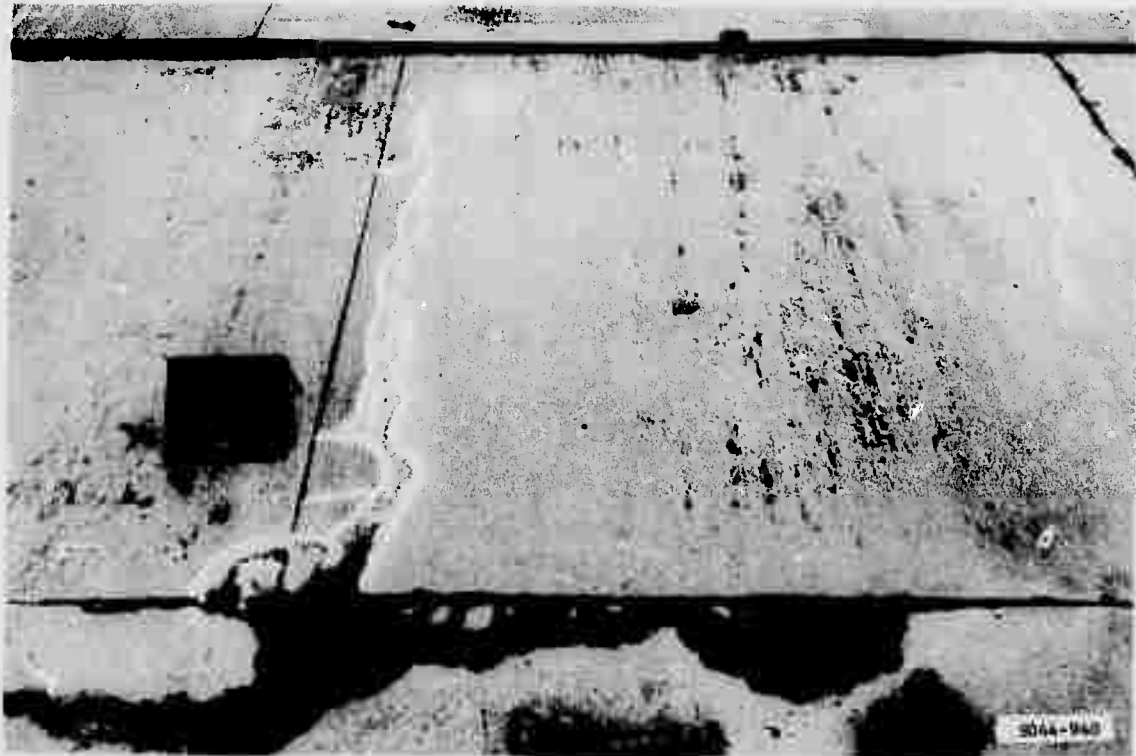


Figure A30. Subitem 5d, lane 1, rigid pavement test section, after 3000 coverages by 200-kip twin-tandem assembly



Figure A31. Item 1, lane 2, rigid pavement test section, prior to traffic

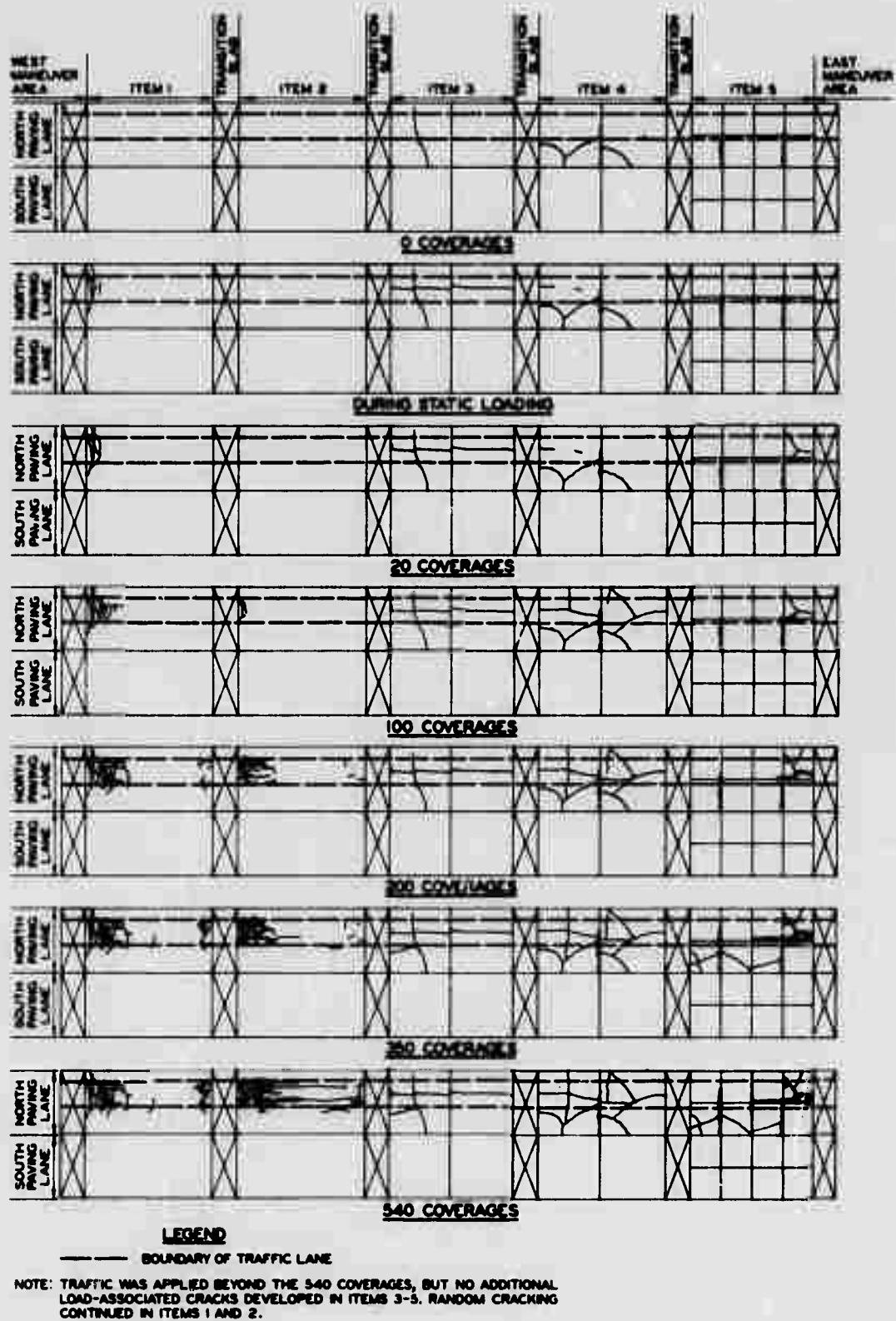


Figure A32. Crack development in lane 2, rigid pavement test section



Figure A33. Item 1, lane 2, rigid pavement test section, after 200 coverages by 240-kip twin-tandem assembly

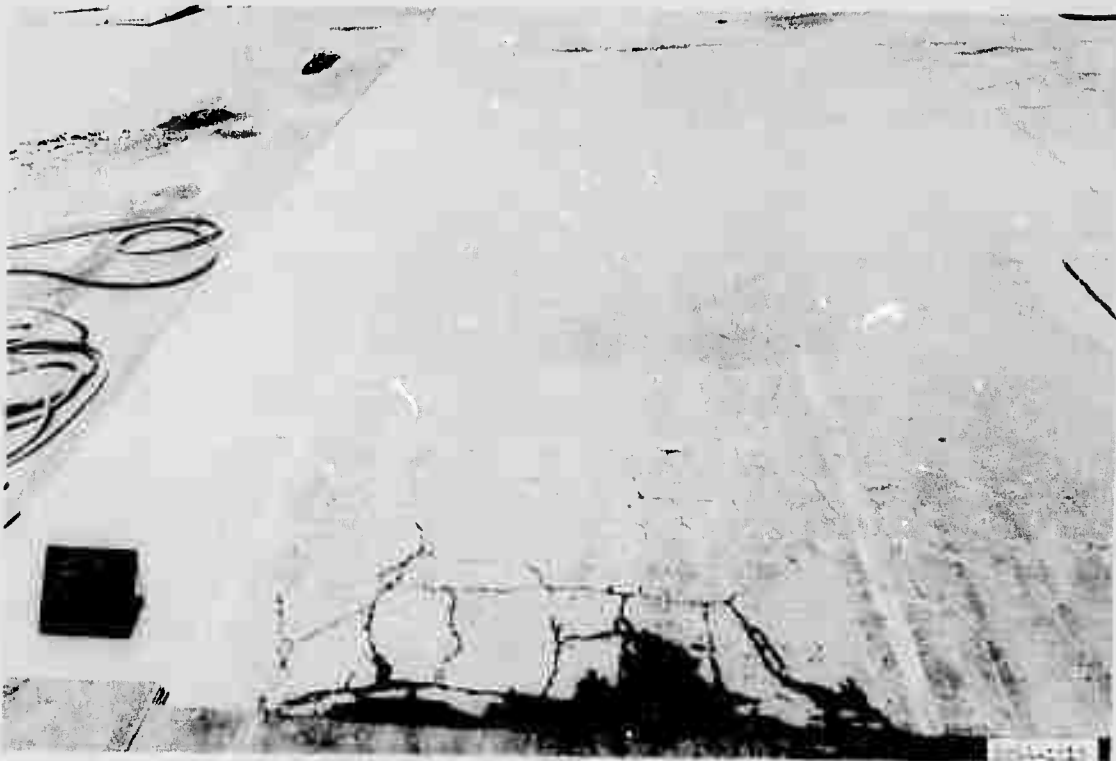


Figure A34. Item 1, lane 2, rigid pavement test section, after 1010 coverages by 240-kip twin-tandem assembly

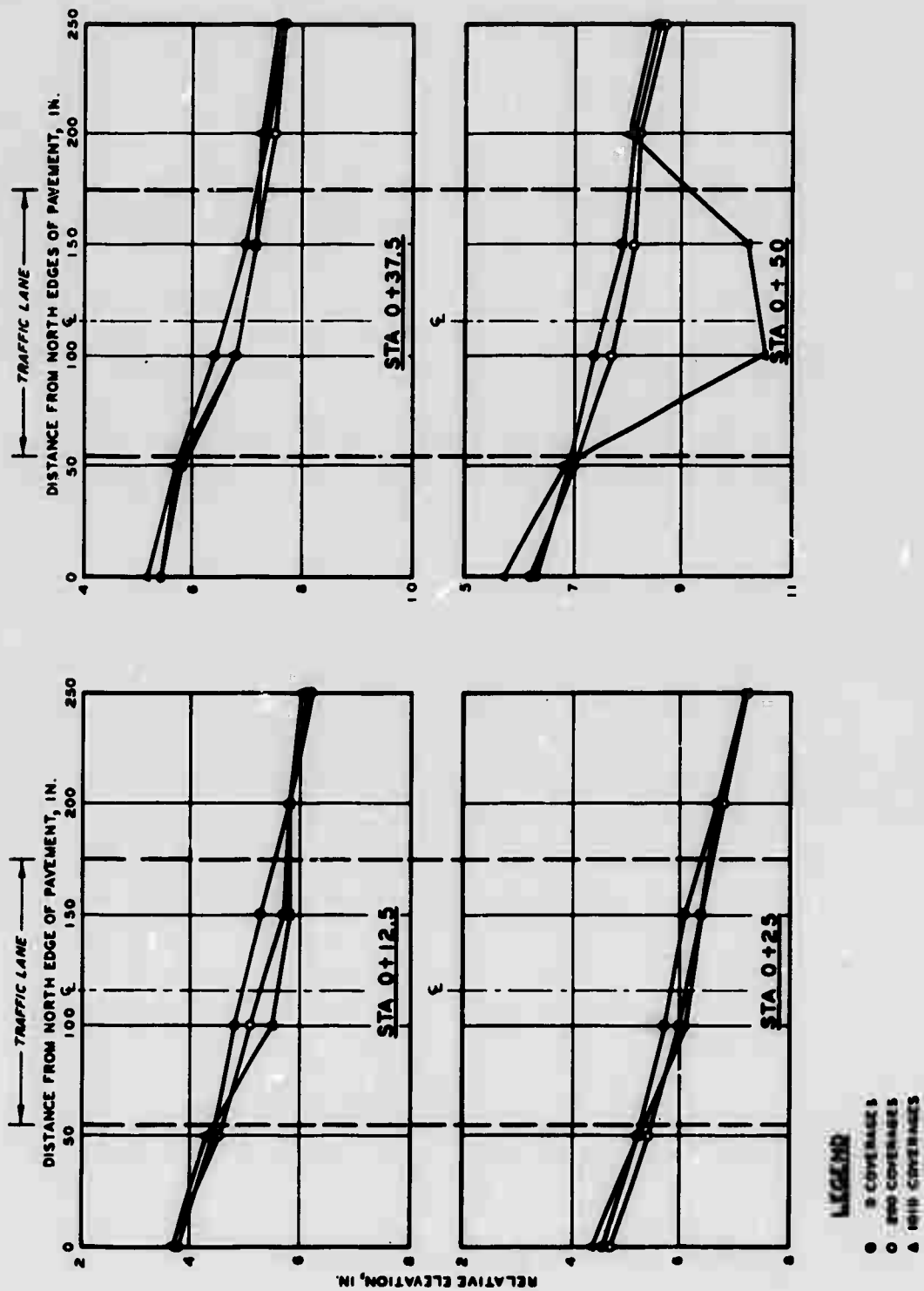


Figure A35. Surface deformation in item 1, lane 2, rigid pavement test section

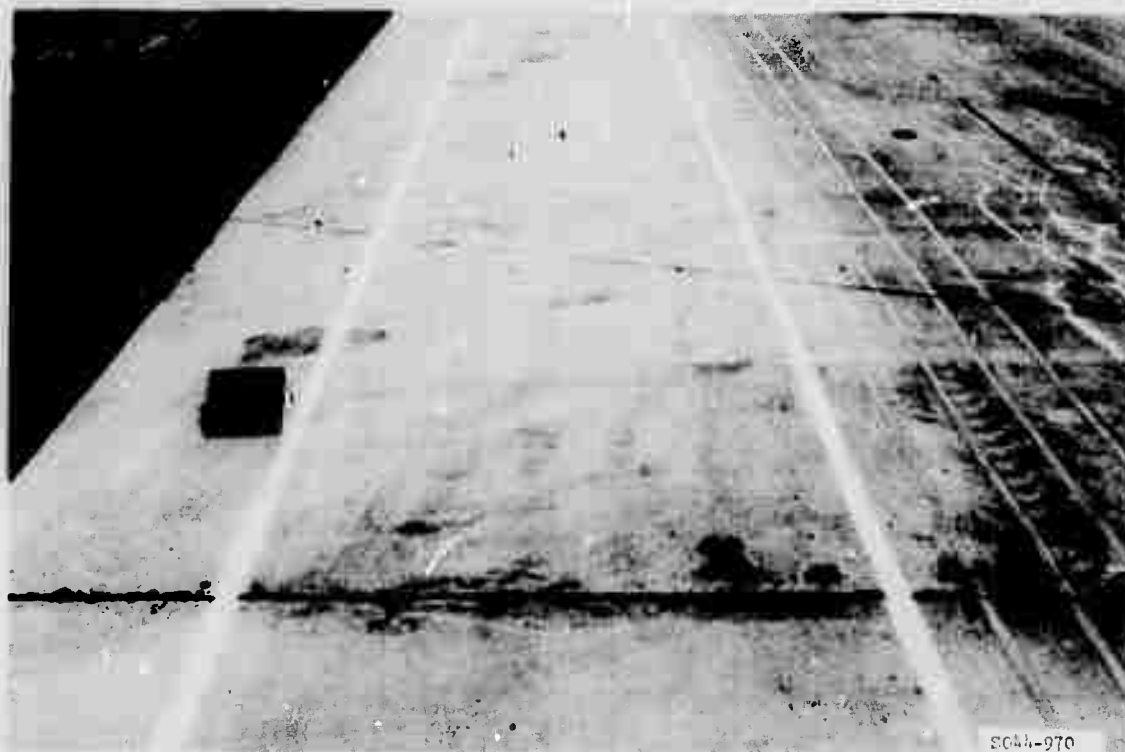


Figure A36. Item 2, lane 2, rigid pavement test section, prior to traffic

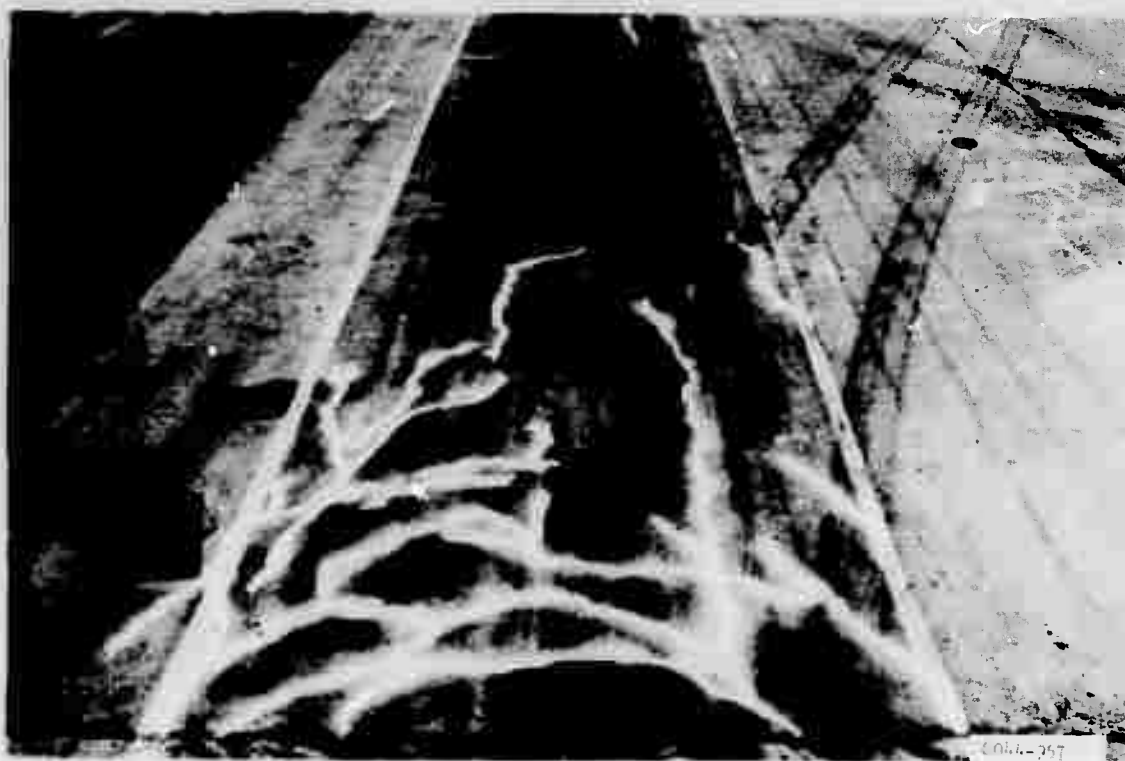


Figure A37. Item 2, lane 2, rigid pavement test section after 200 coverages by 240-kip twin-tandem assembly

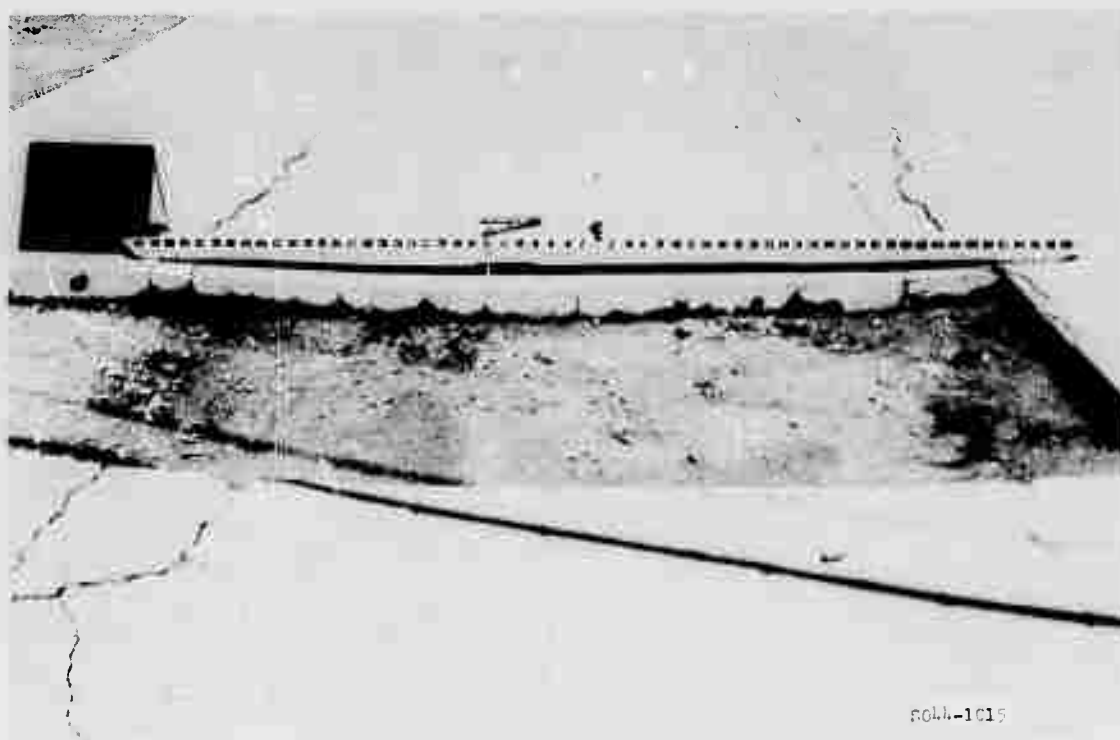


Figure A38. Item 2, lane 2, rigid pavement test section, after 950 coverages by 240-kip twin-tandem assembly

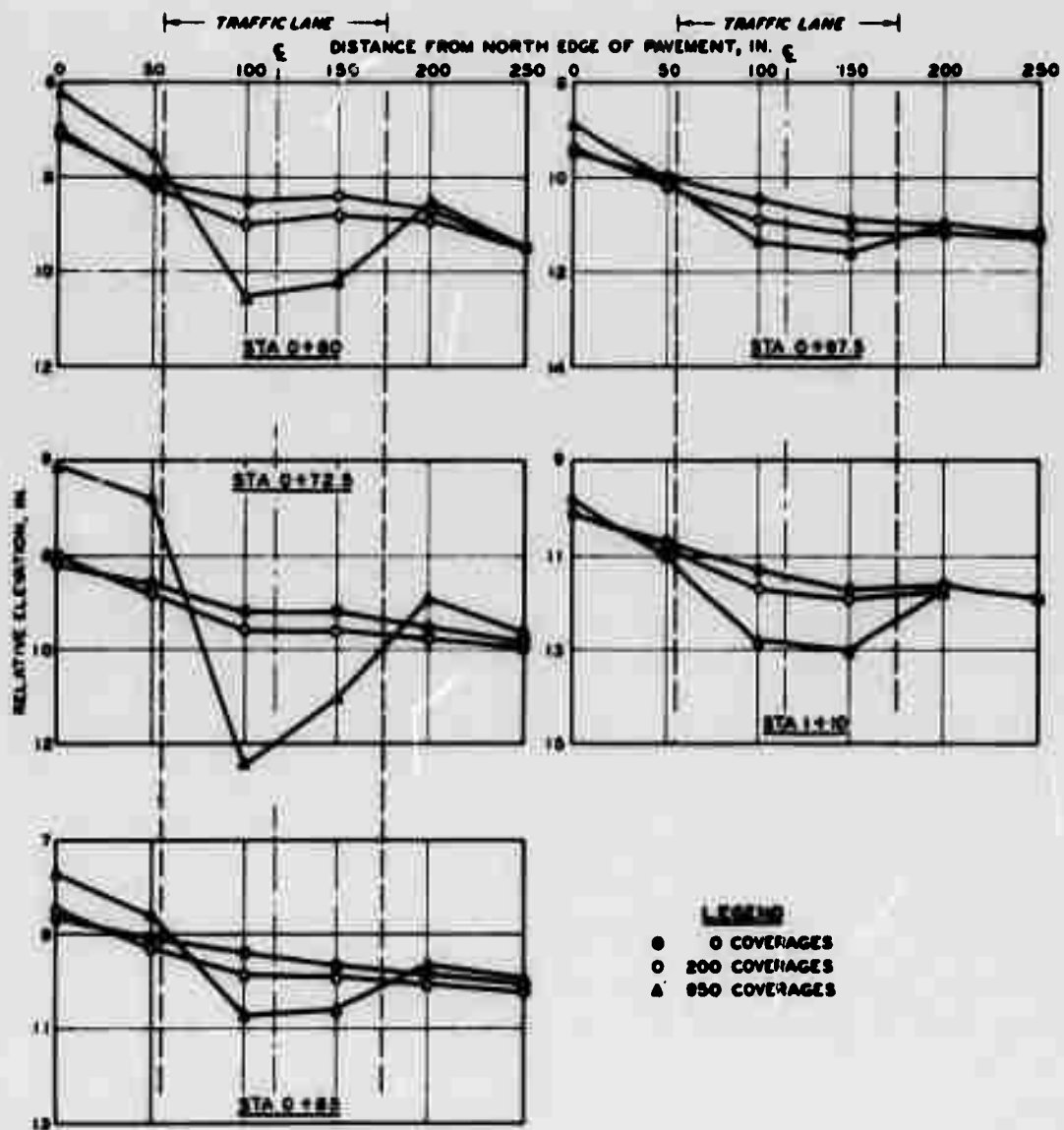


Figure A39. Surface deformation in item 2, lane 2, rigid pavement test section

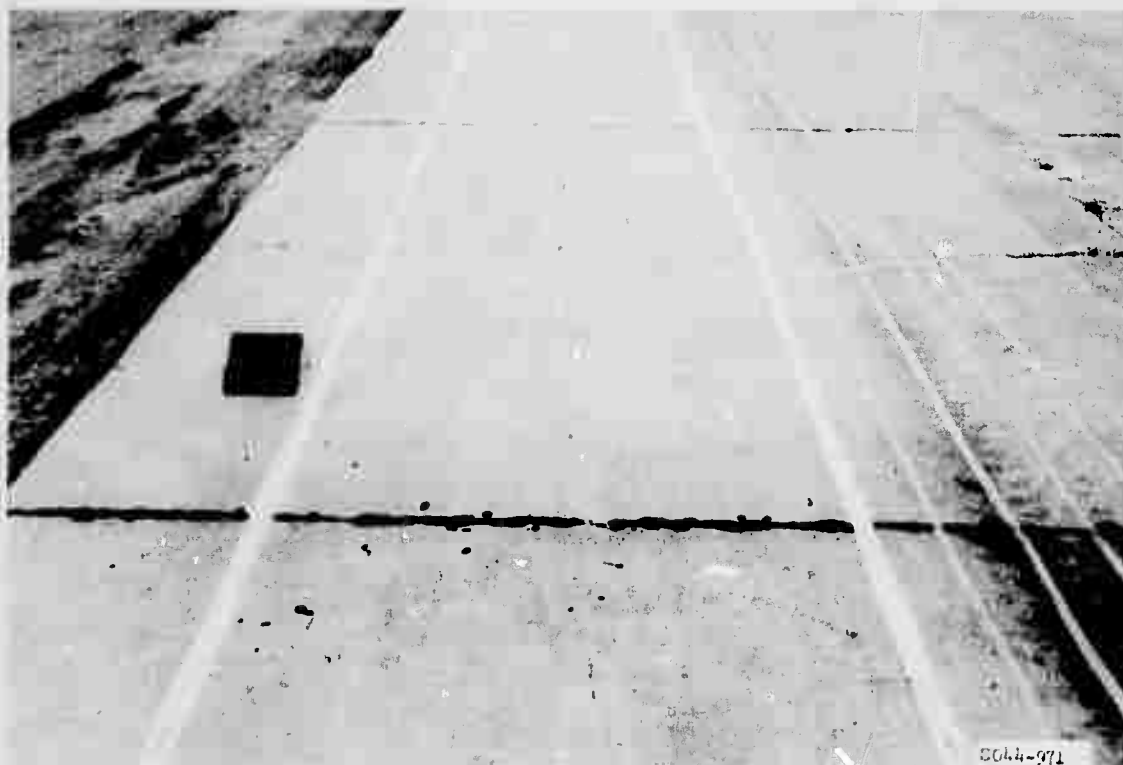


Figure A40. Item 3, lane 2, rigid pavement test section, prior to traffic



Figure A41. Item 3, lane 2, rigid pavement test section, after 200 coverages by 240-kip twin-tandem assembly

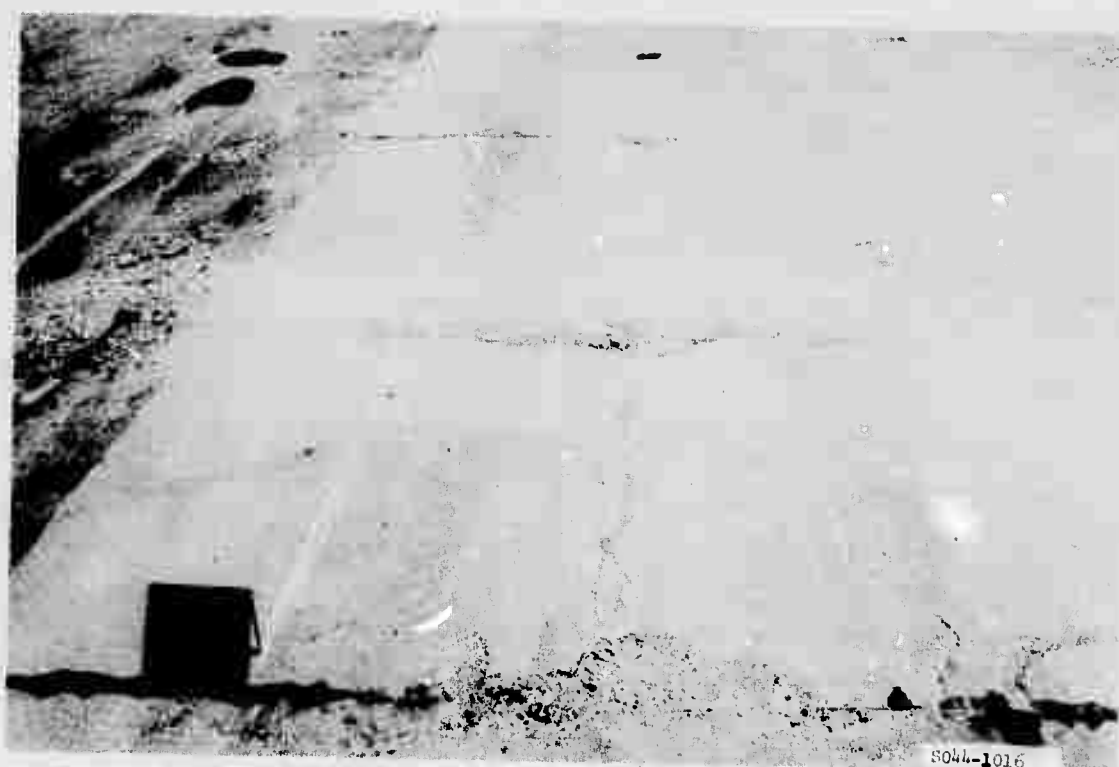


Figure A42. Item 3, lane 2, rigid pavement test section,
after 1200 coverages by 240-kip twin-tandem assembly

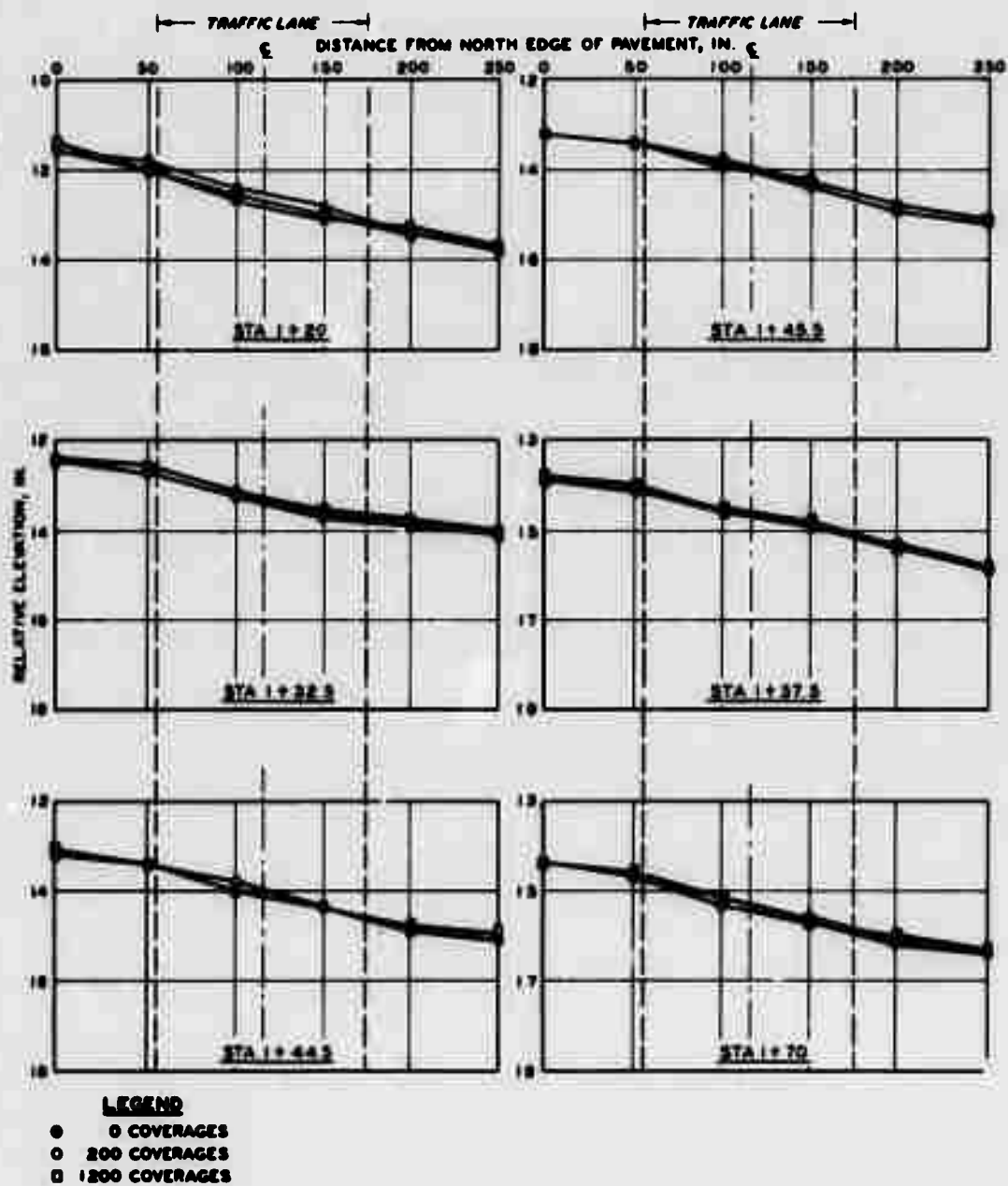


Figure A43. Surface deformation in item 3, lane 2, rigid pavement test section



Figure A44. Item 4, lane 2, rigid pavement test section, prior to traffic



Figure A45. Item 4, lane 2, rigid pavement test section, after 200 coverages by 240-kip twin-tandem assembly

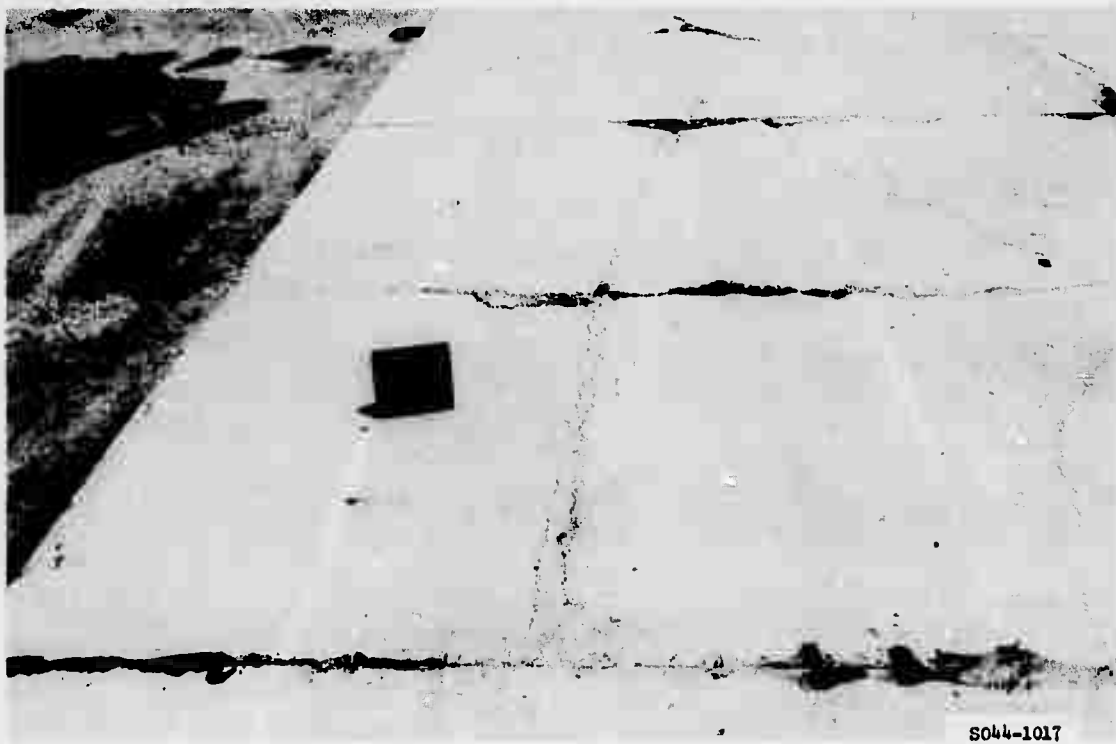


Figure A46. Item 4, lane 2, rigid pavement test section, after 950 coverages by 240-kip twin-tandem assembly

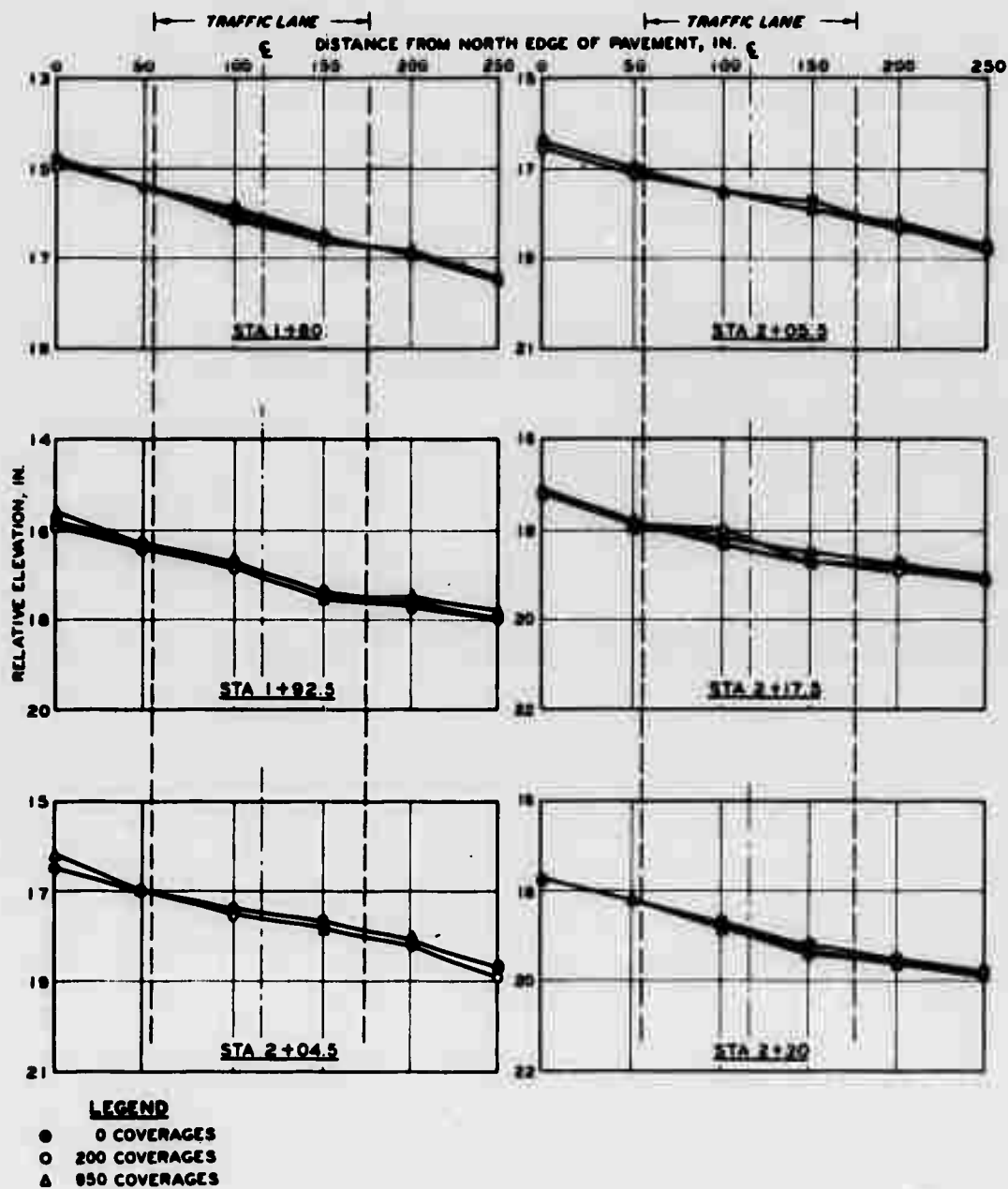


Figure A47. Surface deformation in item 4, lane 2, rigid pavement test section



Figure A48. Subitem 5a, lane 2, rigid pavement test section, after 200 coverages by 240-kip twin-tandem assembly



Figure A49. Subitem 5a, lane 2, rigid pavement test section, after 950 coverages by 240-kip twin-tandem assembly

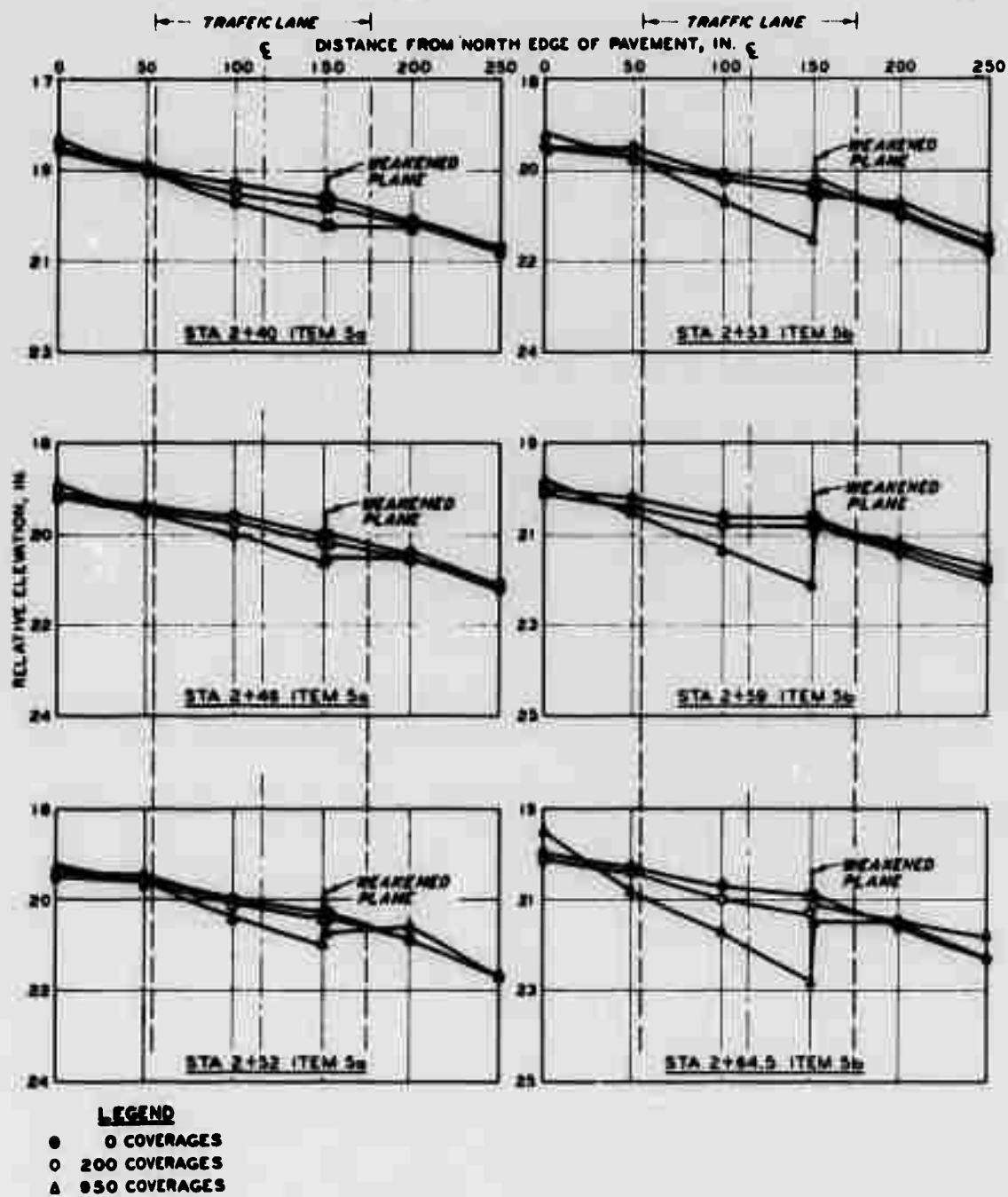


Figure A50. Surface deformation in subitems 5a and b, lane 2, rigid pavement test section



Figure A51. Subitem 5b, lane 2, rigid pavement test section, after 200 coverages by 240-kip twin-tandem assembly

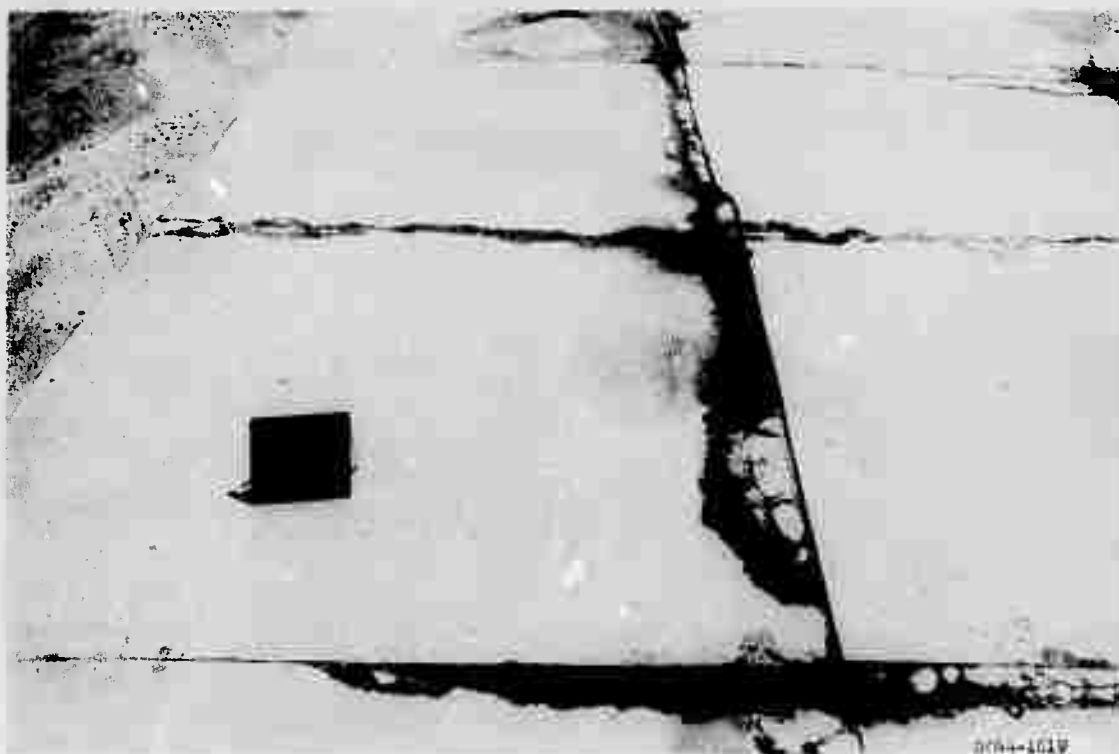


Figure A52. Subitem 5b, lane 2, rigid pavement test section, after 950 coverages by 240-kip twin-tandem assembly

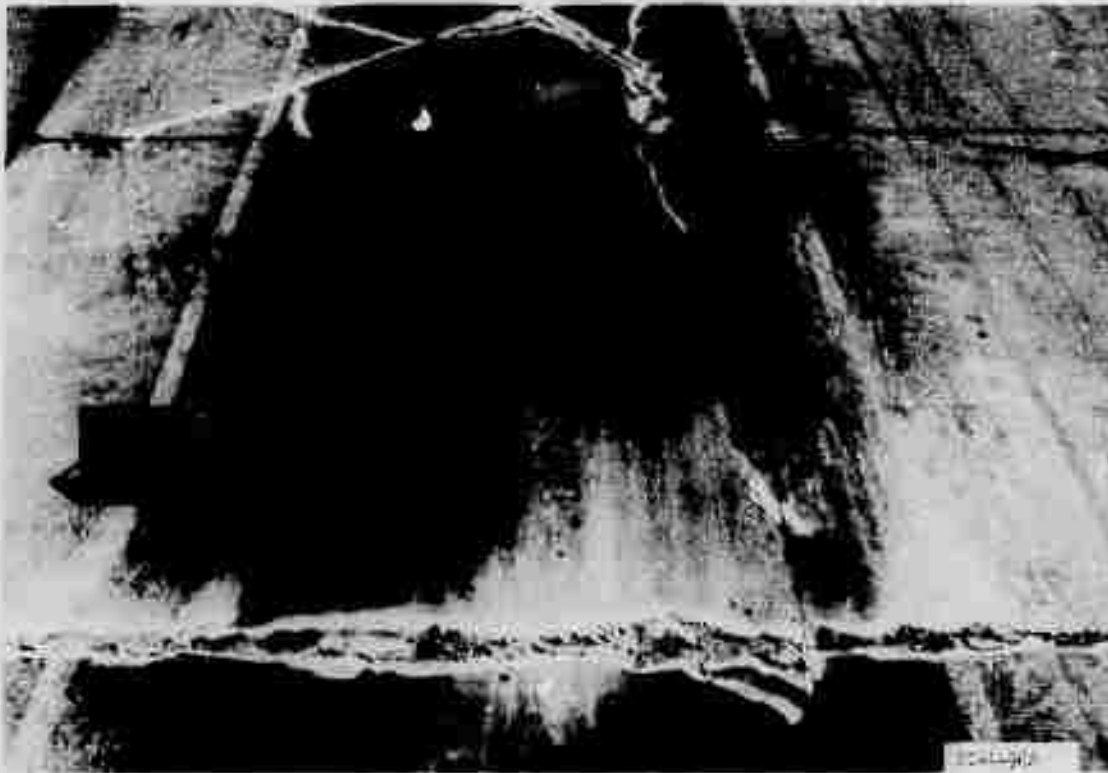


Figure A53. Subitem 5c, lane 2, rigid pavement test section, after 200 coverages by 240-kip twin-tandem assembly



Figure A54. Subitem 5c, lane 2, rigid pavement test section, after 840 coverages by 240-kip twin-tandem assembly

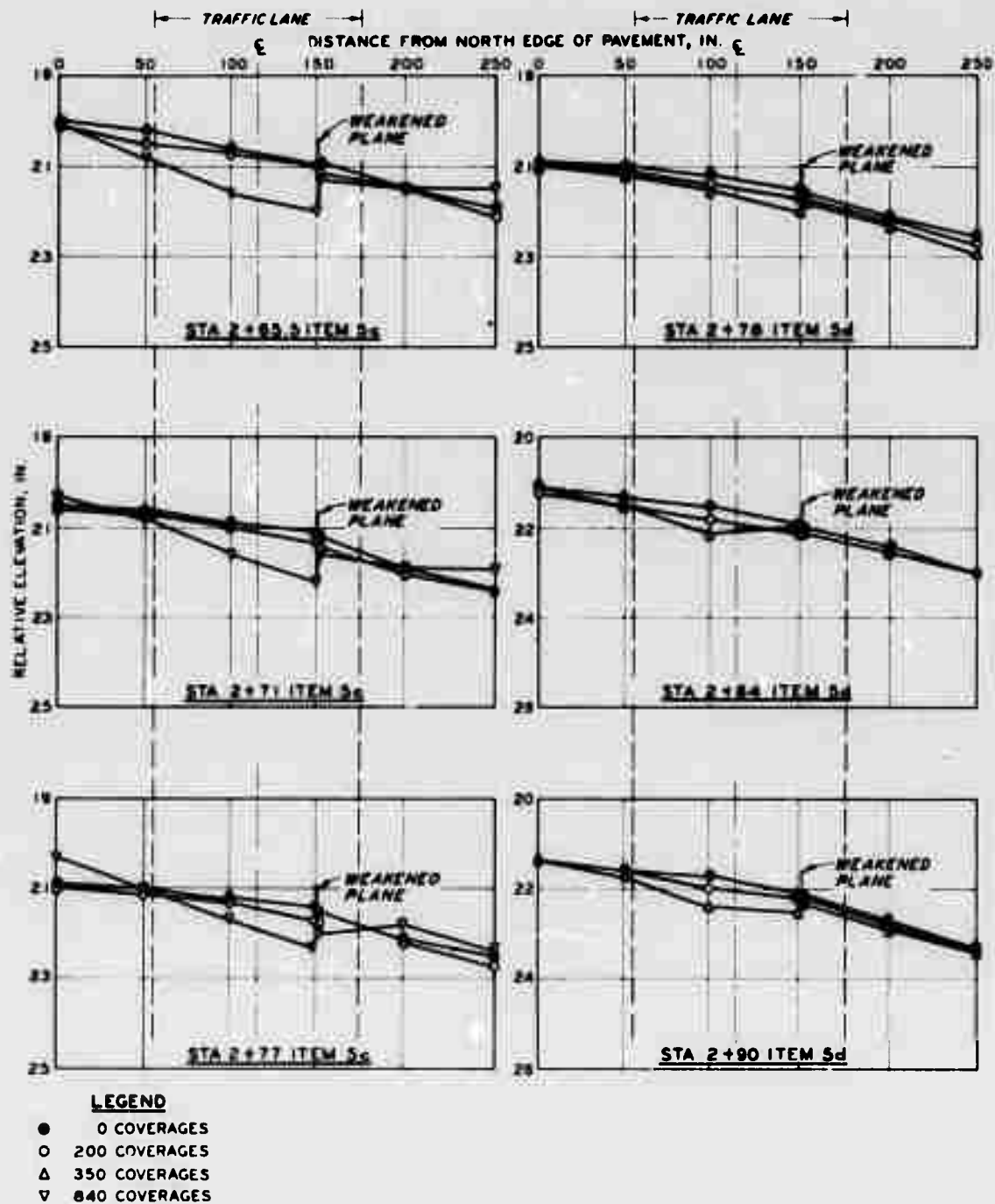


Figure A55. Surface deformation in subitems 5c and d, lane 2, rigid pavement test section

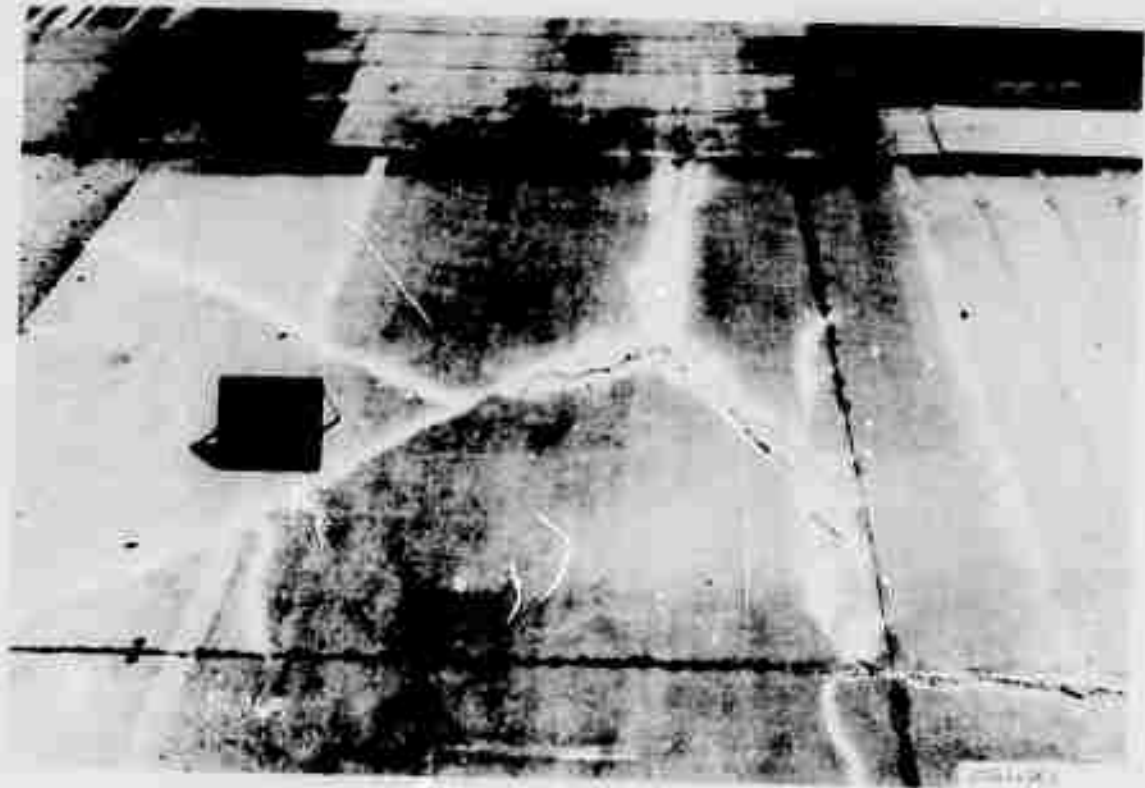


Figure A56. Subitem 5d, lane 2, rigid pavement test section, after 200 coverages by 240-kip twin-tandem assembly

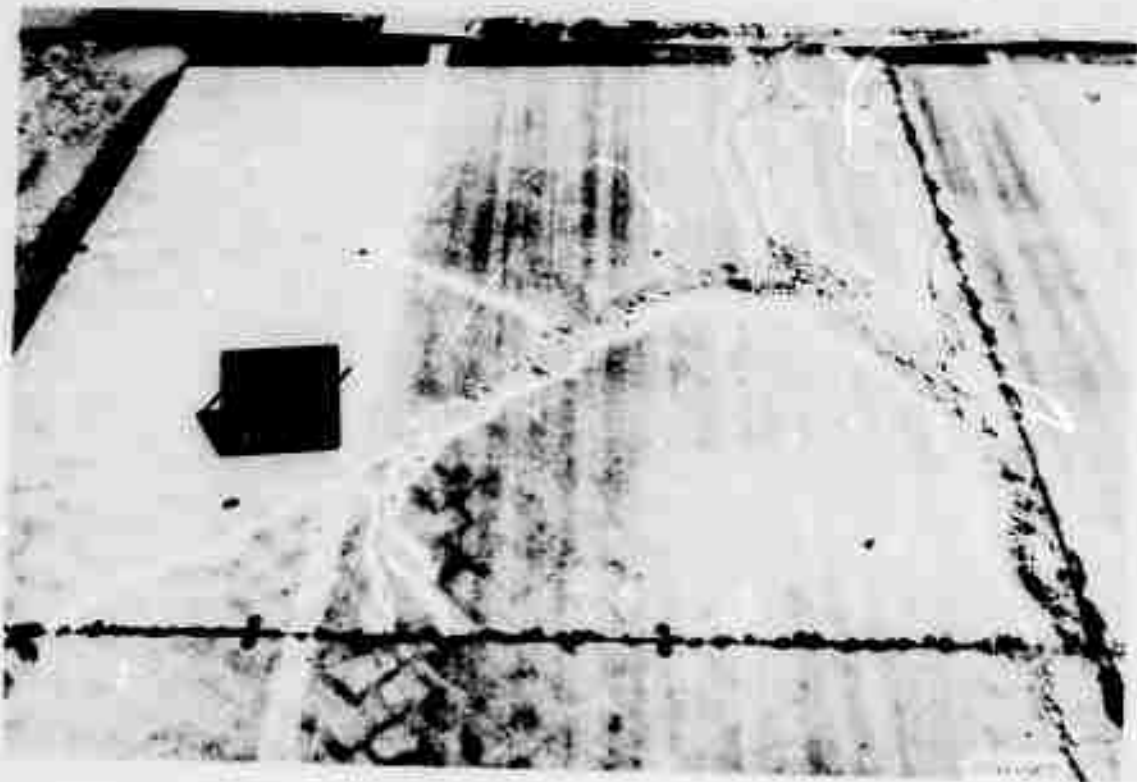
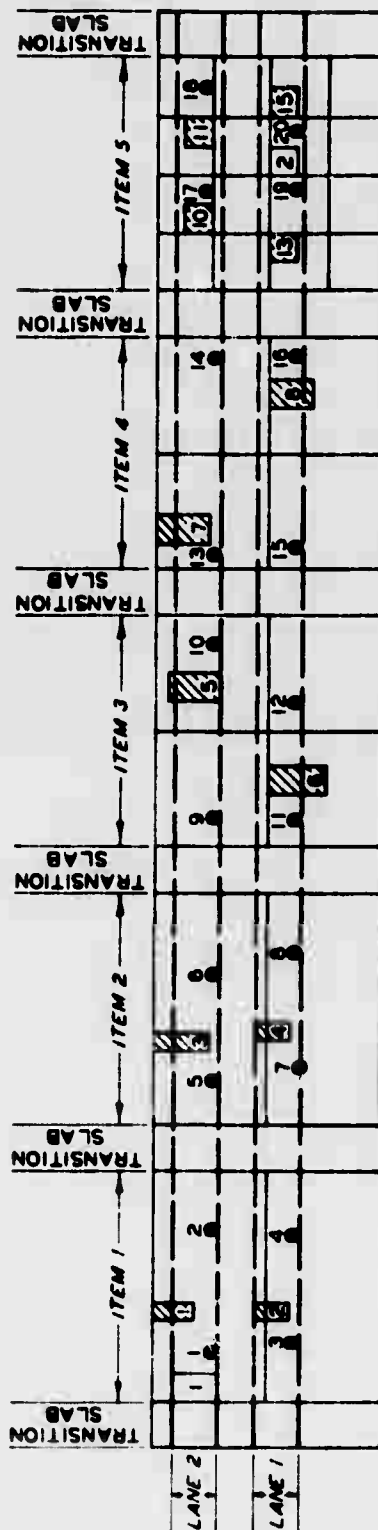


Figure A57. Subitem 5d, lane 2, rigid pavement test section, after 350 coverages by 240-kip twin-tandem assembly



LEGEND




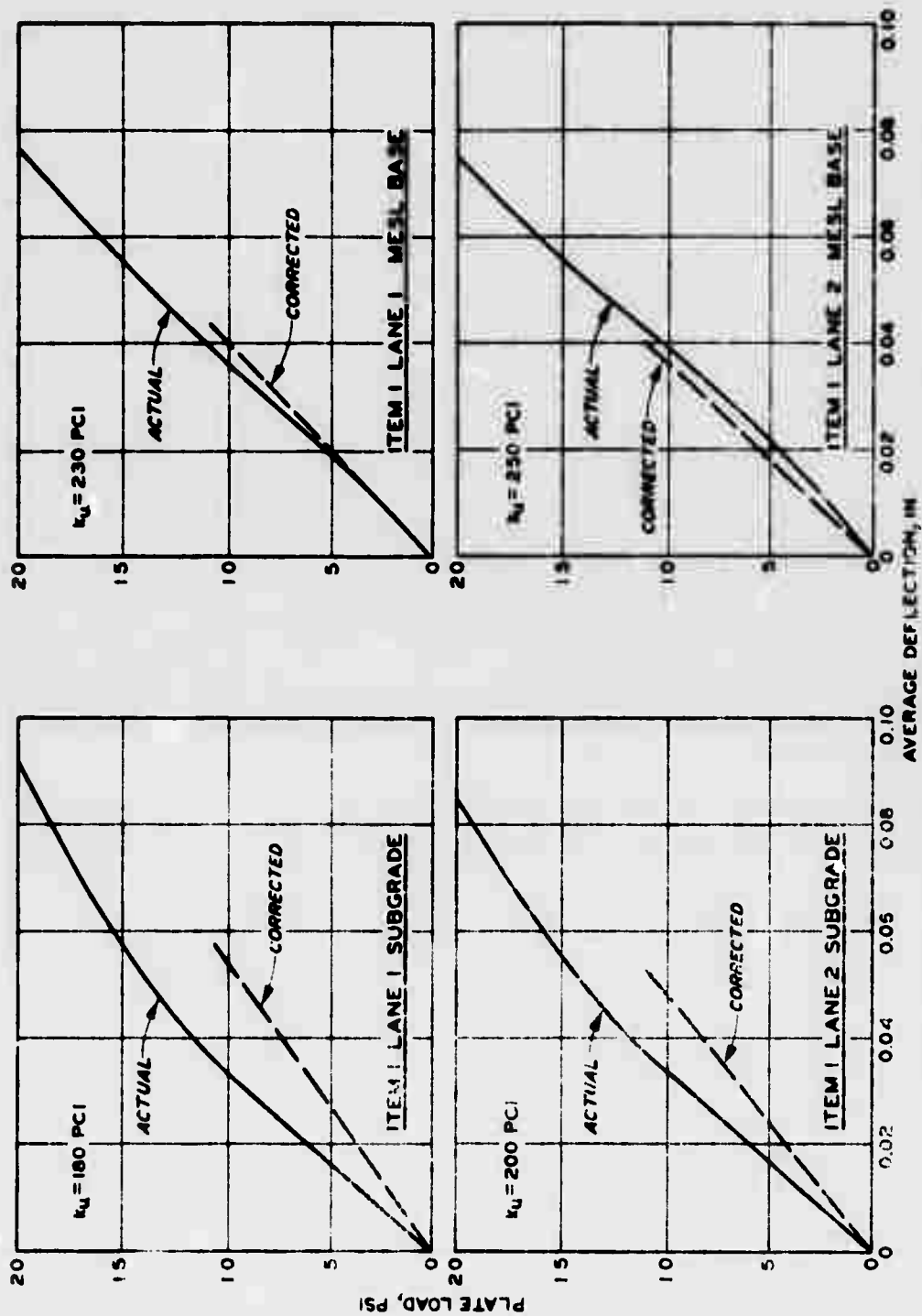
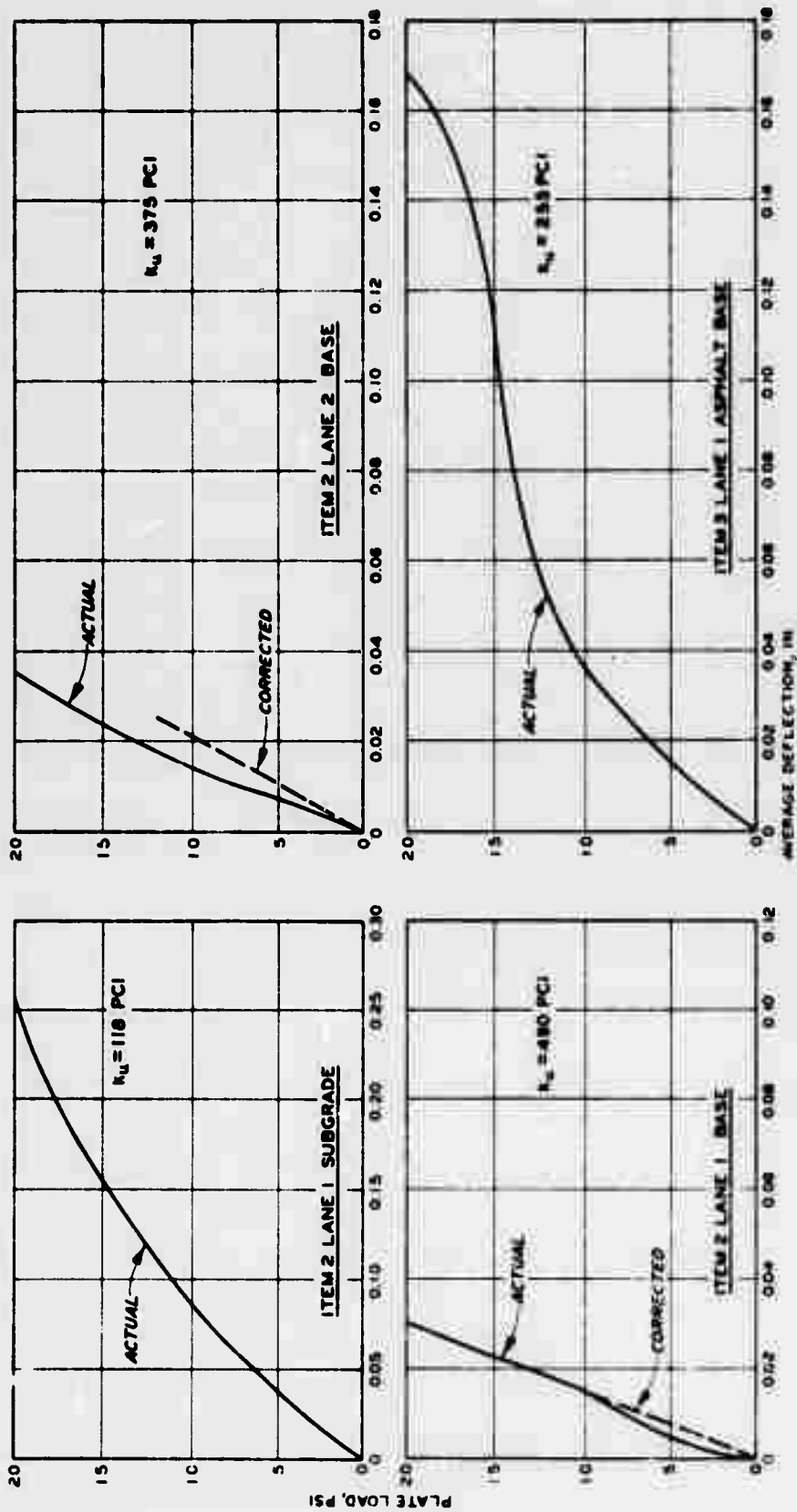
-  TEST PIT
-  OBSERVATION PIT
-  CORE

Figure A58. Locations of test pits, observation pits, and cores in rigid pavement test section



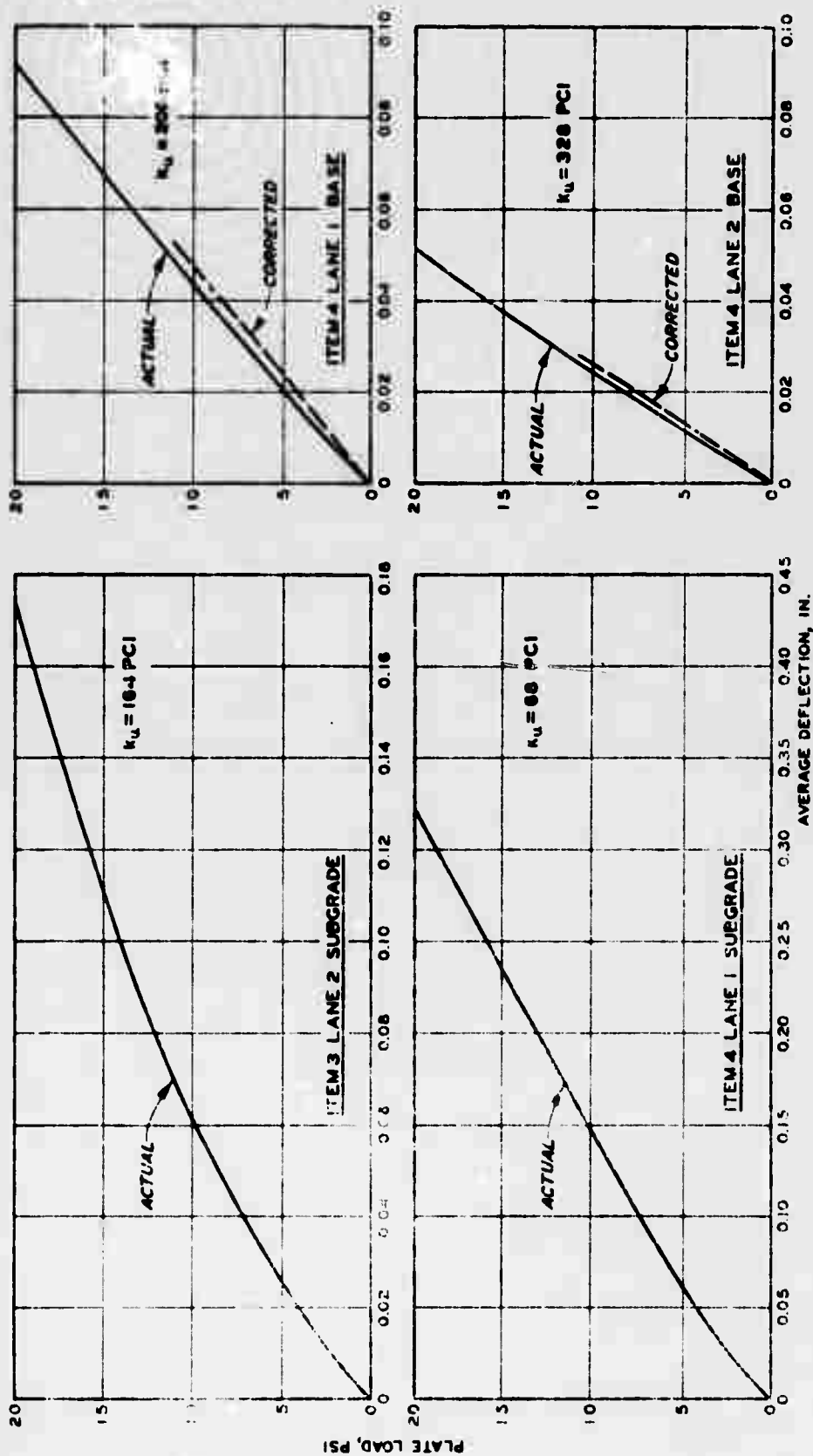
NOTE: k_u IS THE MODULUS OF SOIL REACTION, IN POUNDS PER CUBIC INCH, UNCORRECTED FOR SATURATION.

Figure A59. Plate bearing tests, item 1, lanes 1 and 2, rigid pavement test section



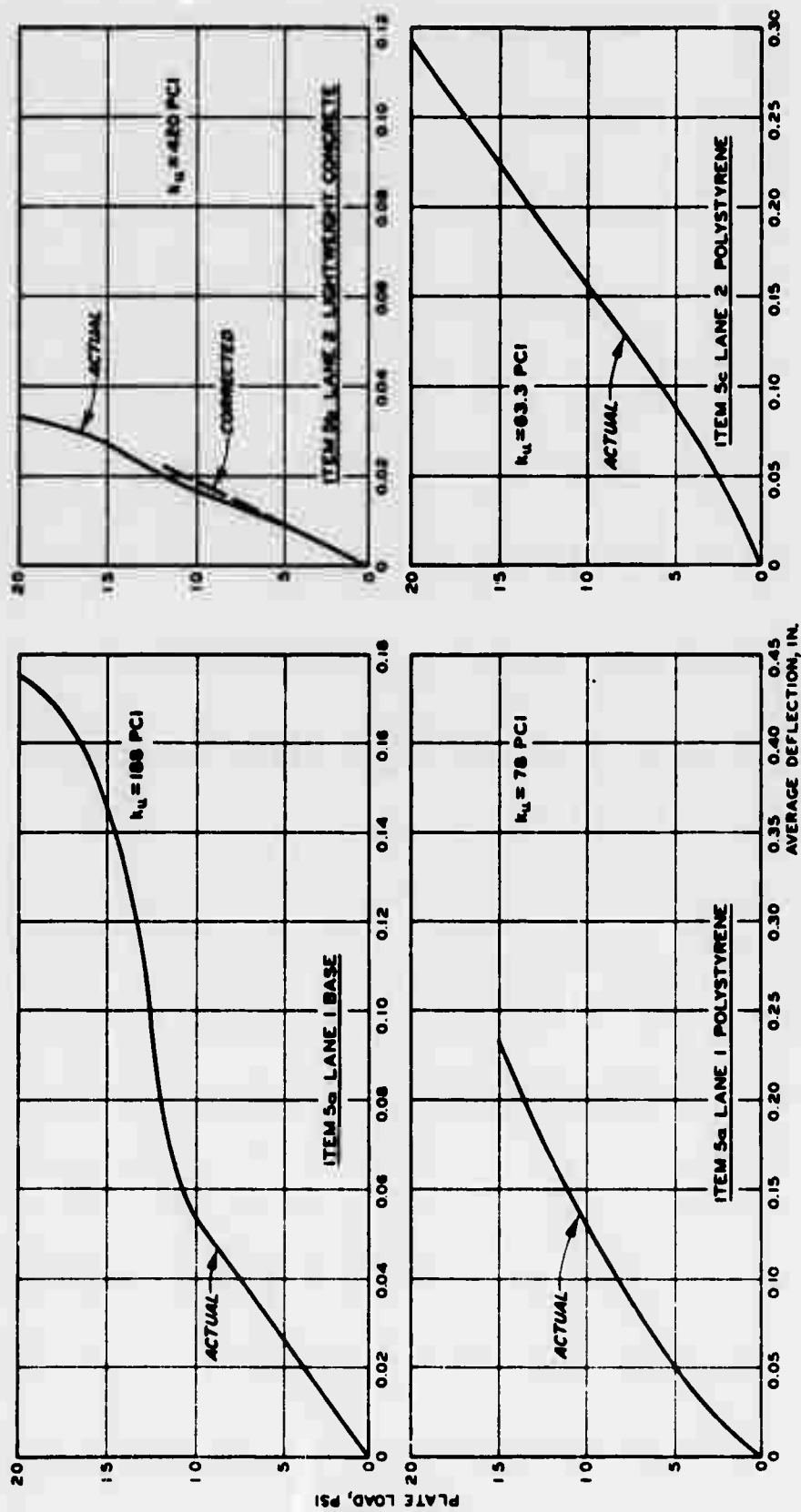
NOTE: k_u IS THE MODULUS OF SOIL REACTION, IN POUNDS PER CUBIC INCH, UNCORRECTED FOR SATURATION.

Figure A60. Plate bearing tests, item 2, lanes 1 and 2, rigid pavement test section



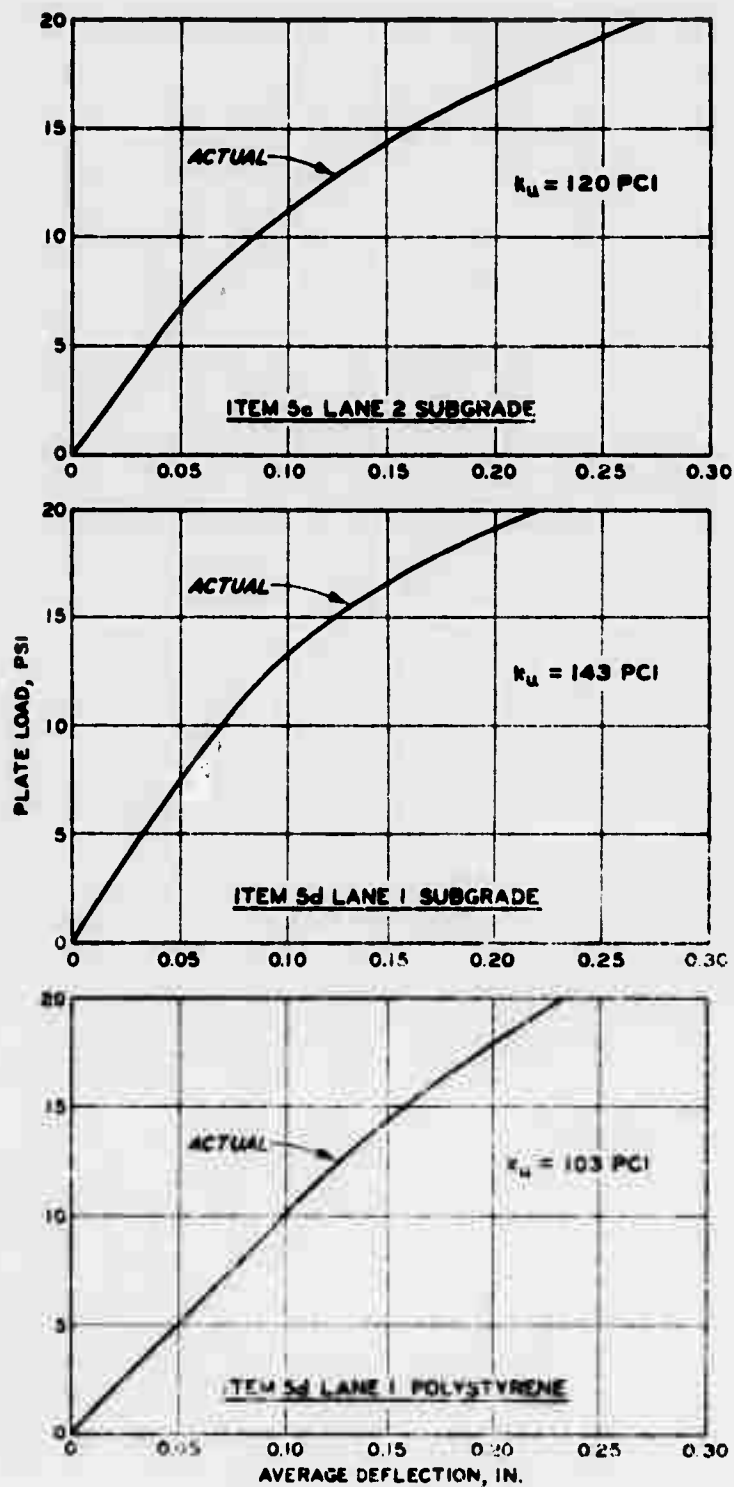
NOTE: k_u IS THE MODULUS OF SOIL REACTION, IN POUNDS PER CUBIC INCH, UNCORRECTED FOR SATURATION.

Figure A61. Plate bearing tests, items 3 and 4, lanes 1 and 2, rigid pavement test section



NOTE: k_u IS THE MODULUS OF SOIL REACTION, IN POUNDS PER CUBIC INCH, UNCORRECTED FOR SATURATION.

Figure A62. Plate bearing tests, items 5a-c, lanes 1 and 2, rigid pavement test section



NOTE: k_u IS THE MODULUS OF SOIL REACTION, IN POUNDS PER CUBIC INCH, UNCORRECTED FOR SATURATION.

Figure A63. Plate bearing tests, items 5c and d, lanes 1 and 2, rigid pavement test section

Table A1
Results of Tests of Beams from Rigid Pavement Test Section

<u>Item No.</u>	<u>Test Pit No.</u>	<u>Lane and Slab</u>	<u>Nominal Beam Size in.</u>	<u>No. of Beams</u>	<u>Average Flexural Strength psi</u>	<u>Static Modulus 10⁶ psi</u>
1	1	2N	8 by 8 by 24	3	1097	4.68
1	2	1S	7 by 7 by 21	3	992	5.33
2	3	2N	4 by 4 by 12	3	1120	6.41
2	4	1S	4 by 4 by 12	3	1177	4.60
3	5	2NE	15 by 15 by 45	2	910	6.30
33	6	1SW	15 by 15 by 45	3	897	6.79
4	7	2NW	15 by 15 by 45	3	605	5.87
4	8	1SE	15 by 15 by 45	3	982	7.23
5a	13	1S	15 by 15 by 45	3	965	7.76
5b*	10	2N	8 by 8 by 24	3	127	0.373
5c	11	2N	15 by 15 by 45	3	868	6.70

* Lightweight concrete base.

Table A2

Results of Tests on Concrete Cores From Rigid Pavement Test Section

Item No.	Date Tested	Core No.	Diam in.	Length in.	Weight lb	Density pcf	Compressive Strength psi	Tensile Strength psi	Dynamic Modulus 10 ⁶ psi	Static Modulus 10 ⁶ psi
1	5-16-73	1	3.89	6.90	6.98	146.9	5840*	--	--	4.34
1	5-16-73	2	3.89	7.05	7.10	145.3	7610	--	--	5.25
1	5-16-73	3	3.89	6.50	6.42	143.6	6690	--	--	4.75
1	5-16-73	4	3.89	6.50	6.53	146.0	6840	--	--	5.00
2	5-16-73	5	5.90	4.50	10.40	146.0	--	830	--	--
2	5-16-73	6	5.90	4.50	10.80	151.0	--	860	--	--
2	5-16-73	7	5.90	4.00	9.20	145.3	--	880	--	--
2	5-14-73	8	5.90	4.50	10.00	147.2	--	905	--	--
3	5-16-73	9	5.90	12.10	28.20	147.3	5880	--	6.09	5.53
3	5-14-73	10	5.90	12.00	28.10	148.0	5820	--	6.23	5.80
3	5-14-73	11	5.90	12.15	28.20	144.5	5020	--	5.43	4.86
3	5-14-73	12	5.90	11.90	27.60	146.6	6660	--	6.00	6.20
4	5-14-73	13	5.90	12.00	28.20	148.5	6480	--	6.36	5.90
4	5-14-73	14	5.90	12.10	28.40	148.3	8580	--	6.45	5.80
4	5-14-73	15	5.90	12.00	27.90	146.9	5670	--	5.81	5.00
4	5-14-73	16	5.90	11.90	27.20	144.5	6990	--	6.22	5.62
5	5-16-73	17	5.90	12.05	27.80	145.7	6590	--	5.81	5.71
5	5-16-73	17**	5.90	8.50	6.06	45.0	270	--	--	0.134
5	5-14-73	18	5.90	12.10	28.20	147.3	5310	--	5.84	5.14
5	5-16-73	19	5.90	12.40	28.50	145.2	7280	--	5.99	6.10
5	5-16-73	19**	5.90	8.00	5.85	46.2	272	--	--	--
5	5-14-73	20	5.90	12.10	27.90	145.7	6220	--	5.62	5.07

* Core had vertical crack prior to testing.

** Lightweight concrete core.

APPENDIX B: BEHAVIOR OF FLEXIBLE PAVEMENT TEST SECTION UNDER TRAFFIC

200-KIP LOAD, LANE 1

ITEM 1

A general view of item 1 prior to traffic is shown in Figure B1. Cracking began at the west end of the item adjacent to the transition area between this test section and the original multiple-wheel heavy gear load test section and progressed with the continued application of traffic. At 2500 coverages, cracking was severe on the western quarter of the item (Figure B2). Traffic was continued on the item to 3660 coverages, when failure occurred. At the time of failure, cracks had penetrated the full depth of the asphaltic concrete. Cracks in the western quarter of the item had become extremely severe and this area had to be covered with landing mat after 2680 coverages in order to continue traffic. Figure B3 shows the eastern three-fourths of the item at failure (3660 coverages).

ITEM 2

A general view of item 2 prior to traffic is shown in Figure B4. At 1200 coverages, a few transverse hairline cracks were observed near the center of the item where the instrumentation gages were installed. As traffic was continued on the section, the transitions at each end of the item failed and were covered with landing mat in order to continue traffic. At 2500 coverages, cracking around the instrumentation grid had increased (Figure B5); cores taken showed that the cracks were not completely through the asphaltic concrete. The item was considered failed at 3660 coverages, with cracks penetrating the full depth of the asphaltic concrete. The condition of the pavement at failure is shown in Figure B6.

ITEM 3

A general view of item 3 prior to traffic is shown in Figure B7. Prior to traffic, a few hairline shrinkage cracks had developed in the item as shown in the figure. These cracks appeared to seal under the

first few coverages of traffic. At about 2500 coverages, the shrinkage crack along the north edge of the traffic lane began to open but did not affect the structural capabilities of the pavement. Traffic was continued on the item. At about 4600 coverages, a few longitudinal hairline cracks were noted in the pavement surface. Traffic was discontinued on the item at 7820 coverages when cracks penetrated the full depth of the asphaltic concrete. The condition of the pavement at 7820 coverages is shown in Figure B8. There was no rutting at the end of traffic; however, the surface of the entire traffic lane was concave.

ITEM 4

A general view of item 4 prior to traffic is shown in Figure B9. Moderate cracking was noted on the west end of the traffic lane at about 760 coverages. At 1200 coverages, severe cracking had occurred over most of the western half of the item (Figure B10). The item was judged failed at 1380 coverages due to cracks penetrating the full depth of the asphaltic concrete. Cracks were about 1/2 in. wide, and some rutting had occurred. Figure B11 shows the condition of the pavement at failure.

ITEM 5

A general view of item 5 prior to traffic is shown in Figure B12. At 1200 coverages, shallow hairline cracks were observed near the west end of the item (Figure B13). Traffic was stopped on the item after 2500 coverages because cracks penetrated the full depth of the asphaltic concrete and the item was considered failed. Figure B14 shows the condition of the item at the time of failure.

PAVEMENT DEFLECTION

Surface deflection measurements were made at one location per item at zero coverages and at various intervals during traffic. These measurements were obtained with level instruments by reading rods (engineer scales) at prearranged positions on lines both transverse and longitudinal to the direction of traffic. Transverse deflection readings were taken along the center line of the rear duals of the twin-tandem assembly. Rod readings were first taken with the load off the

the pavement; the test cart was moved until the centroid of the assembly was at a prearranged position, and a second series of readings was taken with the load on. The difference in rod readings indicated the total vertical movement of the pavement. This deflection was essentially elastic since the pavement surface rebounded to about the original elevation when the load was removed.

Plots of deflection measurements taken transverse to the direction of traffic prior to traffic, about halfway to failure, and at failure or termination of traffic for each of the items are shown in Figures B15-17. These plots show that generally the amount of deflection decreased with the application of traffic except for item 4, where a base course shear failure occurred and the deflection was greater (0.49 in.) at failure than prior to traffic (0.34 in.). The deflection data indicate that, with the application of traffic, the strength of the pavement structure was increasing except for item 4, where the greater deflection readings were obtained after traffic.

PERMANENT PAVEMENT DEFORMATION

Level readings were taken prior to traffic and at various intervals of traffic across the test lane at the quarter points and center of each item. These observations were made to determine the magnitude of pavement deformation resulting from traffic. The results of the cross-section measurements prior to traffic, at approximately half of the total coverages, and at failure or termination of traffic are shown in Figures B18-22. At failure (3660 coverages), items 1 and 2 had approximately 1.2 in. of permanent deformation in the 100 percent traffic area, with no upheaval at the edges of the traffic lane. About 0.3 in. of deformation was measured outside the traffic lane, which was probably due to consolidation of the entire test section. At the termination of traffic (7820 coverages), item 3 had an average deformation of 1.5 in. and no upheaval at the edge of the traffic lane. Item 4 had an average deformation of 1.3 in. at failure (1300 coverages). A slight amount of upheaval (0.4 in.) occurred at the south edge of the traffic lane at station 1+30. Item 5 had 2.3 in. of deformation at failure

(2500 coverages); 2 in. of this deformation occurred between the beginning of traffic and 1380 coverages. A very slight amount of upheaval was measured along the south edge of the traffic lane. As is shown by the cross-section measurements, permanent deformation in item 5, which was of conventional construction, was approximately 1 in. greater at a lower coverage level (2500 coverages) than the deformation in the stabilized items 1, 2, and 3. Deformation in item 4 was less than that in item 5 (0.7 and 2.3 in., respectively) at the time of base course shear failure in item 4.

FAILURE INVESTIGATIONS

After failure of an item, trenches were cut across the traffic lane into untrafficked areas to determine the extent of distortion of the various elements of each pavement structure. In-place CBR tests were conducted and water content and density determinations were made at selected intervals of depth in each layer of the pavement structure. Tests were performed both inside and outside the traffic lane to compare the effects of traffic on each layer. Profiles of the investigation trenches for each item in lane 1 are shown in Figures B23-27, and the CBR test results, moisture and density determinations, and other pertinent data for all test items are presented in Table 14 of the main text. The layer thicknesses shown in the profiles of test trenches were determined from level rod readings taken as each layer was removed. The as-constructed surfaces were determined from rod and level readings taken when construction of the layer was completed. No level readings were taken after construction of the subgrade was completed, but the subgrade was graded to grade stakes set to the design elevation. In items 1 and 5, the bottom of the asphaltic concrete was covered with a layer of crushed limestone, which made the surface of the base course irregular.

Item 1. The profile of the test trench in item 1 (Figure B23) shows that deformation at the surface of the pavement and deformation of the surface of the stabilized lean clay subbase were identical;

therefore, the deformation that occurred during traffic occurred in the subbase material or lower. The small amount of deformation that occurred in the surface of the subgrade was fairly uniform over the entire length of the test trench, which indicates that it probably occurred during compaction of the stabilized lean clay subbase. In-place density determinations in the limestone base course and stabilized subbase showed an increase in density inside the traffic lane when compared with that outside the traffic lane. Subgrade densities were about the same inside and outside the traffic lane.

Item 2. The profile of the test trench in item 2 (Figure B24) shows that deformations on the surface of the pavement and on the surface of the stabilized lean clay base course were approximately the same. The surface of the subgrade was approximately 0.6 in. lower than the design surface but was fairly uniform across the entire test trench, which indicates that the deformation in the subgrade occurred during compaction of the stabilized base. The profiles of these layers indicate that most of the deformation occurred in the cement-stabilized lean clay base course. Densities determined at the surface of the base course inside the traffic lane were less than those outside the traffic lane, but the density determinations made after traffic inside the traffic lane were about 5 percent of laboratory density greater than density determinations made during construction. Therefore, some densification of the stabilized materials occurred during traffic.

Item 3. The profile of the test trench in item 3 is shown in Figure B25. The surface of the asphaltic concrete and the surface of the stabilized base course had approximately the same amount of deformation; therefore, deformation occurred either in the base course or the subgrade. The profile of the subgrade was not taken after traffic, so it was impossible to determine exactly where the deformation occurred. Density determinations were not made in the base course because the material was too hard to accurately test.

Item 4. The profile of the test trench in item 4 is shown in Figure B26. About 1.0 in. of deformation occurred at the center of the

traffic lane, and about 0.4 in. of upheaval occurred at the edge of the traffic lane. The profile indicates that deformation occurred in both the base course and the heavy clay subgrade, but both appeared to have been constructed about 1 in. above the design elevation. In-place CBR tests at the surface of the base course and at 12 in. below the surface showed lower CBR values inside the traffic lane than outside (Table 14 of the main text). This indicates that failure occurred when the base course sheared under traffic. In-place density inside the traffic lane was less at the surface of the base than that outside the traffic lane but was slightly greater at 12 in. below the surface inside the traffic lane. The lower density inside the traffic lane at the surface of the base course also indicates a shear failure in the base course.

Item 5. The profile of the test trench in item 5 is shown in Figure B27. Deformation of the pavement surface at the center of the traffic lane was 2.0 in.; at the surface of the base and subbase courses, the indicated deformation was 2.4 and 1.8 in., respectively. The greater indicated deformation at the surface of the base course was caused by difficulty in determining the exact thickness of pavement due to the prime coat on the base course having penetrated the limestone and some of the limestone base being removed with the asphaltic concrete. The distortion in the surface of the subgrade appeared to have been caused by the rolling of the subbase during construction of the test section. Density determinations taken after completion of traffic (Table 14 of the main text) indicate that the density in the base course increased by about 2 percent during trafficking. The subbase shows an average density increase of 1.8 percent in the traffic lane. The profile data and density determinations indicate that the majority of the deformation occurred due to densification of the subbase material during traffic.

240-KIP LOAD, LANE 2

ITEM 1

A general view of item 1 prior to traffic is shown in Figure B28.

Hairline cracking was first noted at the west end of the item at 320 coverages. Cracking progressed with traffic, and, at 600 coverages, severe cracks penetrated the full depth of the pavement. The condition of the pavement at failure (600 coverages) is shown in Figure B29.

ITEM 2

A general view of item 2 prior to traffic is shown in Figure B30. Cracking was first noted at about 120 coverages and continued with the application of traffic. At 320 coverages, cracks had developed through the full depth of the asphaltic concrete, and the item was considered failed (Figure B31).

ITEM 3

A general view of item 3 prior to traffic is shown in Figure B32. Prior to traffic, a few transverse shrinkage cracks were noted, but the cracks were not considered to be structurally detrimental to the pavement. Cracking of the asphaltic concrete was never severe in item 3, but the item was considered failed at 620 coverages due to excessive deformation and upheaval, which will be discussed later in this appendix. The condition of the pavement at failure (620 coverages) is shown in Figure B33.

ITEM 4

A general view of item 4 prior to traffic is shown in Figure B34. A few transverse hairline cracks were noted in item 4 at 40 coverages. At 120 coverages, severe cracking penetrated the full depth of the pavement. The condition of the pavement at failure (120 coverages) is shown in Figure B35.

ITEM 5

A general view of item 5 prior to traffic is shown in Figure B36. Slight cracking was noted at 40 coverages, and at 340 coverages, the cracks penetrated the full depth of the asphaltic concrete and the item was considered failed (Figure B37).

PAVEMENT DEFLECTION

The procedure described for lane 1 was also followed to obtain deflection measurements in this lane. Plots of deflections taken prior to traffic, about halfway to failure, and at failure are shown in Figures B38-40. These plots show that in all items the amount of deflection increased with the application of traffic. Deflections in items 1-3 were approximately the same before traffic (0.25, 0.24, and 0.21 in., respectively). At 320 coverages, the deflections in items 1-3 had increased to 0.47, 0.44, and 0.38 in., respectively. Item 2 was considered failed at 400 coverages, but deflection readings were not taken. Item 1 had a deflection of 0.60 in. at failure (600 coverages), and item 3 had a deflection of 0.48 in. at failure (620 coverages). Item 4 had a maximum deflection of 0.38 in. before traffic which increased to 0.43 in. at 40 coverages. A base course shear failure developed in the item, and the deflection increased to 0.90 in. at failure (120 coverages). Item 5 had a deflection of 0.30 in. before traffic which increased to 0.39 in. at 120 coverages. At failure (340 coverages), a deflection of 0.40 in. was recorded.

PERMANENT PAVEMENT DEFORMATION

Rod and level readings were taken prior to traffic and at intervals of traffic across the test lane at the quarter points and center of each item. These observations were made to determine the magnitude of pavement deformation resulting from traffic. The results of the cross-section measurements prior to traffic, about halfway to failure, and at failure are shown in Figures B41-45.

Item 1. As can be seen in the cross sections in Figure B41, the permanent deformation for item 1 ranged from about 3.2 in. at the western quarter point (station 0+10) to 1.1 in. at the eastern quarter point (station 0+30). At station 0+10, an upheaval at the edge of the traffic lane of about 1.0 in. was recorded, but only 0.2 in. of upheaval was recorded at station 0+30.

Item 2. Cross sections for item 2 are shown in Figure B42 for 0, 120, and 320 coverages. The item was not considered failed until 400 coverages, but cross sections were not taken at that time. At 320 coverages, the maximum permanent deformation ranged from 0.7 in. at the western quarter point (station 0+50) to 1.4 in. at the eastern quarter point (station 0+70). At the edge of the test section, which was approximately 4 ft north of the edge of the traffic lane, an upheaval of about 0.2 in. was measured at station 0+50 and increased to 1.4 in. at station 0+70.

Item 3. Cross sections for item 3 in Figure B43 show that the maximum permanent deformations at the time of failure (620 coverages) were 2.5 in. at the western quarter point (station 0+90), 2.5 in. at the center, and 1.9 in. at the eastern quarter point (station 1+10). Upheaval at the north edge of the item ranged from 2.3 in. at station 0+90 to 0.3 in. at station 1+10.

Item 4. A cross section was not taken at failure at the eastern quarter point (station 1+50) of item 4 (Figure B44) because landing mat had been placed over the area in order to traffic over an isolated failed area near the transition between items 4 and 5. Permanent deformations at failure (120 coverages) at the western quarter point and at the center of the item were 1.7 and 1.6 in., respectively. Upheaval at the north edge of the item was approximately 0.2 in. at both locations.

Item 5. Permanent deformations at failure (340 coverages) in item 5 (Figure B45) were 2.1 in. at station 1+70, 2.4 in. at station 1+80, and 1.7 in. at station 1+90. Upheaval at the outside edge of the traffic lane was greater on the north side of the traffic lane than on the south side. Upheaval at the north side ranged from 0.9 in. at station 1+70 to 0.6 in. at station 1+80. It can be seen from the results of the cross-section measurements that deformations in item 5, the conventional construction item, were as great as in any of the stabilized items except item 4 and that item 5 failed at a lower coverage level than items 1, 2, and 3.

FAILURE INVESTIGATIONS

Profiles of the trenches for the items in lane 2 are shown in Figures B46-50. CBR test results, density and moisture content determinations, and other pertinent data for all test items are presented in Table 14 of the main text. Precise thickness determinations of the asphaltic concrete in items 1 and 5 were difficult to obtain because the asphalt prime coat used on the limestone base course penetrated the limestone and caused it to bond to the asphaltic concrete. Also, when the asphaltic concrete was removed from the test trench, some limestone adhered to the bottom surface of the pavement and was removed with it.

Item 1. The profile of the test trench in item 1 (Figure B46) shows that deformation occurred in the heavy clay subgrade. The CBR values obtained at the surface of the limestone base were about the same after traffic as the values obtained during construction. In-place tests performed on the surface of the cement-stabilized lean clay subbase showed higher CBR values after traffic than before traffic. CBR values obtained in the subgrade increased from a value of approximately 4 to about 5 from the time of construction to after-traffic testing. Water contents were approximately the same after traffic as before.

Item 2. The profile for the test trench in item 2 shown in Figure B47 indicates that some deformation occurred in the subgrade and that lateral displacement of the subgrade caused upheaval of the pavement surface outside the traffic lane. In-place CBR and density values obtained after traffic were higher at the surface of the stabilized base, both inside and outside the traffic lane, than similar values obtained during construction.

Item 3. The profile of the test trench in item 3 (Figure B48) shows that the deformation in the pavement surface was reflected into the heavy clay subgrade and that lateral displacement of the subgrade caused upheaval of the pavement outside the traffic lane. In-place CBR and density determinations on the surface of the stabilized base course were approximately the same before and after traffic. Subgrade CBR

values were slightly lower at the surface of the subgrade after traffic than during construction, and the water content was about 2 percent higher after traffic.

Item 4. The profile of the test trench in item 4 (Figure B49) shows that most of the deformation that occurred in the traffic lane occurred in the subgrade material. Approximately 0.2 in. of upheaval occurred at the edge of the traffic lane in the pavement and base. CBR and density determinations at the surface of the stabilized clayey sand were the same before and after traffic. Approximately 15 in. below the surface of the pavement, the CBR obtained inside the traffic lane was 26 as compared with values of 112 outside the traffic lane and 93 obtained during construction. This indicates that a shear failure occurred in the lower half of the cement-stabilized clayey sand. CBR and density values were slightly higher in the subgrade after traffic than during construction, and the water content was about 1 percent lower.

Item 5. The profile of the test trench in item 5 is shown in Figure B50. A comparison of the as-constructed elevations with the after-traffic elevations shows that very little (0.2 in.) deformation occurred in the subgrade and that most of the deformation occurred in the gravelly sand subbase material. A comparison of the elevations also shows that gravelly sand material displaced laterally and caused upheaval in the limestone base course and pavement outside the traffic lane. Values for in-place CBR and density determinations in Table 14 of the main text show that the CBR of the base course increased during traffic from 104 to 133 and that the density increased by about 1 percent of laboratory density inside the traffic lane. The CBR value of the subbase decreased during traffic from 46 to 24, and the density remained about the same. This decrease in the CBR value indicates that the subbase developed a shear failure, which resulted in some lateral displacement and upheaval. The CBR value of the subgrade remained about the same after traffic as before traffic, and the density increased by about 1 percent of laboratory density.

50-KIP SINGLE-WHEEL LOAD, LANE 3

SUBITEM 4a

A general view of subitem 4a prior to traffic is shown in Figure B51. At 80 coverages, severe cracking had developed at the west end of the subitem (Figure B52). At 170 coverages, cracks penetrated the full depth of the pavement over the entire subitem, so it was considered failed. Traffic was continued on the subitem to 240 coverages.

SUBITEM 4b

A general view of subitem 4b prior to traffic is shown in Figure B53. Longitudinal hairline cracks were noted in the subitem at 80 coverages. At 170 coverages, cracks penetrated the full depth of the pavement, and the subitem was considered failed. Figure B54 shows the condition of the pavement at failure (170 coverages). Traffic was continued on the item to 240 coverages.

SUBITEM 4c

A general view of subitem 4c prior to traffic is shown in Figure B55. At 170 coverages, minor longitudinal hairline cracks were observed. At 240 coverages, cracks penetrated the full depth of the asphaltic concrete, and the item was considered failed. The condition of the pavement at failure is shown in Figure B56.

SUBITEM 4d

A general view of subitem 4d prior to traffic is shown in Figure B57. Prior to traffic, a crack developed around the perimeter of the subitem at the edge of the lightweight concrete base course, but no cracks were observed within the perimeter. At 170 coverages, moderate surface cracking developed near the east end, and longitudinal cracks developed along the entire length of the subitem (Figure B58). At 240 coverages, severe cracking had developed over the entire subitem, and the subitem was considered failed. The condition of the subitem at failure is shown in Figure B59.

SUBITEM 5a

A general view of subitem 5a prior to traffic is shown in Figure B60. At 170 coverages, moderate cracking had occurred at the west end of the subitem, and a longitudinal crack had developed in the traffic lane near the south edge. An observation pit was opened at the east end of the subitem, and cracks were noted in the lightweight concrete sub-base course that coincided with cracks in the asphaltic concrete surface. At 240 coverages, cracks were severe (Figure B61), and the subitem was considered failed.

SUBITEM 5b

A general view of subitem 5b prior to traffic is shown in Figure B62. At 240 coverages, only minor hairline cracks were observed in the pavement surface, but the pavement was considered failed due to pavement deformation that will be discussed later. The condition of the pavement at 240 coverages is shown in Figure B63.

SUBITEM 5c

A general view of subitem 5c prior to traffic is shown in Figure B64. At 130 coverages, numerous cracks were observed in the pavement surface that did not appear to penetrate the full depth of the asphaltic concrete. At 240 coverages, the cracks had penetrated the full depth of the asphaltic concrete surface, and the item was considered failed. The condition of the pavement at failure is shown in Figure B65.

SUBITEM 5d

A general view of subitem 5d prior to traffic is shown in Figure B66. At 130 coverages, cracks were observed in the pavement surface that did not appear to penetrate the full depth of the asphaltic concrete. At 240 coverages, the cracks had penetrated the full depth of the asphaltic concrete surface, and the item was considered failed. The condition of the pavement at failure is shown in Figure B67.

PAVEMENT DEFLECTION

The procedure described previously was followed to obtain deflection measurements, except that the measurements were taken under the single-wheel assembly load instead of the twin-tandem multiple-wheel assembly load. Plots of deflections taken prior to traffic and at 170 coverages are shown in Figures B68-71. These plots indicate that, except for subitem 4d, the deflections obtained on the subitems that incorporated the lightweight concrete material were less than the deflections obtained on subitems that incorporated the polystyrene panels, both before and after traffic. In subitem 4d, the deflection at 170 coverages was about the same as that in subitems that incorporated the polystyrene panels.

PERMANENT PAVEMENT DEFORMATION

Rod and level readings were taken prior to traffic and at intervals during traffic at the center and each end of the subitem. These observations were made to determine the magnitude of pavement deformation resulting from traffic. The results of the cross-section measurements prior to traffic, at 170 coverages, and at 240 coverages taken at the center of each subitem are shown in Figures B72 and B73. Upheaval was noted at the edge of the traffic lane in all subitems as indicated in the plots. Only very minor upheaval, about 0.2 in., was recorded in subitems 5a-d.

FAILURE INVESTIGATIONS

After all items in lane 3 had failed, trenches were excavated across the traffic lane into untrafficked areas. In-place CBR tests were conducted and water content and density determinations were made inside and outside the traffic lane in test trenches in subitems 4a, 4c, 5a, and 5c. In-place water content was measured on the surface of the stabilized base course in subitem 4b. In-place tests were performed at selected intervals of depth in each of the pavement structures. Observation trenches were excavated in subitems 4d, 5b, and 5c for visual inspection of performance of the insulating materials used in each

subitem. Profiles of the investigation trenches are shown in Figures B74-77, and the CBR test results and moisture content and density determinations are shown in Table 14 of the main text.

Subitem 4a. The results of CBR tests at the surface of the stabilized base course in subitem 4a showed a CBR of 67 inside the traffic lane and 114 outside the traffic lane. The density of the base course was higher outside the traffic lane than inside. The base course material above the polystyrene appeared to have sheared during traffic, causing the lower CBR and density values. Below the polystyrene, the indicated density was still lower inside the traffic lane than outside, but the CBR value obtained inside the traffic lane was 56 and outside the traffic lane was 22. Subgrade CBR values in the top 12 in. inside the traffic lane averaged 2.8 and outside the traffic lane averaged 3.7. The polystyrene panels in subitem 4a were laid transverse to traffic, and cracks had developed the full depth of the panels inside the traffic lane as shown in Figure B78.

Subitem 4b. The condition of the surface of the polystyrene inside the traffic lane in the observation trench in subitem 4b is shown in Figure B79. The polystyrene was placed transverse to the direction of traffic, and cracking was primarily parallel to traffic. The cracks occurred throughout the traffic lane.

Subitem 4c. In subitem 4c, CBR values at the surface of the stabilized base course were lower inside the traffic lane than outside, 104 and 130+, respectively. The density inside the traffic lane was 85.0 percent of laboratory density, and outside the traffic lane it was 88.3 percent of laboratory density. Under the lightweight concrete, the CBR values were 51 and 18 inside and outside the traffic lane, respectively, but the density was less inside the traffic lane than outside (86.2 and 91.0 percent of laboratory density, respectively). CBR values inside the traffic lane in the subgrade averaged 5.1 and outside the traffic lane averaged 6.3. Cracks had developed parallel to traffic in the lightweight concrete at the edge of the traffic lane and near the center of the traffic lane.

Subitem 4d. An observation test trench was opened at the east end of subitem 4d and the west end of subitem 5a at 170 coverages to observe the condition of the lightweight concrete. The cracking that had developed is shown in Figure B80. As can be seen, the crack pattern in the lightweight concrete in subitem 4d to the right in the figure coincides with the crack pattern in the asphaltic concrete. Small hairline cracks had developed parallel to traffic near the edge of the traffic lane in the lightweight concrete in subitem 5a.

Subitem 5a. In subitem 5a, in-place CBR values inside and outside the traffic lane were 63 and 53, respectively, with corresponding densities of 100.2 and 101.7 percent of laboratory density. In-place CBR values in the gravelly sand subbase both inside and outside the traffic lane were 20. The subbase showed an increase in density inside the traffic lane when compared with that outside the traffic lane (104.1 and 100.3 percent of laboratory density, respectively). Test values obtained on the subgrade were approximately the same inside and outside the traffic lane. Hairline cracks parallel to traffic were noted in the surface of the lightweight concrete. These cracks corresponded to cracks in the asphaltic concrete surface.

Subitem 5b. An examination of the surface of the lightweight concrete in subitem 5b showed one small longitudinal hairline crack near the center of the traffic lane. An observation trench was located at the center of the subitem, and it was determined that only about 0.4 in. of permanent deformation had occurred.

Subitem 5c. The results of in-place tests performed in the test trench in subitem 5c showed no significant difference for values obtained inside and outside the traffic lane. Data obtained in the test trench are shown in Table 14 of the main text. The polystyrene in subitem 5c was placed with the long dimension of the panels parallel to the direction of traffic. No cracks were noted in the polystyrene panels, although about 1 in. of permanent deformation occurred at the surface of the pavement in the traffic lane. A view of the surface of the panels is shown in Figure B81.

Subitem 5d. Figure B82 shows the surface of the polystyrene in subitem 5d. The panels were placed with the long dimension parallel to the direction of traffic. No cracks were noted in the polystyrene panels, although permanent deformation of about 1.2 in. occurred at the surface of the pavement.

VARIATION IN CEMENT CONTENT

During excavation of the test trenches that were cut in the flexible pavement for collection of past-failure test data, it was observed that there was noticeable layering in the chemically treated soils, indicating possible nonuniformity of distribution of the chemical additives. (See Figure B83.) In order to properly assess this condition, it was decided to undertake a special sampling program to determine actual additive content for comparison with the design mix values. The sampling program was conducted in item 2 since the lean clay is a more uniformly graded material and only one additive, portland cement, was used. The program consisted of first obtaining samples of the treated soils at incremental depths from the top of the base course, i.e., directly underneath the asphaltic concrete surface course to the top of the heavy clay subgrade. Samples were obtained from the vertical walls of the observation trenches at five locations in the item (see Figure B84.) At each sampling site, specimens were obtained in successive increments in thicknesses of about 1 to 3 in. each for the full depth of the stabilized base layer. The procedure for determining the cement content of each specimen consisted first of determining the calcium oxide (CaO) content of the treated soil, the raw soil, and the portland cement used in construction of the test item. By calculating the relative CaO content in the specimen, the cement content was then determined and expressed as a percent of the dry soil weight. Results of this sampling program are presented in Table B1. For each sampling location, the applicable depths of each specimen below the subgrade along with computed cement contents are indicated. From this data, it can be seen that there was considerable variation in cement content both

horizontally and vertically. These data are also presented in bar graph form in Figure B85.

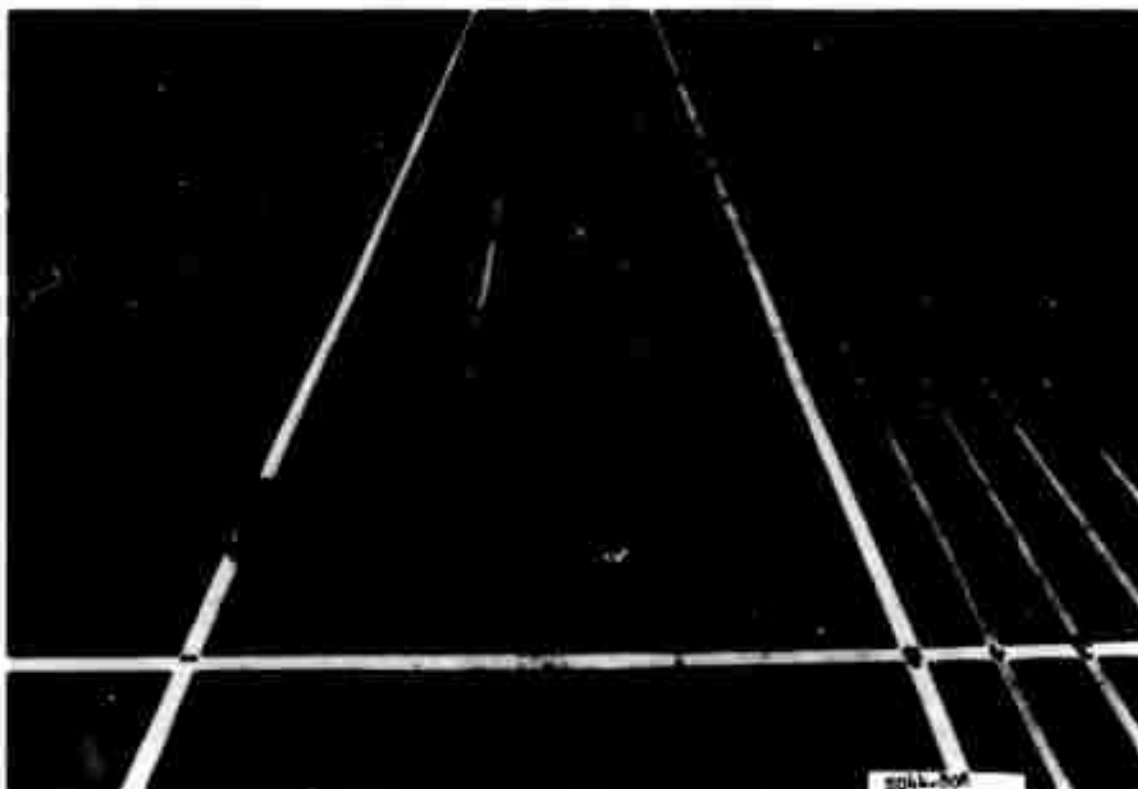


Figure B1. Item 1, lane 1, flexible pavement test section, prior to traffic



Figure B2. Cracking in western quarter of item 1, lane 1, flexible pavement test section, at 2500 coverages of 200-kip twin-tandem assembly



Figure B3. Cracking in eastern three-fourths of item 1, lane 1, flexible pavement test section, at 3660 coverages of 200-kip twin-tandem assembly

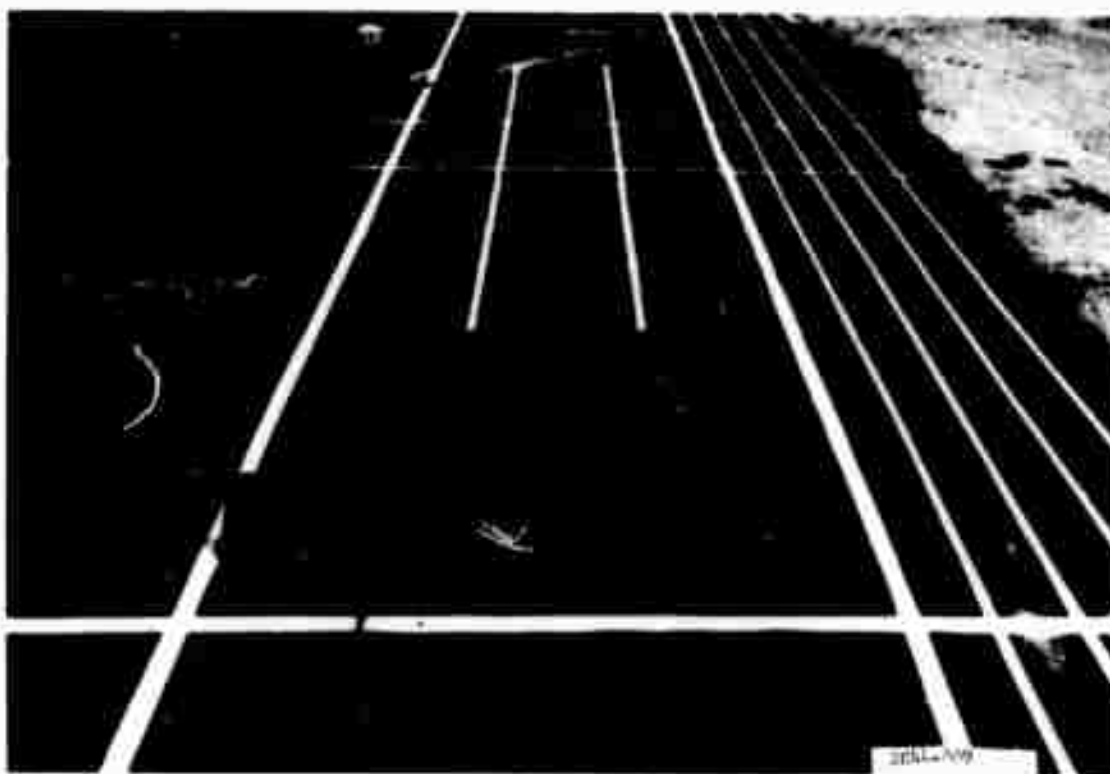


Figure B4. Item 2, lane 1, flexible pavement test section, prior to traffic

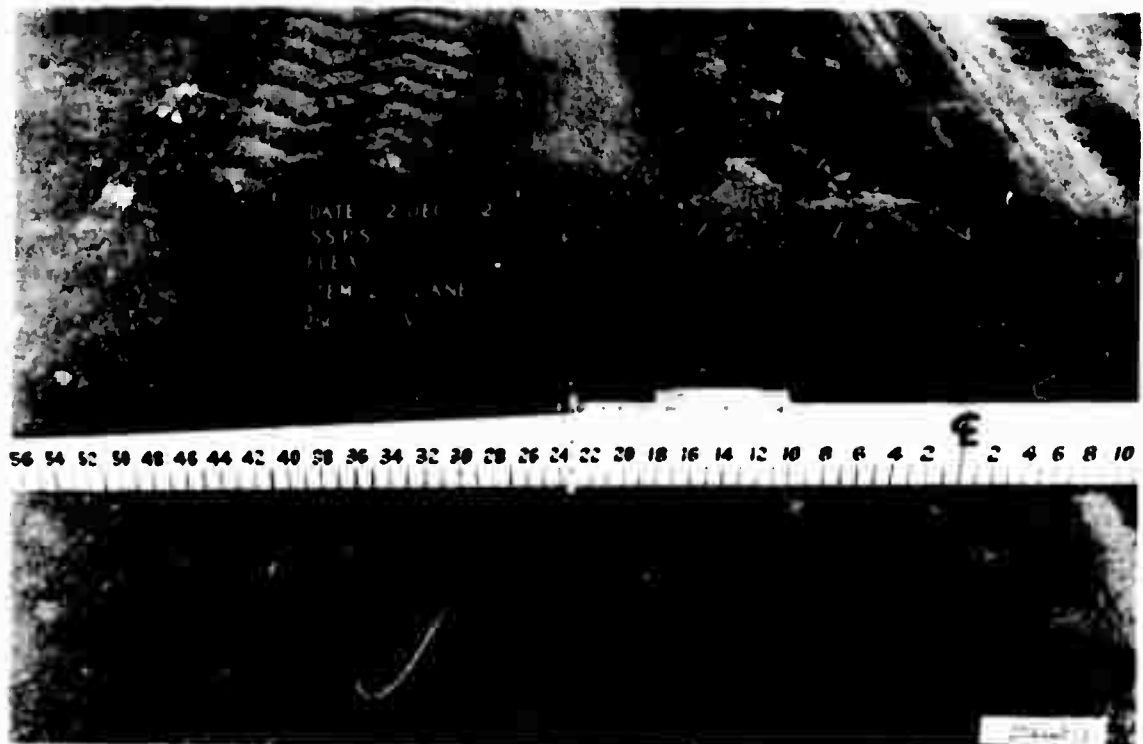


Figure B5. Cracking at instrumentation grid in item 2, lane 1, flexible pavement test section, at 2500 coverages of 200-kip twin-tandem assembly



Figure B6. Item 2, lane 1, flexible pavement test section, at 3660 coverages of 200-kip twin-tandem assembly

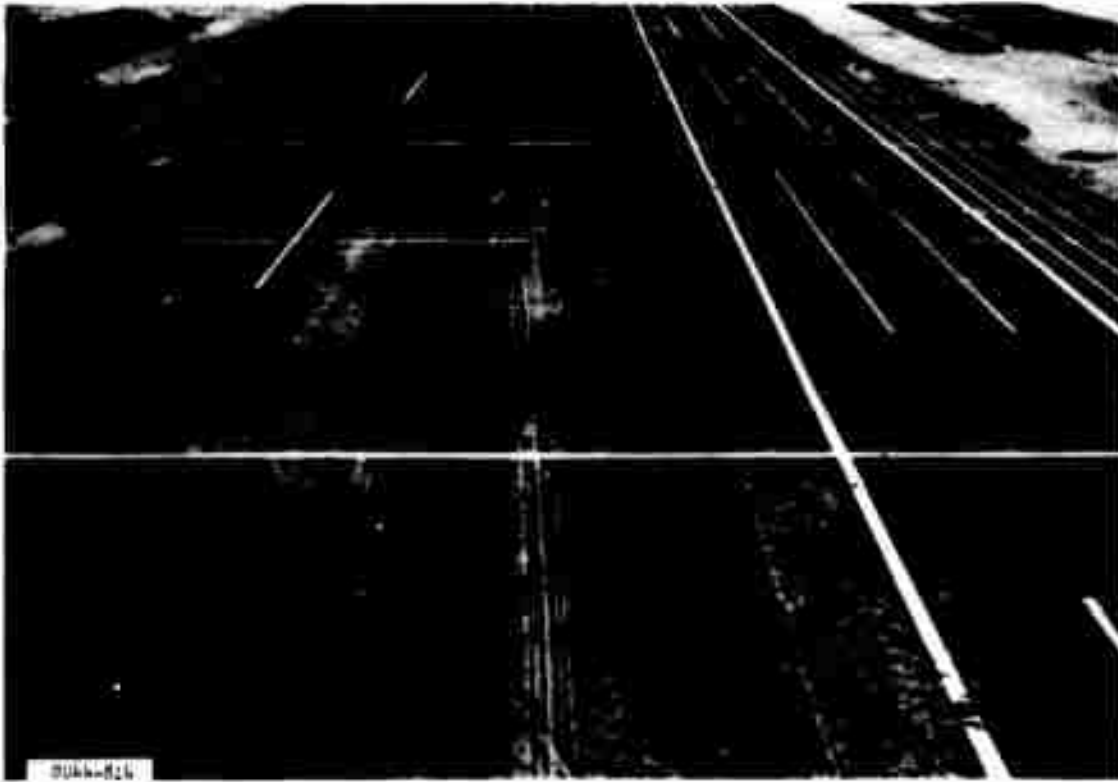


Figure B7. Item 3, lane 1, flexible pavement test section, prior to traffic

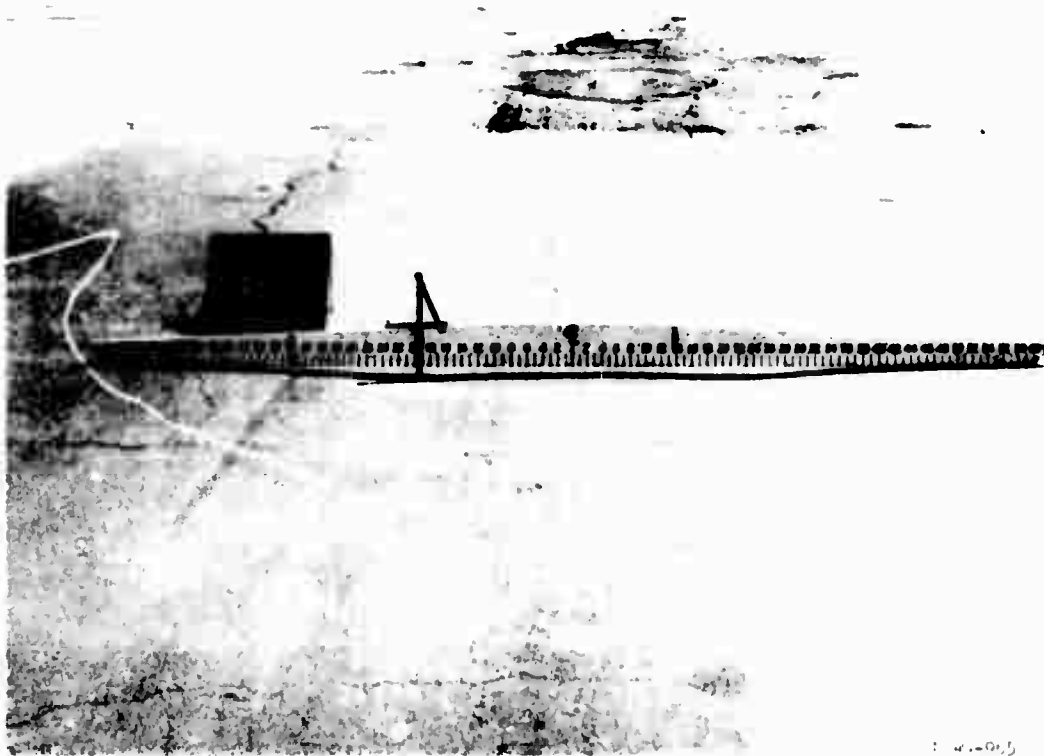


Figure B8. Item 3, lane 1, flexible pavement test section, when traffic was terminated after 7820 coverages of 200-kip twin-tandem assembly

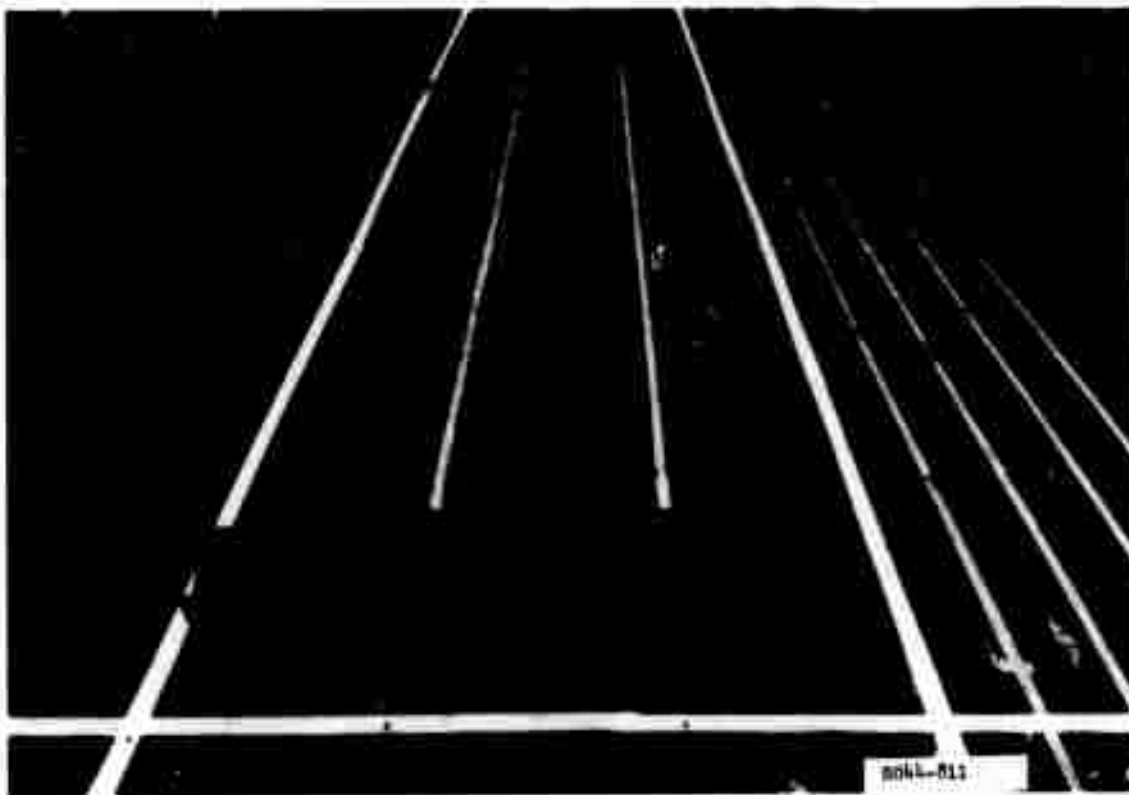


Figure B9. Item 4, lane 1, flexible pavement test section, prior to traffic

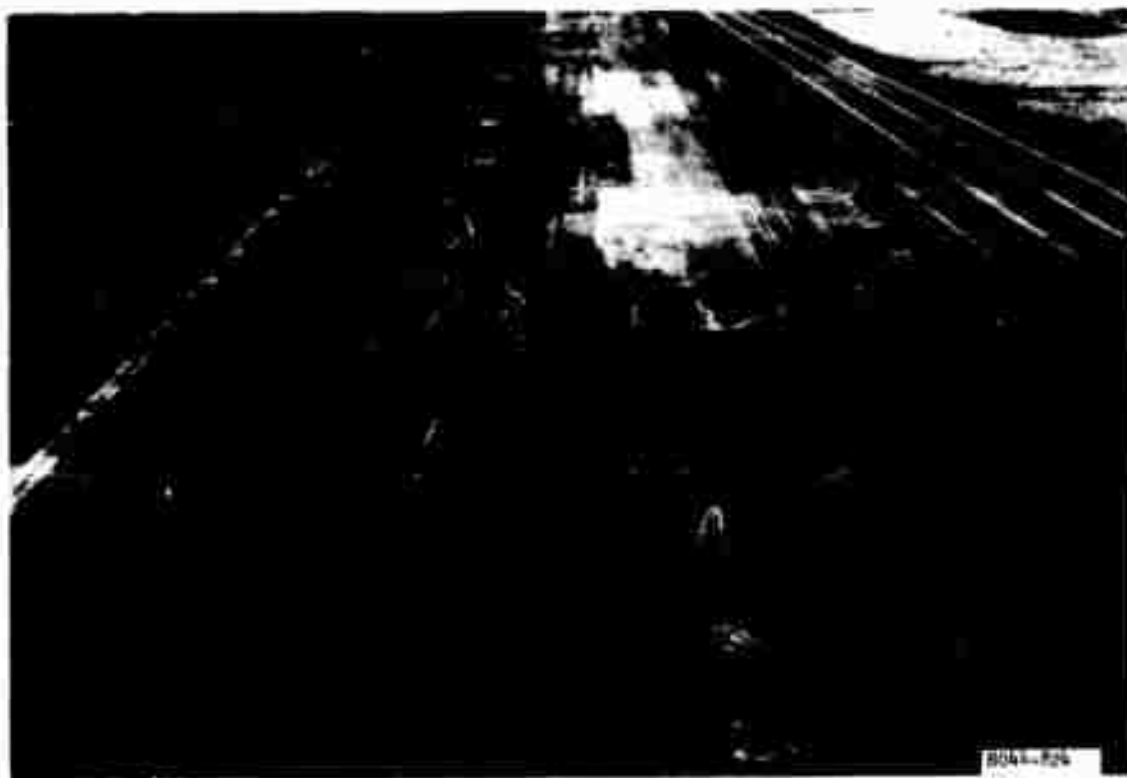


Figure B10. Cracking in item 4, lane 1, flexible pavement test section, after 1200 coverages of 200-kip twin-tandem assembly

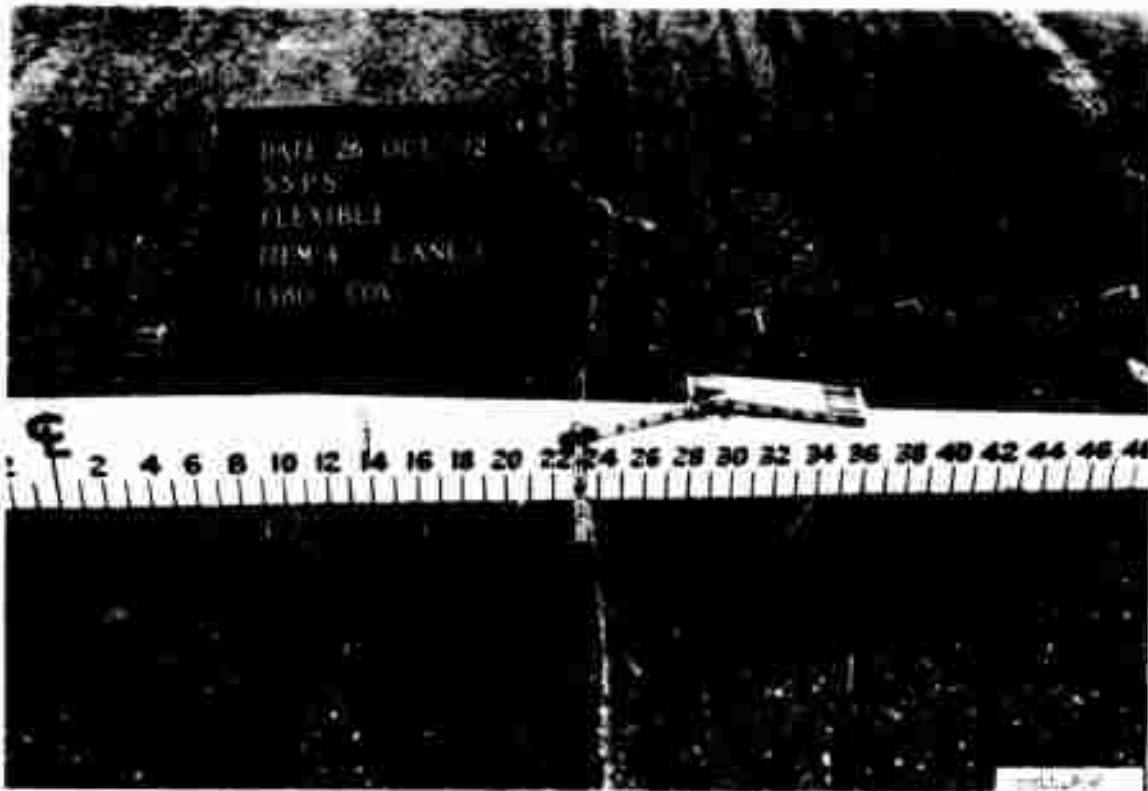


Figure B11. Item 4, lane 1, flexible pavement test section,
at 1380 coverages of 200-kip twin-tandem assembly

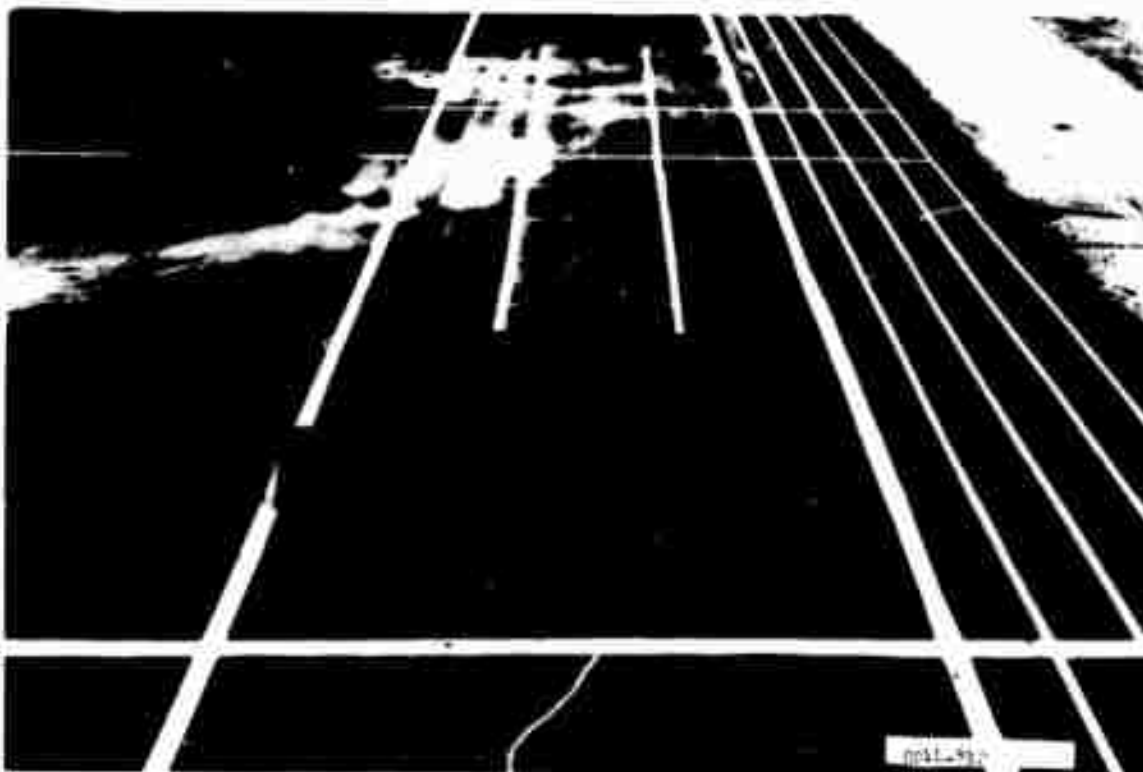


Figure B12. Item 5, lane 1, flexible pavement test section prior to
traffic

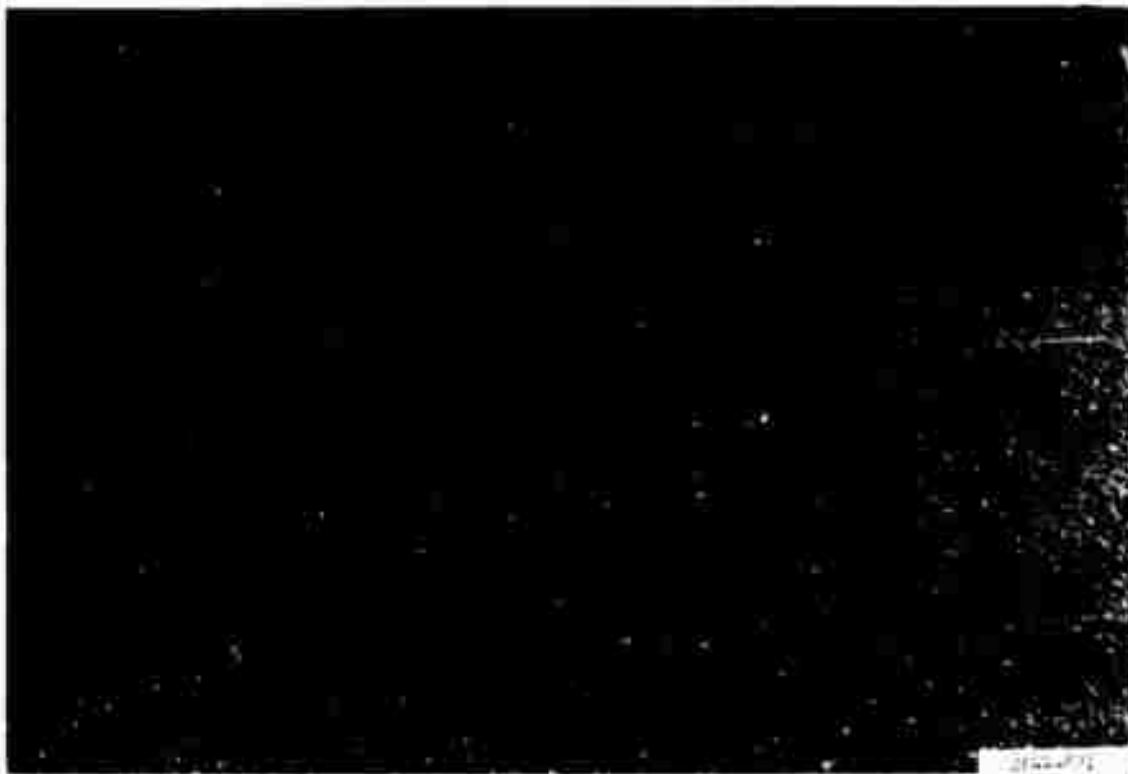


Figure B13. Cracking in item 5, lane 1, flexible pavement test section, after 1200 coverages of 200-kip twin-tandem assembly

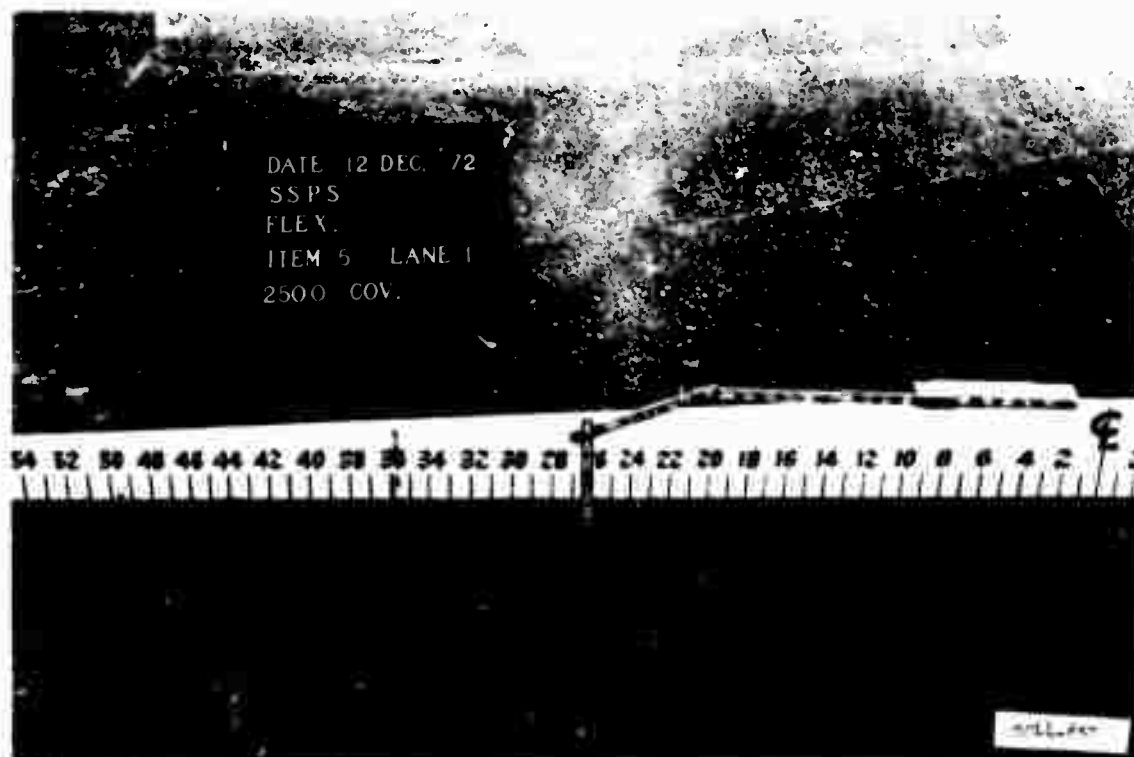


Figure B14. Item 5, lane 1, flexible pavement test section, at 2500 coverages of 200-kip twin-tandem assembly

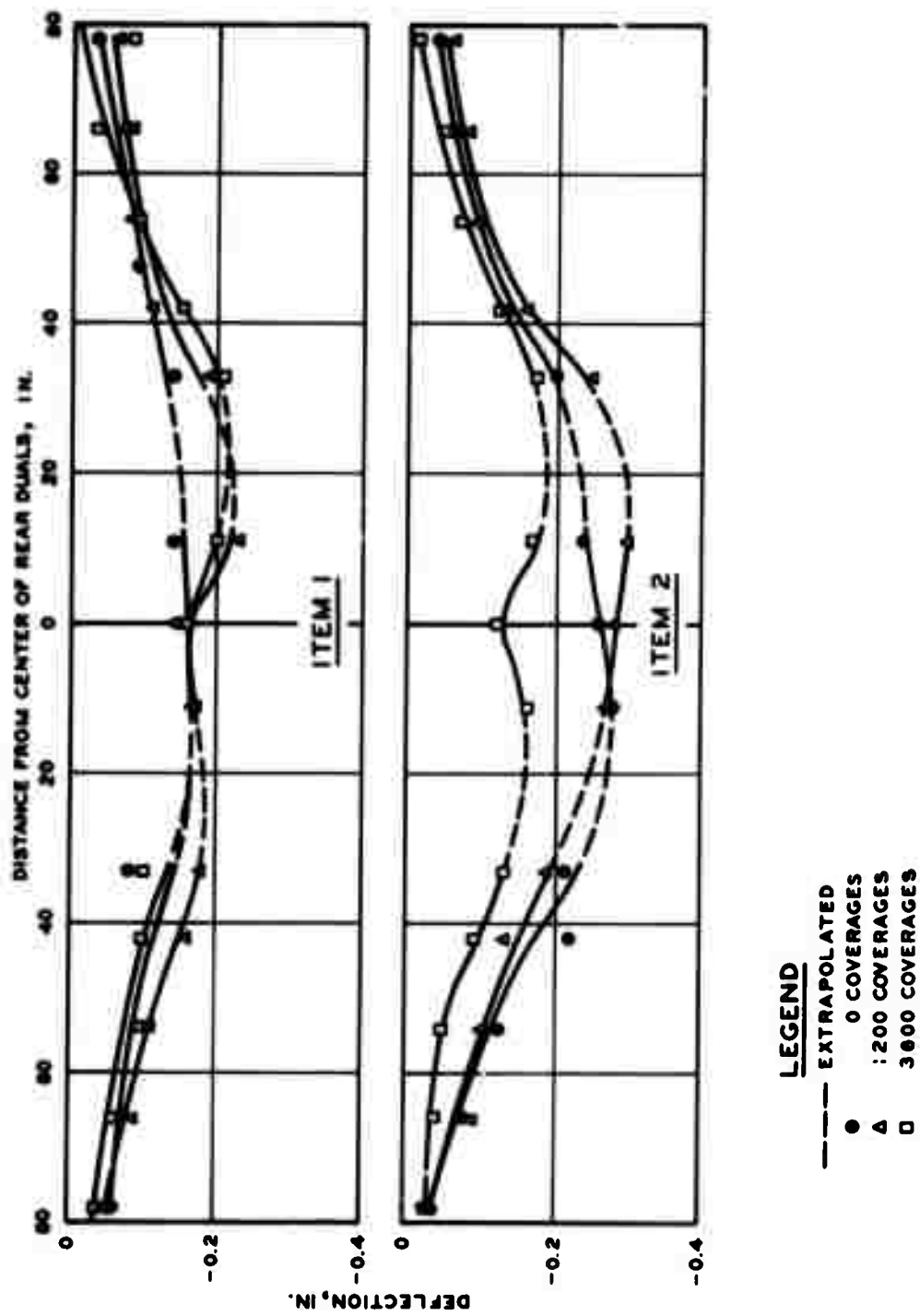


Figure B15. Deflections measured transverse to direction of traffic in items 1 and 2, lane 1, flexible pavement test section

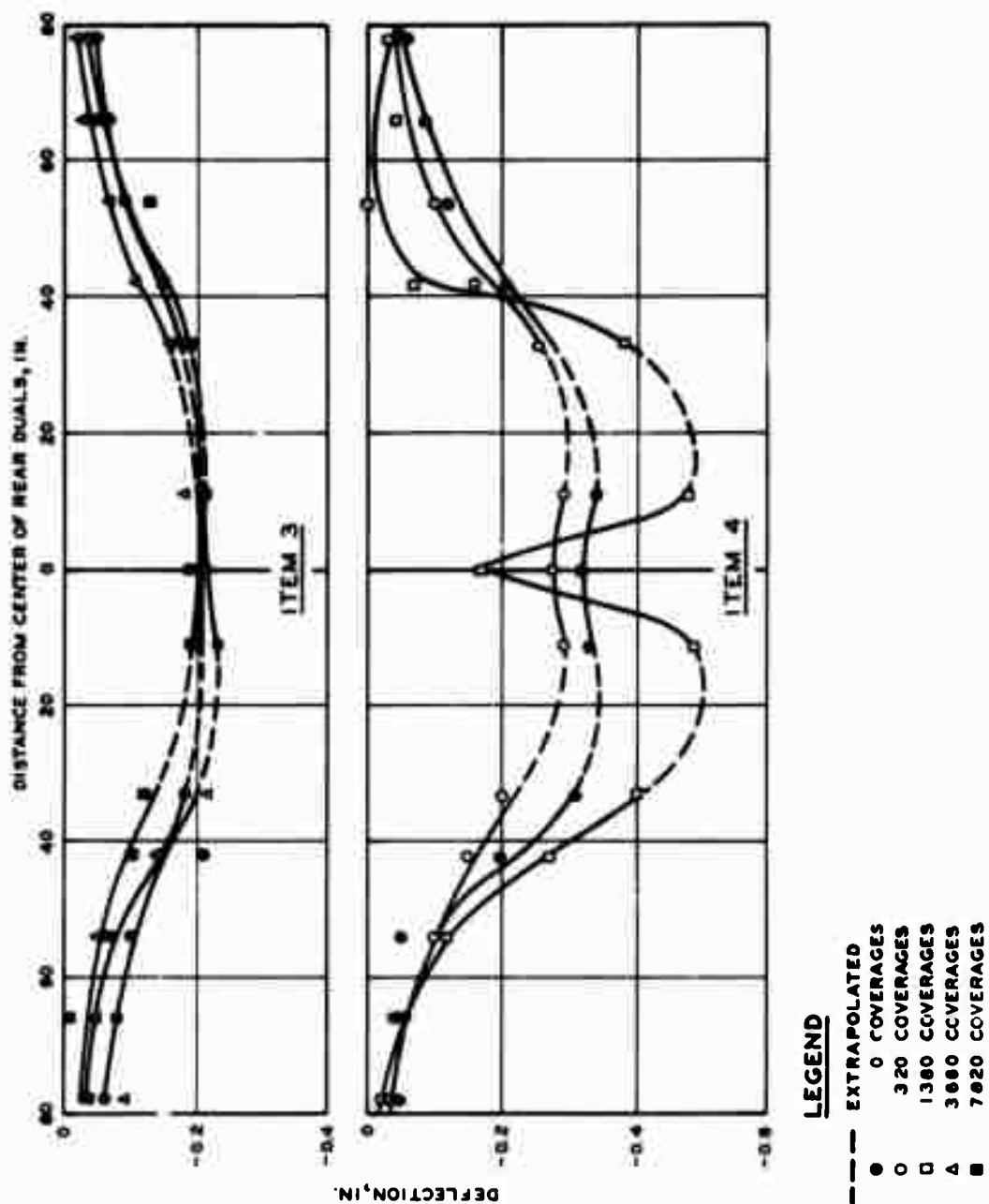


Figure B16. Deflections measured transverse to direction of traffic in items 3 and 4, lane 1, flexible pavement test section

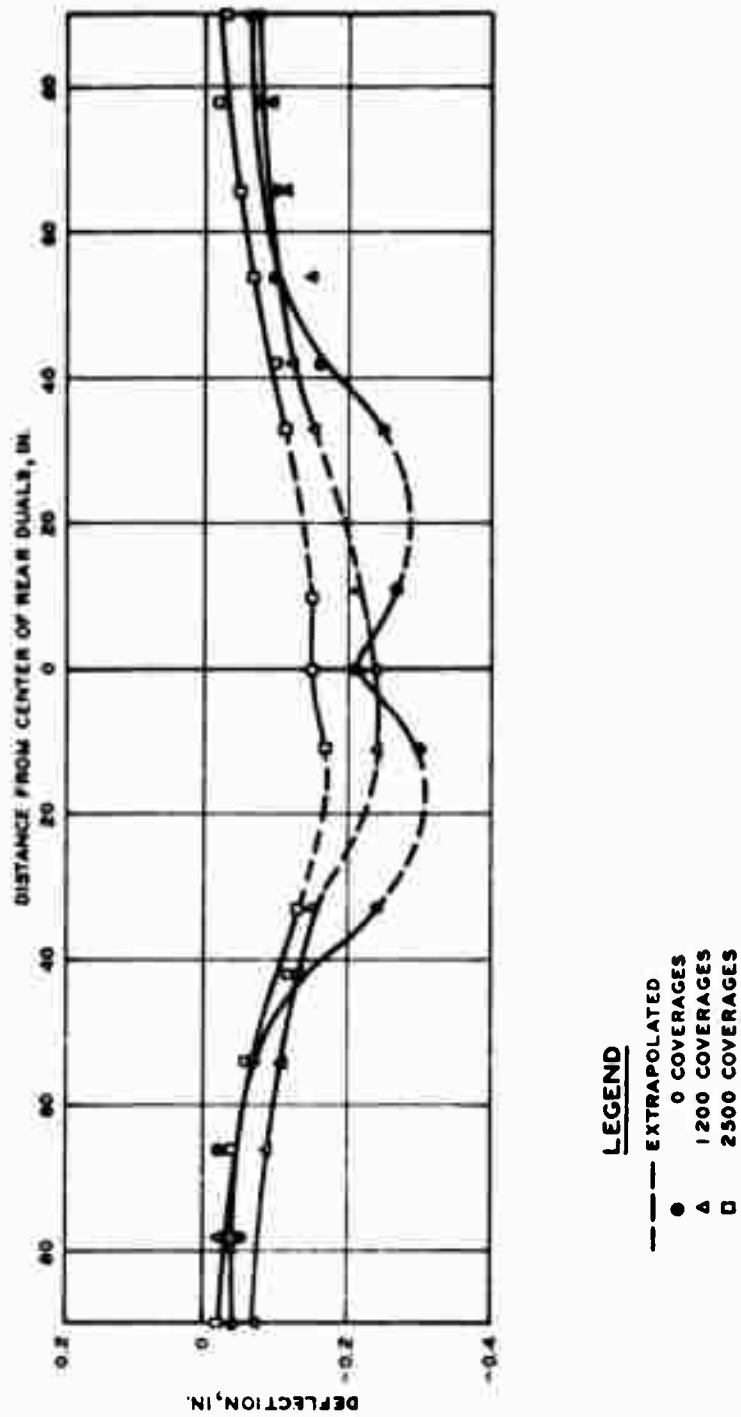


Figure B17. Deflections measured transverse to direction of traffic in item 5, flexible pavement test section

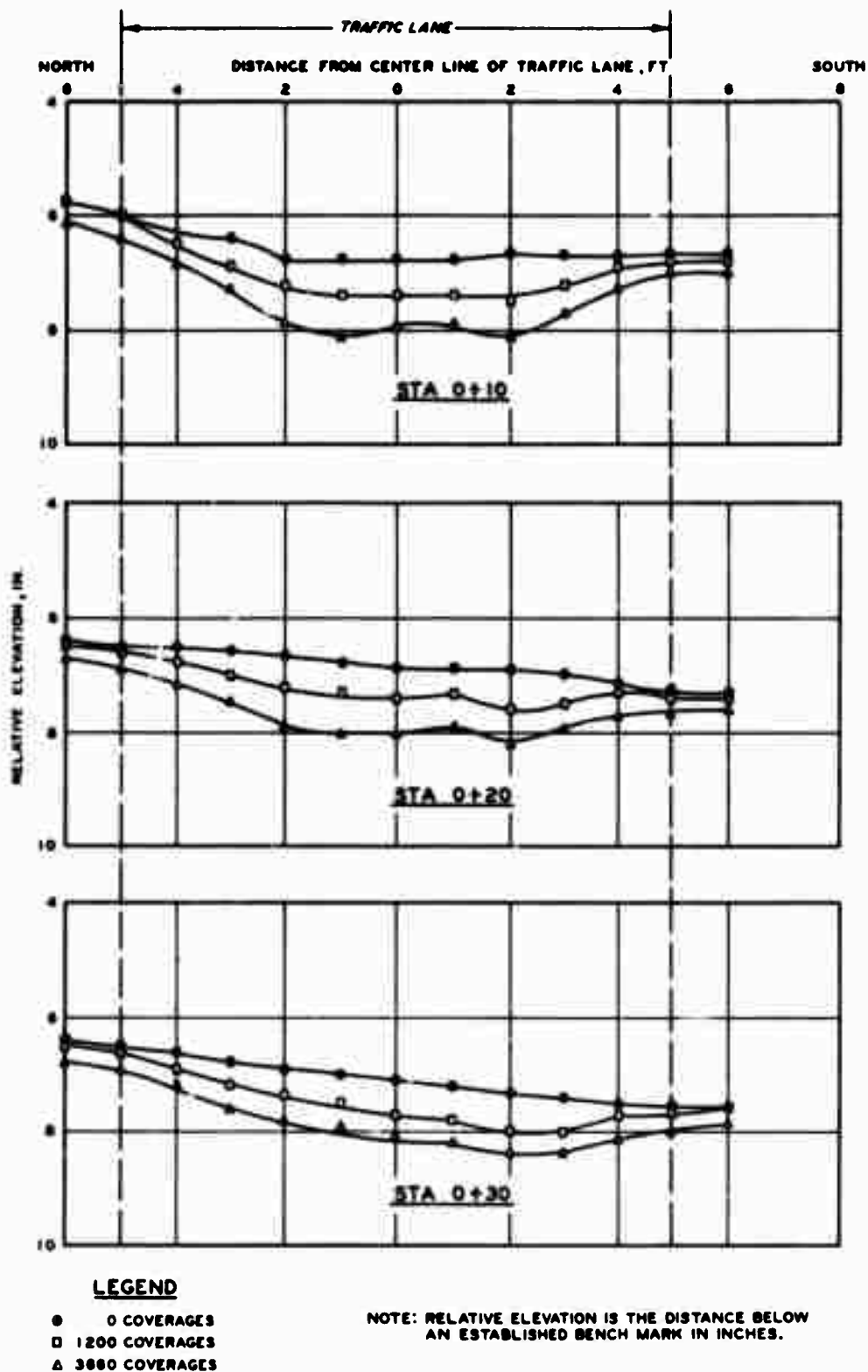


Figure B18. Surface deformation in item 1, lane 1, flexible pavement test section

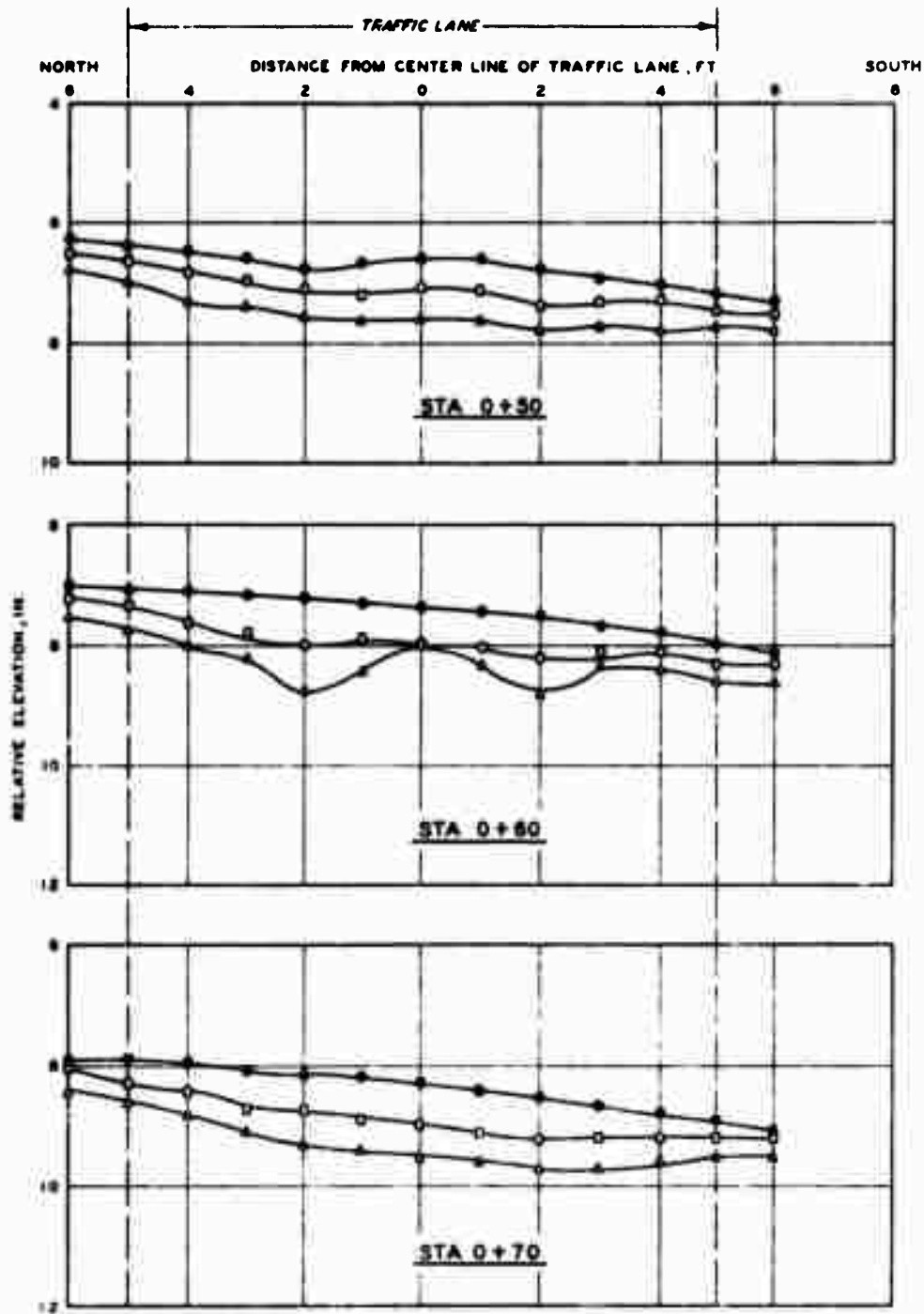
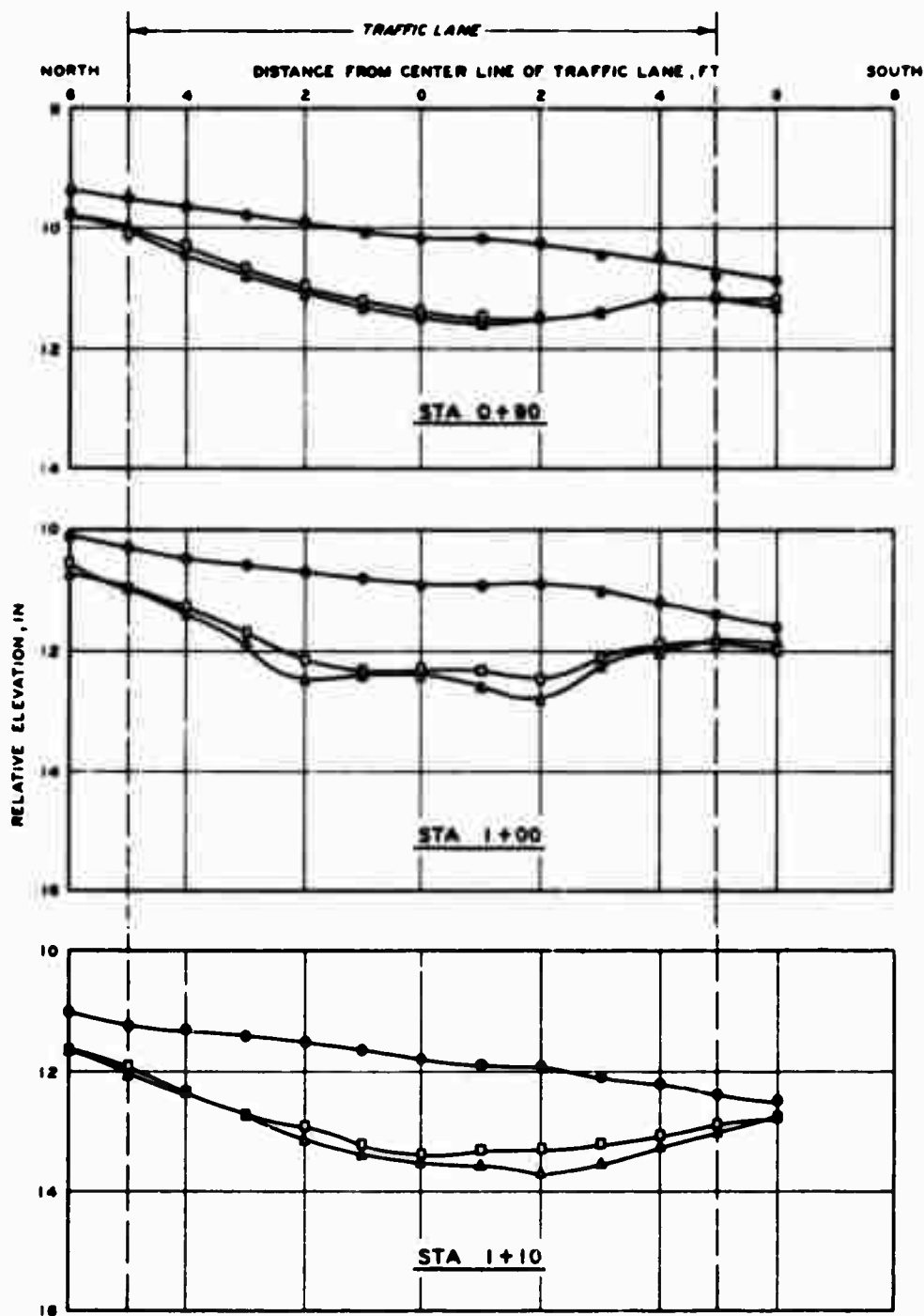


Figure B19. Surface deformation in item 2, lane 1, flexible pavement test section



LEGEND

- 0 COVERAGES
- 3000 COVERAGES
- ▲ 7020 COVERAGES

Figure B20. Surface deformation in item 3, lane 1, flexible pavement test section

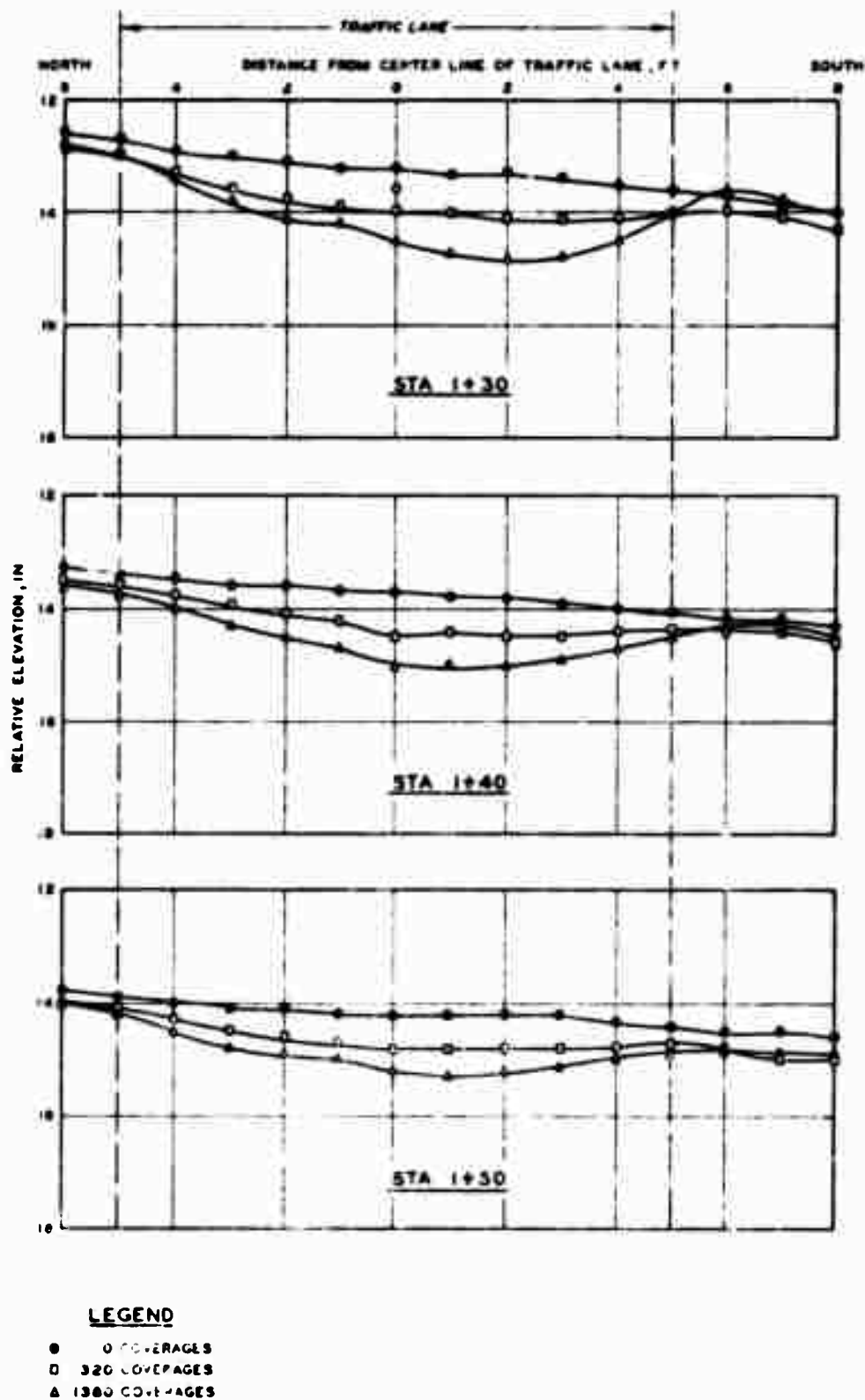
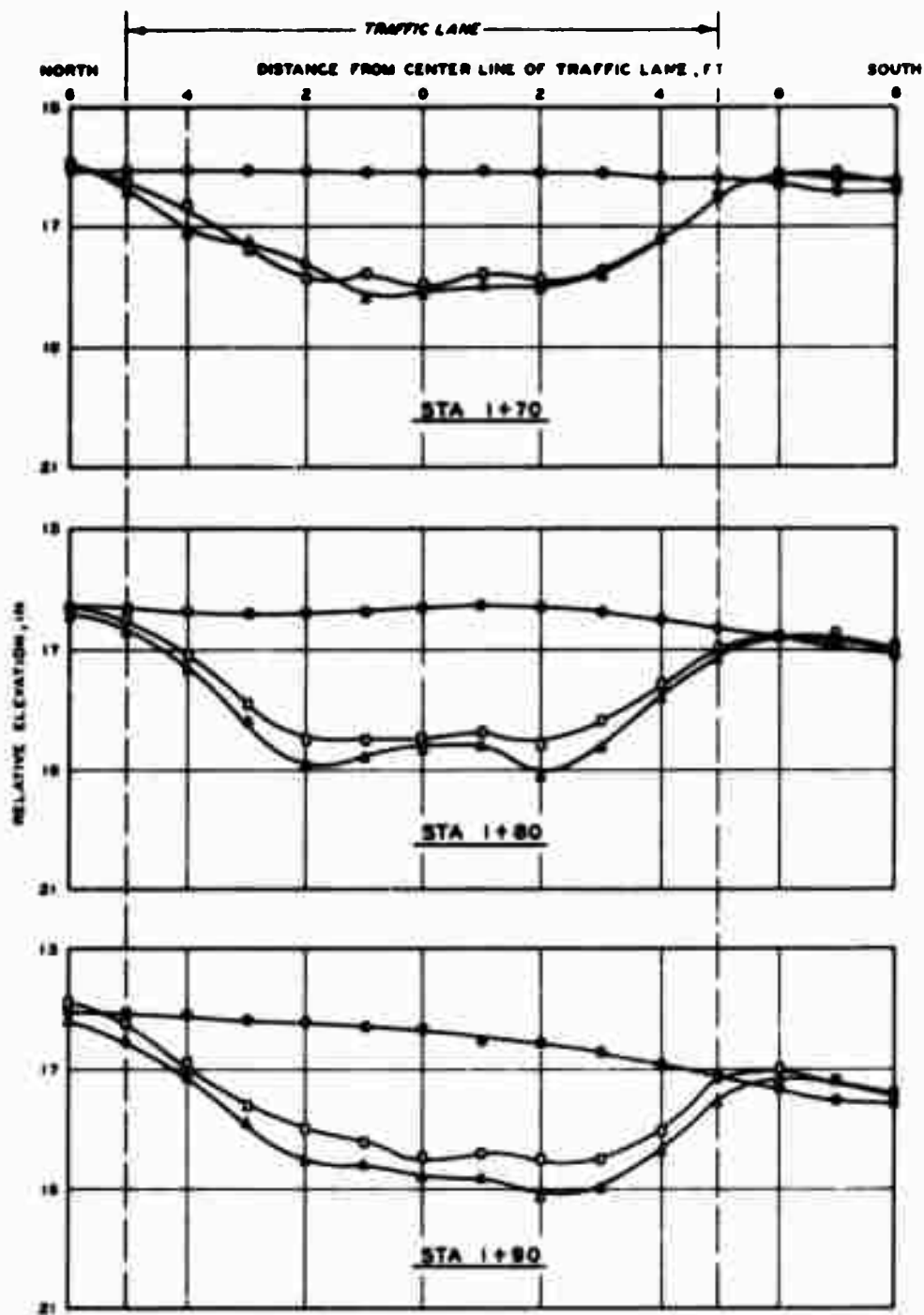


Figure B21. Surface deformation in item 4, lane 1, flexible pavement test section



LEGEND

- 0 COVERAGES
- 1200 COVERAGES
- ▲ 2500 COVERAGES

Figure B22. Surface deformation in item 5, lane 1, flexible pavement test section

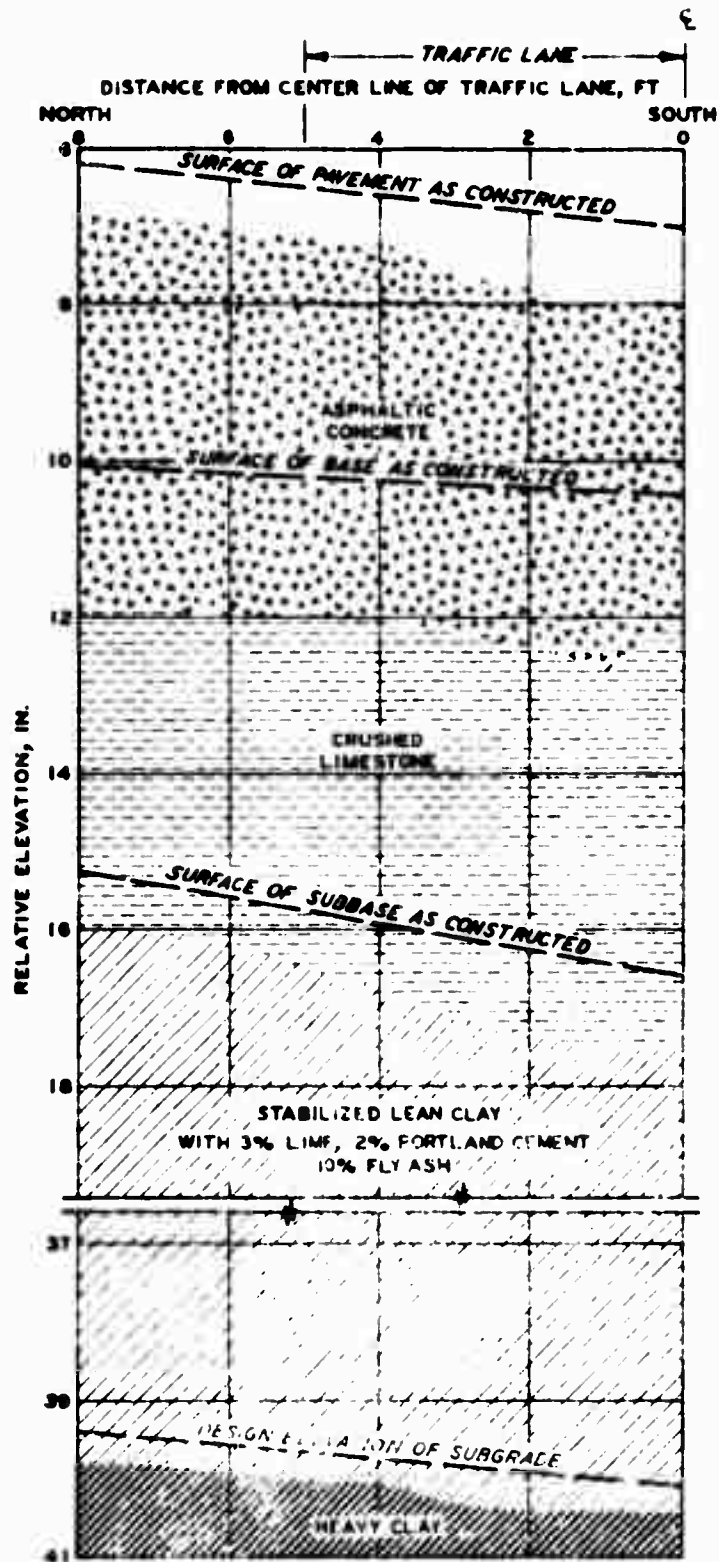


Figure 223. Test pit profile of item 1, lane 1, flexible pavement test section. Station 0+26.5 after 3660 coverages of 200-kip twin-tandem assembly

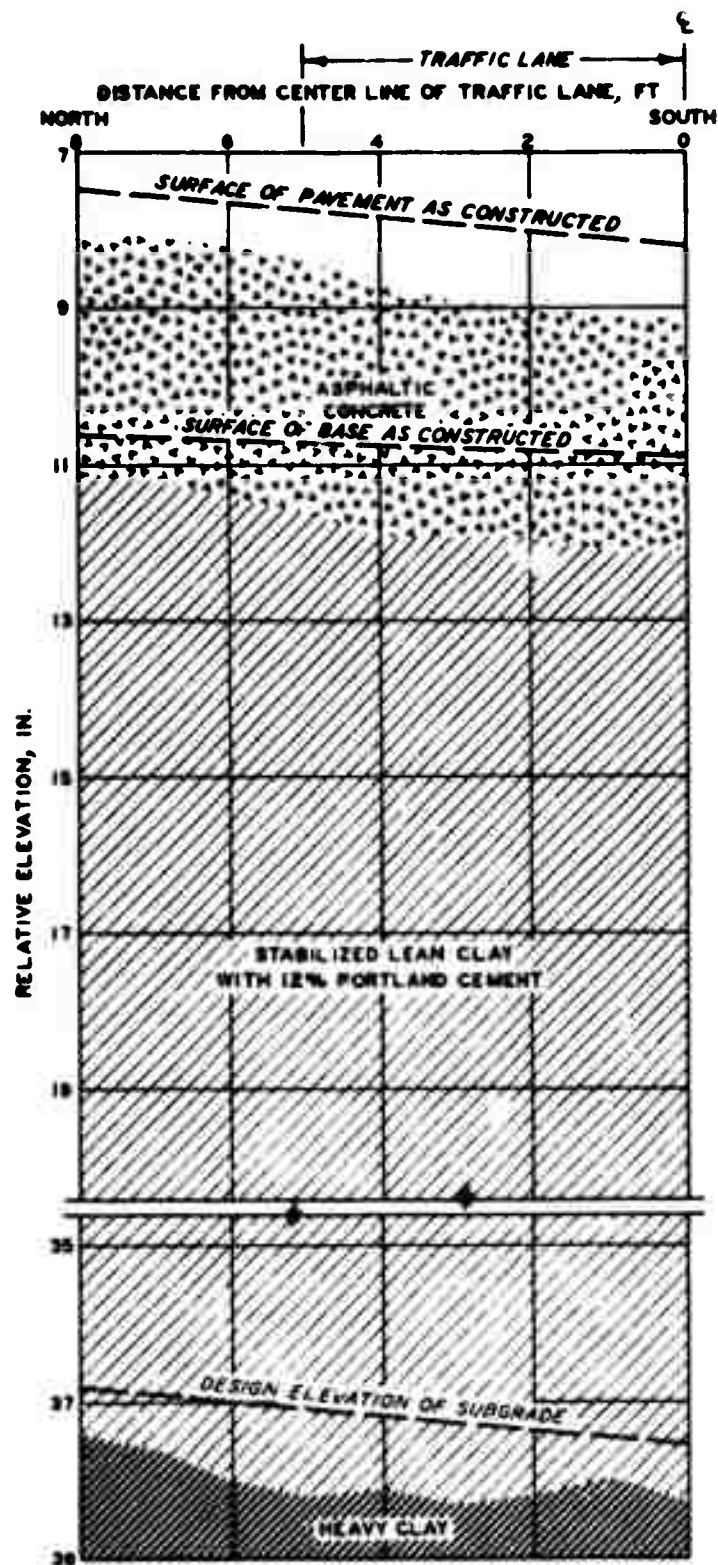


Figure B24. Test pit profile of item 2, lane 1, flexible pavement test section. Station 0+65 after 3660 coverages of 200-kip twin-tandem assembly

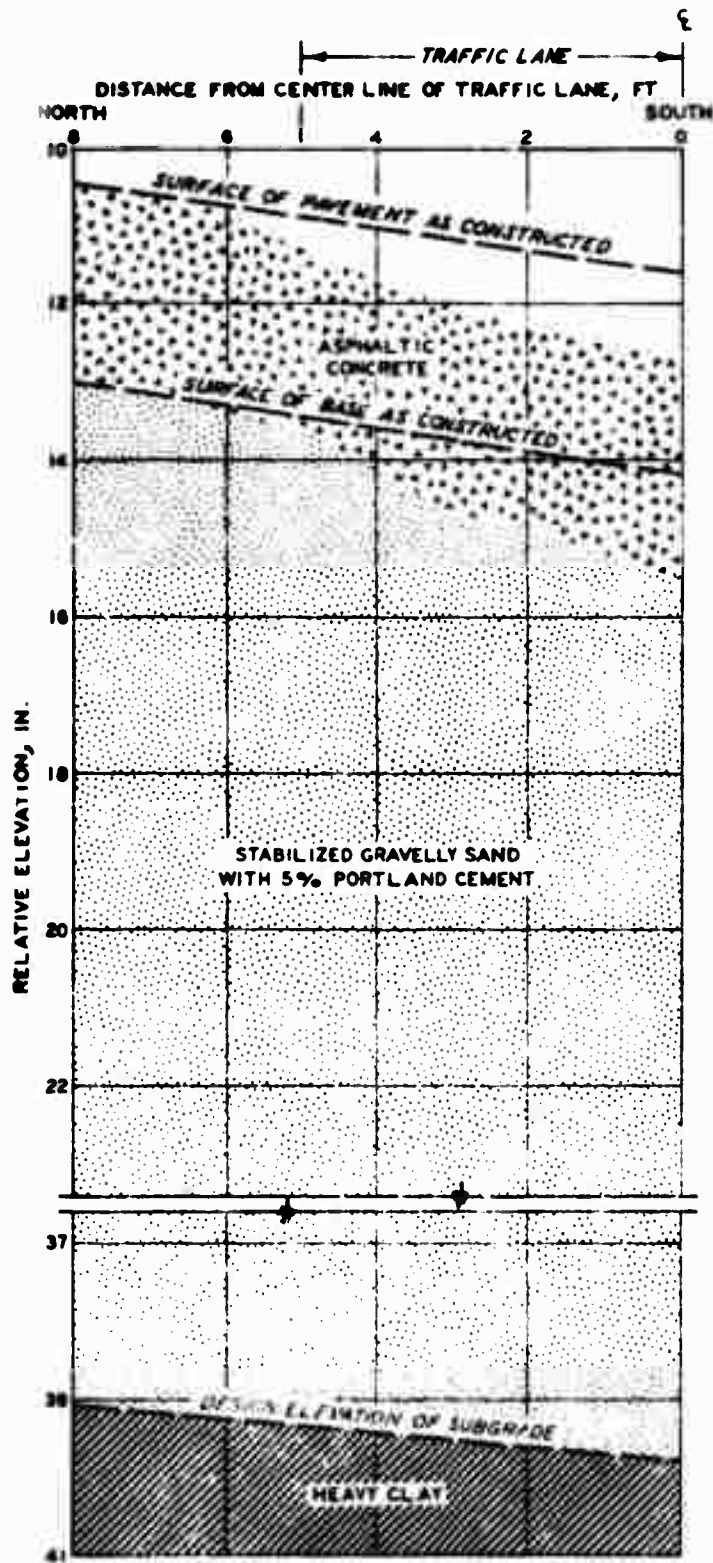


Figure 125. Test pit profile of item 3, lane 1, flexible pavement test section. Station 1+04 after 7820 coverages of 200-kip twin-tandem assembly

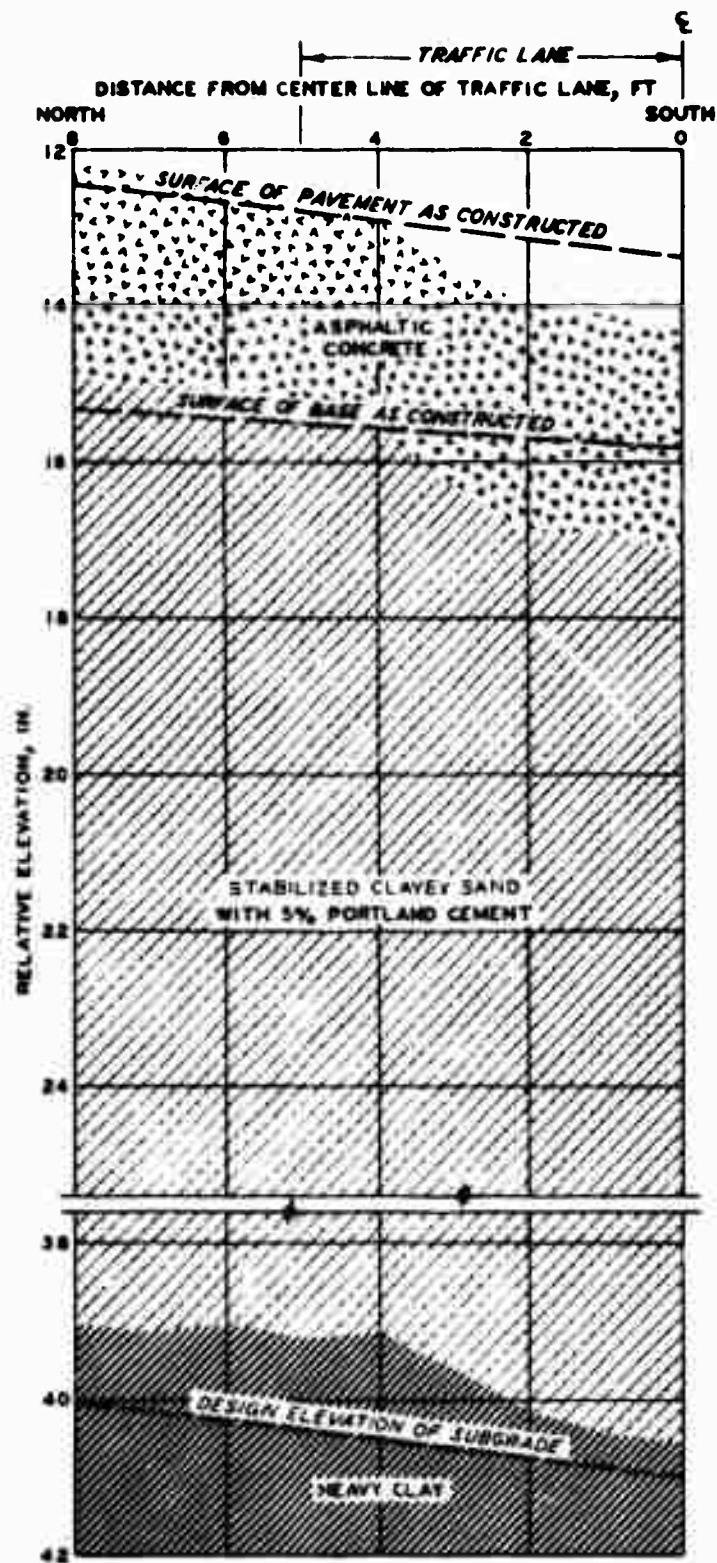


Figure B26. Test pit profile of item 4, lane 1, flexible pavement test section. Station 1+27 after 1380 coverages of 200-kip twin-tandem assembly

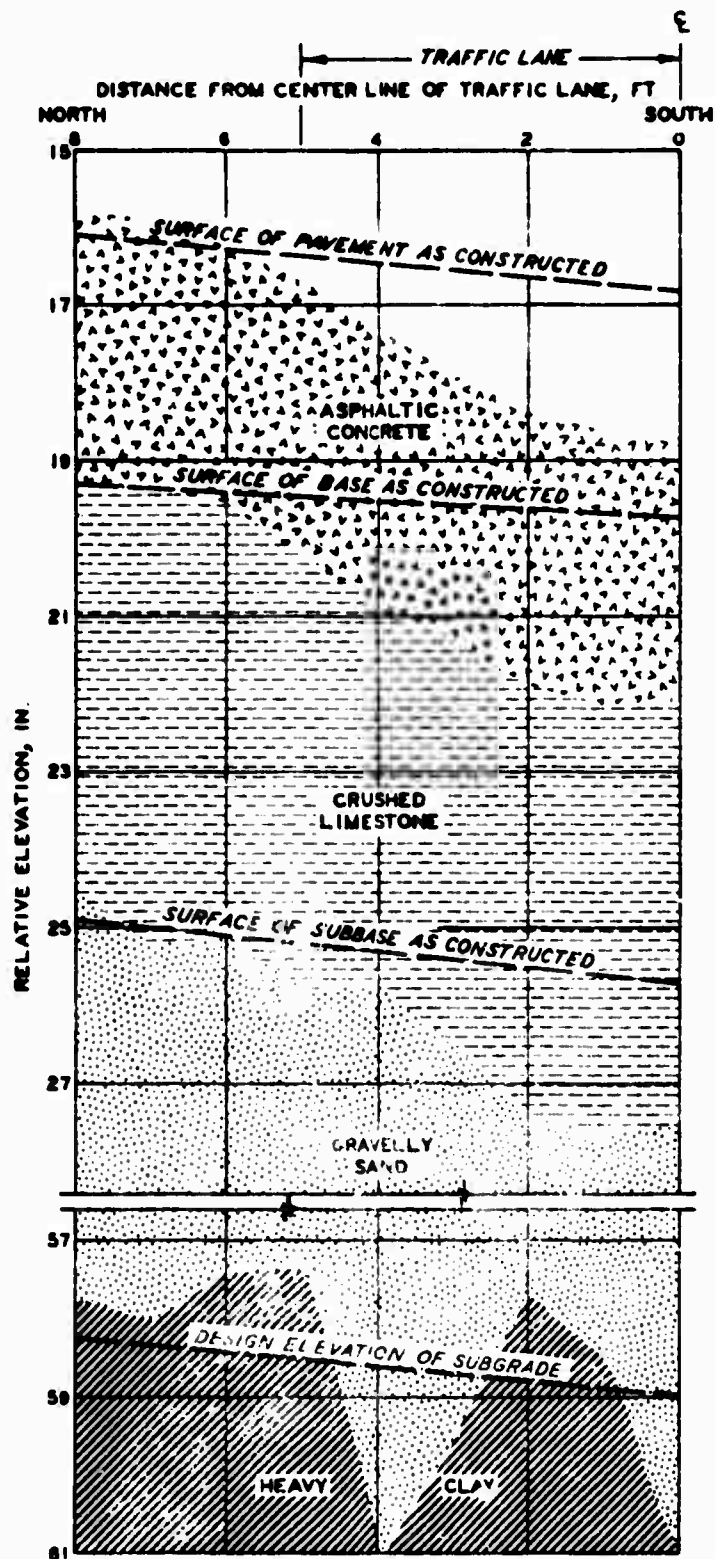


Figure B27. Test pit profile of item 5, lane 1, flexible pavement test section. Station 1+89 after 2500 coverages of 200-kip twin-tandem assembly



Figure B28. Item 1, lane 2, flexible pavement test section prior to traffic

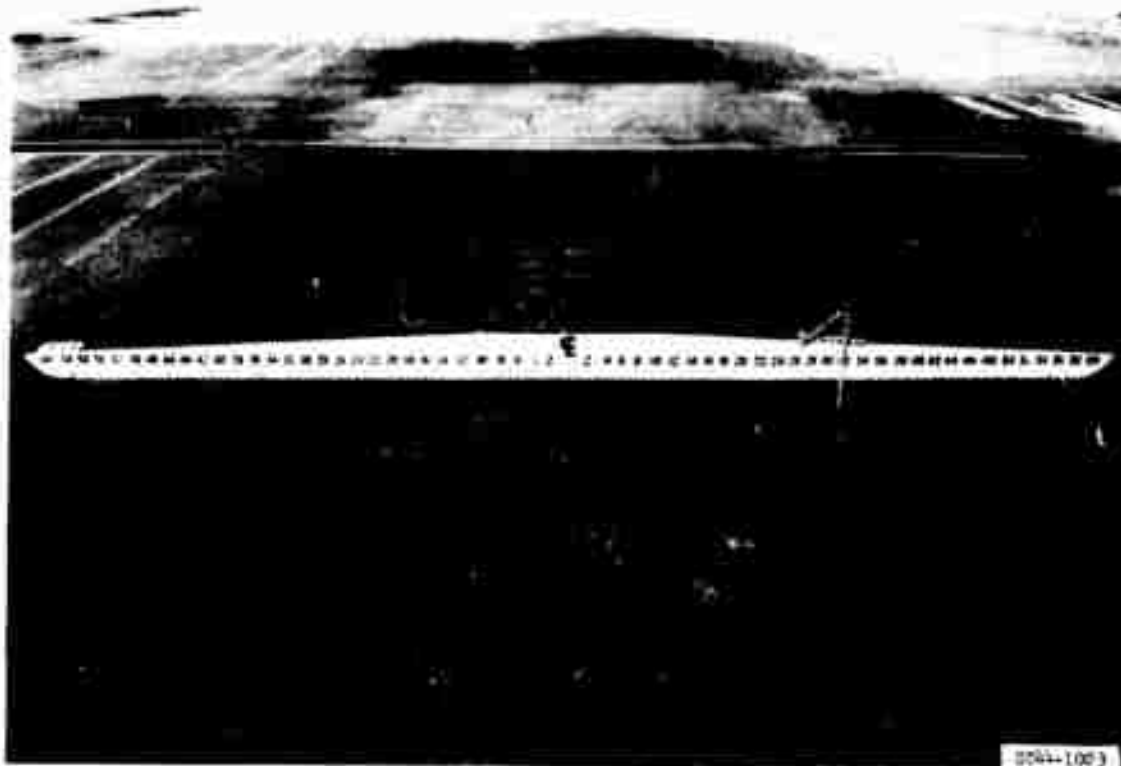


Figure B29. Cracking and deformation in item 1, lane 2, flexible pavement test section, after 600 coverages of 240-kip twin-tandem assembly

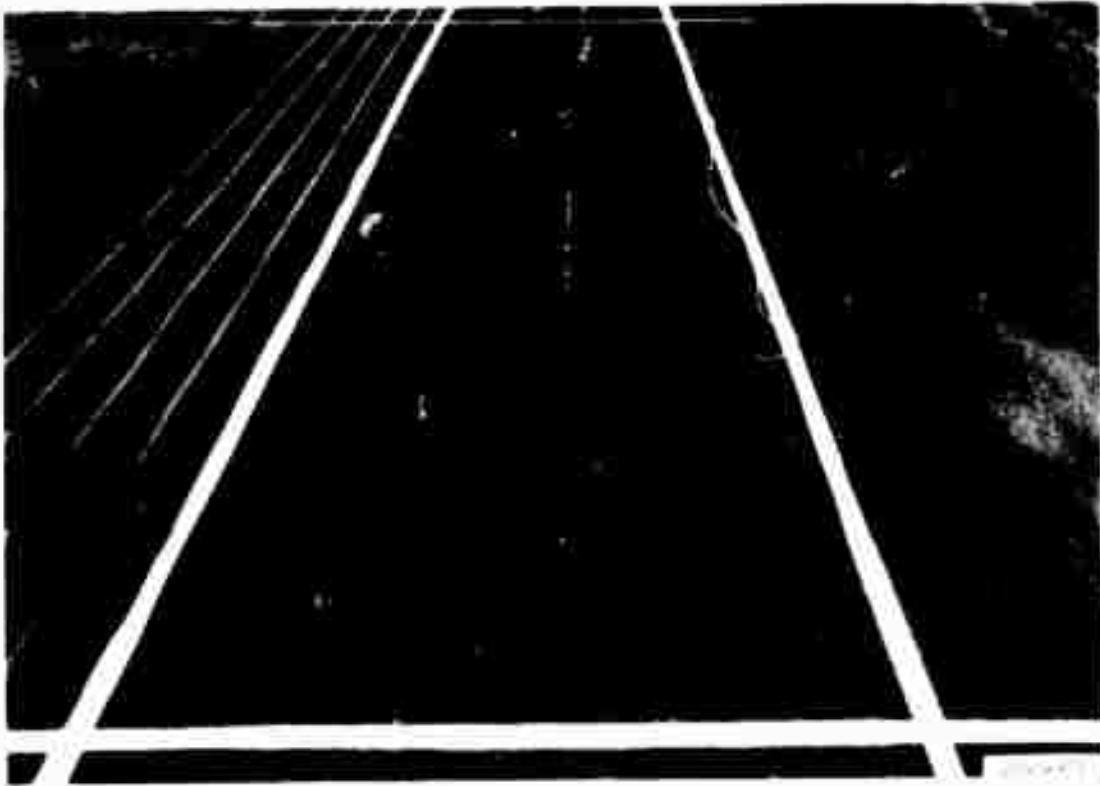


Figure B30. Item 2, lane 2, flexible pavement test section, prior to traffic



Figure B31. Item 2, lane 2, flexible pavement test section, after 320 coverages of 240-kip twin-tandem assembly

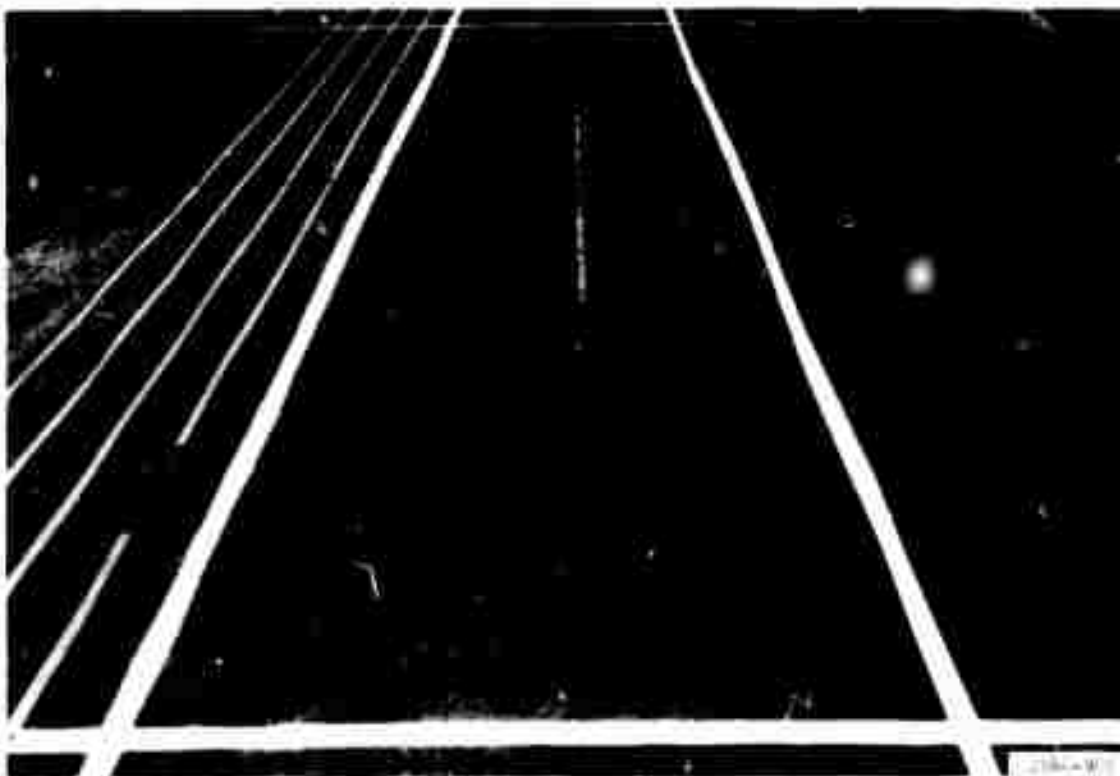


Figure B32. Item 3, lane 2, flexible pavement test section, prior to traffic

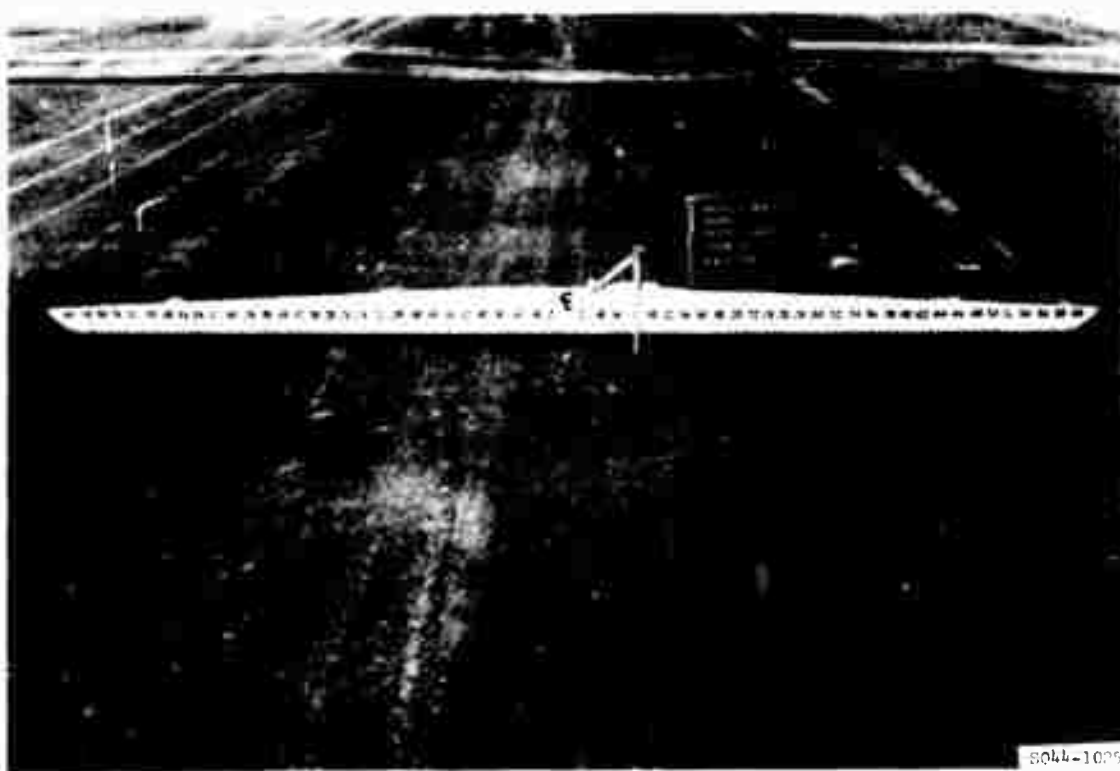


Figure B33. Deformation in item 3, lane 2, flexible pavement test section, at failure after 620 coverages of 240-kip twin-tandem assembly

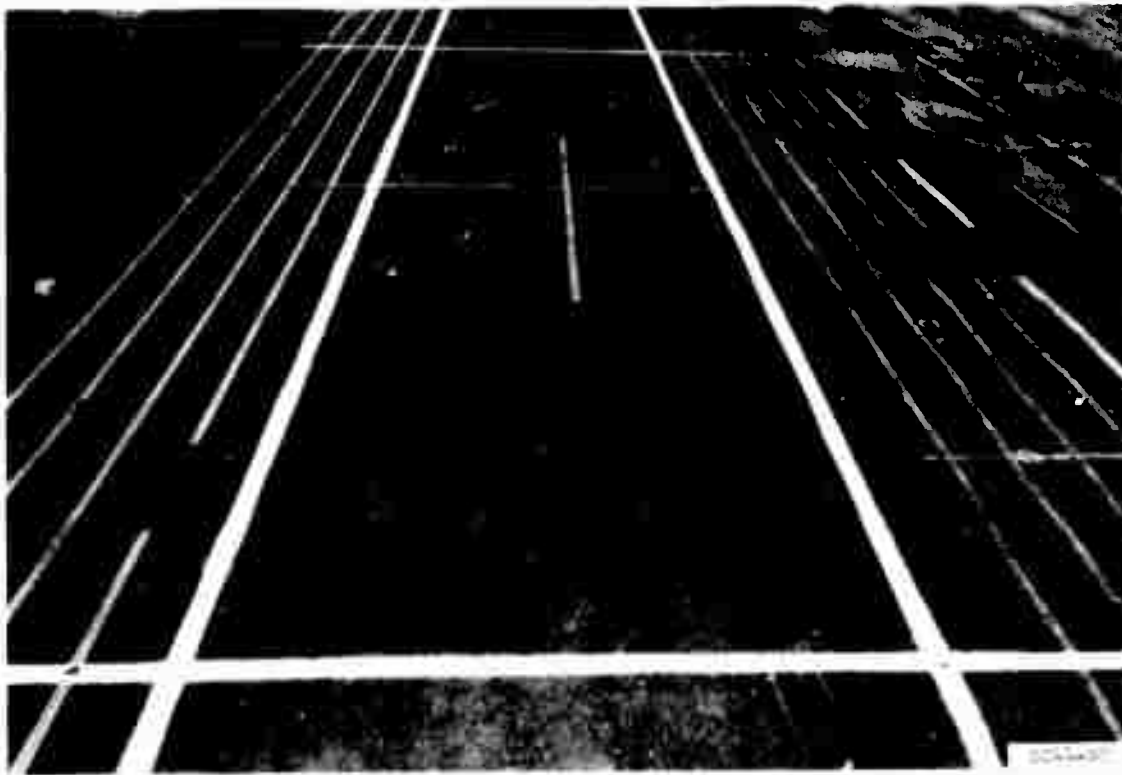


Figure B34. Item 4, lane 2, flexible pavement test section, prior to traffic



Figure B35. Cracking and deformation in item 4, lane 2, flexible pavement test section, at failure after 120 coverages of 240-kip twin-tandem assembly

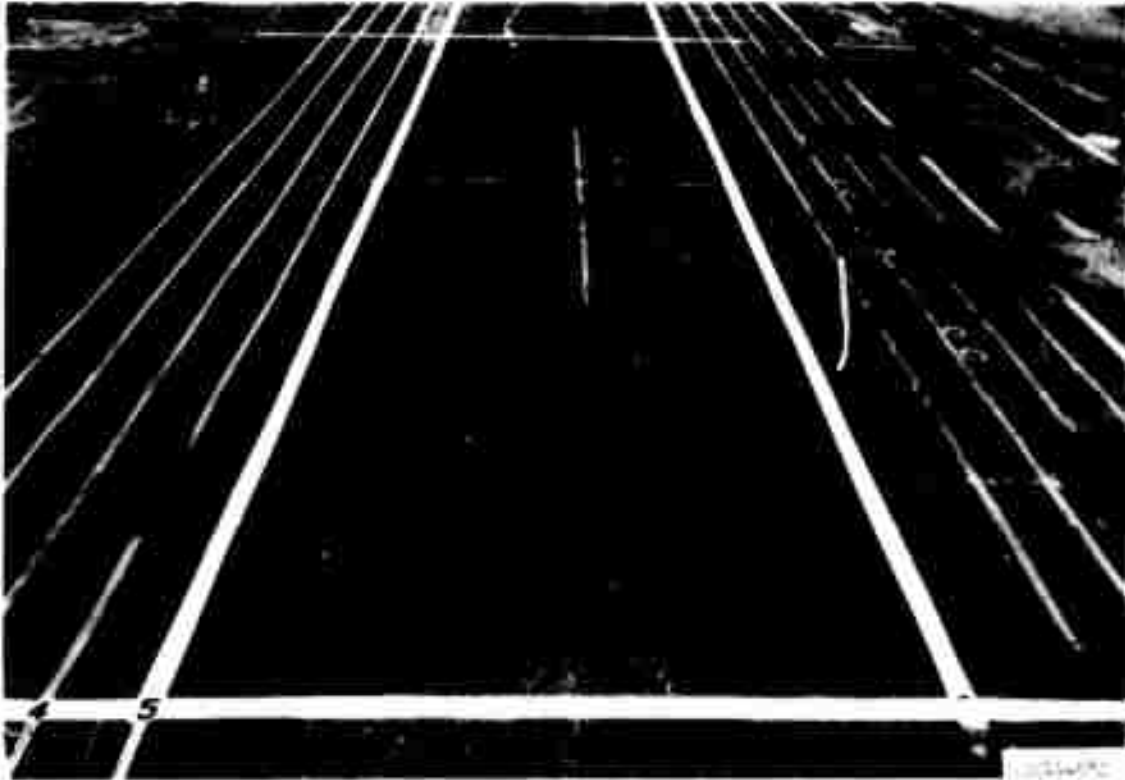


Figure B36. Item 5, lane 2, flexible pavement test section, prior to traffic

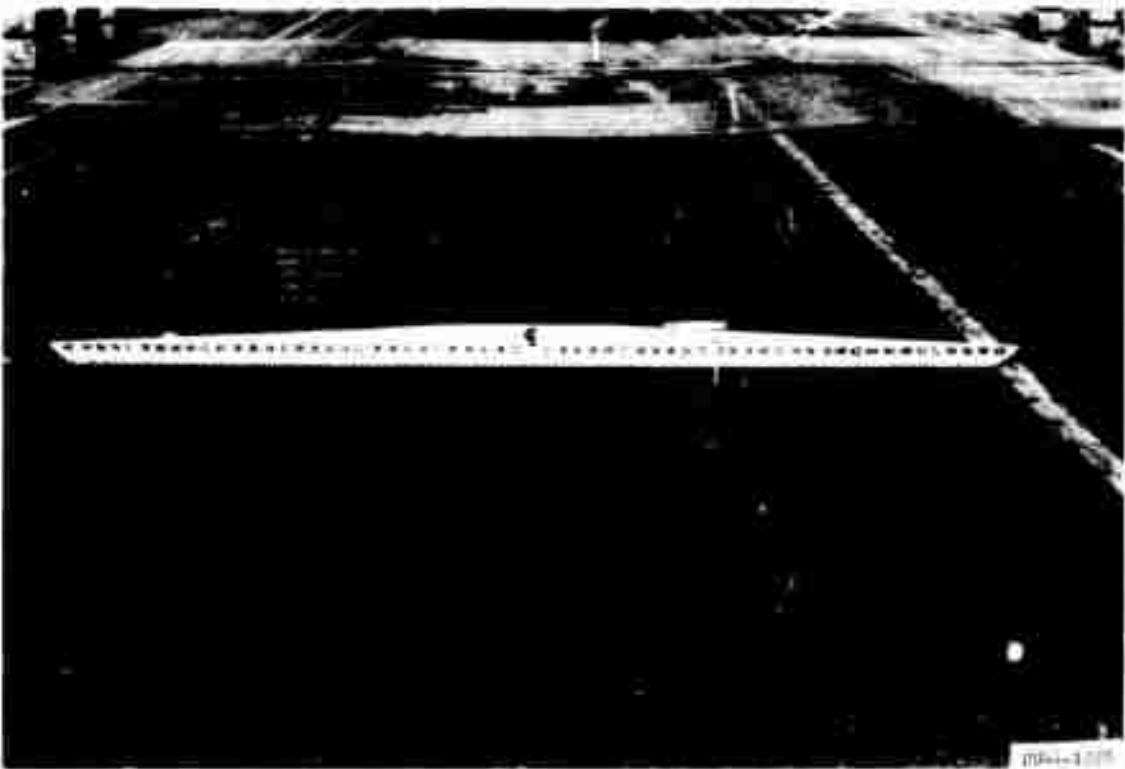


Figure B37. Cracking and deformation in item 5, lane 2, flexible pavement test section, at failure after 340 coverages of 240-kip twin-tandem assembly

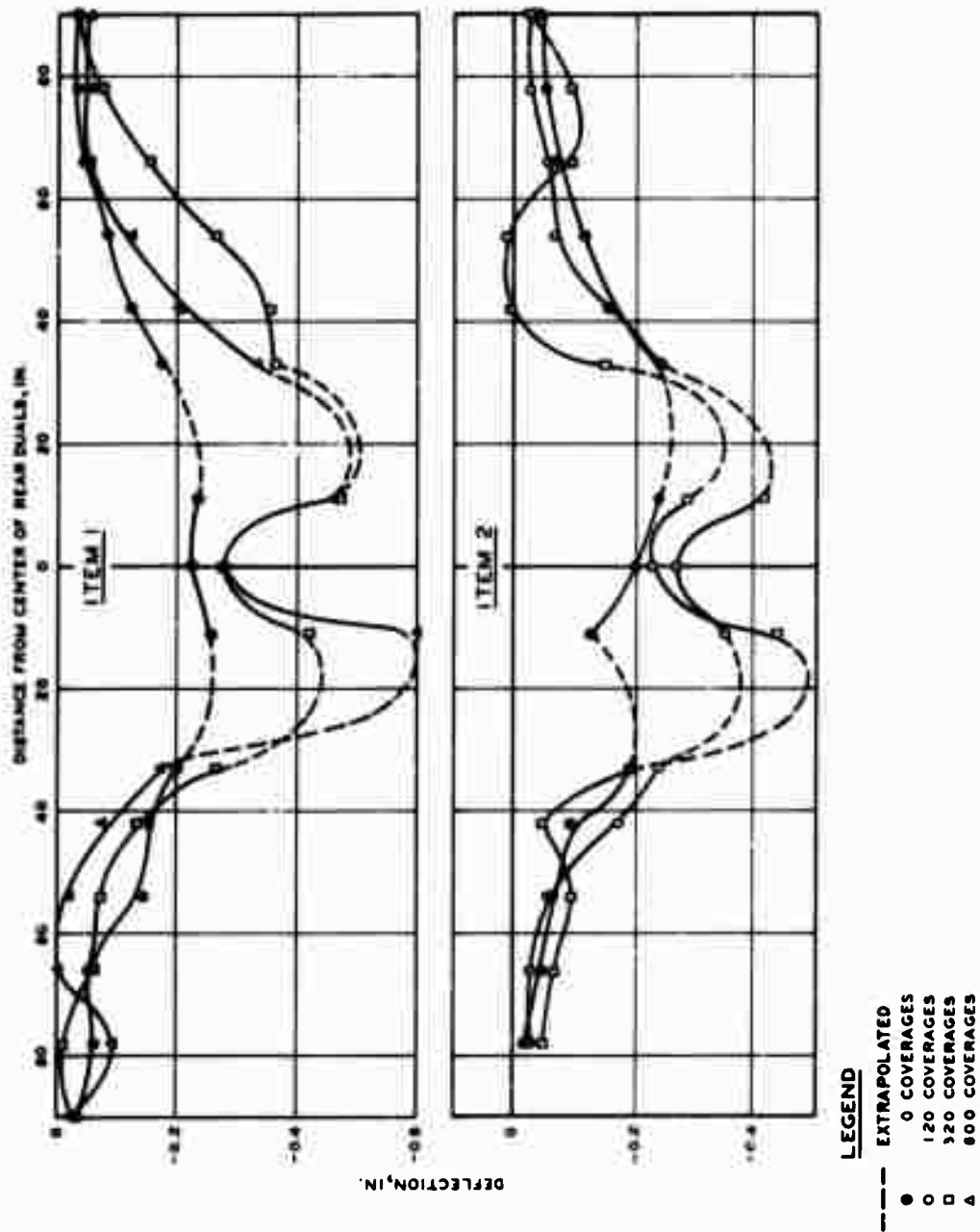


Figure B38. Deflections measured transverse to direction of traffic in items 1 and 2, lane 2, flexible pavement test section

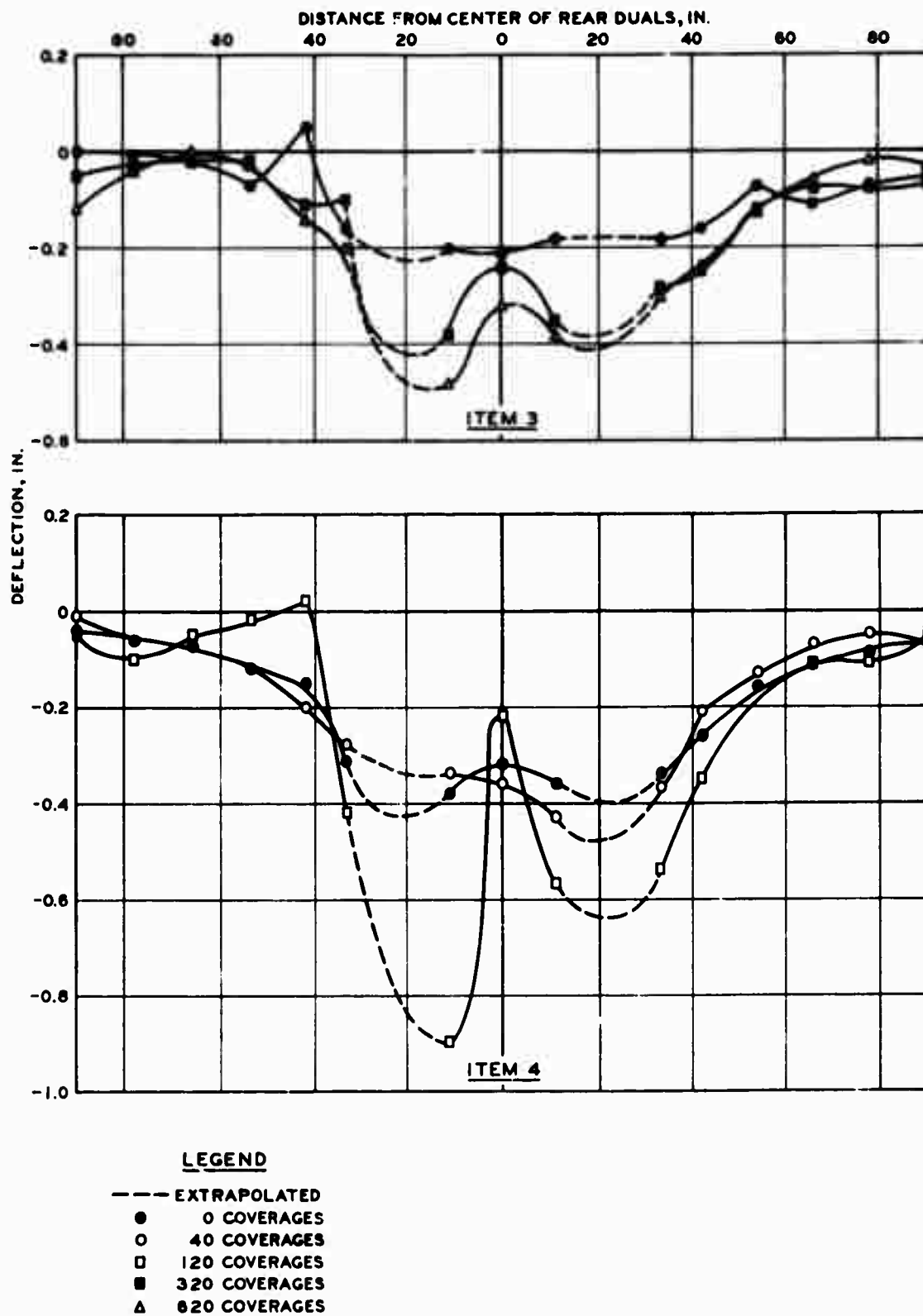
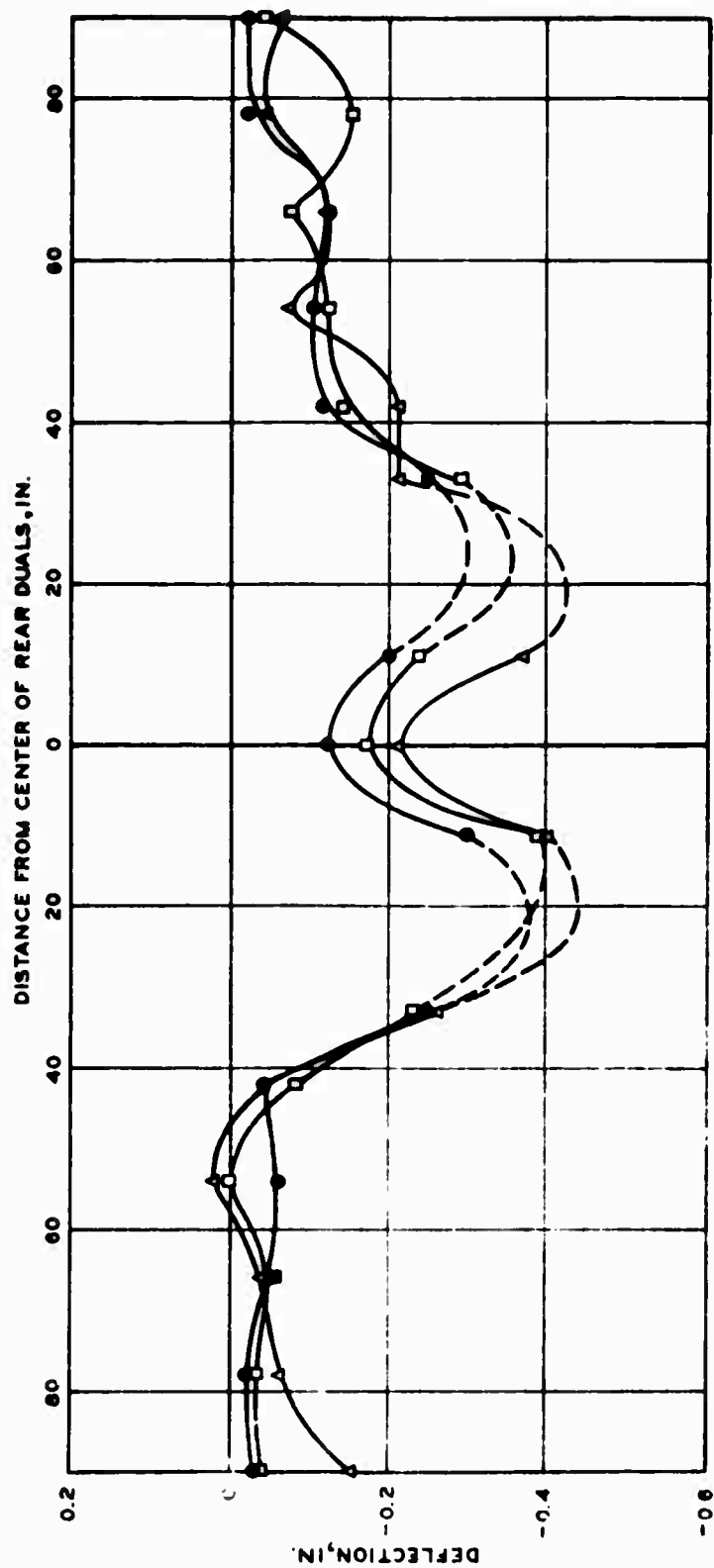


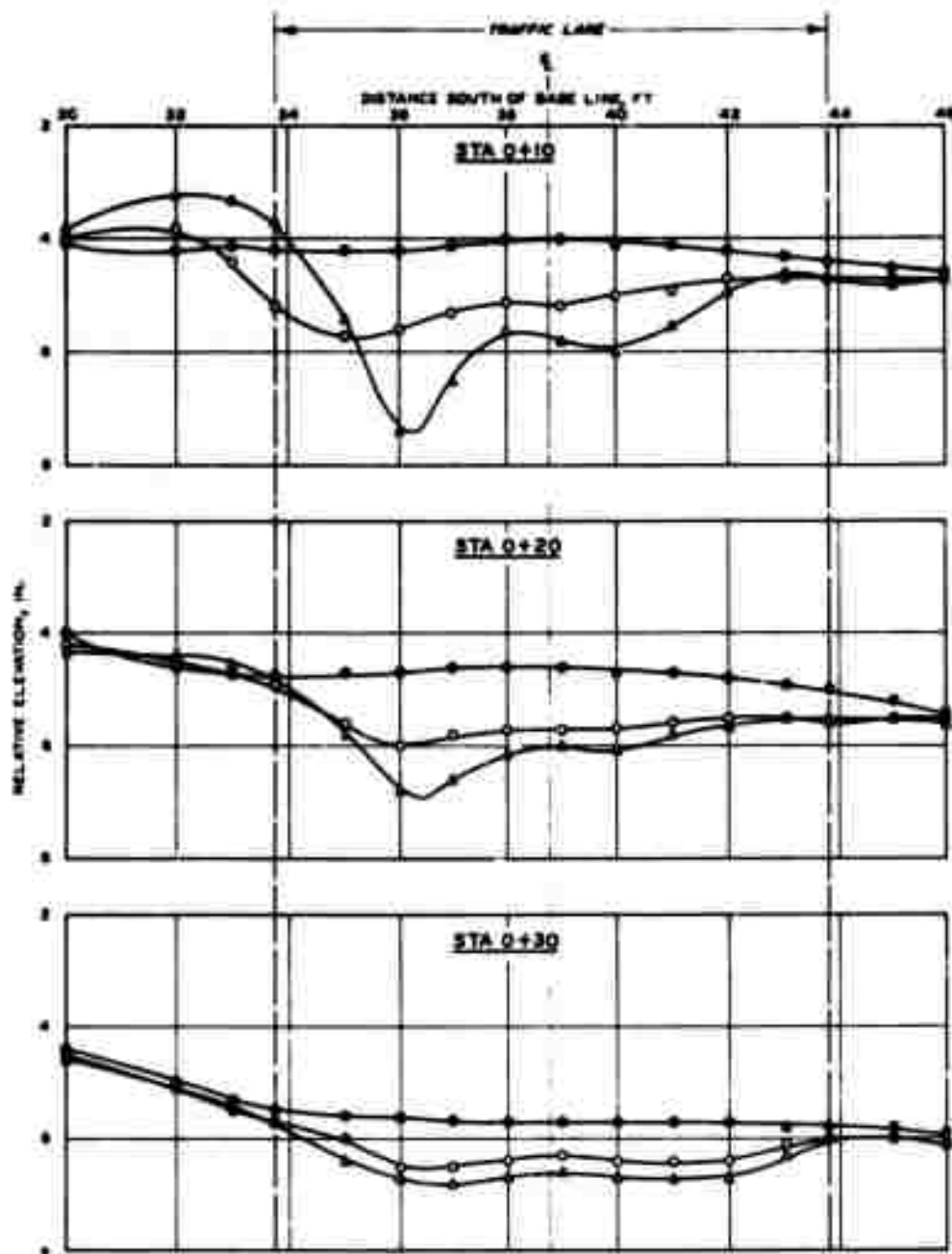
Figure B39. Deflections measured transverse to direction of traffic in items 3 and 4, lane 2, flexible pavement test section



LEGEND

- EXTRAPOLATED
- 0 COVERAGES
- 120 COVERAGES
- △ 340 COVERAGES

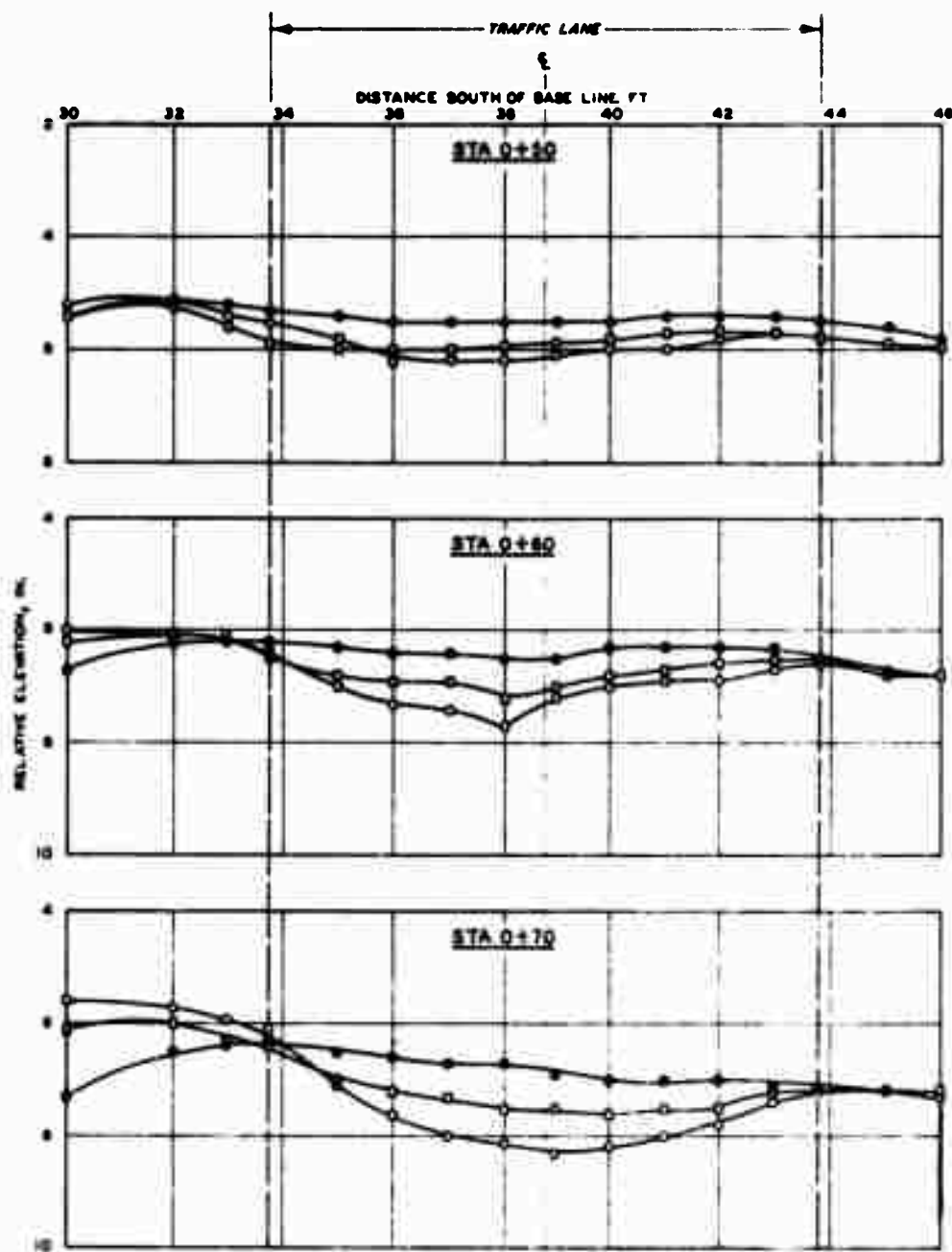
Figure B40. Deflections measured transverse to direction of traffic in item 5, lane 2, flexible pavement test section



LEGEND

- 0 COVERAGES
- 320 COVERAGES
- △ 600 COVERAGES

Figure B41. Surface deformation in item 1, lane 2, flexible pavement test section



LEGEND

- 0 COVERAGES
- 120 COVERAGES
- 320 COVERAGES

Figure B42. Surface deformation in item 2, lane 2, flexible pavement test section

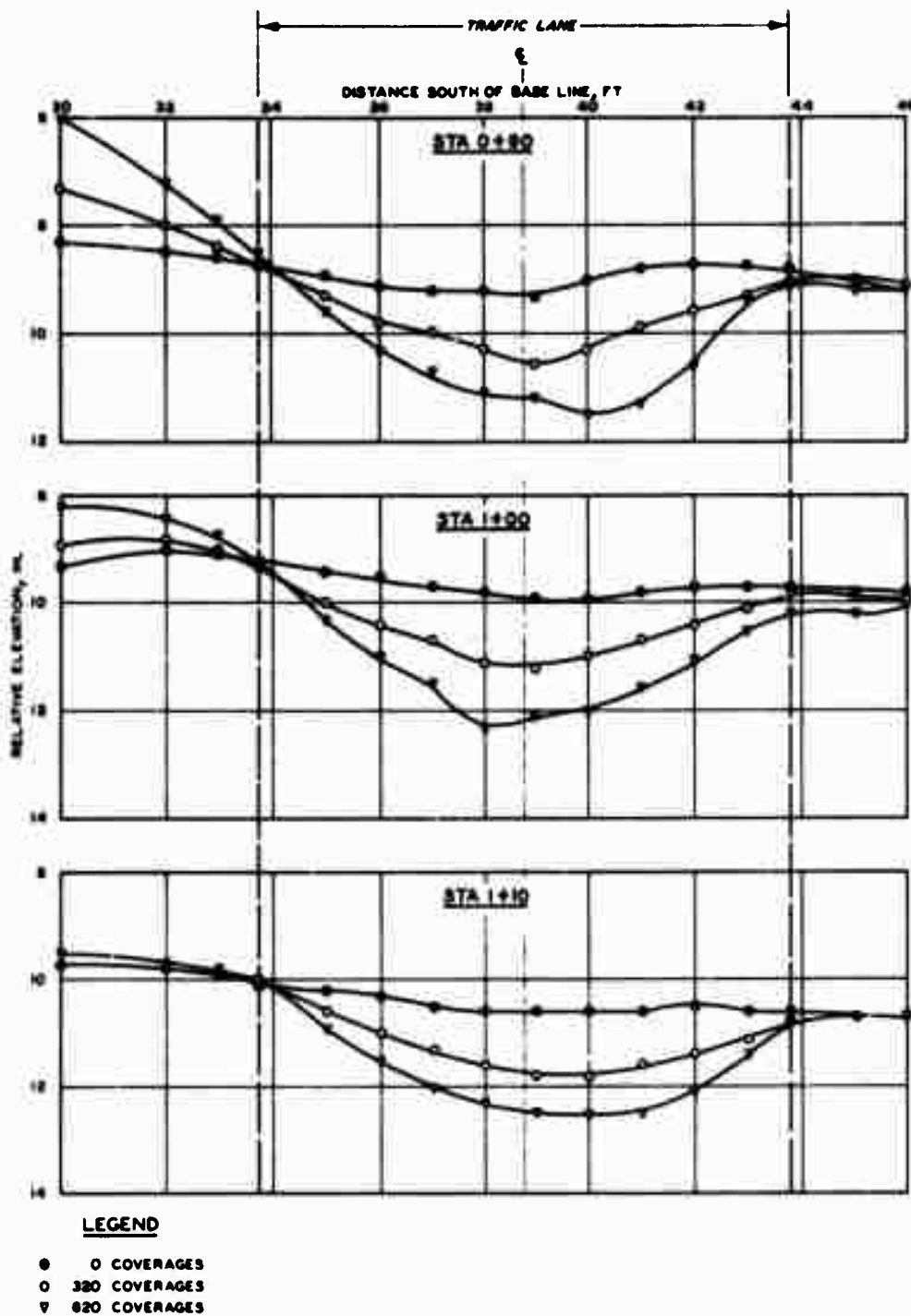


Figure B43. Surface deformation in item 3, lane 2, flexible pavement test section

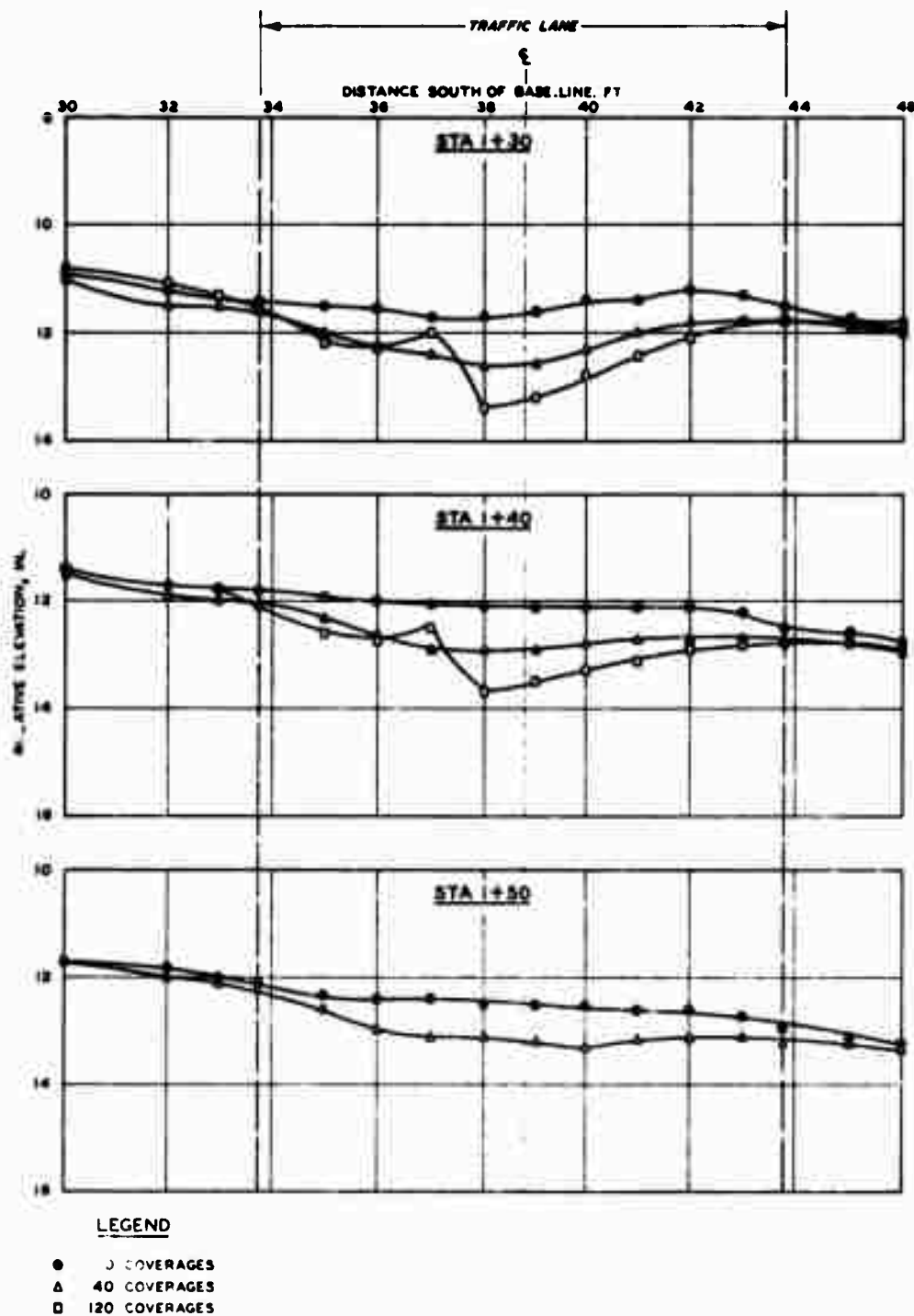


Figure B44. Surface deformation in item 4, lane 2, flexible pavement test section

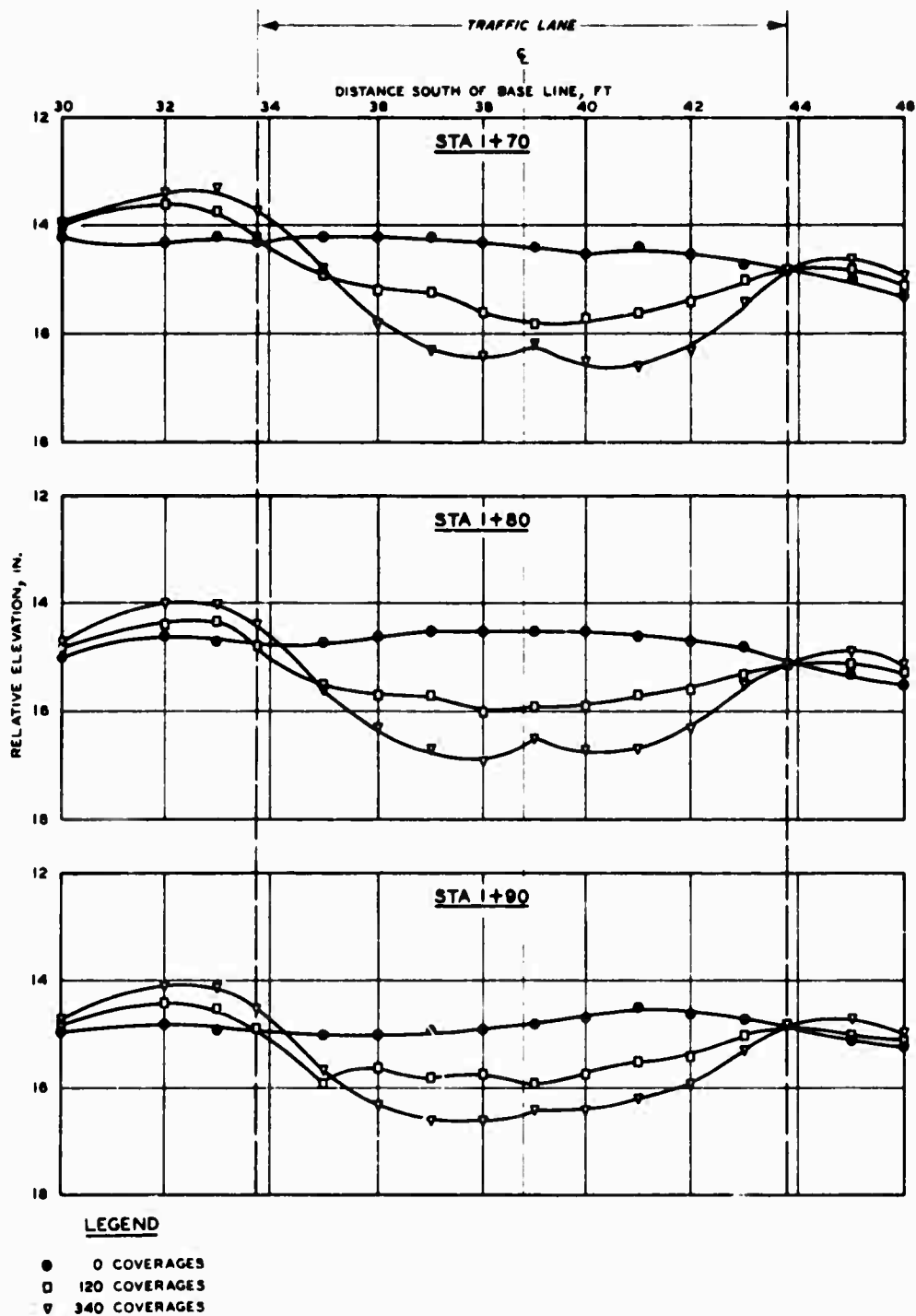


Figure B45. Surface deformation in item 5, lane 2, flexible pavement test section

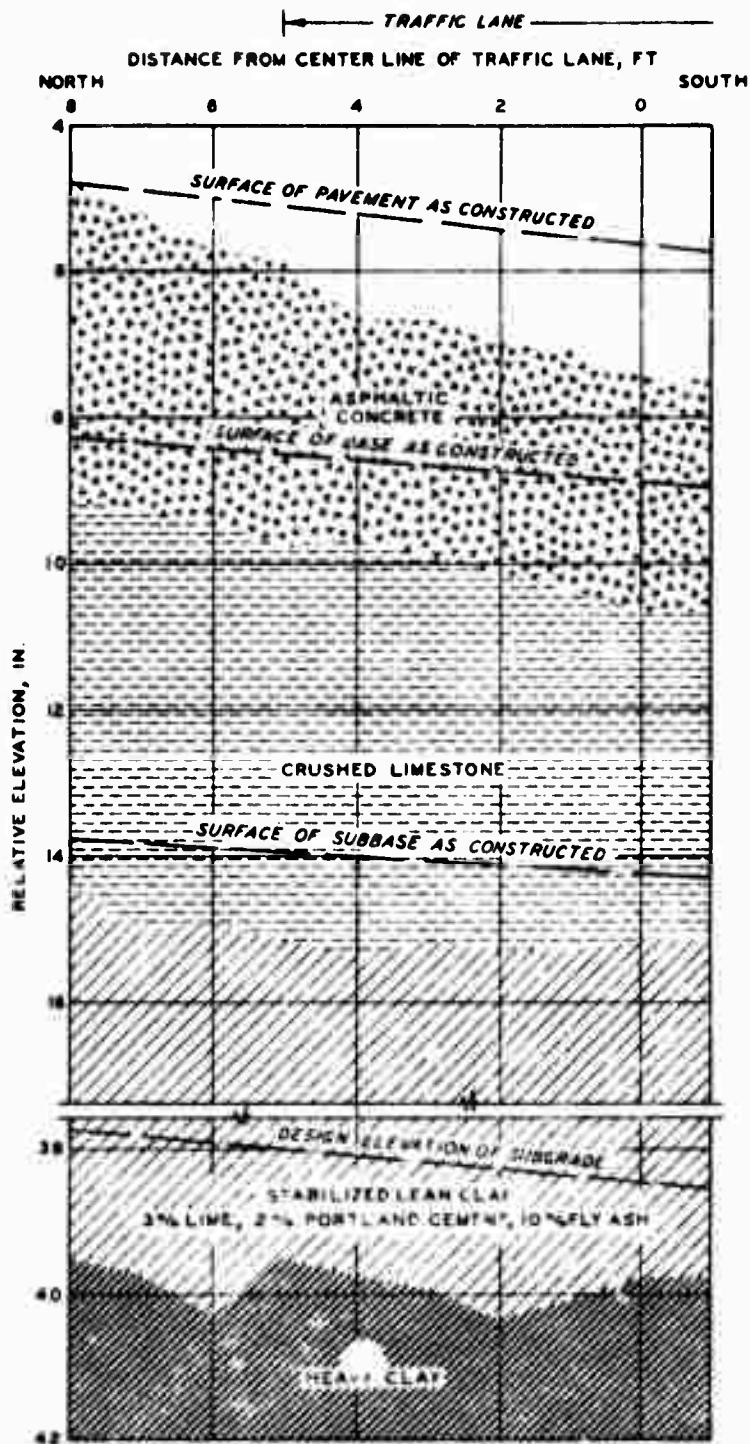


Figure B46. Test pit profile of item 1, Lane 2, flexible pavement test section. Station 0+28 after 600 coverages of 240-kip twin-tandem assembly

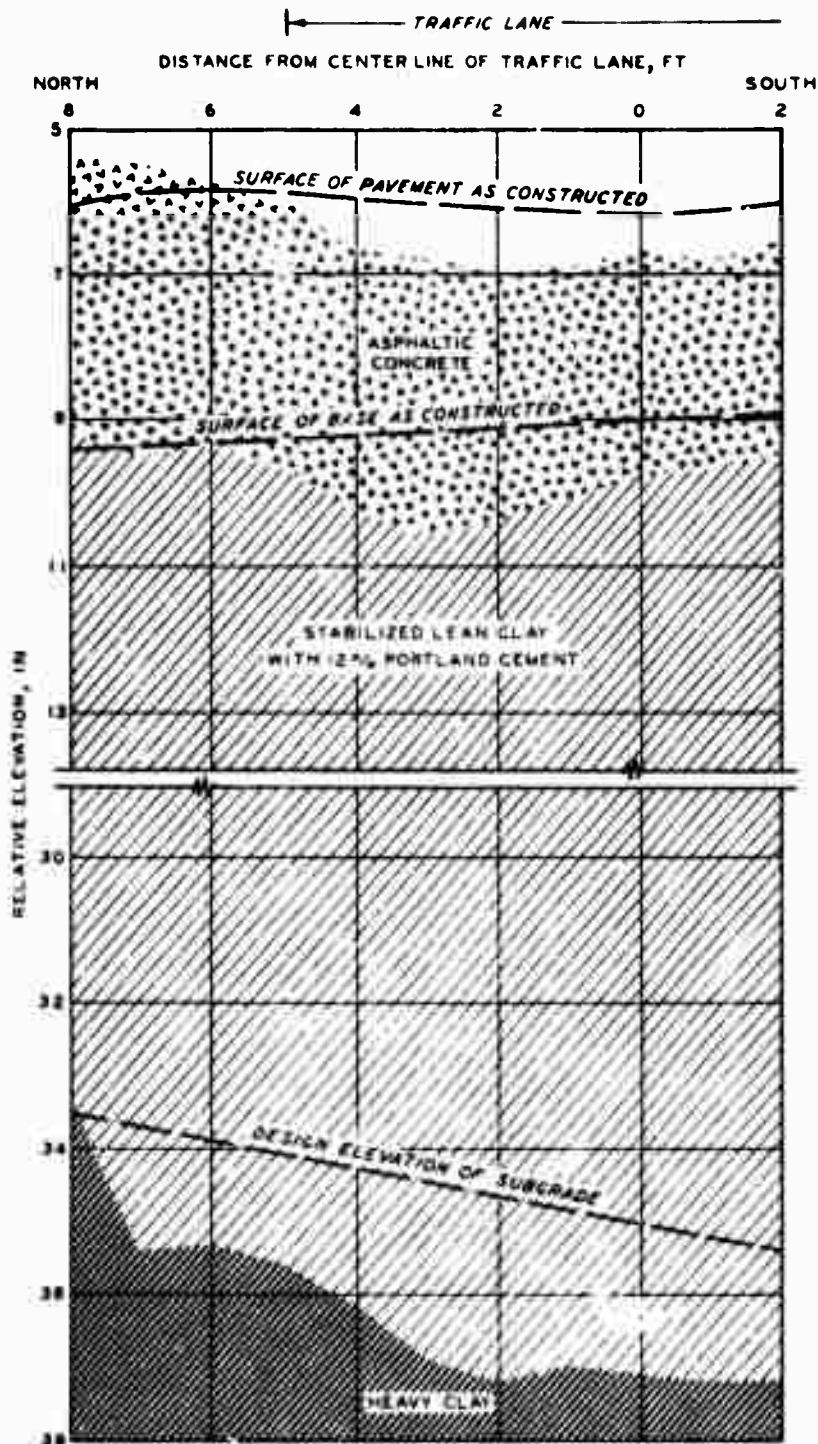


Figure B47. Test pit profile of item 2, lane 2, flexible pavement test section. Station 0+56 after 320 coverages of 240-kip twin-tandem assembly

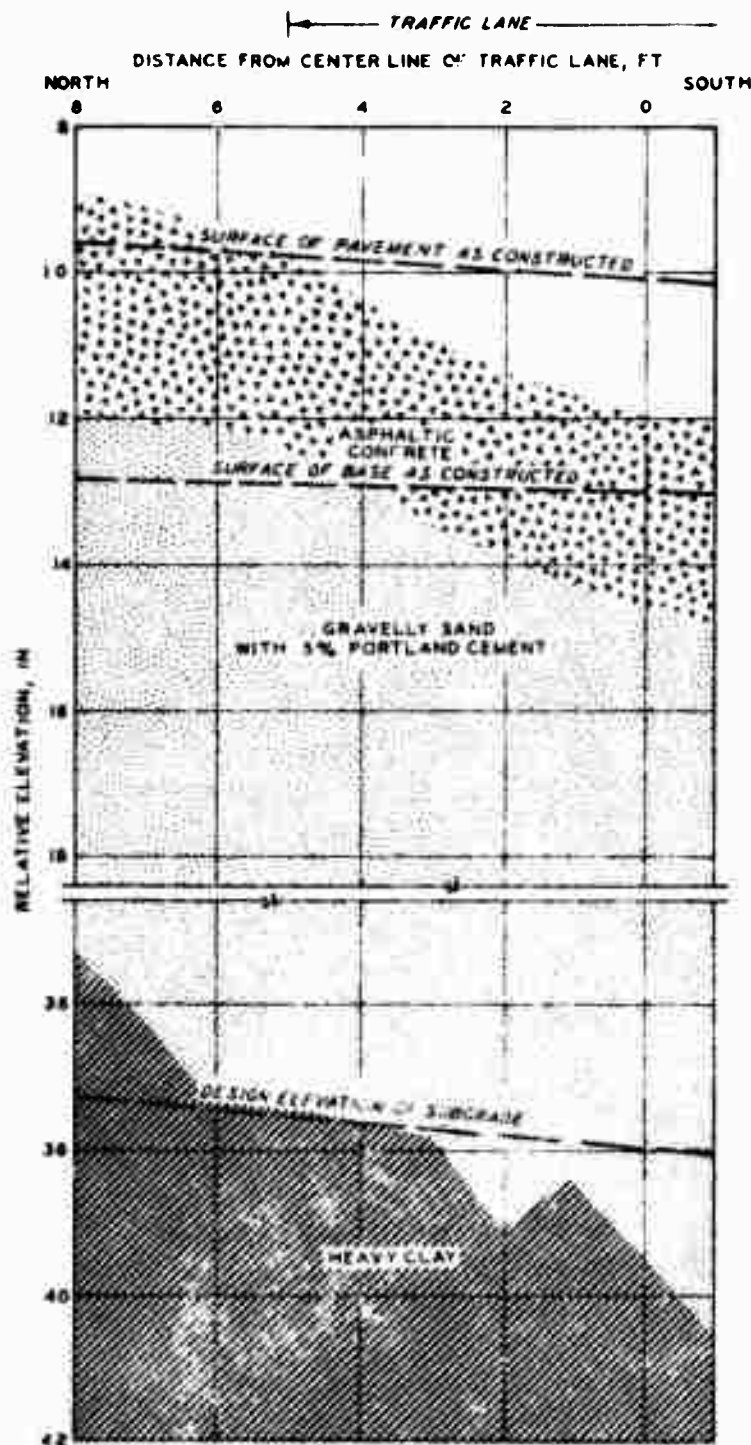


Figure B48. Test pit profile of item 3, lane 2, flexible pavement test section. Station 1+05 after 620 coverages of 240-kip twin-tandem assembly

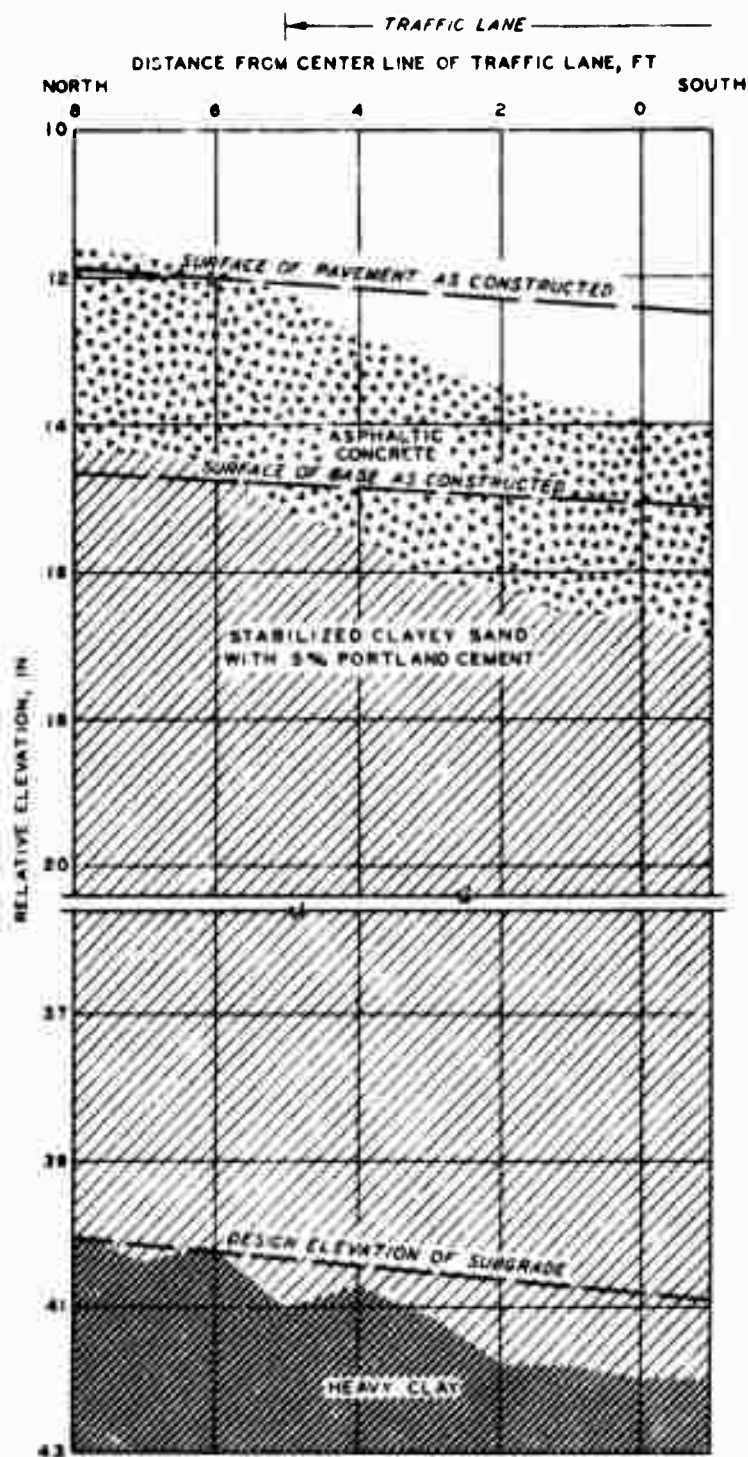


Figure B49. Test pit profile of item 4, lane 2, flexible pavement test section. Station 1+51 after 120 coverages of 240-kip twin-tandem assembly

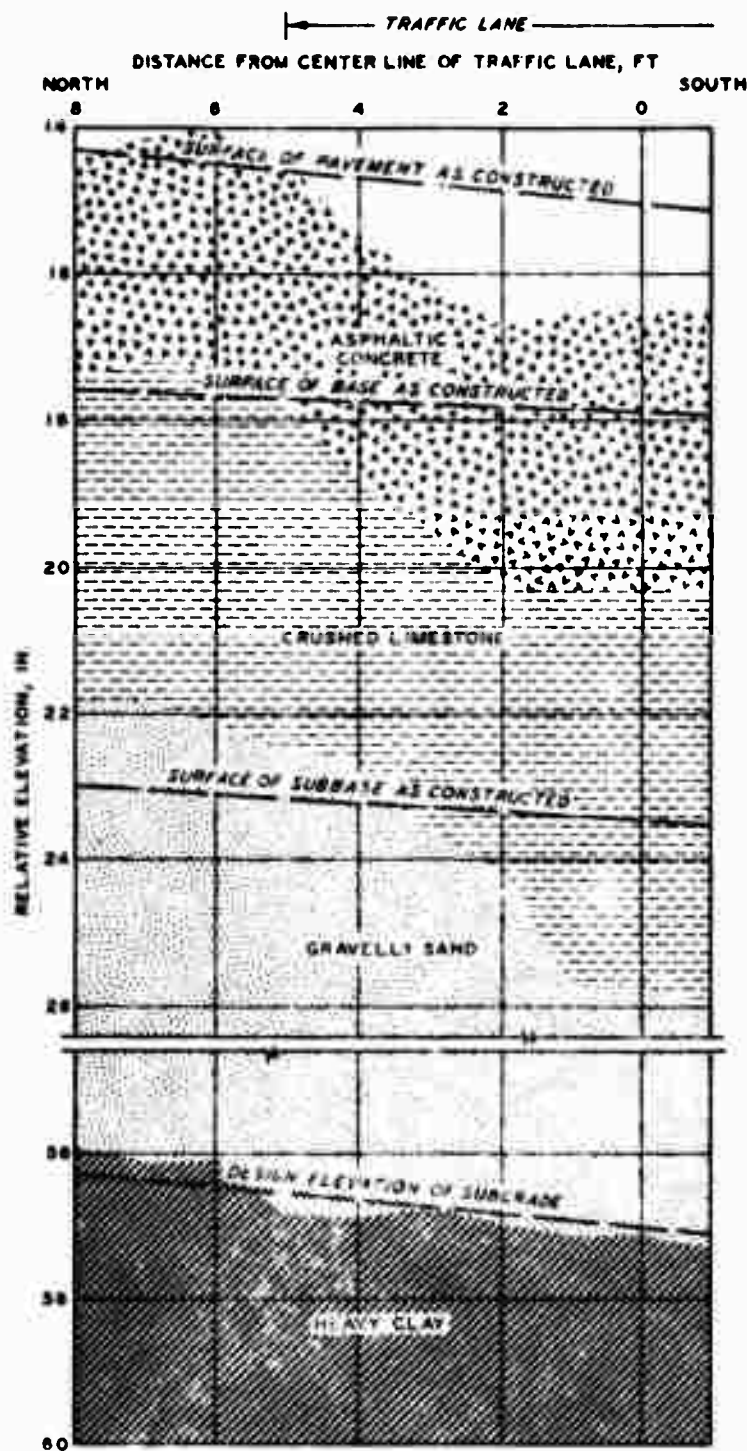


Figure B50. Test pit profile of item 5, lane 2, flexible pavement test section. Station 1+88 after 340 coverages of 240-kip twin-tandem assembly

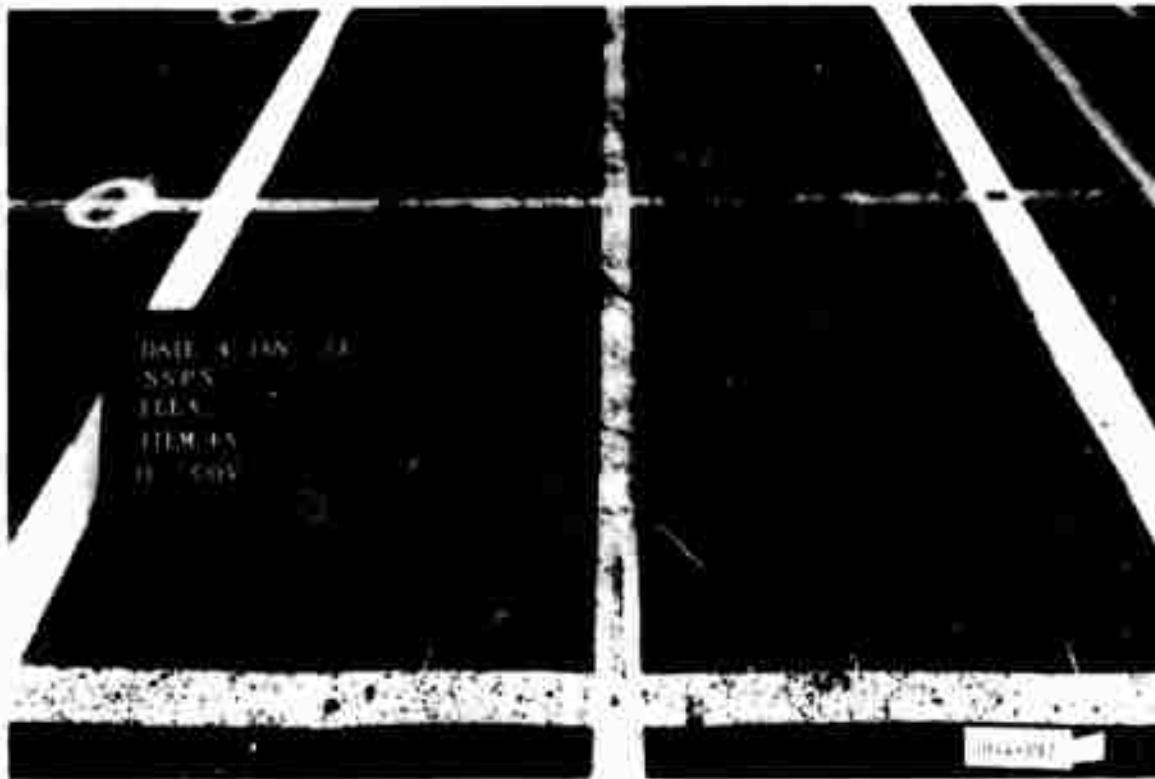


Figure B51. Subitem 4a, lane 3, flexible pavement test section, prior to traffic

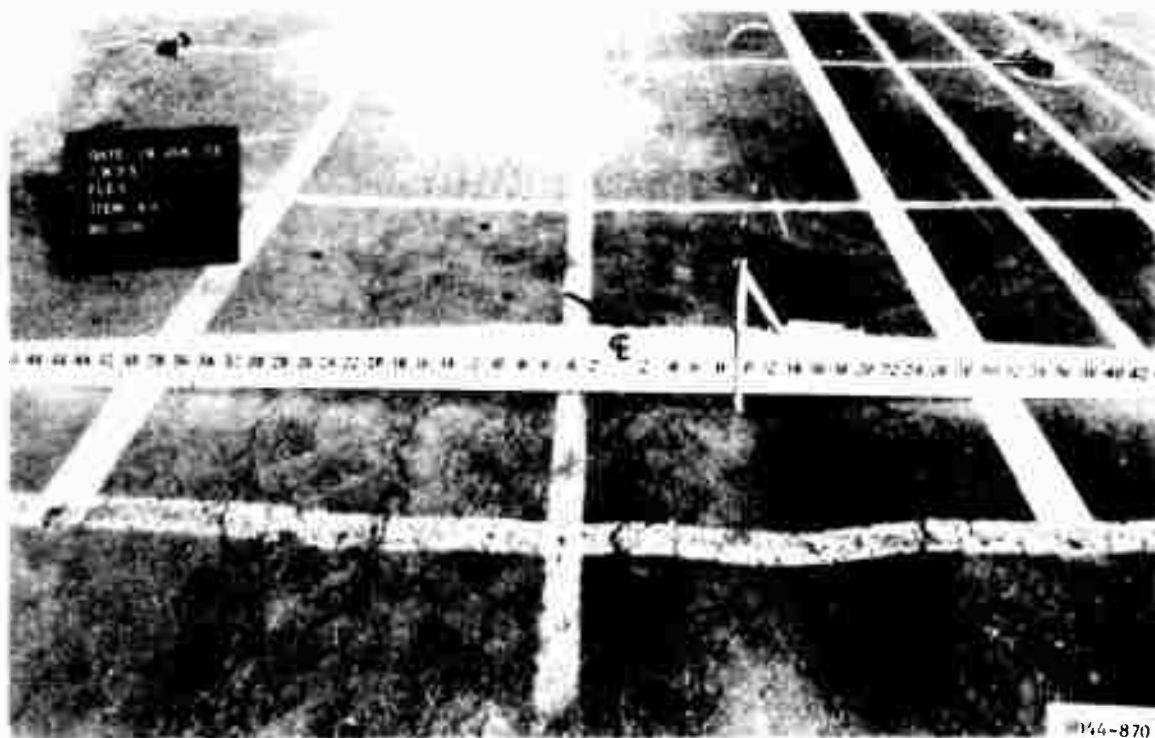


Figure B52. Cracking in subitem 4a, lane 3, flexible pavement test section, after 80 coverages of 50-kip single-wheel assembly



Figure B53. Subitem 4b, lane 3, flexible pavement test section, prior to traffic



Figure B54. Cracking and deformation in subitem 4b, lane 3, flexible pavement test section, at failure after 170 coverages of 50-kip single-wheel assembly



Figure B55. Subitem 4c, lane 3, flexible pavement test section, prior to traffic

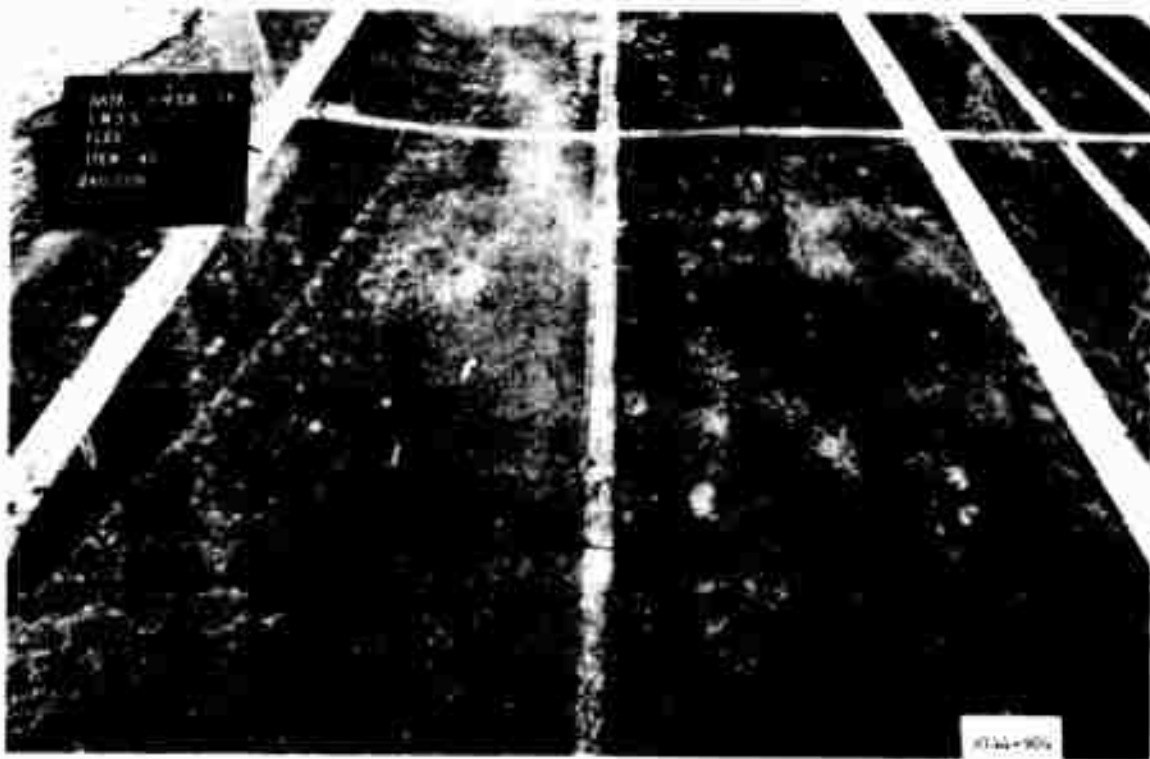


Figure B56. Cracking in subitem 4c, lane 3, flexible pavement test section, at failure after 240 coverages of 50-kip single-wheel assembly

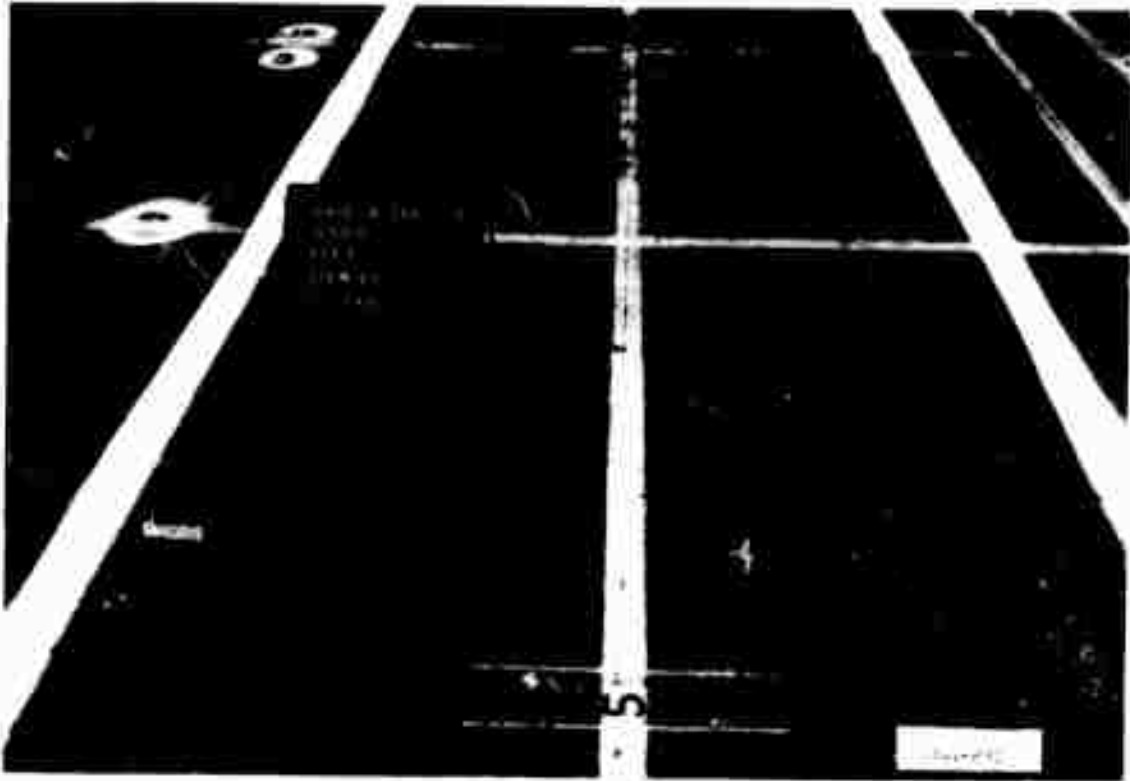


Figure B57. Subitem 4d, lane 3, flexible pavement test section, prior to traffic

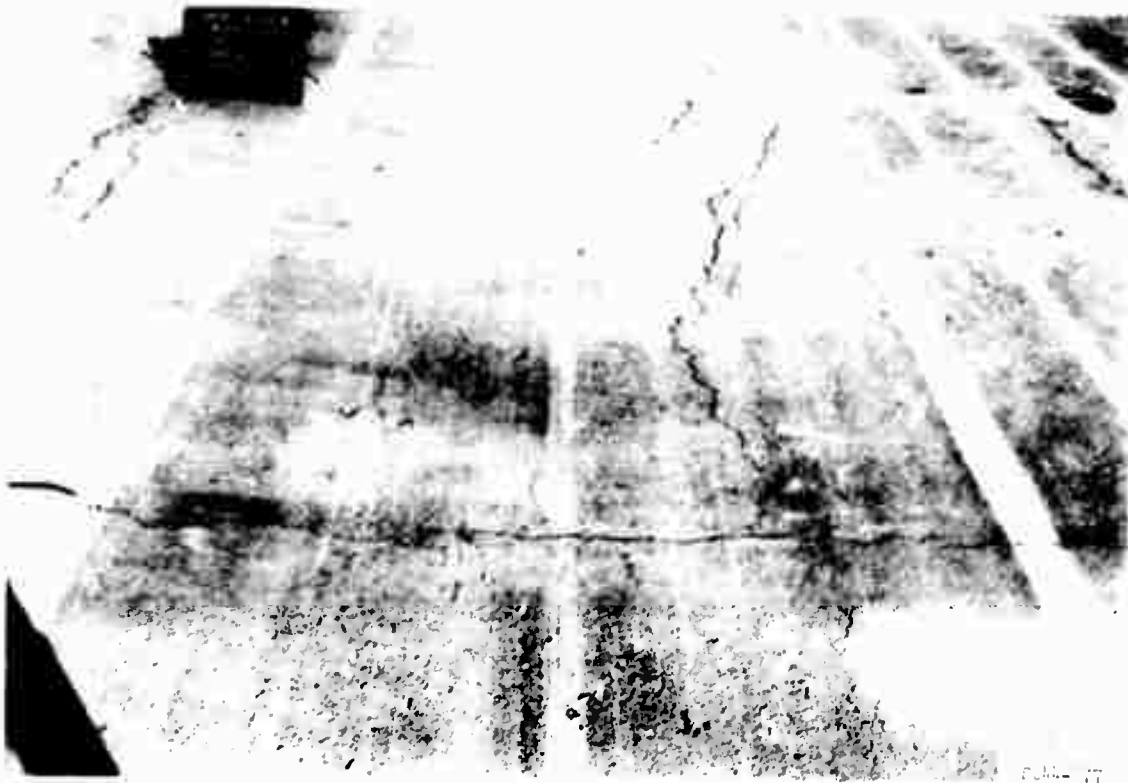


Figure B58. Cracking in subitem 4d, lane 3, flexible pavement test section, at 170 coverages of 50-kip single-wheel assembly

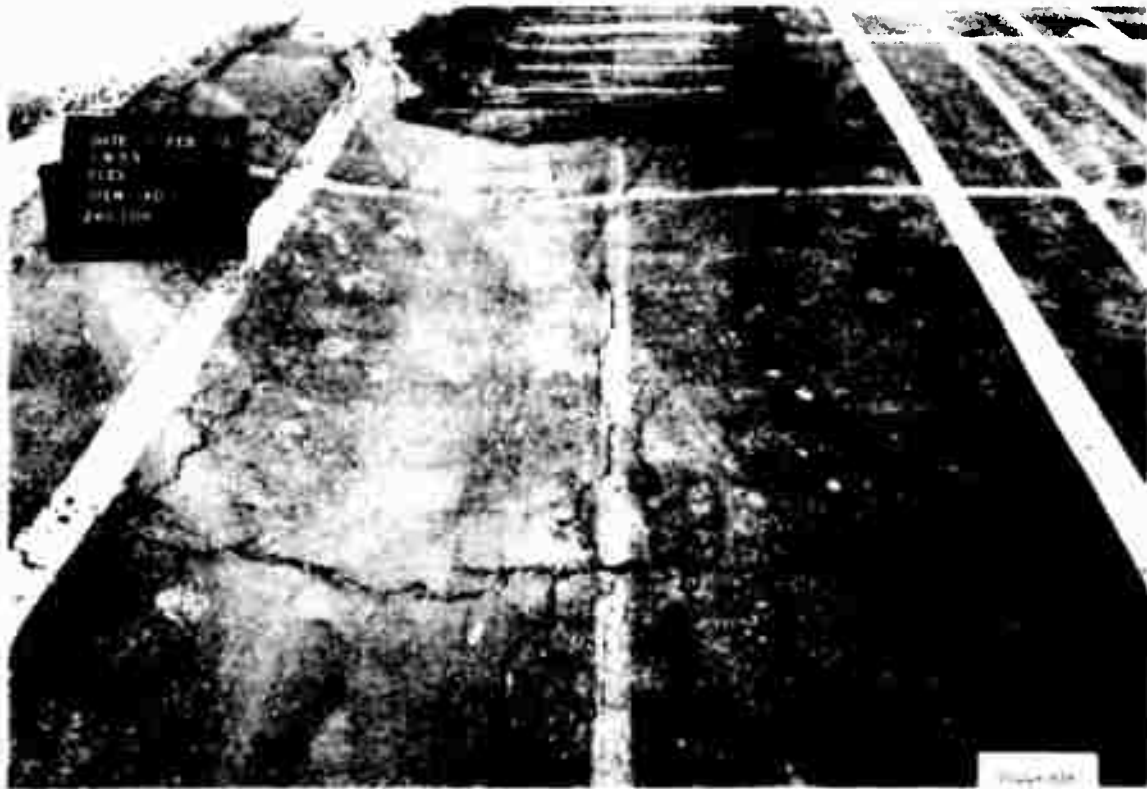


Figure B59. Cracking in subitem 4d, lane 3, flexible pavement test section, at failure after 240 coverages of 50-kip single-wheel assembly

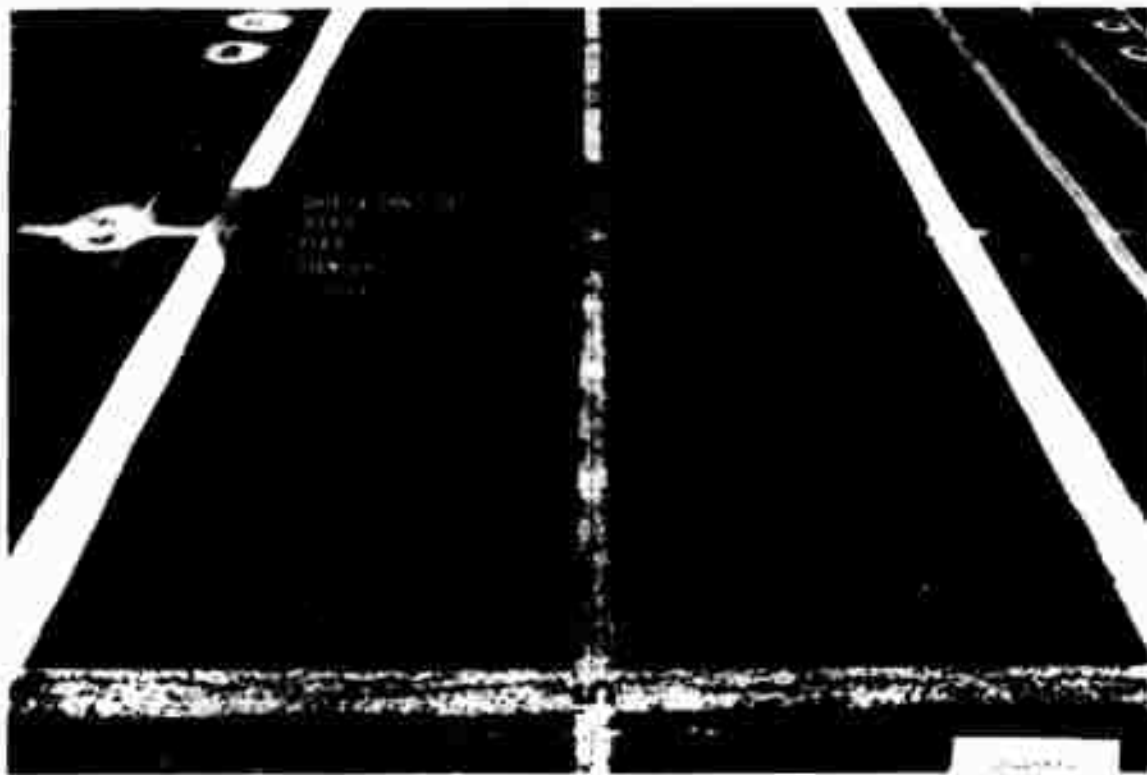


Figure B60. Subitem 5a, lane 3, flexible pavement test section, prior to traffic



Figure B61. Cracking in subitem 5a, lane 3, flexible pavement test section, at failure after 240 coverages of 50-kip single-wheel assembly



Figure B62. Subitem 5b, lane 2, flexible pavement test section, prior to traffic

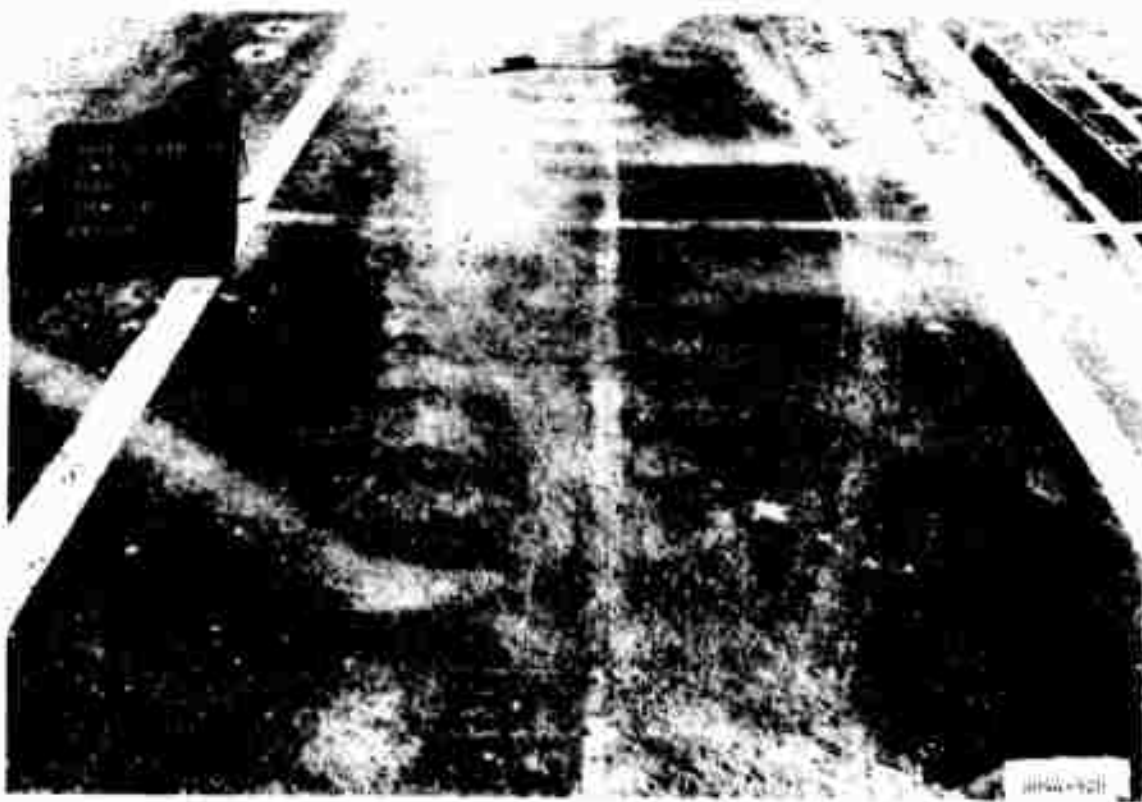


Figure B63. Subitem 5b, lane 3, flexible pavement test section, at failure after 240 coverages of 50-kip single-wheel assembly

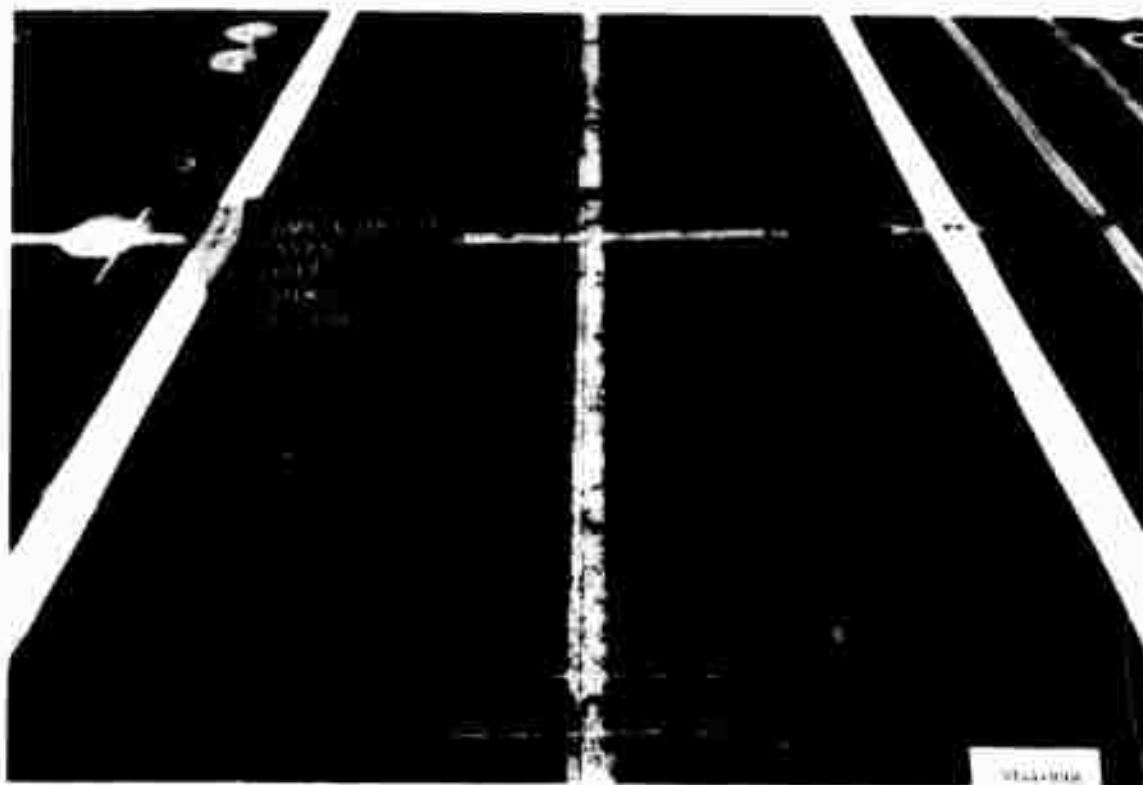


Figure B64. Subitem 5c, lane 3, flexible pavement test section, prior to traffic



Figure B65. Cracking in subitem 5c, lane 3, flexible pavement test section, at failure after 240 coverages of 50-kip single-wheel assembly

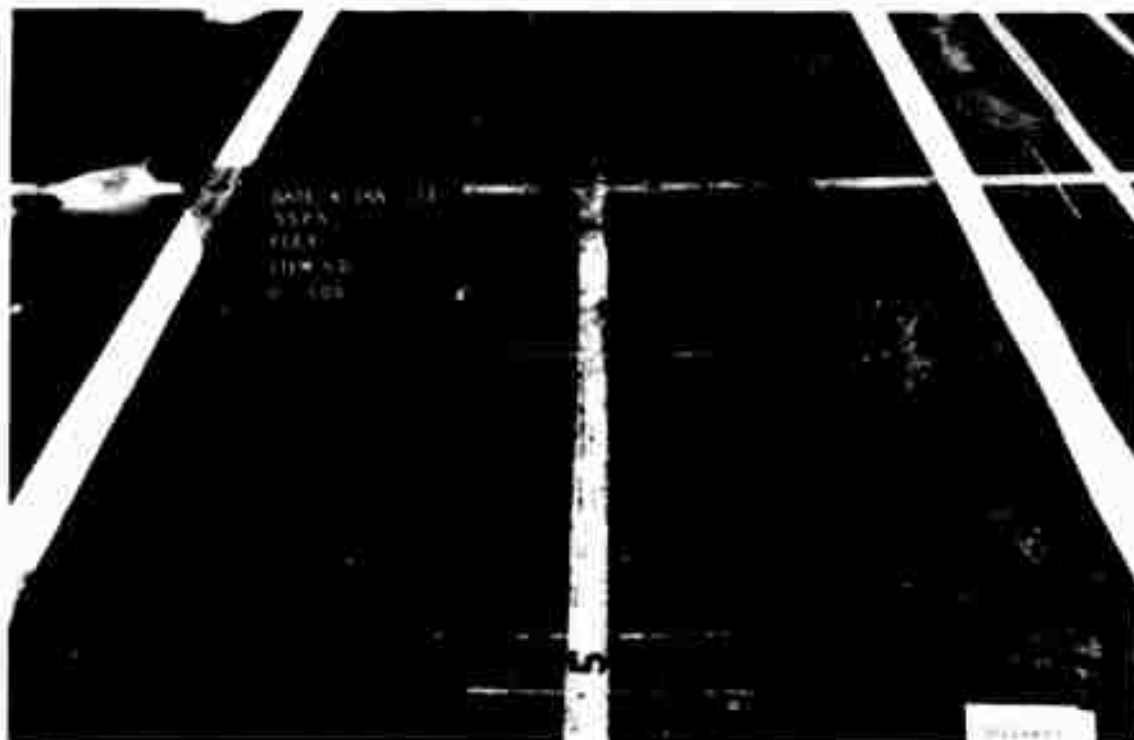
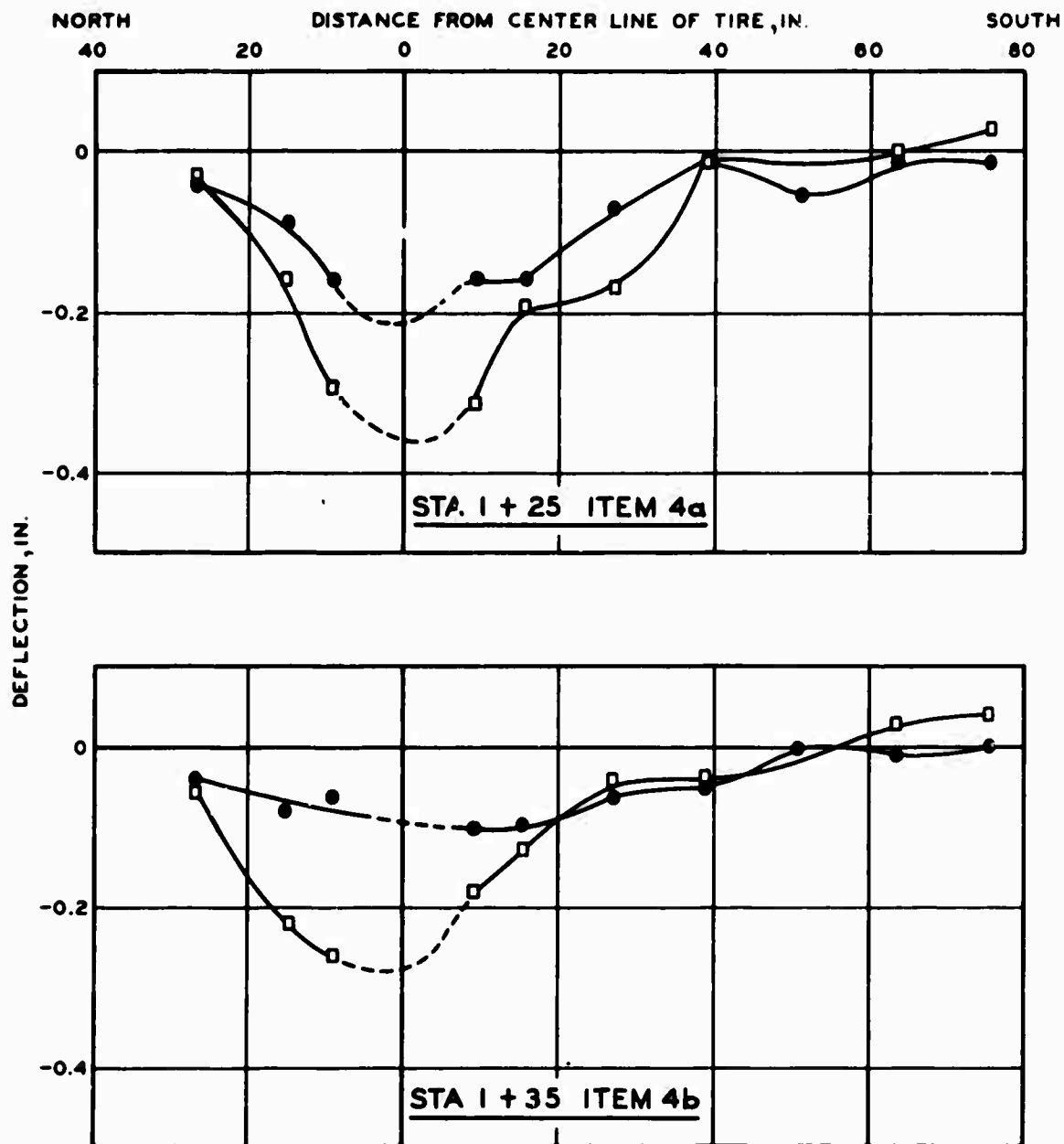


Figure B66. Subitem 5d, lane 3, flexible pavement test section, prior to traffic



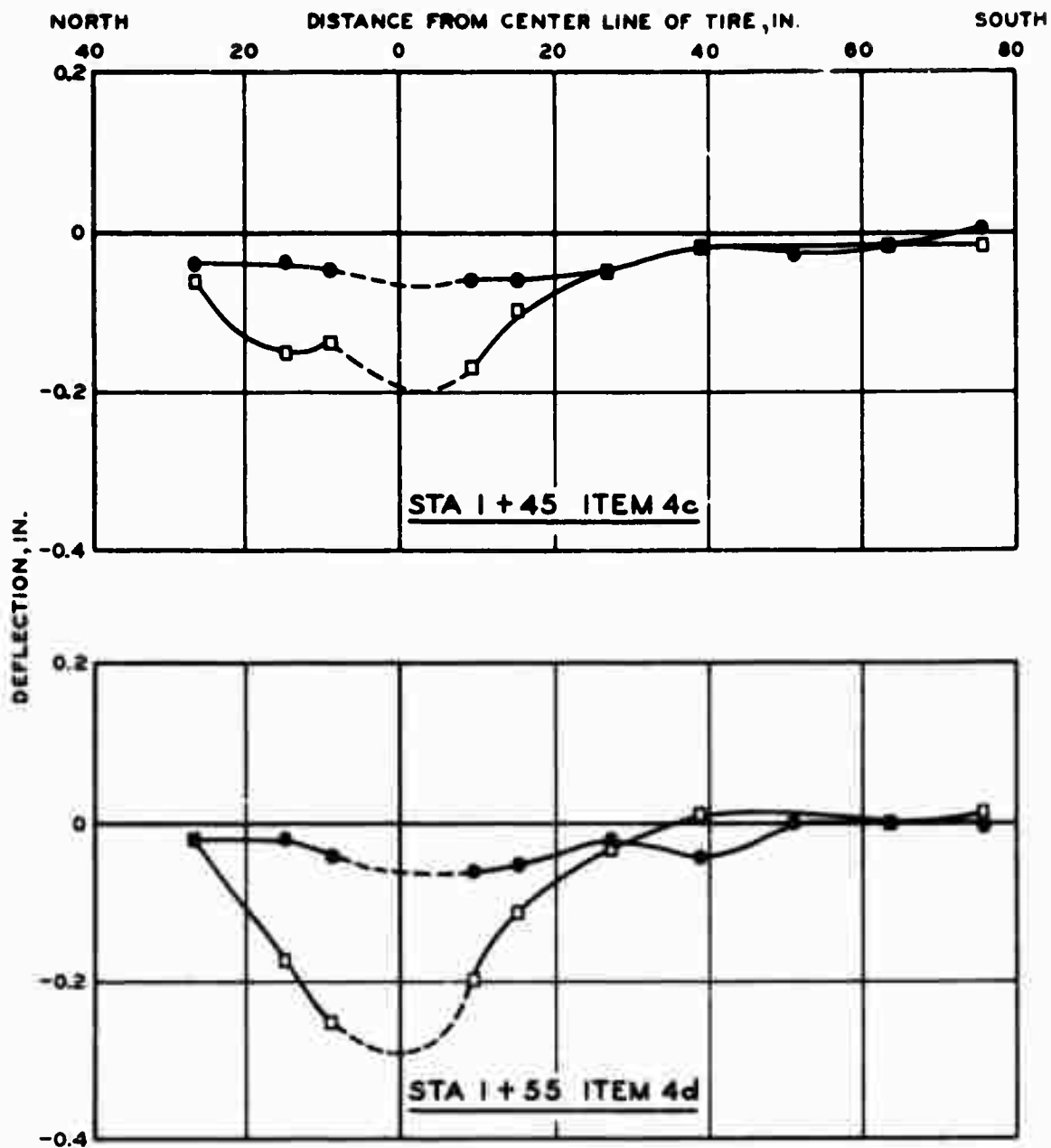
Figure B67. Cracking in subitem 5d, lane 3, flexible pavement test section, at failure after 240 coverages



LEGEND

- EXTRAPOLATED
- 0 COVERAGES
- 170 COVERAGES

Figure B68. Deflections measured transverse to direction of traffic in subitems 4a and b, lane 3, flexible pavement test section



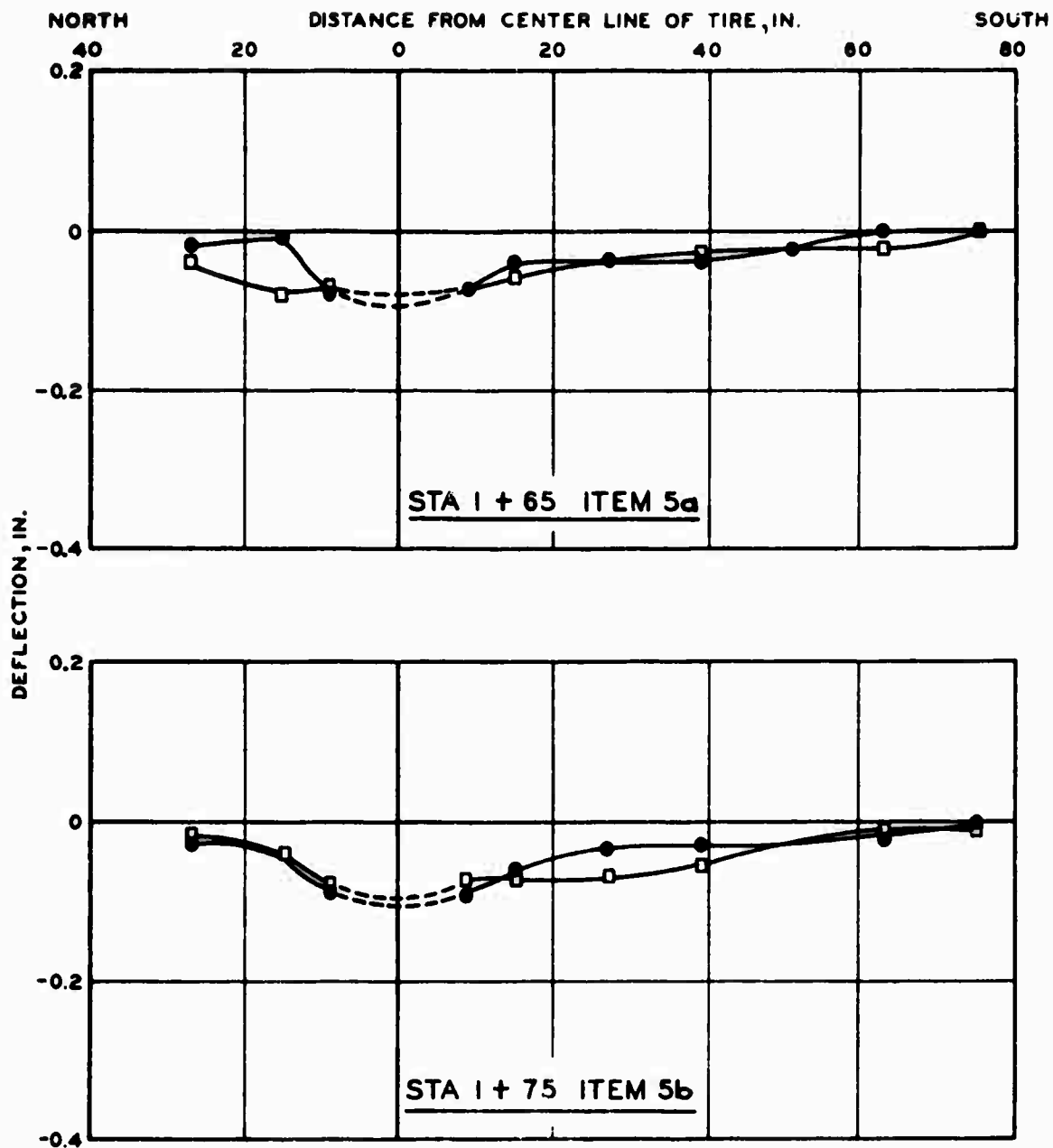
LEGEND

----- EXTRAPOLATED

● 0 COVERAGES

□ 170 COVERAGES

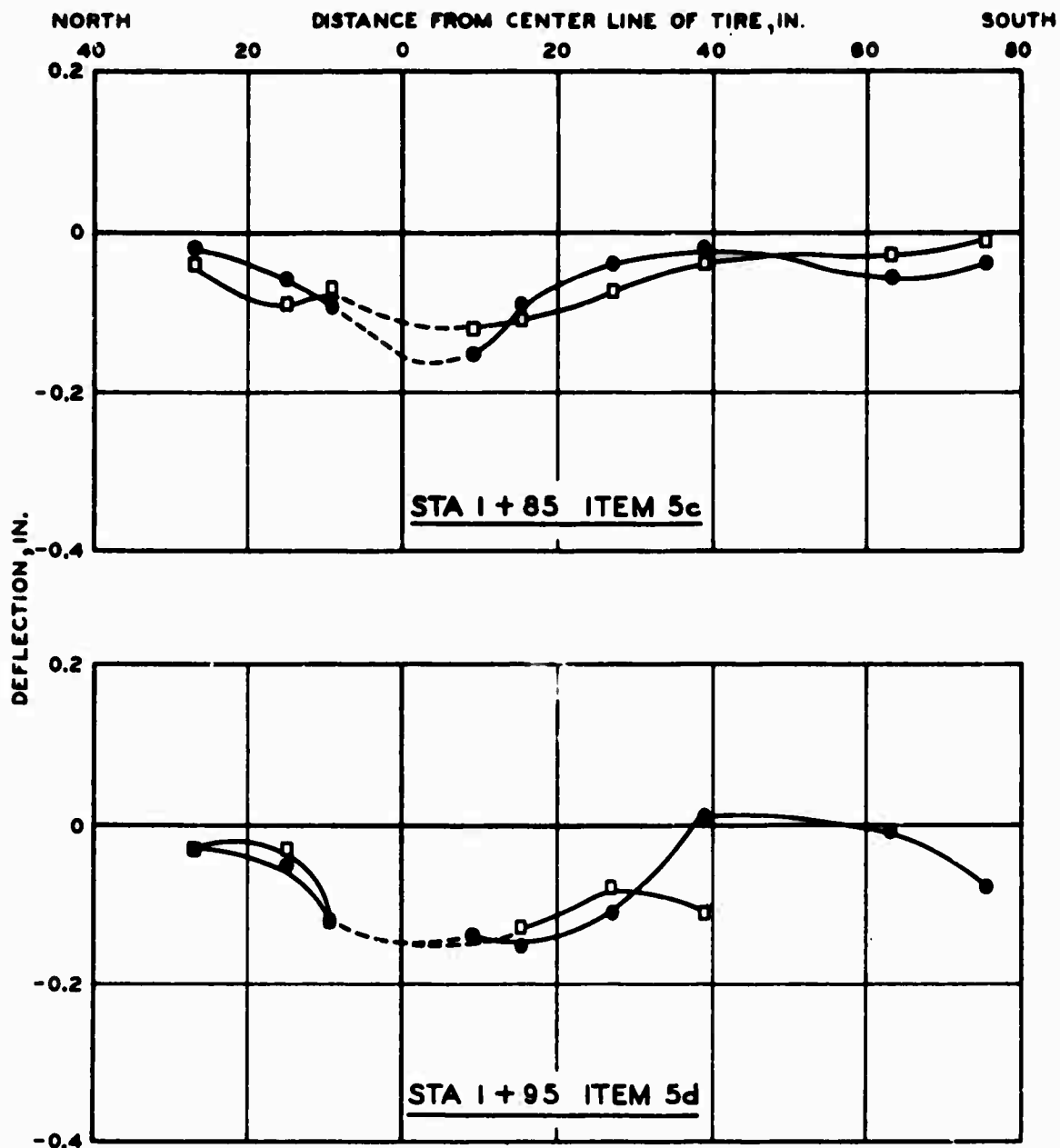
Figure B69. Deflections measured transverse to direction of traffic in subitems 4c and d, lane 3, flexible pavement test section



LEGEND

- EXTRAPOLATED
- 0 COVERAGES
- 170 COVERAGES

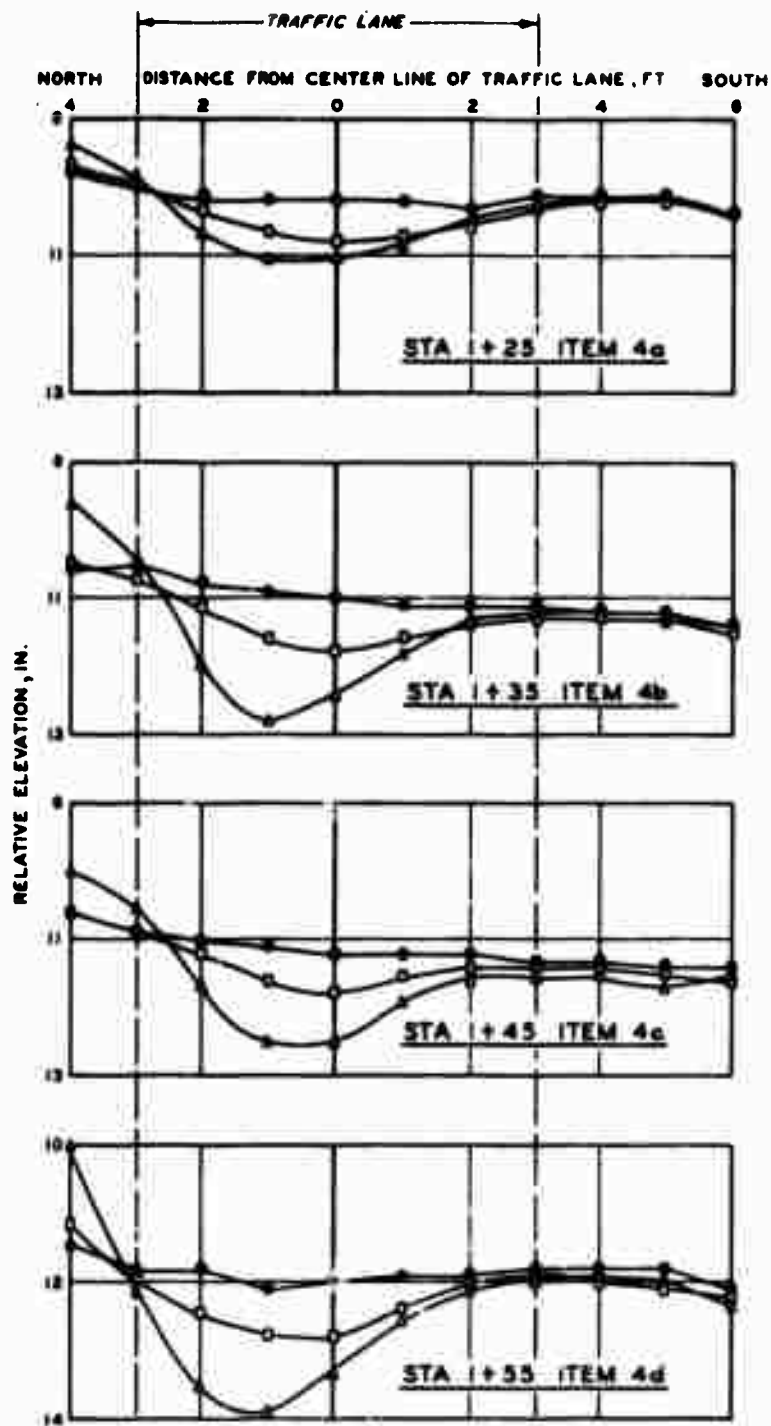
Figure B70. Deflections measured transverse to direction of traffic in subitems 5a and b, lane 3, flexible pavement test section



LEGEND

- EXTRAPOLATED
- 0 COVERAGES
- 170 COVERAGES

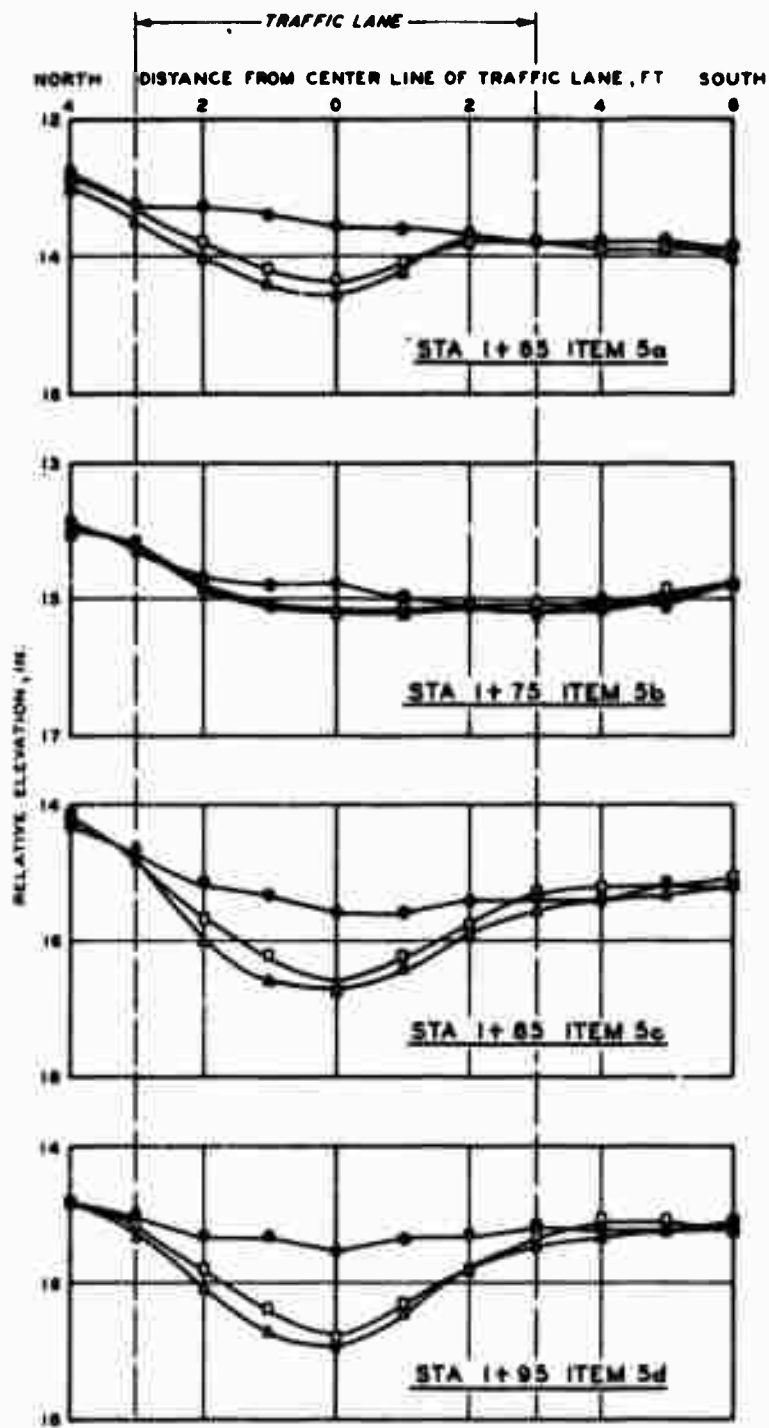
Figure B71. Deflections measured transverse to direction of traffic in subitems 5c and d, lane 3, flexible pavement test section



LEGEND

- 0 COVERAGES
- 170 COVERAGES
- △ 240 COVERAGES

Figure B72. Surface deformation in subitems 4a-d, lane 3, flexible pavement test section



LEGEND

- 0 COVERAGES
- 170 COVERAGES
- △ 240 COVERAGES

Figure B73. Surface deformation in subitems 5a-d, lane 3, flexible pavement test section

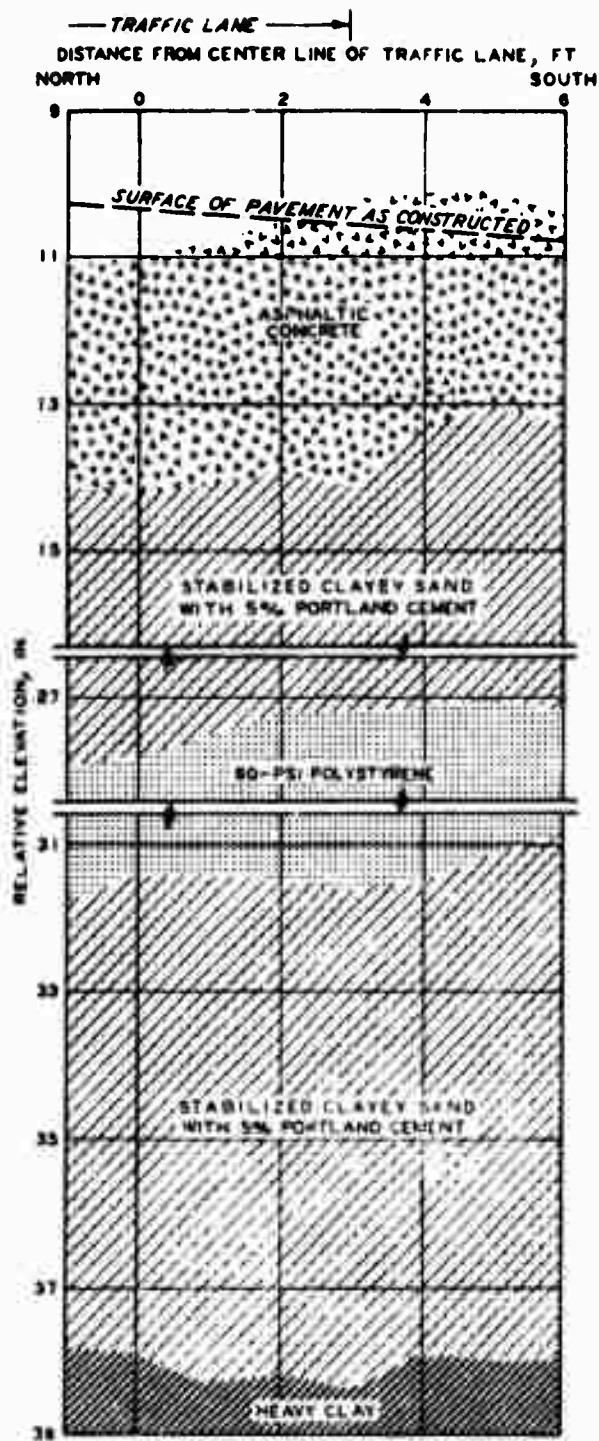


Figure B7⁴. Test pit profile of subitem 4a, lane 3, flexible pavement test section. Station 1+25 after 240 coverages of 50-kip single-wheel assembly

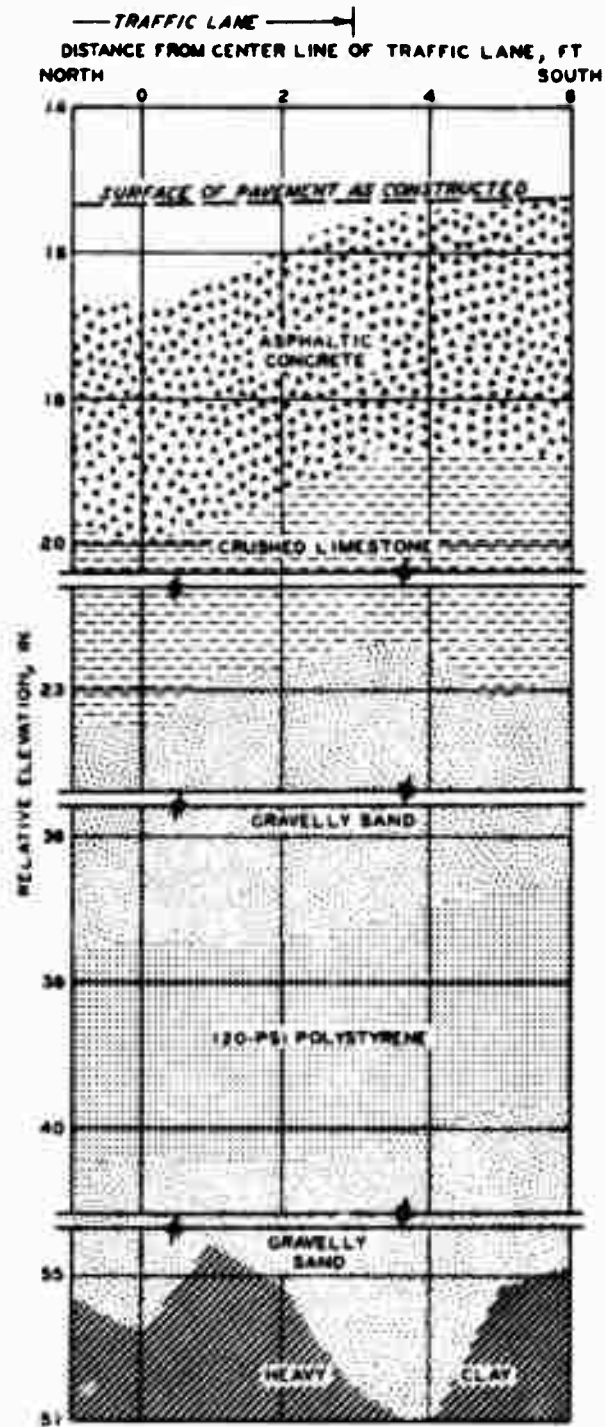


Figure B75. Test pit profile of subitem 5c, lane 3, flexible pavement test section. Station 1+85 after 240 coverages of 50-kip single-wheel assembly

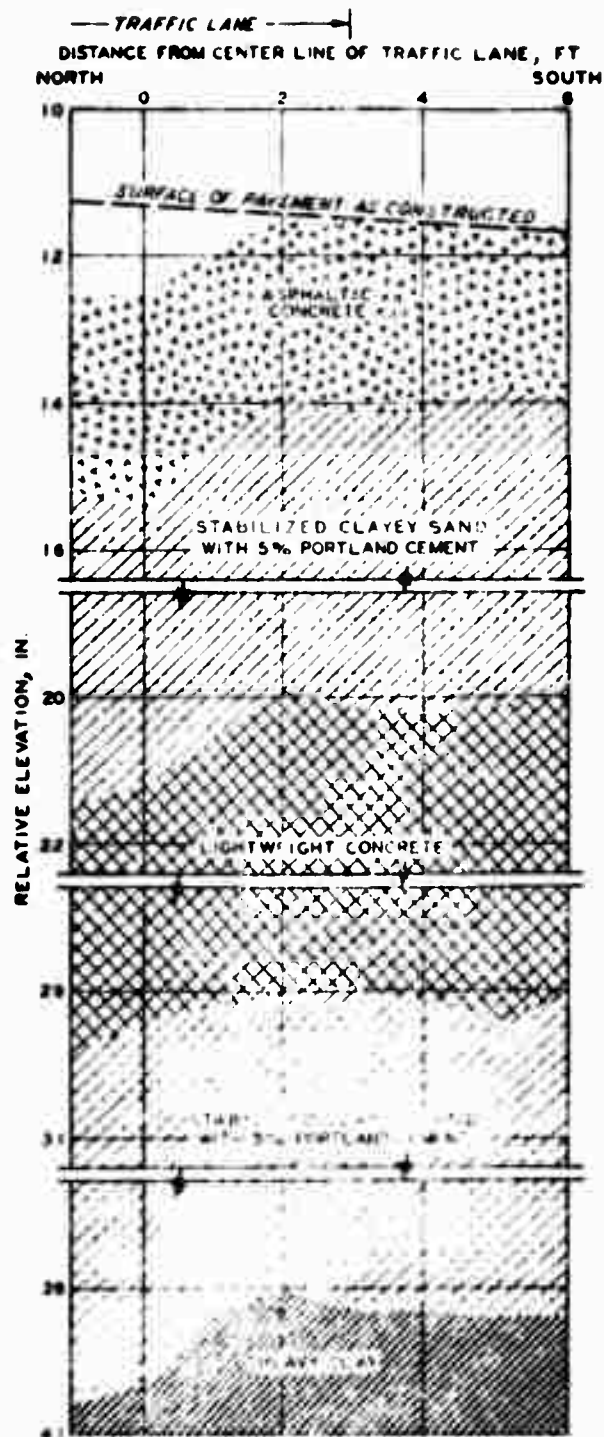


Figure 10. Top profile of sublayer 10, 11, 12, 13, 14, 15, 16, 17, 18, 19, 20, 21, 22, 23, 24, 25, 26, 27, 28, 29, 30, 31, 32, 33, 34, 35, 36, 37, 38, 39, 40, 41, 42, 43, 44, 45, 46, 47, 48, 49, 50, 51, 52, 53, 54, 55, 56, 57, 58, 59, 60, 61, 62, 63, 64, 65, 66, 67, 68, 69, 70, 71, 72, 73, 74, 75, 76, 77, 78, 79, 80, 81, 82, 83, 84, 85, 86, 87, 88, 89, 90, 91, 92, 93, 94, 95, 96, 97, 98, 99, 100 after 140 coverages of 1/2-in. single-wheel assembly

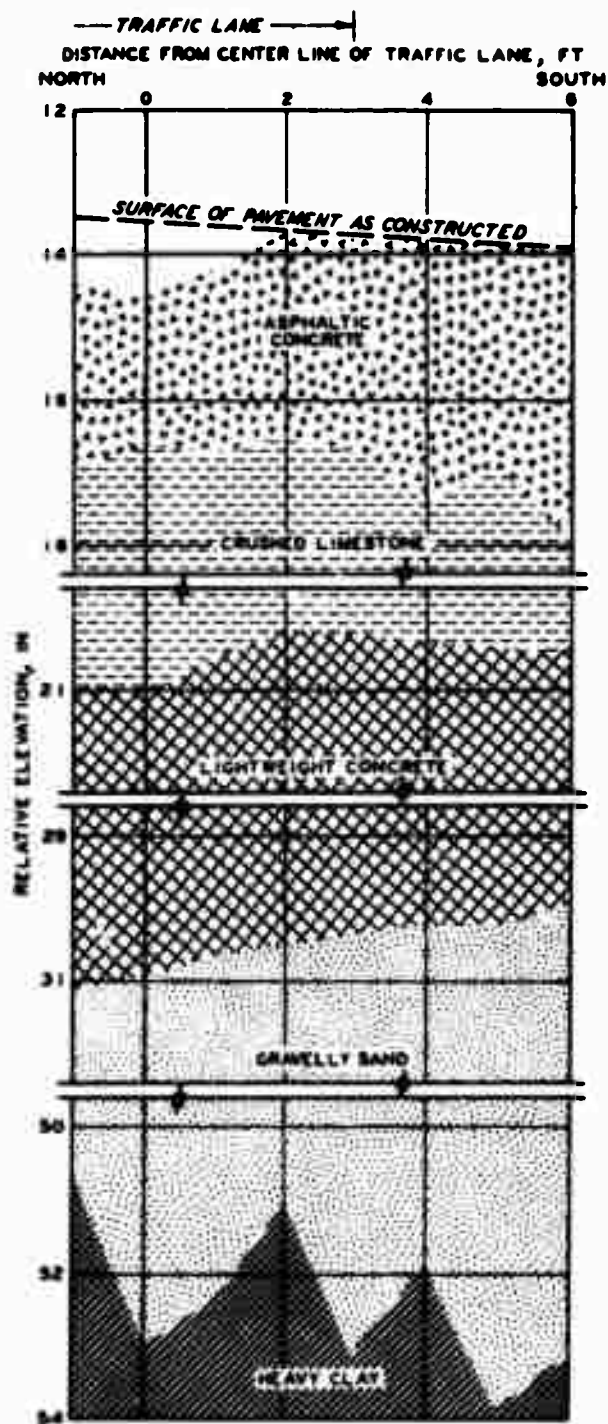


Figure B77. Test pit profile of subitem 5a, lane 3, flexible pavement test section. Station 1+65 after 240 coverages of 50-kip single-wheel assembly



Figure B78. Cracks in polystyrene panels in subitem 4a, lane 3, flexible pavement test section, after traffic



Figure B79. Cracks in polystyrene panels in subitem 4b, lane 3, flexible pavement test section, after traffic



Figure B80. Cracks in lightweight concrete in subitems 4d and 5a, lane 3, flexible pavement test section, after 170 coverages of 50-kip load



Figure B81. Surface of polystyrene panels in subitem 5c, lane 3, flexible pavement test section, after traffic



Figure B82. Surface of polystyrene panels in subitem 5d, lane 3, flexible pavement test section, after traffic



Figure B83. Vertical wall of test pit where samples were obtained to determine cement content of cement-stabilized soil layer (see Figure B84)

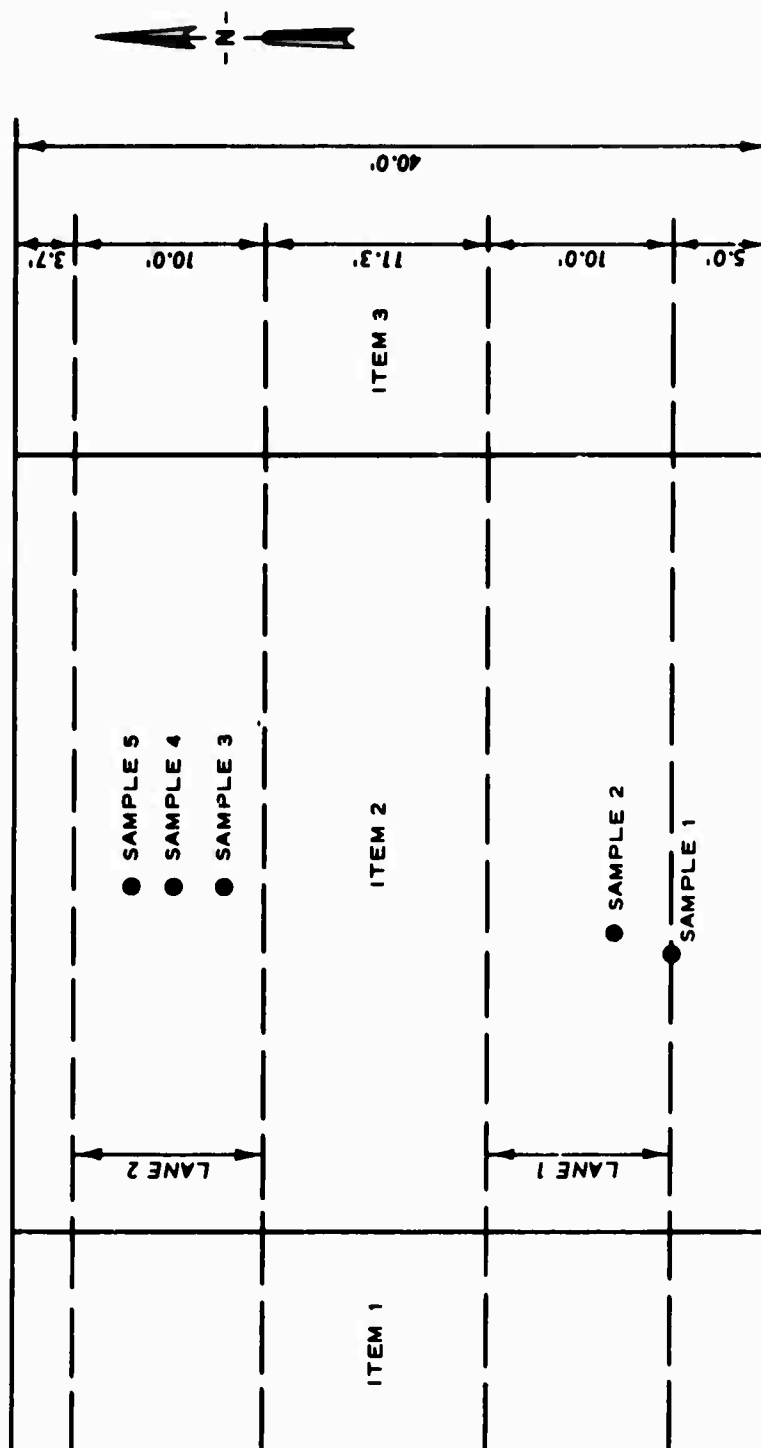


Figure B84. Locations of observation trenches for cement content determinations

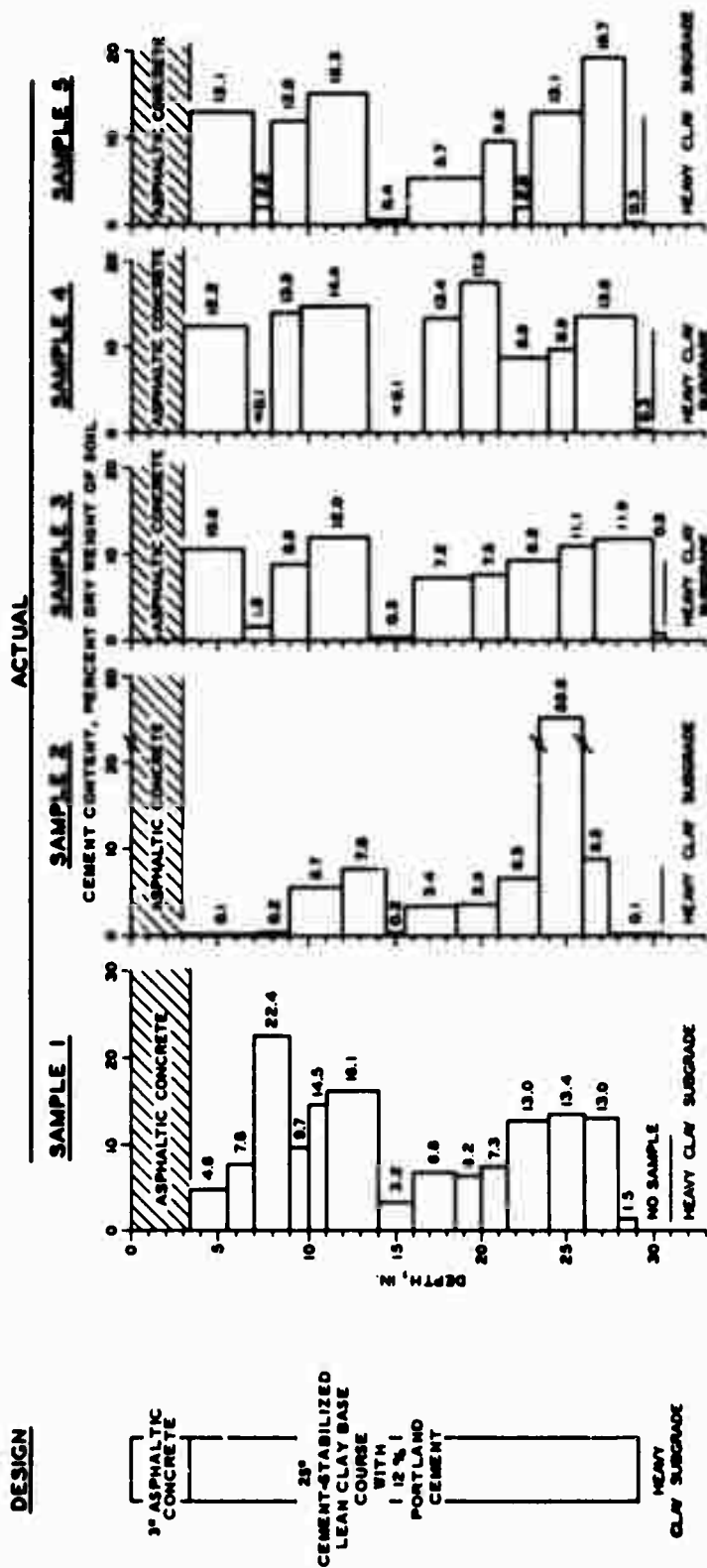


Figure B85. Cement content versus depth. Samples from cement-stabilized lean clay base course, item 2, flexible pavement test section

Table B1

Summary of Cement Content Data for Item 2 of the Flexible Pavement Test Section

Sample 1, Station 0+54.4 South Edge of Lane 1			Sample 2, Station 0+55.8 3 ft North of South Edge of Lane 1			Sample 3, Station 0+58 11.4 ft South of North Edge of Item			Sample 4, Station 0+58 8.7 ft South of North Edge of Item			Sample 5, Station 0+58 6.5 ft South of North Edge of Item		
Depth in.	Cement Content percent		Depth in.	Cement Content percent		Depth in.	Cement Content percent		Depth in.	Cement Content percent		Depth in.	Cement Content percent	
0-3.5	AC*		0-3.0	AC		0-3.0	AC		0-3.0	AC		0-3.5	AC	
3.5-5.5	4.6		3.0-6.0	0.1		3.0-6.5	10.6		3.0-6.75	12.2		3.5-7.0	13.1	
5.5-7.0	7.8		6.0-7.5	0.1		6.5-8.0	1.8		6.75-8.0	<0.1		7.0-8.0	2.0	
7.0-9.0	22.4		7.5-9.0	0.2		8.0-10.0	8.9		8.0-9.5	13.9		8.0-10.0	12.0	
9.0-10.0	9.7		9.0-12.0	5.7		10.0-13.5	12.0		9.5-13.5	14.4		10.0-13.5	15.3	
10.0-11.0	14.3		12.0-14.5	7.8		13.5-16.0	0.3		13.5-16.75	<0.1		13.5-15.7	0.4	
11.0-14.0	16.1		14.5-15.5	0.2		16.0-19.5	7.2		16.75-18.75	13.4		15.7-20.2	5.7	
14.0-16.0	3.2		15.5-18.5	3.4		19.5-21.5	7.5		18.75-21.0	17.5		20.2-22.0	9.8	
16.0-18.5	6.8		18.5-21.0	3.5		21.5-24.5	9.2		21.0-24.0	8.6		22.0-22.8	2.0	
18.5-20.0	6.2		21.0-23.5	6.5		24.5-26.5	11.1		24.0-25.5	8.9		22.8-25.0	13.1	
20.0-21.5	7.3		23.5-26.0	55.6		26.5-30.0	11.9		25.5-29.0	13.6		26.0-28.5	19.7	
21.5-24.0	13.0		26.0-27.5	9.5		30.0-30.75	0.9		29.0-30.0	0.3		28.5-29.5	0.3	
24.0-26.0	13.4		27.5-30.5	0.1										
26.0-28.0	13.0													
28.0-29.0	1.5													

* Denotes asphaltic concrete surfacing.

REFERENCES

1. Rice, J. L., "Proposed Design Criteria for Fibrous Concrete Pavement," Preliminary Report S-5, U. S. Army Construction Engineering Research Laboratory, CE, Champaign, Ill.
2. Department of Defense, "Unified Soil Classification System for Roads, Airfields, Embankments, and Foundations," Military Standard No. MIL-STD-619B, Jun 1968, Washington, D. C.
3. Federal Aviation Administration, "Airport Paving," Advisory Circular AC 150/5320-6A, Sep 1971, Washington, D. C.
4. American Society for Testing and Materials, "Standard Methods of Test for Moisture-Density Relations of Soils Using 10-lb Rammer and 18-in. Drop," Designation: D 1557-70, 1972 Annual Book of ASTM Standards, Part 11, 1972, Philadelphia, Pa.
5. Burns, C. D. et al., "Multiple-Wheel Heavy Gear Load Pavement Tests; Design, Construction, and Behavior Under Traffic," Technical Report S-71-17, Vol II, Nov 1971, U. S. Army Engineer Waterways Experiment Station, CE, Vicksburg, Miss.
6. Department of Defense, "Test Methods for Pavement, Subgrade, Subbase, and Base-Course Materials," Military Standard No. MIL-STD-621A, Dec 1964, Washington, D. C.
7. American Society for Testing and Materials, "Standard Methods of Test for Moisture-Density Relations of Soils Using 5.5-lb Rammer and 12-in. Drop," Designation: D 698-70, 1972 Annual Book of ASTM Standards, Part 11, 1972, Philadelphia, Pa.
8. General Services Administration, "Cement, Portland," Federal Specification SS-C-192G, Nov 1971, Washington, D. C.
9. Grau, R. W., "Strengthening of Keyed Longitudinal Construction Joints in Rigid Pavements," Miscellaneous Paper S-72-43, Aug 1972, U. S. Army Engineer Waterways Experiment Station, CE, Vicksburg, Miss.
10. Burns, C. D. et al., "Study of Behavior of Bituminous-Stabilized Pavement Layers," Miscellaneous Paper S-73-4, Mar 1973, U. S. Army Engineer Waterways Experiment Station, CE, Vicksburg, Miss.
11. Grau, R. W., "Evaluation of Structural Layers in Flexible Pavement," Miscellaneous Paper S-73-26, May 1973, U. S. Army Engineer Waterways Experiment Station, CE, Vicksburg, Miss.
12. Brabston, W. N. and Hammitt, G. M. II, "Soil Stabilization for Roads and Airfields in the Theater of Operations," Miscellaneous Paper (in preparation), U. S. Army Engineer Waterways Experiment Station, CE, Vicksburg, Miss.

13. Hohwiller, F. and Köhling, K., "Styropor-Concrete: A Status Report," Badische Anilin- & Soda-Fabrik AG, 1970, Munich.
14. American Society for Testing and Materials, "Standard Specification for Hydrated Lime for Masonry Purposes," Designation: C 207-49, 1972 Annual Book of ASTM Standards, Part 9, 1972, Philadelphia, Pa.
15. General Services Administration, "Pozzolan (For Use in Portland-Cement Concrete)," Federal Specification SS-P-570, Apr 1969, Washington, D. C.
16. U. S. Army, Office, Chief of Engineers, "Guide Specification for Military Construction, Graded-Crushed-Aggregate Base Course," Guide Specification CE-807.07, Oct 1972, Washington, D. C.
17. Federal Aviation Administration, "Standard Specifications for Construction of Airports," Advisory Circular AC 150/5370-1A, May 1968, Washington, D. C.
18. Portland Cement Association, "Soil-Cement Laboratory Handbook," Engineering Bulletin, 1971, Skokie, Ill.
19. American Society for Testing and Materials, "Standard Methods for Freezing-and-Thawing Tests of Compacted Soil-Cement Mixtures," Designation: D 560-57, 1972 Annual Book of ASTM Standards, Part 11, 1972, Philadelphia, Pa.
20. _____, "Standard Method for Laboratory Determination of Pulse Velocities and Ultrasonic Elastic Constants of Rock," Designation: D 2845-69, 1972 Annual Book of ASTM Standards, Part 11, 1972, Philadelphia, Pa.
21. Ledbetter, R. H. et al., "Multiple-Wheel Heavy Gear Load Pavement Tests; Presentation and Initial Analysis of Stress-Strain-Deflection and Vibratory Measurements; Instrumentation," Technical Report S-71-17, Vol IIIA, Nov 1971, U. S. Army Engineer Waterways Experiment Station, CE, Vicksburg, Miss.
22. Horn, W. J., "Aircraft Dynamic Load Effects," Report No. FAA-RD-74-32 (in preparation), Federal Aviation Administration, Washington, D. C.
23. American Society for Testing and Materials, "Standard Specification for Cationic Emulsified Asphalt," Designation: D 2397-71, 1972 Annual Book of ASTM Standards, Part 11, 1972, Philadelphia, Pa.
24. General Services Administration, "Sealing Compound, Hot Poured Type, For Joints in Concrete," Federal Specification SS-S-164(4), Aug 1964, Washington, D. C.
25. American Society for Testing and Materials, "Standard Method of Test for Density of Soil in Place by the Drive-Cylinder Method," Designation: D 2937-71, 1972 Annual Book of ASTM Standards, Part 11, 1972, Philadelphia, Pa.

26. American Society for Testing and Materials, "Standard Method of Test for Density of Soil in Place by the Rubber-Balloon Method," Designation: D 2167-66, 1972 Annual Book of ASTM Standards, Part 11, 1972, Philadelphia, Pa.
27. _____, "Standard Method of Test for Flexural Strength of Concrete (Using Simple Beam with Third-Point Loading)," Designation: C 78-64, 1972 Annual Book of ASTM Standards, Part 10, 1972, Philadelphia, Pa.
28. Barker, W. R. et al., "An Investigation of the Structural Properties of Stabilized Layers in Flexible Pavement Systems," Air Force Weapons Laboratory Technical Report No. AFWL-TR-73-21, Oct 1973, prepared by the U. S. Army Engineer Waterways Experiment Station, CE, Vicksburg, Miss., for the Air Force Weapons Laboratory, Kirtland Air Force Base, N. Mex.
29. U. S. Army Engineer Waterways Experiment Station, CE, "Handbook for Concrete and Cement," Aug 1949 (with quarterly supplements), Vicksburg, Miss.